

**SYNTHESIS OF IMMUNOGENIC  
MYCOBACTERIAL CELL WALL LIPIDS**

Satvika Burugupalli

Submitted in total fulfilment of the requirements of the degree of

Doctor of Philosophy

December 2017

School of Chemistry

The University of Melbourne



## ABSTRACT

This thesis is comprised of two parts: Part I describes the synthesis and immunology of mycobacterial cell wall lipids and Part II describes the development of oxime-based activated esters as safer alternatives to hydroxylbenzotriazoles for chemo- and regioselective benzylation.

### *Part I: Synthesis of immunogenic mycobacterial cell wall lipids*

Tuberculosis is the most devastating infectious disease in the world. It is caused by infection with *Mycobacterium tuberculosis* (*M.tb*), a bacterium with a complex lipid rich cell wall that contributes to virulence and antibiotic resistance. The outer cell wall lipids are known to mingle with receptors of the host immune system. In Chapters 1-3, we report the synthesis of immunogenic glycolipids and phospholipid antigens present in the outer cell surface of the mycobacterial cell wall that can be presented by CD1 proteins. These antigens are characterized by the presence of a branched methyl fatty acid, 10-methyl stearic acid, called tuberculostearic acid (TBSA).

Chapter 1 describes the synthesis of (*R*) and (*S*) enantiomers of TBSA. We developed efficient two-step and three-step approaches for the synthesis of TBSA. We used citronellyl bromide, a commercially available chiral pool starting material available as both enantiomers, and built the fatty acid chain by copper mediated cross-coupling and subsequent tandem cross metathesis/hydrogenation using Hoveyda-Grubbs second generation catalyst. In an attempt to ascertain the stereochemistry of natural TBSA we developed a chiral discrimination method using an anthracene based chiral derivatizing reagent; while some discrimination was possible, baseline separation of the key peaks could not be achieved.

Chapter 2 describes the synthesis of an *M.tb* phosphatidyl glycerol (PG). Recently, a PG fraction containing a range of lipofoms was isolated from *M.tb* and shown to activate type II NKT cells by binding to CD1d. Towards this end, we undertook the synthesis of a homogenous representative PG bearing *R*-TBSA and two other analogues lacking the methyl

branch. A one pot synthesis of a diacylglycerol was achieved by epoxide ring opening with *R*-TBSA using Jacobsen's catalyst, and phosphoramidite chemistry was used to assemble the PG fragments. The availability of pure synthetic *M.tb* PG and analogues facilitated the immunological studies of their ability to activate CD1b-restricted T cells.

Chapter 3 describes the development of a second-generation synthesis of mycobacterial glycolipid, Gl-A, an  $\alpha$ -glucuronosyl diacylglyceride, in a short 8 step sequence using just a single protecting group. A highlight of this approach include a high fidelity regioselective acylation of a bromohydrin intermediate, synthesized by Jacobsen hydrolytic kinetic resolution of allyl  $\alpha$ -D-glucoside derived epoxide and subsequent epoxide ring opening with  $\text{Li}_2\text{NiBr}_4$ . Using this method, Gl-A, and  $\alpha$ -glucosyl and  $\alpha$ -glucuronosyl analogues bearing (*R*)-TBSA and (*S*)-TBSA, were synthesized. Immunological studies of all the analogues on an assortment of NKT cells revealed that while type Ia NKT cells were tolerant to glucose and glucuronosyl head groups, type II NKT cells preferred glucuronosyl head group only.

*Part II: Development of oxime-based activated esters as safer alternatives to hydroxybenzotriazoles for chemo- and regioselective benzylation*

Benzoyloxybenzotriazole (BBTZ), is a useful selective benzoylating reagent, but has safety limitations owing to the explosive nature of its precursor HOBt. In Chapter 4, we have explored a range of benzoylated oxime-based reagents as alternatives to BBTZ, for the selective benzylation of carbohydrate polyols. Of the reagents synthesized, the most effective reagent was identified as benzoyl-Oxyma, a highly crystalline, readily prepared alternative to BBTZ, which was shown to be useful in the selective benzylation of carbohydrate polyols.

## **DECLARATION**

This is to certify that

- (i) the thesis comprises only my original work towards the PhD except where indicated in the Preface
- (ii) due acknowledgment has been made in the text to all the material used
- (iii) the thesis is less than 100,000 words in length, exclusive of tables, bibliographies and appendices

Satvika Burugupalli

December 2017

## **PREFACE**

All work reported herein has been conducted by the candidate Satvika Burugupalli except where indicated. Bromohydrin intermediate used in the synthesis of G1-A is a kind gift from Dr. Sayali Shah, a previous lab member. NKT cell immunoassays as described in chapter 4 were conducted by Dr. Catrina Almeida in the laboratory of Prof. Dale Godfrey, Department of Microbiology and Immunology, University of Melbourne. Samples of *M.tb* PG were given to Dr. Daniel Pellici who conducted immunological studies.

This thesis has been published in part:

1. Satvika Burugupalli, Sayali Shah, Phillip L. van der Peet, Seep Arora, Jonathan M. White, Spencer J. Williams. “Investigation of benzoyloximes as benzoylating reagents: Benzoyl-Oxyma as a selective benzoylating reagent”, *Org. Biomol. Chem.*, **2016**, 14, 97-104.
2. Satvika Burugupalli, Mark B. Richardson, Spencer J. Williams. “Total synthesis and mass spectrometric analysis of a *Mycobacterium tuberculosis* phosphatidylglycerol featuring a two-step synthesis of (*R*)-tuberculostearic acid” *Org. Biomol. Chem.*, **2017**, 15, 7422-7429.

## **ACKNOWLEDGEMENTS**

I sincerely thank my supervisor, Prof. Spencer Williams for his guidance and encouragement throughout my PhD.

I appreciate the assistance of past and present Williams group members and recognize the contributions they have made to my training as a scientist. I thank my friends at the University of Melbourne, Dr. Sayali Shah, Katherine Shang and Dr. Aysa Pourvaly who made this journey a memorable experience.

I am forever thankful to my family for their support and unwavering belief in me. I especially appreciate the significant sacrifices made by my parents.

Most importantly, I thank my husband, Raj for his unconditional love, faith and support throughout all the years.



## TABLE OF CONTENTS

### PART I

#### CHAPTER ONE

##### Introduction

<b>1</b>	<b>Chapter 1: Introduction.....</b>	<b>1</b>
1.1	Introduction to tuberculosis.....	1
1.2	Mycobacteria possess a unique cell wall important for its virulence.....	4
1.3	The mycobacterial cell-wall is rich in lipids and glycolipids .....	6
1.4	Immune sensing of microbial lipids and lipid-like molecules by T cells.....	9
1.4.1	Lipid antigen recognition by the immune system .....	9
1.4.2	Lipid antigen presentation by CD1 molecules .....	10
1.4.3	CD1-restricted T cells.....	11
1.4.4	CD1d-restricted T cells (NKT cells) .....	13
1.4.5	Type II NKT cells (dNKT cells).....	17
1.4.6	Atypical Type Ia NKT cells.....	21
1.5	Mycobacterial lipids capable of inducing CD1d-restricted T-cell responses. 22	
1.6	CD1b presents a wide range of mycobacterial lipids.....	23
1.7	Summary.....	26
1.8	Thesis outline for Chapters 2-4.....	26

#### CHAPTER TWO

##### Synthesis and NMR discrimination of tuberculostearic acid (TBSA) enantiomers

<b>2.1</b>	<b>Introduction.....</b>	<b>31</b>
2.1.1	Methyl branched fatty acids in mycobacteria.....	31
2.1.2	Tuberculostearic acid, a branched fatty acid produced by mycobacteria..	31
2.1.3	Chirality of natural TBSA .....	32
2.2	TBSA is present in a wide range of mycobacterial lipid-like species.....	35
2.3	Biosynthesis of TBSA.....	38
2.4	10-Hydroxy stearate: a case study .....	39
2.5	Summary of enantioselective syntheses of ( <i>R</i> )-TBSA.....	40
2.6	Aims of this chapter .....	43
2.7	Results and Discussion.....	43
2.7.1	Cross metathesis concept and optimization.....	44
2.7.2	A new two-step approach for the synthesis of TBSA .....	50

<b>2.8 Aim 2: NMR discrimination of TBSA enantiomers using a chiral derivatizing agent.....</b>	<b>51</b>
<b>2.9 Results and discussion .....</b>	<b>56</b>
2.9.1 <sup>1</sup> H NMR analysis of the cyclohexanol esters of TBSA.....	57
2.9.2 Mosher's ester synthesis and NMR analysis .....	58
<b>2.10 Summary.....</b>	<b>60</b>
<b>2.11 Experimental .....</b>	<b>61</b>

### CHAPTER THREE

#### Synthesis of *Mycobacterium. tuberculosis* phosphatidylglycerol

<b>3.1 Introduction.....</b>	<b>72</b>
3.1.1 Discovery of PG .....	72
<b>3.2 The mycobacterial cell wall is rich in PLs .....</b>	<b>73</b>
<b>3.3 Biosynthesis and metabolism of PG .....</b>	<b>73</b>
<b>3.4 Structural characterization of PG .....</b>	<b>74</b>
<b>3.5 PG and cardiolipin can modulate host immune system .....</b>	<b>76</b>
3.5.1 CD1d-dependent activation .....	76
3.5.2 CD1b-dependent activation .....	79
<b>3.6 Synthesis of PG and related PLs.....</b>	<b>80</b>
3.6.1 Synthesis of 1,2-diacylglycerols.....	80
3.6.2 Regioselective glycidol opening reactions .....	81
<b>3.7 Previous syntheses of PG and related phospholipids .....</b>	<b>85</b>
3.7.1 Baer's total synthesis of PG.....	86
3.7.2 Minnaard's synthesis of phosphatidylethanolamine.....	87
3.7.3 Painter's synthesis of PIM <sub>2</sub> .....	88
<b>3.8 Aim .....</b>	<b>89</b>
<b>3.9 Results and discussion .....</b>	<b>90</b>
3.9.1 Synthesis of dibenzyl glycerol.....	91
3.9.2 Assembly of the fragments onto the phosphorus linchpin .....	92
<b>3.10 ESI CID- MS/MS of PG analogues.....</b>	<b>95</b>
<b>3.11 Conclusion .....</b>	<b>97</b>
<b>3.12 Experimental .....</b>	<b>98</b>

### CHAPTER FOUR

#### A second generation synthesis of Gl-A, a GlcA-DAG from *M. smegmatis*

<b>4.1 Introduction.....</b>	<b>112</b>
<b>4.2 Mycobacterial glycosyl diacylglycerols .....</b>	<b>112</b>
4.2.1 Gentiobiosides .....	112

4.2.2	$\alpha$ -Glucuronides .....	113
4.3	Determination of the structure of Gl-A lipofoms .....	114
4.4	Structural role of Gl-A in the biosynthesis of corynebacterial lipomannan .....	116
4.5	Gl-A can act a selective agonist for V $\alpha$ 10 NKT cells .....	119
4.6	Previous synthesis of Gl-A .....	120
4.6.1	Chiral glycerol fragment synthesized from D-mannitol.....	121
4.6.2	Chiral auxiliary approach to ( <i>R</i> )-TBSA.....	121
4.6.3	Formation of the challenging 1,2-cis glucosidic bond by halide-ion catalysis .....	122
4.6.4	Assembly of the fragments .....	123
4.6.5	Shortcomings of the synthesis .....	124
4.7	Strategies for the synthesis of glycosyl diglycerides and limitations.....	124
4.8	Allyl glycosides: masked precursors for glycosyl diglyceride synthesis ..	125
4.9	A new approach to access glucosyl diacylglycerols via a bromohydrin intermediate.....	126
4.9.1	Synthesis of glycolipids utilizing the bromohydrin intermediate.....	127
4.10	Aim of this project .....	129
4.11	Results and discussion .....	130
4.11.1	Synthesis of glucosyl diacylglycerols (GlcDAGs).....	130
4.11.2	Synthesis of glucuronosyl diacylglycerols (GlcADAGs).....	132
4.12	Summary.....	135
4.13	Biological activity of $\alpha$ -glucosyl and $\alpha$ -glucuronosyl diacylglycerides.....	135
4.13.1	Activation of NKT cells .....	137
4.14	Summary and conclusions.....	139
4.15	Experimental .....	141

## CHAPTER FIVE

### Development of oxime-based activated esters

5.1	Introduction.....	150
5.1.1	Hydroxyl protecting groups in carbohydrate chemistry .....	150
5.2	Principles of selective hydroxyl group protection.....	151
5.3	Esters as hydroxyl protecting groups.....	152
5.3.1	Intramolecular migration .....	153
5.3.2	Neighboring group participation .....	153
5.3.3	“Armed/disarmed” principle.....	154
5.4	Use of benzoates in carbohydrate chemistry .....	154
5.4.1	Selective installation of benzoyl groups .....	155

<b>5.5</b>	<b>An introduction to HOBt and BBTZ .....</b>	<b>157</b>
5.5.1	Safety considerations .....	160
<b>5.6</b>	<b>Oxime based reagents .....</b>	<b>161</b>
5.6.1	Other Oxime based reagents .....	162
5.6.2	Safety .....	163
<b>5.7</b>	<b>Aim and Overview .....</b>	<b>164</b>
<b>5.8</b>	<b>Results and discussion .....</b>	<b>164</b>
5.8.1	Design of oxime-based reagents .....	164
5.8.2	Preparation of benzoylated oxime-based reagents .....	165
5.8.3	$pK_a$ values of the oximes .....	169
5.8.4	Initial screening of the reagents with a primary alcohol .....	170
5.8.5	Selective benzoylation of carbohydrate alcohols .....	173
<b>5.9</b>	<b>Summary and Conclusions .....</b>	<b>177</b>
<b>5.10</b>	<b>Experimental .....</b>	<b>178</b>
	<b>References.....</b>	<b>189</b>

## ABBREVIATIONS

<b>Ac</b>	acetyl
<b>Aq.</b>	aqueous
<b><math>\alpha</math>-GalCer</b>	$\alpha$ -galactosyl ceramide
<b><math>\alpha</math>-GlcCer</b>	$\alpha$ -glucosyl ceramide
<b>APC</b>	antigen presenting cell
<b>APM</b>	antigen presenting molecule
<b>Ar</b>	aromatic
<b><math>\beta</math>2m</b>	$\beta$ -2 microglobulin
<b>BAIB</b>	bis(acetoxy)iodobenzene
<b>BBTZ</b>	benzoyloxy benzotriazole
<b>BDA</b>	butane diacetal
<b>BSA</b>	bovine serum albumin
<b>Bu</b>	butyl
<b>Bn</b>	benzyl
<b>Bz</b>	benzoyl
<b>CAN</b>	cerium ammonium nitrate
<b>Cat.</b>	catalytic
<b>CDR</b>	complementarity determining region
<b>CID</b>	collision induced dissociation
<b>CIP</b>	contact ion-pair
<b>COMU</b>	1-[(1-cyano-2-ethoxy-2-oxoethyl)diaminoxy]diaminomorpholinomethylene)]methanaminium hexafluorophosphate
<b>CD</b>	cluster of differentiation

<b>CFSE</b>	carboxyfluorescein diacetate succinimidyl ester
<b>CM</b>	cross metathesis
<b>D</b>	day (s)
<b>DAG</b>	diacylglyceride
<b>DCC</b>	<i>N,N'</i> -dicyclohexylcarbodiimide
<b>DIPEA</b>	<i>N,N</i> -diisopropylethylamine
<b>DMAP</b>	<i>N,N</i> -dimethyl-4-aminopyridine
<b>DMF</b>	<i>N,N</i> -dimethylformamide
<b>DMSO</b>	dimethyl sulfoxide
<b>EDC</b>	1-Ethyl-3-(3-dimethylaminopropyl) carbodiimide
<b>ESI</b>	electrospray ionization
<b>Et</b>	ethyl
<b>Eq.</b>	molar equivalents
<b>FAB</b>	fast-atom bombardment
<b>FT</b>	Fourier transform
<b>GC</b>	gas chromatography
<b>GMM</b>	glucose monomycolate
<b>GSL</b>	glycosphingolipid
<b>H</b>	hour (s)
<b>HBTU</b>	<i>O</i> -benzotriazole- <i>N,N,N',N'</i> -triamethyl-uronium-hexafluoro-phosphate
<b>HG-II</b>	Hoveyda Grubbs second generation catalyst
<b>HKR</b>	hydrolytic kinetic resolution
<b>HOBt</b>	<i>N</i> -hydroxybenzotriazole
<b>HONM</b>	isonitroso Meldrum's acid

<b>HPLC</b>	high performance liquid chromatography
<b>HRMS</b>	high resolution mass spectrometry
<b>IFN</b>	interferon
<b>iGb3</b>	isoglobotrihexosylceramide
<b>IL</b>	interleukin
<b>iNKT cell</b>	invariant natural killer T cell
<b>LAM</b>	lipoarabinomannan
<b>LDA</b>	lithium diisopropylamide
<b>LIT</b>	linear ion trap
<b>LM</b>	lipomannan
<b>mCPBA</b>	<i>meta</i> -chloroperoxybenzoic acid
<b>Mincle</b>	macrophage-inducible C-type lectin receptor
<b>MCL</b>	macrophage C-type lectin receptor
<b>Me</b>	methyl
<b>MeOAc</b>	methoxyacetyl
<b>MeOH</b>	methanol
<b>MHC</b>	major histocompatibility complex
<b>Min</b>	minute(s)
<b>MS</b>	mass spectrometry
<b><i>M.tb</i></b>	<i>Mycobacterium tuberculosis</i>
<b>NIS</b>	<i>N</i> -iodosuccinimide
<b>NKT</b>	natural killer T
<b>NMR</b>	nuclear magnetic resonance
<b>o/n</b>	overnight

<b>PAMP</b>	pathogen-associated molecular pattern
<b>PBB</b>	<i>p</i> -bromobenzyl
<b>PG</b>	phosphatidylglycerol
<b>Ph</b>	phenyl
<b>PIM</b>	phosphatidylinositol mannoside
<b>PMB</b>	<i>p</i> -methoxybenzyl
<b>PRR</b>	pattern recognition receptor
<b>pyr.</b>	pyridine
<b>quant.</b>	quantitative
<b>Rt</b>	room temperature
<b>SAM</b>	s-adenosyl methionine
<b>sat.</b>	saturated
<b>TB</b>	tuberculosis
<b>TBAB</b>	tetrabutylammonium bromide
<b>TBSA</b>	tuberculostearic acid
<b>TCR</b>	T cell receptor
<b>TFA</b>	trifluoroacetic acid
<b>T<sub>H</sub></b>	T helper
<b>THF</b>	tetrahydrofuran
<b>THP</b>	tetrahydropyranyl
<b>TMS</b>	trimethylsilyl
<b>Tol</b>	tolyl
<b>Tps</b>	<i>tert</i> -butyldiphenyl silyl







## **PART I**

**Synthesis of immunogenic mycobacterial cell wall**

**lipids**



## Chapter 1: Introduction

### 1.1 Introduction to tuberculosis

Tuberculosis (TB), caused by *Mycobacterium tuberculosis* (*M.tb*), remains a major cause of death. TB was declared a “global health emergency” by the World Health Organization (WHO) in 1993.<sup>1</sup> According to the WHO Global Tuberculosis Report 2017, nearly 10.4 million people were diagnosed with TB, with 11% (1.1 million) of cases involving people who are HIV positive. Although the mortality rate has decreased 45% since 1990, the rise of TB/HIV co-infection and multidrug resistant TB (MDR-TB) remains a cause for concern.<sup>2</sup> There were an estimated 1.4 million TB deaths in 2015, and an additional 0.4 million deaths resulting from TB disease among people living with HIV infection. Although the number of TB deaths decreased by 22% between 2000 and 2015, TB remained one of the top 10 causes of death worldwide in 2015.<sup>3</sup> With the rise in cases of MDR-TB and extensively drug-resistant TB (XDR-TB), there is a need to develop new effective diagnostic tools for rapid and early detection of drug-resistant TB, effective new drugs with a shorter treatment regimen, and enhanced vaccination methods to prevent infection.

*M. tuberculosis* is spread by inhalation of ‘droplet nuclei’ exhaled by infected persons. TB is manifested in four stages: latency, primary disease, primary progressive disease, and extra-pulmonary disease, with each stage being correlated with the effectiveness of the individual’s immune system.<sup>4</sup> The majority of TB infections remain asymptomatic with only 10% of cases proceeding towards active TB, most commonly assuming as pulmonary TB with symptoms including chest pain, prolonged and labored coughing, and blood in the sputum.<sup>4</sup> The infection process begins when the tubercle

bacilli penetrate the alveoli of the host where they are phagocytized by macrophages.<sup>4</sup> If the bacteria survives this first line of defense, they start actively replicating, diffuse to nearby cells including epithelial and endothelial cells, and in a few weeks of exponential growth cause high bacterial burden. Thereafter, once the adaptive immune system responds to the infection, lymphocytes and other immune cells form a cellular infiltrate that later assumes the typical structure of a granuloma, restricting the spread of the infection and segregating the bacteria from the immune system. At this stage, *M.tb* can adopt a dormant state and remain viable for years without observable symptoms. Weakening of the immune system (e.g. through age or infection by HIV) triggers the bacteria to activate and cause infection.

The initial empiric treatment for TB is the administration of a four drug regimen of rifampicin, isoniazid, ethambutol and pyrazinamide for a period of 6-9 months.<sup>5</sup> This regimen has changed little since the 1960s and suffers from complexity, toxicity and bacterial drug resistance. Two new drugs, bedaquiline (a quinolone based drug) and delamanid (a nitroimidazole based drug), are now available; however, they have been only rarely prescribed thus far owing to concerns over toxicity and integrating into established methods for treatment (Figure 1.1).<sup>5</sup>

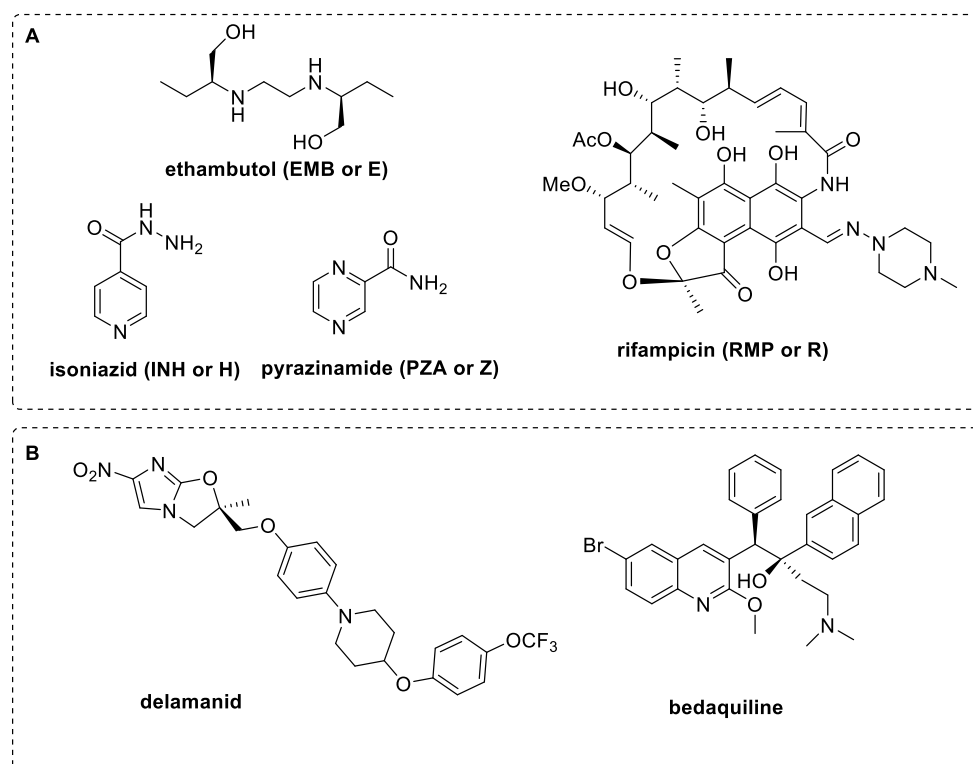


**Figure 1.1** A) First-line anti-tuberculosis drugs; B) Recently approved anti-tuberculosis drugs.

Vaccination is widely used for the prevention of TB. *M. bovis* BCG, an attenuated strain developed at the Institute Pasteur and first used in 1921, is now widely used worldwide. It is a live vaccine strain derived from repeated culture of a virulent *M. bovis* strain on a glycerin-bile-potato mixture by successive sub culturing every three weeks. After 230 sub cultures the bacterial strain was so weakened that it could confer immunity without causing disease in humans. It is listed on the WHO list of essential medicines, yet studies have shown it reduces infection rates by only 19-27%, and has limited effectiveness against pulmonary TB.<sup>6</sup> There remains substantial scope for improved vaccines, and the development of recall antigens<sup>1</sup> that can bolster the immune response

<sup>1</sup> Recall antigens are molecules to which an individual has previously been sensitized and which is subsequently administered as a challenging dose to elicit a hypersensitivity reaction.

to restore the protective and therapeutic potential of BCG. Other adjunct immunotherapy approaches that can enhance host immune responses include mycobacterial-specific antibodies, mycobacterial antigens, or whole cell inactivated environmental mycobacterial preparations to enhance the immune responses elicited by T-helper cells.<sup>7</sup>

Genome sequencing of the *M.tb* H37Rv<sup>8-9</sup> strain and that of other clinical isolates and important vaccine strains (*M. bovis*, *M. avium*, *M. leprae*, *M. marinum*, *M. ulcerans*)<sup>8, 10-13</sup> have facilitated the study of pathogenic mycobacteria. *Mycobacterium smegmatis*, an important model bacterium and related Corynebacteria (e.g. *Corynebacterium glutamicum*) have now been sequenced allowing integration of results from the study of these biochemical model organisms with those of *M.tb*.<sup>14-15</sup>

## **1.2 Mycobacteria possess a unique cell wall important for its virulence.**

Mycobacteria are characterized by their uniquely complex lipid rich cell wall. The mycobacterial cell wall consists of the outer and inner layers, which surround the plasma membrane. The cell wall is rich in lipids that are both covalently and non-covalently associated with the cell wall (Figure 1.2).<sup>16</sup>



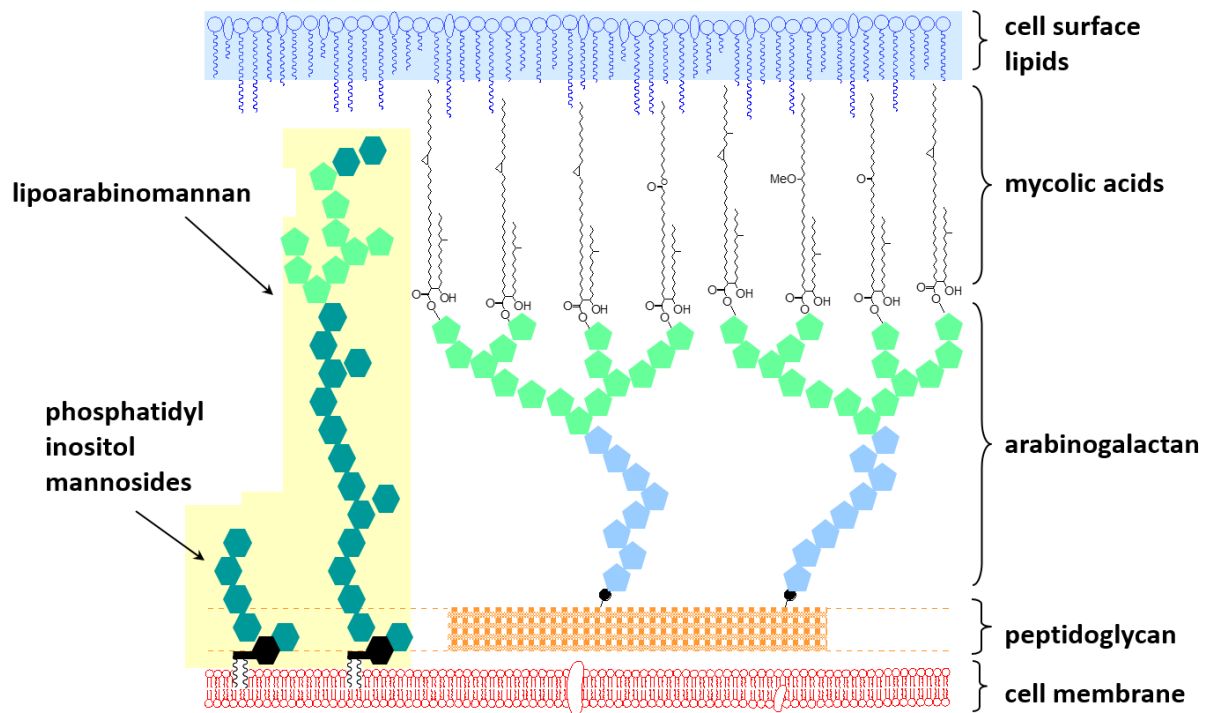


**Figure 1.2** The mycobacterial cell wall.

The *inner layer* consists of peptidoglycan (PG), arabinogalactan (AG), and mycolic acids (MA) covalently-linked to form the macromolecule mycolyl-AG-peptidoglycan, which extends outwards from the plasma membrane.<sup>17</sup> The inner layer is the target for anti-tubercular drugs such as isoniazid (inhibits MA biosynthesis) and ethambutol (inhibits arabinan biosynthesis).<sup>5</sup> The AG layer consists of approximately 30 galactofuranose residues arranged linearly with alternating 1,5- and 1,6-linkages, and bearing branched arabinan units. AG is covalently attached to the PG by a phosphoryl-*N*-acetylglucosaminyl-rhamnosyl linkage. The AG layer is important for the integrity of cell wall and for anchoring mycolic acids to the PG. Mycolic acids (MA) are  $\alpha$ -alkyl- $\beta$ -hydroxyl long-chain fatty acids and are critical determinants of cell wall permeability. Most antibacterial agents cannot pass through the mycolic acid layer and are ineffective against mycobacteria. Lipophilic drugs, such as fluoroquinolones or rifampicin, pass more easily through the lipid-rich cell wall and thus are active against mycobacteria.<sup>17</sup>

Lipidic molecules associated with the *outer cell wall* include: lipids, glycolipids, glycophospholipids, glycopeptides, sulfolipids, and sulfoglycolipids. Among the most abundant of these are a family of glycophospholipids that contain mannose and share a phosphatidyl-*myo*-inositol core, termed phosphatidylinositol mannosides (PIMs), lipomannan (LM), and lipoarabinomannan (LAM).<sup>16</sup> Biochemical and genetic studies show a biosynthetic relationship of PI → PIMs → LM → LAM.<sup>18</sup>

### 1.3 The mycobacterial cell-wall is rich in lipids and glycolipids

Goldman *et al.* studied the chemical composition of the cell wall of *M. tuberculosis* H37Ra and reported that the cell wall is composed of 22% amino acids: mainly alanine, glutamate and diaminopimelate (a carboxy derivative of lysine, and one of the key linking units of peptidoglycan); 25% reducing sugars: mainly D-arabinose and D-galactose; 4% aminosugars: D-glucosamine, D-muramic acid and D-galactosamine; and 32% lipids.<sup>19</sup> 55% of the lipids were two series of mycolic acids, one containing cyclopropane rings and the other with an unsaturation; 22% of the lipids were saturated fatty acids. The most abundant saturated fatty acids were palmitic acid (C<sub>16:0</sub>), 10-methylstearic acid (C<sub>19:0</sub>; tuberculostearic acid, TBSA), and cerotic acid (C<sub>26:0</sub>) in a ratio of 2.7:1.1:0.67.<sup>19</sup> The keen interest in combatting TB led to it being just the second bacterium to have its genome sequenced (after *Mycoplasma genitalium*). Of the approximate 4000 genes in *M. tb* H37Rv, 250 genes are devoted to fatty acid metabolism.<sup>20</sup> The high proportion of lipids in the mycobacterial cell wall enhances resistance to antibiotics, resistance to killing by acid, alkaline, and reactive oxygen/nitrogen species, and resistance to osmotic lysis via complement deposition on the bacterial surface. Furthermore it is increasingly apparent that mycobacterial glycolipids possess the ability to modulate the host immune response.<sup>17</sup>

Belisle *et al.* have attempted to catalogue these diverse lipids into a database named *M.tb* Lipid DB spanning 47 lipid subclasses (14,489 mass entries) according to LIPID MAPS nomenclature.<sup>21</sup> However, this database represents an incomplete view of the mycobacterial lipid repertoire as the mass spectrometry based lipidomic systems detect many hundreds of species whose mass values do not appear in the database.<sup>22</sup> Later Moody *et al.* developed two databases: mycomass and mycomap summarizing 58 lipid types. Many unnamed molecules were identified from fragmentation, detection of unexpected adducts, or not yet discovered mycobacterial lipids.<sup>22</sup>

Category	Main Class	Subclass	Level 4 / "Family" (abbreviated name)	Alkylforms Molecules	
Fatty acyls	Fatty acids and Conjugates	straight chain fatty acids	-	11	
		branched fatty acids	-	8	
			mycocerosic acids	6	
			mycosanoic acids	9	
			phthioceranic acids	9	
			-	18	
		unsaturated fatty acids	mycolipodienic acid	1	
			phthienoic acids	5	
		hydroxy fatty acids	hydroxyphthioceranic acid (HPA)	18	
			mycolipanic acid	1	
Fatty esters	lactones	mycolic acids	150		
		mycolactones	7		
Fatty acyl glycosides	fatty acyl glycosides of mono- and disaccharides	glucose monomycolates (GMM)	150		
Glycerolipids	Monoradylglycerols	monoacylglycerols	monoacylglycerols (MAG) glycerol monomycolates (GroMM)	44 150	
	Diradylglycerols	diacylglycerols	diacylglycerols (DAG)	129	
	Triradylglycerols	triacylglycerols	triacylglycerols (TAG)	255	
	Glycosyldiradylglycerols	glycosyldiacylglycerols	glucuronosyl diacylglycerols	81	
			diglycosylated diacylglycerols	6	
Glycero-phospholipids	Glycerophosphoglycerols	diacylglycerophosphoglycerols	phosphatidylglycerols (PG)	129	
			lysinylated diacylglycerophosphoglycerols	1	
			lysophosphatidylglycerols	44	
	Glycerophosphoinositols	diacylglycerophosphoinositols	phosphatidylinositols (PI)	129	
			lysophosphatidylinositols (LPI)	44	
	Glycerophosphates	monoacylglycerophosphates	phosphatidic acids (PA)	141	
			lysophosphatidic acids (LPA)	47	
	Glycerophosphoglycerophosphoglycerols	diacylglycerophosphoglycerophosphodiradylglycerols	cardiolipins (CL)	425	
	Glycero-phosphoinositolglycans	monoacylglycerophosphoinositolglycans	lysophosphatidylinositol mannosides (Lyso-PIMx)	12	
			phosphatidylinositol mannosides (PIMx)	12	
			monoacylated diacylglycerophosphoinositolglycans	monoacyl phosphatidylinositol mannosides (PIMxAc <sub>1</sub> )	12
			diacylated diacylglycerophosphoinositolglycans	diacyl phosphatidylinositol mannosides (PIMxAc <sub>2</sub> )	18
			phosphatidyl-ethanolamines (PE)	148	
	Glycero-phosphoethanolamines	monoacylglycerophosphoethanolamines	lysophosphatidyl-ethanolamines (LPE)	44	
			phosphatidyl-ethanolamines (PE)	44	
	Prenol lipids	Isoprenoids	C20 isoprenoids	decaprenyl phosphoribose (DPPR)	1
			C40 isoprenoids	β-carotene	1
Quinones and hydroquinones			ubiquinones	menaquinone (MK)	35
Saccharolipids	Polyprenols	bactoprenols	undecaprenol	1	
		monoacylamino sugars	glycopeptidolipids (GPL)	720	
	Acyltrehaloses	monoacyltrehaloses	trehalose monomycolates (TMM)	150	
			diacyltrehaloses	diacyl trehaloses (DAT)	131
			trehalose dimycolate (TDM)	52	
			triacyltrehaloses	triacyl trehaloses (TAT)	255
			polyacyltrehaloses	polyacyl trehalose (PAT)	19
acylsulfotrehaloses	sulfoglycolipids (Ac,SGL)	859			
Polyketides	Linear polyketides		lipooligosaccharides	6	
			mannosylphosphomycoketides	26	
	Aromatic polyketides	monocyclic aromatic polyketides	phthiocerol dimycocerosates (PDIM)	179	
			monoglycosyl phenylphthiocerol dimycocerosate	157	
			diglycosylated phthiocerol dimycocerosates	6	
			triglycosyl phenylphthiocerol dimycocerosates (PGL)	142	
			parahydroxybenzoic acid derivatives (HBAD)	2	
			leprosol	1	
			Non-ribosomal peptide/polyketide hybrids	mycobactins	126
	carboxymycobactins	252			
exocheilins	2				
Others		lipopentapeptides (L5P)	6		
		mycothiol (MSH)	1		

**Figure 1.3** List of the lipids in the MycoMass database. This database follows the Lipid Maps organizational tree and uses lipid families' names found in the mycobacterial literature in level 4. Phosphatidylinositol mannosides (PIMx) contain 1 to 6 mannosyl residues (x) and sulfoglycolipids (AcxSGL) contain 2 to 4 fatty acyl chains (x). Alkyl forms vary by the saturation and by the length of carbon backbone.<sup>22</sup>

## **1.4 Immune sensing of microbial lipids and lipid-like molecules by T cells**

### **1.4.1 Lipid antigen recognition by the immune system**

The immune system encompasses a powerful collection of defense mechanisms, fundamental to our survival. The innate immune system receptors called the pattern recognition receptors (PRR) recognize specific molecular structures, which include the self-associated molecular patterns (SAMPs), damage-associated molecular patterns (DAMP), microbe-associated molecular patterns (MAMPs), and pathogen-associated molecular patterns (PAMPs). Based on their localization, PRRs may be classified as: *Transmembrane PRRs*, which include the Toll like receptors (TLRs) and C-type lectin receptors (CLRs) and *Cytoplasmic PRRs*, which include NOD-like receptors (NLRs) and RIG-I-like receptors (RLRs). CLRs and TLRs play a crucial role in sensing glycolipids.<sup>23</sup> The most significant CLRs responsible for glycolipid sensing include the macrophage inducible C-type lectin (Mincle) and macrophage C-type lectin (MCL).<sup>23</sup> Engagement of an appropriate glycolipid with these PRRs produces cytokines that modulate recruitment of immune cells and orient T cell responses (Figure 1.4).

Cell-mediated immunity is initiated by the recognition of antigens presented on antigen presenting molecules (APM) by the T-cell receptors (TCRs) on T cells. Three main groups of APMs have been discovered. Major histocompatibility complexes (MHC I and II), which are polymorphic APMs, present peptide antigens to MHC restricted T-cells. Cluster of differentiation (CD1) glycoproteins, a non-polymorphic group of APMs, present lipidic antigens such as lipids, peptidolipids and glycolipids to CD1 restricted T cells. The MHC class-I related molecule (MR1), a monomorphic APM, presents vitamin B metabolites to innate-like mucosal associated invariant T (MAIT) cells.

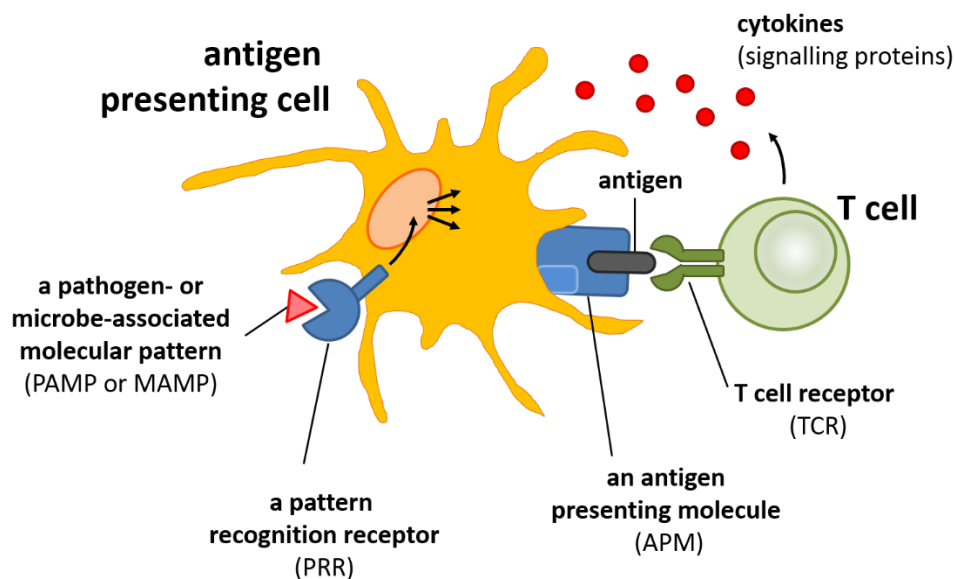


**Figure 1.4** Simplified schematic representation of glycolipid sensing by antigen-presenting cells. Binding of pathogen- or microbe-associated molecular patterns to pattern recognition receptors, leads to signaling and cellular activation. Binding of the T cell receptor protein to the presented antigen triggers cytokine release and differentiation of T cell lineages.<sup>24</sup>

#### 1.4.2 Lipid antigen presentation by CD1 molecules

CD1 is a group of antigen-presenting molecules that has evolved to present lipid and glycolipid antigens. The human genome encodes five CD1 genes CD1a, CD1b, CD1c, CD1d, and CD1e, which, depending on their amino acid sequence homology, can be further classified into three groups: group 1 (CD1a, CD1b, and CD1c), group 2 (CD1d) and group 3 (CD1e).<sup>25</sup> While CD1a-d mediate lipid presentation to T cells, CD1e does not have this capacity but rather functions as a lipid transfer protein that assists loading of CD1 proteins.<sup>26</sup> Structurally, CD1 consists of a heavy chain with three extracellular domains, non-covalently linked to a  $\beta$ 2-microglobulin ( $\beta$ 2m). The antigen binding grooves of the CD1 molecules are defined by two  $\alpha$  helices ( $\alpha$ 1 and  $\alpha$ 2) placed above the  $\beta$  sheet.<sup>27</sup> The archetypal presentation mode involves CD1 proteins binding to the hydrophobic region of the lipid molecules, with the hydrophilic head group protruding out of the binding groove and recognition by the TCRs. This trimolecular interaction

between the TCR, CD1 and the glycolipid activates CD1 restricted T-cells to release a cascade of signaling molecules, called cytokines (interferons (IFN) and interleukins (IL)) (Figure 1.5).<sup>28</sup>

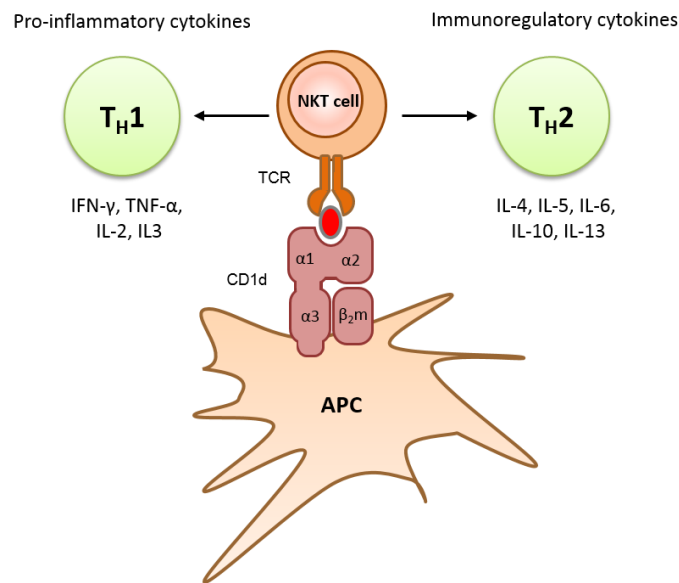


**Figure 1.5** Representation of CD1d presentation of a glycolipid antigen to the TCR of murine NKT cells, resulting in T cell activation and T<sub>H</sub>1 and T<sub>H</sub>2 cytokine production.

### 1.4.3 CD1-restricted T cells

#### 1.4.3.1 Structure of T-cell receptors (TCRs) on the surface of T cells

T-cells are a subset of white blood cells, characterized by the presence of T cell receptors (TCRs) on their cell surface. They originate from hematopoietic stem cells in the bone marrow and migrate to the thymus where they develop under positive and negative selection process and mature into double positive (CD4<sup>+</sup> CD8<sup>+</sup>) and finally into single positive (CD4<sup>+</sup> CD8<sup>-</sup> or CD4<sup>-</sup> CD8<sup>+</sup>) T cells.<sup>29</sup> Each TCR is a heterodimer, composed of two different protein chains: one  $\alpha$  and one  $\beta$  chain or one  $\gamma$  and  $\delta$  chain. The  $\alpha$  chain is encoded by TRAV genes,  $\beta$  chain by TRBV genes,  $\gamma$  and  $\delta$  chains are encoded by TRGV and TRDV genes respectively. 95% of human T cell TCRs consists of  $\alpha$  and  $\beta$  chains, the remaining 5% consists of  $\gamma$  and  $\delta$  chains.<sup>30</sup> The  $\alpha$  and  $\beta$  chains

contain two extracellular domains, the variable (V) and constant (C) domains (Figure 1.6). During their development in the thymus, the V domains of  $\alpha$  chains are encoded by V (TRAV) and joining (J; TRAJ) gene segments; the V domain of TCR  $\beta$  chain is encoded by V (TRBV), diversity (D; TRBD) and joining (J; TRBJ) gene segments. There are three complementarity determining regions (CDRs) in each TCR chain, which collectively form the antigen binding site for the TCR. While the CDR1 and CDR2 loops are encoded in the V gene segments, CDR3 loop is encoded at the junction of the rearranged V and J gene segment (for TCR  $\alpha$ ) and V, D, J gene segments (for TCR  $\beta$ ) thus endowing the CDR3 loop with the greatest diversity (Figure 1.6).<sup>29</sup>

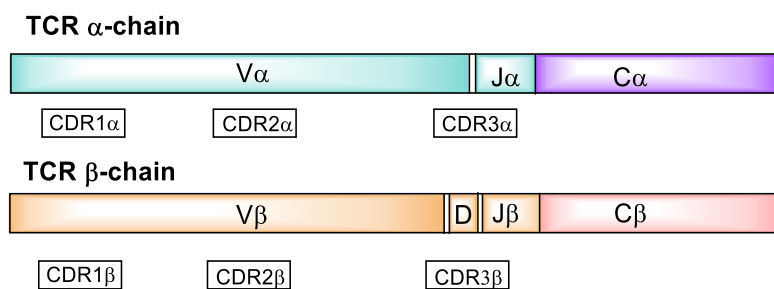


**Figure 1.6** The  $\alpha\beta$  TCR is a heterodimer composed of two chains. The V domains contain the complementarity-determining region (CDR) loops (C, constant; D, diversity; J, joining).

#### 1.4.3.2 Classification of T-cells based on conservation of the TCR chains

T cells stimulated by lipid antigens can be divided into two categories according to their functional behavior and mode of antigen recognition (Figure 1.7). T cells that recognize group 1 CD1 molecules (CD1a, CD1b and CD1c) typically (but not exclusively) have a diverse TCR composition. However, information about their biology and TCR diversity is limited because no specific surface markers are known, and efficient methods to capture clones for TCR sequencing have not been developed because little is known about their antigen-recognition properties. Moody *et al.* identified CD1b restricted T cell lines called the germline encoded mycolyl reactive (GEM) and LDN5-like T cells



that possess strictly conserved TCR  $\alpha$ -chains with conserved or biased TCR  $\beta$ -chains and are considered innate-like (Figure 1.7).<sup>31</sup> The group 2 CD1 restricted T-cells are called natural killer (NK) T cells, and are characterized by the presence of the NK1.1 marker on their cell surface. NKT cells are the most widely studied lipid-reactive T cells owing to their ability to recognize glycosyl ceramide-based antigens presented on CD1d.

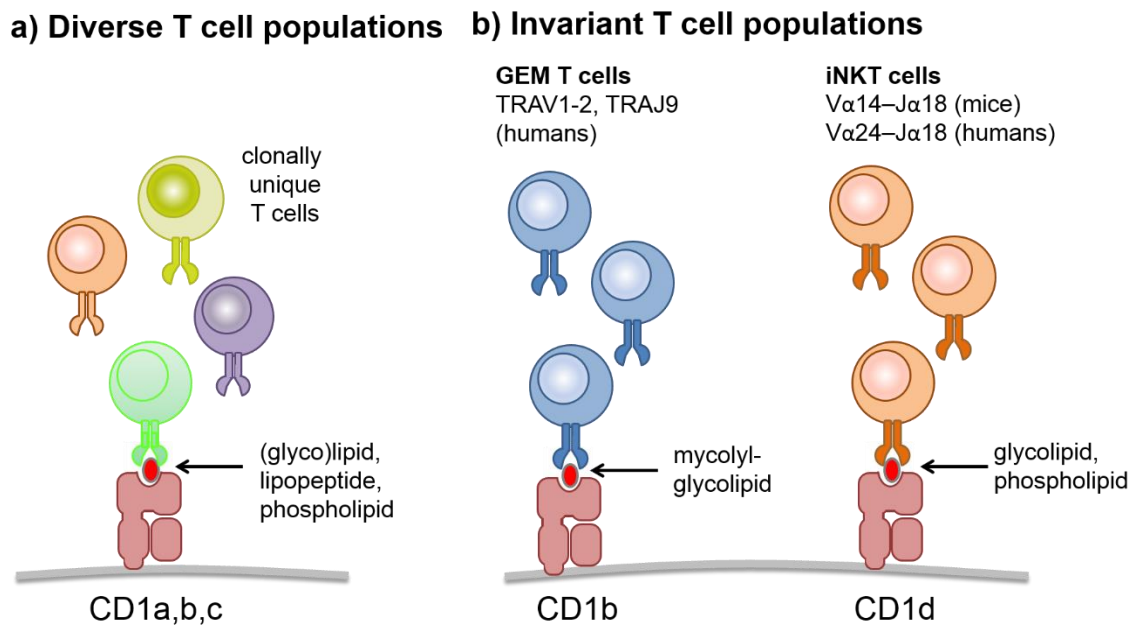


**Figure 1.7** Overview of CD1 ligand presentation and recognition by T cells and NKT cells. a) Diverse T cells populations of clonally unique T cells receptors recognize ligands bound to group 1 CD1 molecules. b) Populations of CD1b restricted T cells (GEM and LDN5-like T cells) are characterized by conserved or biased TCR  $\alpha$  and  $\beta$  chains and can recognize ligands presented by CD1b molecules; and NKT cells with conserved  $\alpha$  and  $\beta$  chains can recognize ligands presented by CD1d molecules.

#### 1.4.4 CD1d-restricted T cells (NKT cells)

The term NKT cells was first coined in 1995 and broadly defines a subset of T cells that share common characteristics of NK cells, especially expression of NK1.1 marker.<sup>32</sup> NKT cells are a distinct lineage of T cells characterized by CD1d reactivity, memory T-cell markers, and a potent cytokine producing capacity.<sup>32</sup> Based on the conservation of the TCR chains they can be broadly classified as type I and type II NKT cells.<sup>32-33</sup>

#### 1.4.4.1 Type I NKT cells (iNKT cells)

Type I NKT cells are defined by the expression of TCRs with limited diversity. Murine type I NKTs express an invariant V $\alpha$ 14-J $\alpha$ 18 TCR  $\alpha$  chain (TRAV11-TRAJ18) paired with a limited set of TCR  $\beta$  chains biased towards V $\beta$ 8 (TRBV13), V $\beta$ 7 (TRBV29) and V $\beta$ 2 (TRBV1). Human type I NKTs express V $\alpha$ 24-J $\alpha$ 18 TCR  $\alpha$  chain paired predominantly with V $\beta$ 11. Type I NKTs can also be defined by their exceptional reactivity to CD1d-presented  $\alpha$ -GalCer.<sup>32, 34</sup>

#### 1.4.4.2 Type I NKT- $\alpha$ -GalCer-CD1d

Much of our understanding about CD1d must be attributed to the discovery of the glycolipid  $\alpha$ -GalCer. In 1994, scientists at Kirin Brewing Company isolated several glycosphingolipids called agelasphins from the marine sponge *Agelas mauritanus* that were shown to have strong anti-tumor properties in mice.<sup>35-36</sup> Agelasphin-9b (AGL-9B), comprising an  $\alpha$ -galactosyl head group linked to a ceramide, exhibited potent anti-tumor properties against murine tumor cells *in vivo* (Figure 1.8). To simplify the chemical synthesis and optimize biological activity, structural alterations were made, and from this work a purely synthetic glycolipid, KRN7000 was developed as a more suitable candidate for therapeutic studies (Figure 1.8).<sup>37</sup> In contrast to AGL-9b, KRN7000 (commonly known as  $\alpha$ -GalCer) has a linear phytosphingosine chain and lacks the hydroxyl group at the 2-position of the *N*-acyl group.  $\alpha$ -GalCer was the first agonist identified capable of activating NKT cells in a CD1d-dependent manner.

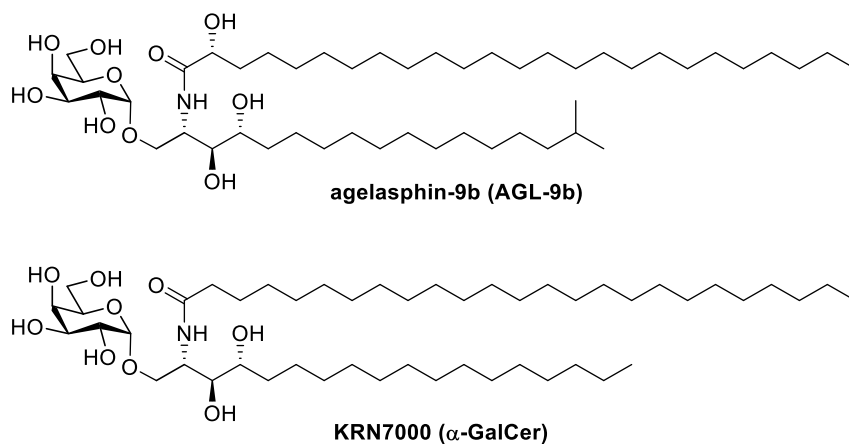


**Figure 1.8** Structures of agelasphin-9b and KRN7000 ( $\alpha$ -GalCer). While both of these structures contain an  $\alpha$ -galactosyl head group and a ceramide aglycon,  $\alpha$ -GalCer lacks the 2-hydroxyl group on the acyl chain and the branching in the phytosphingosine chain.

In 2007, Borg *et al.* published a crystal structure of a CD1d/ $\alpha$ -GalCer/TCR ternary complex that provided a breakthrough in the understanding of CD1d-antigen mediated activation of iNKT cells.<sup>28</sup> The TCR docks parallel to the binding axis of CD1d and the TCR recognition of the CD1d-antigen complex was shown to be mediated by three CDRs present on  $\alpha$  and  $\beta$  chains. Specifically the CDR2 $\beta$  and CDR3 $\alpha$  loops dominate interactions with the glycosyl head group of  $\alpha$ -GalCer (Figure 1.9).

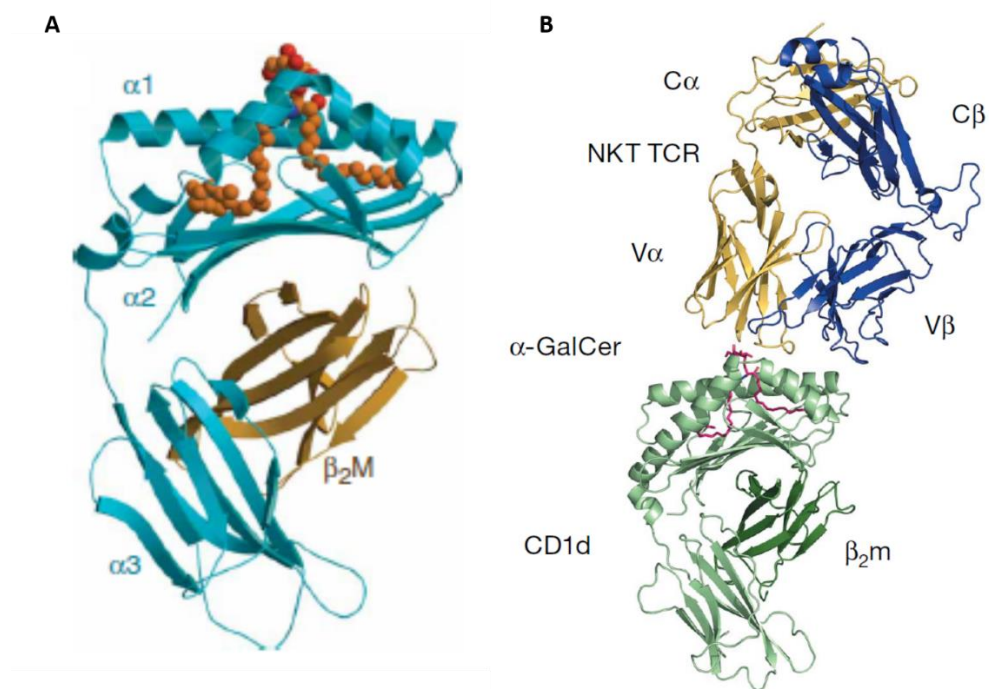


**Figure 1.9** A) Structural overview of human CD1d (blue) bound to  $\alpha$ -GalCer (orange). B) The docking mode of the T cell receptor (TCR) in a type I natural killer T (NKT) cell TCR–lipid–CD1d ternary complex. Figures adapted from Koch *et al.*<sup>38</sup> and Borg *et al.*<sup>28</sup>

#### 1.4.4.3 Type-I NKT ligands

Type I NKT TCRs bind to a diverse array of chemically distinct antigens when presented on CD1d (Figure 1.10). Isoglobotrihexosylceramide (iGb3), a  $\beta$ -glucosylceramide, is an endogenous ligand for type I NKT cells,<sup>39</sup> though the absence of iGb3 in humans questions the significance of this molecule in human health and disease.<sup>40</sup> A range of microbial antigens for type I NKT cells have been identified. These include the glycosyl diacylglycerides from *Borrelia burgdorferi*<sup>41-42</sup> and *Streptococcus pneumoniae*,<sup>43</sup> and glycosphingolipids in the cell wall of *Sphingomonas*, *Ehrlichia* and *Novosphingobium*,<sup>44-45</sup> as well as asperamide B from the fungus *Aspergillus fumigatus*.<sup>46</sup> *Helicobacter pylori*, a gastric pathogen, releases a cholesteryl  $\alpha$ -glucoside that is capable of activating iNKT cells in a CD1d-restricted manner.<sup>47</sup> *Entamoeba histolytica*, a protozoan parasite produces a lyso-phosphatidyl (acyl) inositol (a

lipopeptidophosphoglycan with a phosphatidylinositol anchor) which is capable of producing interferon- $\gamma$  in a CD1d-dependent manner along with TLR signaling.<sup>48</sup> It is noteworthy that these bacteria, fungi and protozoa lack lipopolysaccharide, which is typically an effector for innate immune responses against Gram negative bacteria through TLRs. Thus, the iNKT cell recognition of these microbial lipidic species provide a mechanism for innate-like recognition of LPS negative cell wall.

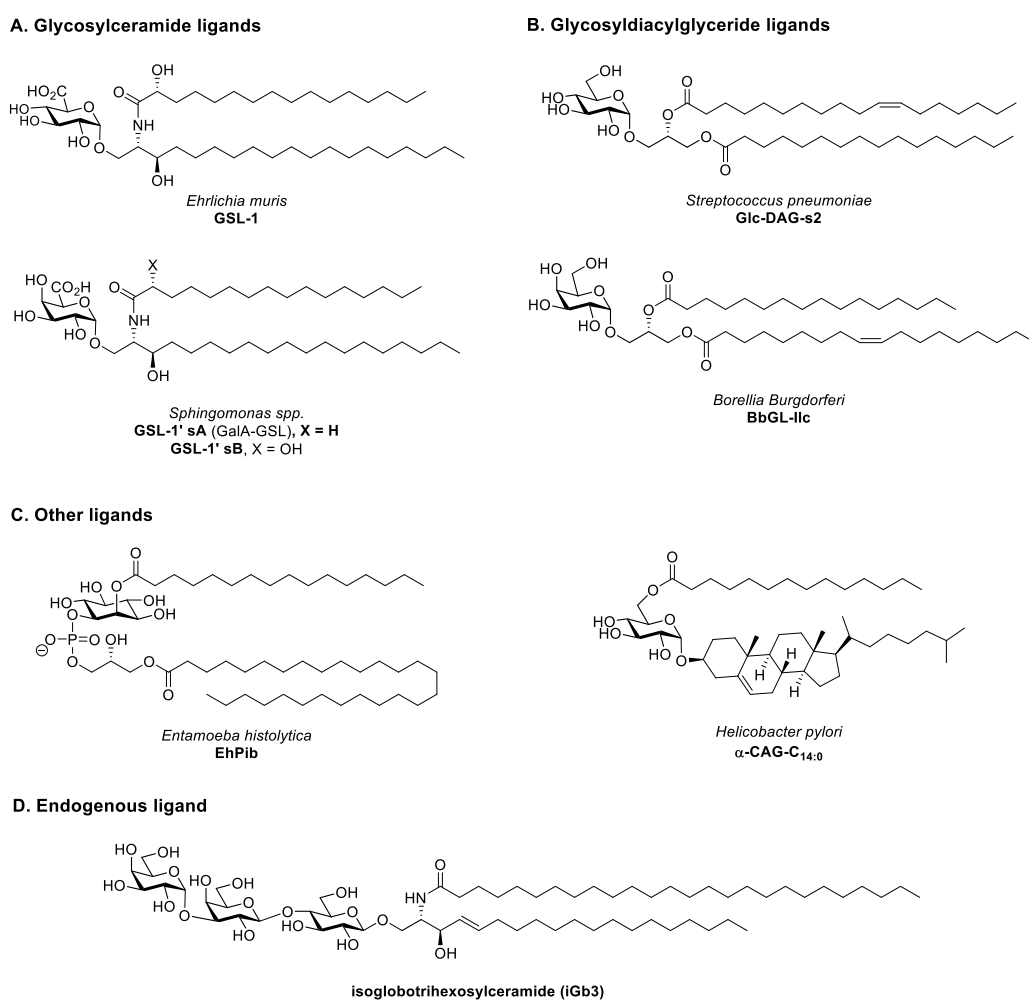


**Figure 1.10** Structures of assorted lipid antigens recognized by type I NKT cells.

### 1.4.5 Type II NKT cells (dNKT cells)

Although type I NKT cells are widely studied, CD1d-restricted lipid reactive type II NKT cells are the predominant NKT cells found in humans.<sup>49</sup> They possess diverse

TCR  $\alpha$  and  $\beta$  chains and typically do not recognize  $\alpha$ -GalCer-CD1d. Emerging evidence supports roles in the regulation of immunity to pathogens/tumors and in autoimmune disorders.

#### 1.4.5.1 Type II NKT ligands

Sulfatide, a sulfated glycolipid found in myelin of the CNS, pancreas, kidney and liver, was the first antigen identified to activate a subset of murine type II NKT cells.<sup>50-51</sup> Subsequently, sulfatide was also found to activate a subset of human type II NKT cells.<sup>52-53</sup>  $\beta$ -GlcCer and  $\beta$ -GalCer have been identified as endogenous ligands capable of activating type II NKT cells.<sup>54-55</sup> Interestingly, no microbial glycosphingolipids have yet to been shown to activate type II NKT cells. It has been shown sulfatide-mediated type II NKT cell stimulation *in vivo* results in the cross-regulation of type I NKT cells and also inhibition of pathogenic Th1/Th17 cells. By contrast, activation of type I NKT cells following  $\alpha$ GalCer administration predominantly activates hepatic dendritic cells.<sup>56</sup>

Phospholipids are a more significant class of type II NKT cell ligands from both self and microbes. Chang *et al.* identified lysophosphatidylcholine (LPC) from mammals as an activator of type II NKT cells (Figure 1.11).<sup>57</sup> It is interesting to note that several LPCs can be recognized by human type II NKT cells, but not by murine type II NKT cells.<sup>57</sup> PI, PG and DPG from mammals can activate type II NKT cells by binding to CD1d (Figure 1.11).<sup>58</sup> Microbe-derived type II NKT cell ligands include phospholipids such as PG from *M.tb* and PG and DPG from *C. glutamicum*.<sup>58</sup> Recently Wolf *et al.* identified PG and DPG from *Listeria monocytogenes* as more potent type II NKT cell antigens than mammalian PG and DPG which could be attributed to the length of the fatty acid chain, fully saturated fatty acids and the anteiso methyl-branching.<sup>59</sup> The ability of

type II NKTs to recognize both mammalian and microbial PG, DPG and PI implicates a role for type II NKTs during infection.<sup>58</sup>

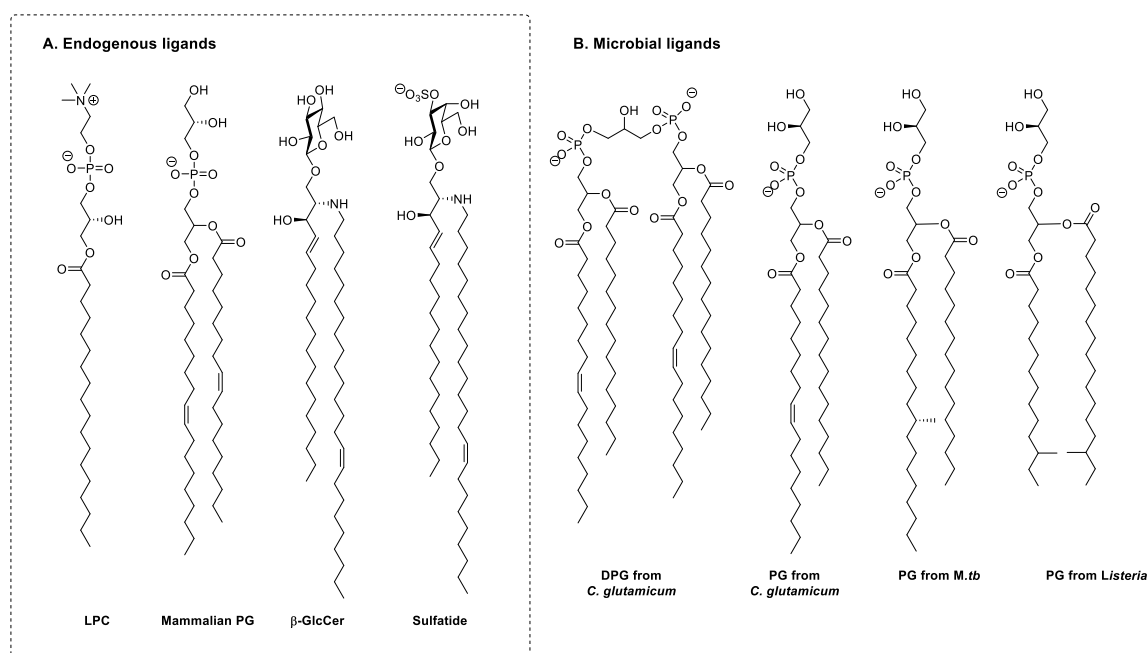


**Figure 1.11** A) Structures of endogenous ligands recognized by type II NKT cells.<sup>2</sup> B) Structures of exogenous ligands recognized by type II NKT cells. C) Structure of synthetic ligand recognized by type II NKT cells.

More atypical ligands for type II NKTs include self *lyso*-phosphatidylethanolamine, which is only generated upon infection by hepatitis B virus, through the deacylation of phosphatidylethanolamine by virus-induced phospholipases.<sup>60</sup> One unique case is the identification of a type II NKT clone that can recognize non-lipidic small molecules such as PPBF (phenyl 2,2,4,6,7-pentamethyldihydrobenzofuran-5-sulfonate) and the 3-methyl analogue, which have been suggested to resemble certain

<sup>2</sup> In order to designate the configuration of glycerol derivatives, the carbon atoms of glycerol are numbered stereospecifically. The carbon atom that appears on top in that Fischer projection that shows a vertical carbon chain with the hydroxyl group at carbon-2 to the left is designated as C-1. To differentiate such numbering from conventional numbering conveying no steric information, the prefix 'sn' (for stereospecifically numbered) is used.

sulfa drugs; the relevance of this observation to human health or disease is unclear (Figure 1.12).<sup>61</sup>

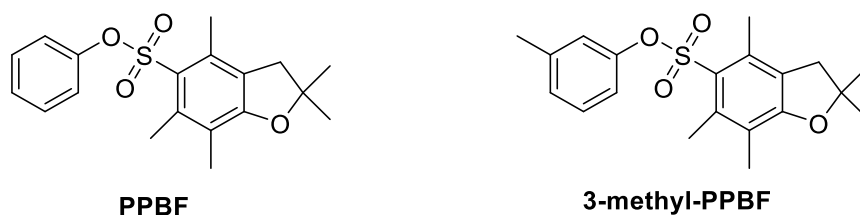


**Figure 1.12** Structure of synthetic ligands recognized by type II NKT cells.

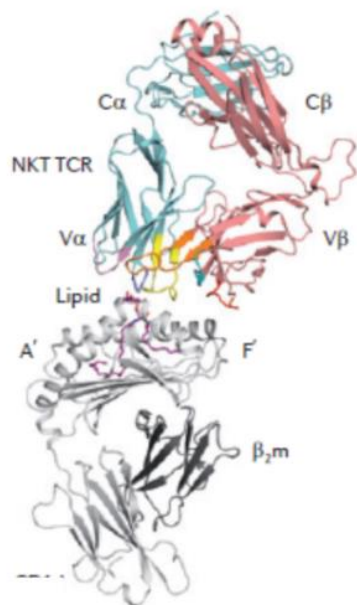
In summary, type II NKT cells seem to recognize diverse antigens presented by CD1d, and given that these cells seem to be more abundant than type I NKT cells in humans, it is important to understand their roles and therapeutic potential.

#### **1.4.5.2 Type II-NKT-TCR-sulfatide-CD1d ternary complex**

Few structures are available for type II NKT TCRs in complex with CD1d-lipid. A complex of CD1d-sulfatide with a type II NKT TCR revealed docking above the A' pocket of CD1d in an anti-parallel fashion resembling the situation with conventional T cells, but distinct from that seen for type I NKT TCRs (Figure 1.13). It is not yet known whether all other type II NKT TCRs will dock to CD1d in a similar fashion. While the type I NKT TCR binds parallel, above the F' pocket, the type II NKT TCR binds diagonally at one end of the CD1d molecule, above the A' pocket similar to the diagonal footprint observed for MHC-reactive TCRs.<sup>50</sup>

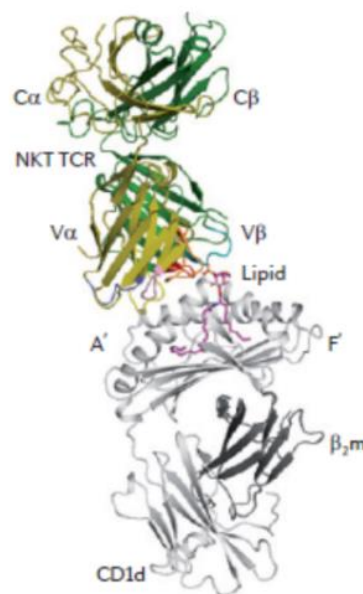


### A. Type I NKT-TCR-lipid-CD1d



C

### B. Type II NKT-TCR-lipid-CD1d



D

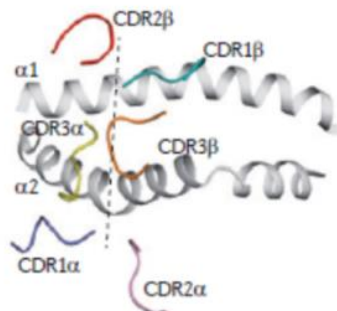
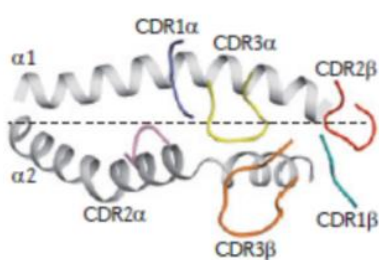


**Figure 1.13** Structural comparison between type I NKT TCR- $\alpha$ -GalCer-CD1d and type II NKT TCR-sulfatide-CD1d complexes. A) The docking mode of the TCR in a type I NKT cell TCR- $\alpha$ -GalCer-CD1d complex and B) shows a type II NKT TCR-lipid-CD1d complex. C) Top view of the antigen-binding groove of CD1d showing the parallel docking mode in the type I complex; D) Top view of the antigen-binding groove of CD1d showing the orthogonal docking mode in the type II complex.

#### 1.4.6 Atypical Type Ia NKT cells

Not all NKT cells fit neatly into the current type I/II NKT cell classification system. One such group are atypical NKT cells (Type Ia) that lack the invariant V $\alpha$ 14-J $\alpha$ 18 TCR  $\alpha$  chain (TRAV11-TRAJ18) and the TRBV25-1  $\beta$ -chain that are inherent to type I NKT cells.<sup>62</sup> Type Ia TCRs from mice show differing specificities to lipid antigens compared to type I NKT cells. The recent characterization of murine V $\alpha$ 10<sup>+</sup>J $\alpha$ 50<sup>+</sup>V $\beta$ 8<sup>+</sup>

NKT cells provides a clear example of NKT cells that fall within this grey zone.<sup>63</sup> These type Ia NKT cells can respond to  $\alpha$ -GalCer-CD1d, but they show greater reactivity to  $\alpha$ -glucosylceramide ( $\alpha$ -GlcCer), compared to type I NKT cells. They preferentially recognize mycobacterial  $\alpha$ -glucuronosyl diacylglycerol (GI-A) (Figure 1.14), and produce super-abundant levels of T<sub>H</sub>2 cytokines: IL-4, IL-5, IL-10, and IL-13 (*vide infra*).<sup>63</sup>

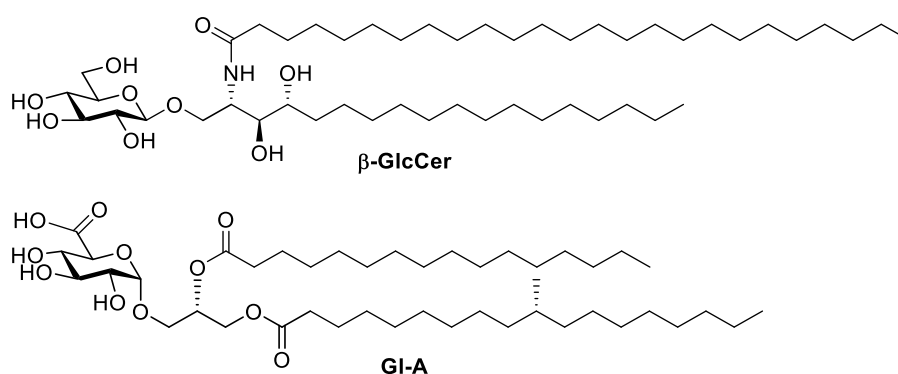


**Figure 1.14** Structures of ligands recognized by atypical type I NKT cells.

### 1.5 Mycobacterial lipids capable of inducing CD1d-restricted T-cell responses.

The first mycobacterial lipid identified to be able to stimulate CD1d-restricted NKT cells was PIM<sub>4</sub>.<sup>64</sup> Fisher *et al.* isolated a material with  $m/z$  1460 Da by fractionation of a lipid extract from *M. bovis*. This was consistent with the structure of PIM<sub>4</sub> bearing two palmitoyl chains. PIM<sub>4</sub> stimulated mouse V $\alpha$ 14-J $\alpha$ 28 (equivalent to V $\alpha$ 14-J $\alpha$ 18) NKT cells, but subsequent studies failed to reproduce this result.<sup>41</sup> Our group has recently showed that  $\alpha$ -D-glucuronic acid diacylglyceride (GI-A) found in *M. smegmatis* is a potent CD1d-presented antigen that activates a subset of type Ia NKT cells to elicit a T<sub>H</sub>2-biased immune response.<sup>63</sup> In 2013, Brenner *et al.* showed that phosphatidylglycerol (PG) and diphosphatidylglycerol (DPG) from *M.tb/C. glutamicum* (*Cg*) could stimulate type II NKT cells in a CD1d-restricted manner (Figure 1.15).<sup>58</sup>

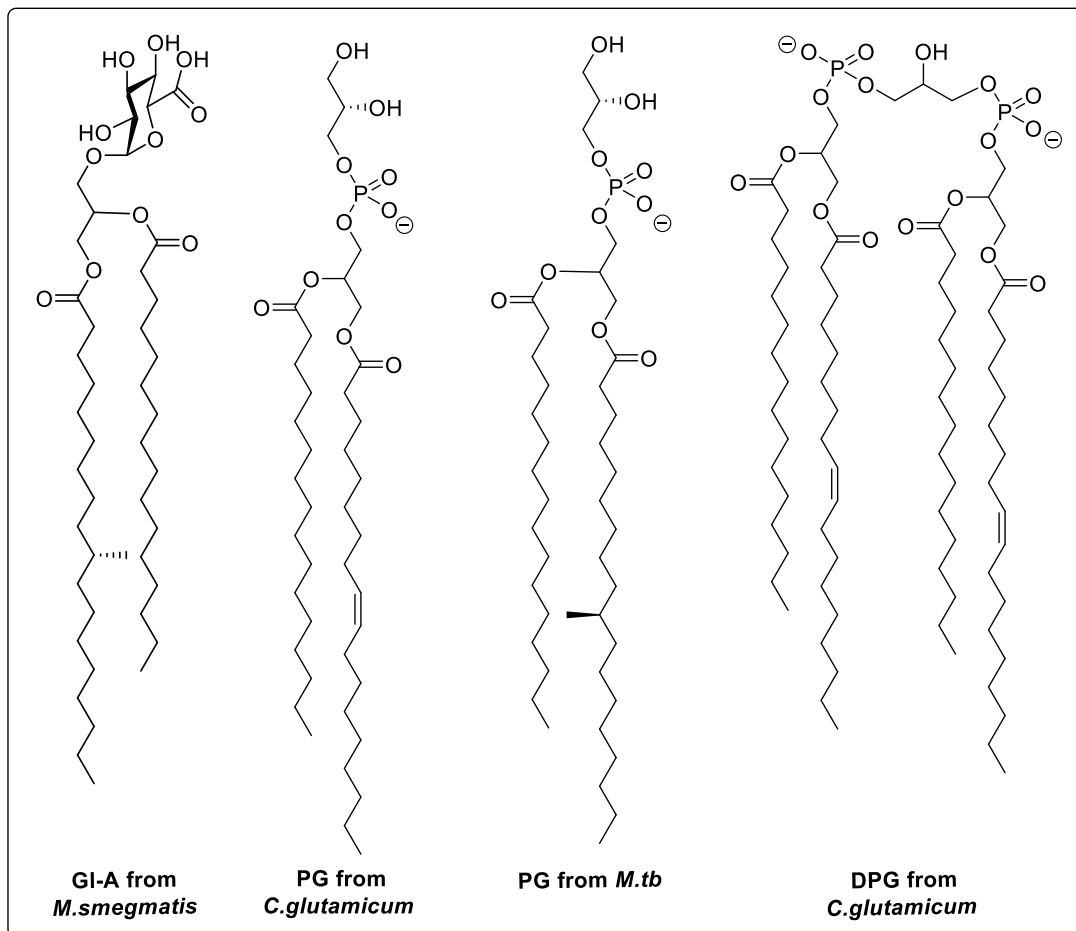


**Figure 1.15** Structures of CD1d presented mycobacterial lipids.

### 1.6 CD1b presents a wide range of mycobacterial lipids

CD1b is characterized by a large hydrophobic pocket ( $2200 \text{ \AA}^3$ ) made of four interconnected chambers, thus accommodating lipid antigens with alkyl chains as long as 80-carbons.<sup>65</sup> CD1b was the first CD1 protein for which an antigen was identified: mycolic acids.<sup>66</sup> Other CD1b-presented mycobacterial antigens are glucose and glycerol monomycolates, PIMs, LAM, diacylated sulfoglycolipids and PIs (Figure 1.16).<sup>67</sup>

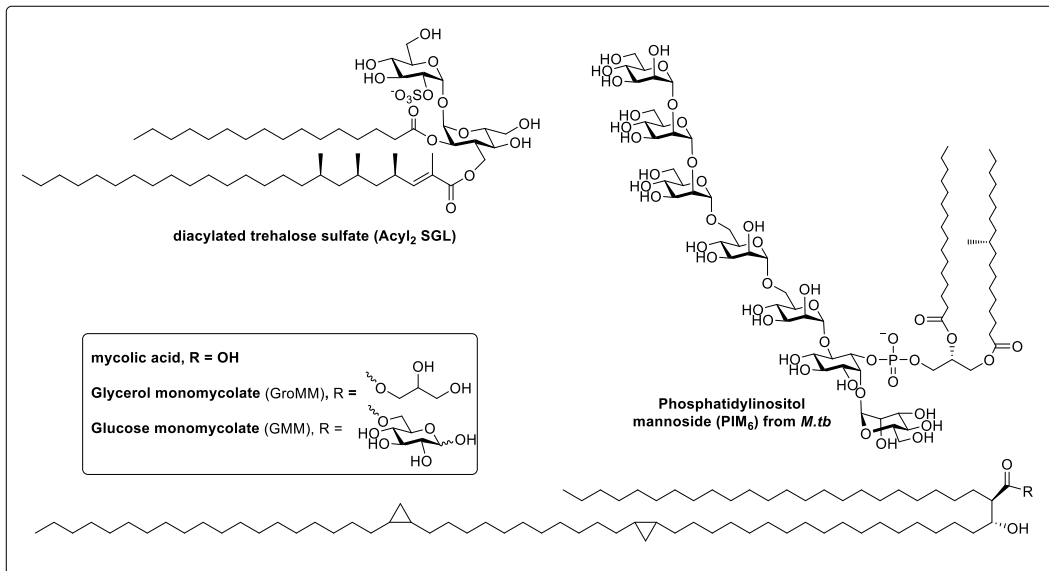


**Figure 1.16** Structures of CD1b presented mycobacterial lipids.

Mycolic acids are long-chain fatty acids bearing an  $\alpha$ -alkyl chain and a  $\beta$ -hydroxyl group. Glucose monomycolate (GMM) is synthesized upon infection from host glucose and is capable of inducing a T cell response by binding to CD1b.<sup>68</sup> Glycerol monomycolate (GroMM) is produced by *Mycobacteria*, *Corynebacteria* and *Nocardia* and produces a CD1b-restricted T cell response.<sup>69</sup> Until recently, CD1b-reactive TCRs were thought to be highly diverse in their TCR gene usage. However, CD1b tetramers loaded with GMM have allowed broader sampling of the human TCR repertoire and detects two sets of conserved TCRs: TRAV1-2<sup>+</sup>TRAJ9<sup>+</sup> GEM (‘germline-encoded mycolyl-reactive’) T cells and TRBV4-1<sup>+</sup> ‘LDN5-like’ T cells.<sup>31</sup>

PIMs and LAM represent the second class of lipid antigens capable of binding to CD1b. LAM from different bacteria differ in the number and branching of the mannose units, thus enabling species specific recognition by T cells.<sup>70</sup> A mixture of PIM<sub>6</sub> and PIM<sub>2</sub> was found to stimulate CD1b restricted T cells.<sup>71</sup> A few studies have shown that larger lipoglycans such as PIM<sub>6</sub> require trimming of the mannose units to PIM<sub>2</sub> to be able to bind to CD1b.<sup>72</sup>

Sulfoglycolipids represent the third class of CD1b binding lipid antigens.<sup>73</sup> Although SGLs do not affect the replication and pathogenicity of *M.tb*, their abundance is associated with strain virulence.<sup>74</sup> Structurally SGLs contain a trehalose sulfate core, acylated with 2, 3, or 4 fatty acids. Structural activity studies have shown that for CD1b-restricted T cell activation it is essential to have a saturated, or monosaturated polymethylated fatty acid, with (*S*)-configured stereocenters in the polymethyl branched fatty acid at the 3-position of the trehalose.<sup>75</sup>

In 2016, PG from a range of bacteria were shown to be able to bind to CD1b (Figure 1.17). PG and DPG from *C.glutamicum* was able to activate CD1b restricted T cells by binding to CD1b. It was not reported whether *M.tb* PG could stimulate CD1b restricted T cells. It would be interesting to explore its ability to bind to CD1b and also see if the structural variation caused by the presence of TBSA results in difference in potency.

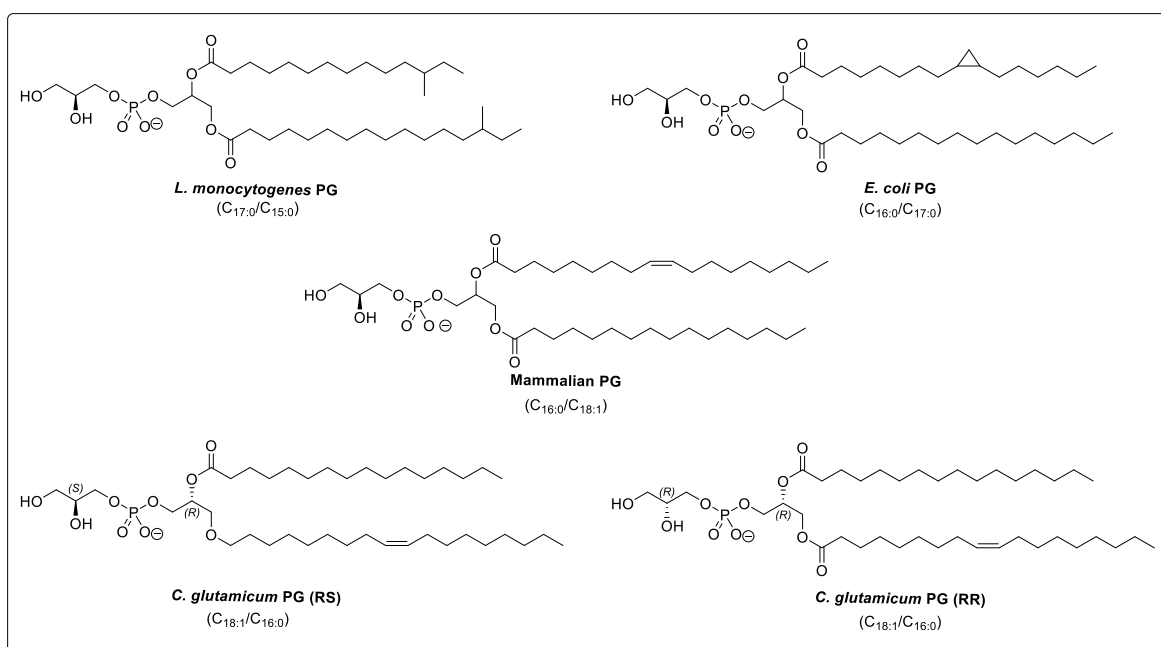


**Figure 1.17** Structures of PG capable of binding to CD1b.<sup>76</sup>

## 1.7 Summary

The highly lipidic and immunogenic mycobacterial cell wall has been a major source of antigen species that have shaped and supported our understanding of lipid-mediated immunity. However, acquisition of these materials from the natural source is hampered by the difficulty of culturing pathogenic mycobacteria, their heterogeneity from natural sources and low abundance. Chemical synthesis has an important role in facilitating immunological studies by providing pure synthetic antigens and their analogues. In this project, we undertook the synthesis of mycobacterial lipids, glycolipids and phospholipids.

## 1.8 Thesis outline for Chapters 2-4

### **Chapter 2: Synthesis and NMR discrimination of tuberculostearic acid enantiomers**

In this chapter we have new two-step and three-step routes for the synthesis of *R*- and *S*-tuberculostearic acid (TBSA) enantiomers from commercially available citronellyl bromide. In an attempt to define the stereochemistry of the natural TBSA, we explored a NMR-based chiral discrimination technique utilizing chiral derivatizing agents.

### **Chapter 3: Synthesis of TBSA containing phosphatidylglycerol from *Mycobacterium tuberculosis***

This chapter describes the synthesis of a representative *M.tb* PG bearing *R*-TBSA and two regioisomeric analogues lacking the methyl branch of TBSA. Phosphoramidite chemistry was used to assemble these PGs. These compounds are being used to study the immunological properties through the CD1b binding axis.

### **Chapter 4: A second generation synthesis of GI-A, a GlcADAG from *M. smegmatis***

In this chapter we report a new concise synthesis of  $\alpha$ -glucuronosyl diacylglycerides and  $\alpha$ -glucosyl diacylglycerides. This new approach proceeds via a bromohydrin intermediate

and provides exquisite acylation fidelity at the glycerol, providing the diglyceride as a highly pure regioisomer. Moreover, unlike the previously reported method, this new approach utilizes only one protecting group, the methoxyacetyl group, which is compatible with lipid unsaturation, allowing synthesis of the oleic acid-containing GlcADAG isolated from *M. smegmatis* and *C. glutamicum*, and its regioisomer. These synthetic  $\alpha$ -glucosyl and  $\alpha$ -glucuronosyl diacylglycerides were used to establish glycolipid recognition preferences for a selection of type I, Ia and II NKT TCRs.







## **Chapter 2**

### **Synthesis and NMR discrimination of tuberculostearic acid (TBSA) enantiomers**

## 2.1 Introduction

### 2.1.1 Methyl branched fatty acids in mycobacteria

Mycobacteria produces an extraordinary variety of saturated methyl-branched fatty acids. These include the characteristic 10-methylstearic acid (tuberculostearic acid), 2,4-dimethyl-C<sub>14</sub> fatty acids, mono-, di-, and tri-methyl branched fatty acids from C<sub>14</sub>-C<sub>25</sub>, mycosanoic acids and phthioceranic acids (Figure 2.1).<sup>77</sup> These fatty acids are found as esters in various cell wall components such as PIMs, sulfolipids (SL), and trehalose mycolates.<sup>77</sup> For the purpose of this chapter, we are interested in the simplest of these methyl-branched fatty acids, tuberculostearic acid.

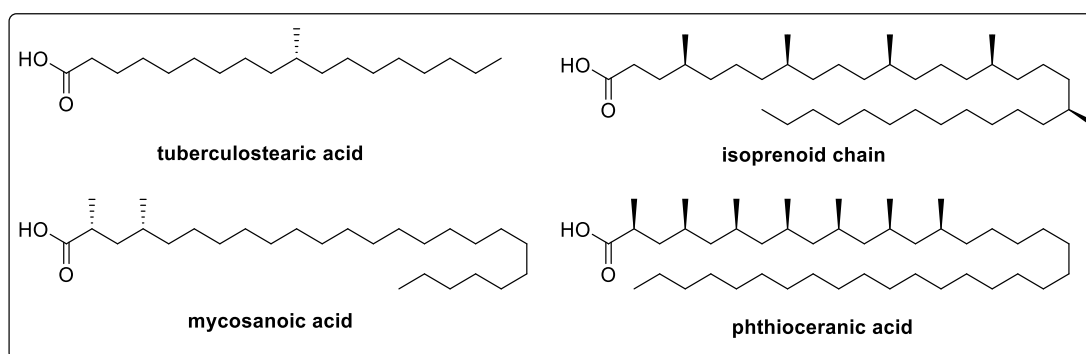


**Figure 2.1** Various methyl branched fatty acids in mycobacteria.

### 2.1.2 Tuberculostearic acid, a branched fatty acid produced by mycobacteria

In 1927 Anderson *et al.* isolated a novel fatty acid from the H37Rv strain of *M. tuberculosis* and termed it tuberculostearic acid (TBSA).<sup>78</sup> In their work, Anderson isolated 240 grams of an acetone soluble fatty acid fraction from 400 L of *M.tb* (H37v) bacterial culture and converted the fatty acid fraction to the corresponding methyl esters. This mixture was subjected to fractional distillation, and a lower-boiling fraction was saponified to give an acid that was determined to be isomeric to stearic acid (C<sub>18</sub>H<sub>36</sub>O<sub>2</sub>), and was named tuberculostearic acid (TBSA).<sup>78</sup> In 1934, Speilman and co-workers oxidized a sample of natural TBSA and isolated 2-decanone and azelaic acid (Figure 2.2)

as the main products; this prompted a revision of the formula as C<sub>19</sub>H<sub>38</sub>O<sub>2</sub> and proposal of its structure as 10-methylstearic acid **201**.<sup>79</sup>

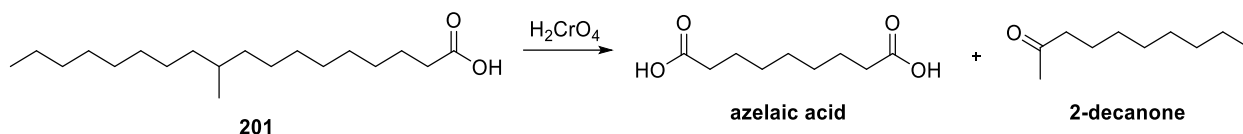


**Figure 2.2** Oxidation of TBSA.<sup>79</sup>

Ryhage *et al.* studied the mass spectral fragmentation pattern of the methyl ester of TBSA **202** by bombardment with low energy electrons (Figure 2.3).<sup>80</sup> They found characteristic peaks at *m/z* 171 and 199, corresponding to methyl nonanoate **203** and methyl undecanoate **204** and a strong peak at *m/z* 167 corresponding to the ketene **205**. This fragmentation pattern ascertained the methyl branching of TBSA to be at tenth carbon.<sup>80</sup>

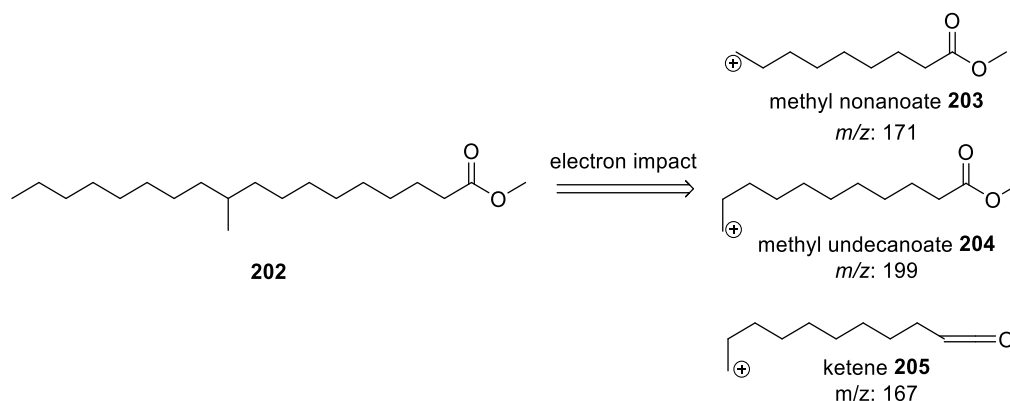
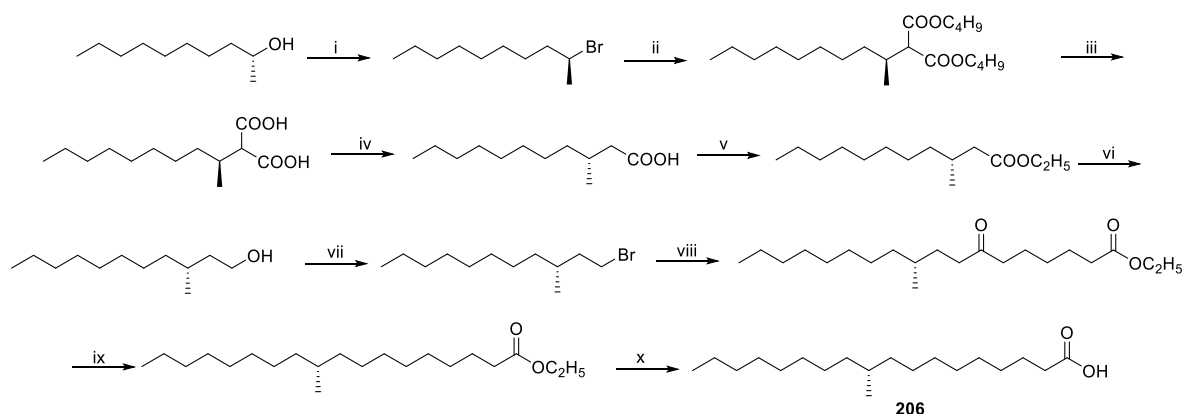


**Figure 2.3** Electron-impact mass spectral fragmentation pattern observed for the methyl ester of TBSA **202**.<sup>80</sup>

### 2.1.3 Chirality of natural TBSA

In 1948, Prout *et al.* reported the synthesis of the two enantiomers of TBSA.<sup>81</sup> Prout's synthesis of (*R*)-TBSA **206** is historically notable dating from 1947/1948. It commenced with the synthesis of 2-decanol and its resolution as a brucine salt via a hydrogen phthalate half ester, to afford optically pure (+)- and (-)-2-decanol. The optically pure alcohols were converted to the bromides and treated with diethyl malonate

and sodium butoxide to afford the dibutyl 2-decylmalonates, which were saponified to afford 2-decyl malonic acid. The acid was subjected to fractional crystallization and heated to 160-180 °C to afford the 3-methyl hendecanoic acids. The acids were converted to the ethyl esters and reduced to afford 3-methylhendecanols. These alcohols were brominated and subjected to further chain elongation. The bromo-3-methyl-hendecane enantiomers were treated with carbethoxycaproyl chloride in presence of cadmium chloride to afford the ethyl-7-keto-10-methyl octadecanoates, which upon reduction afforded the ethyl esters of TBSA. The ethyl esters were saponified to afford optically pure TBSA **206** (Scheme 2.1) and its enantiomer.<sup>81</sup>



**Scheme 2.1** Synthesis of (*R*)-tuberculostearic acid by Prout *et al.*<sup>81</sup> Reagents and conditions: (i) PBr<sub>3</sub>, 65-86%; (ii) CH<sub>2</sub>(COOC<sub>2</sub>H<sub>5</sub>)<sub>2</sub>, NaOC<sub>4</sub>H<sub>9</sub>, 65-84%; (iii) a) KOH b) H<sub>2</sub>SO<sub>4</sub>, 80-98%; (iv) 160-180 °C, 97-98%; (v) C<sub>2</sub>H<sub>5</sub>OH, H<sub>2</sub>SO<sub>4</sub>, 85-96%; (vi) Na, C<sub>4</sub>H<sub>9</sub>OH, 84-87%; (vii) HBr, 70-89%; (viii) 1. Mg, 2. CdCl<sub>2</sub>, 3. ClOC(CH<sub>2</sub>)<sub>5</sub>COOC<sub>2</sub>H<sub>5</sub>, 52-56%; (ix) Zn(Hg), HCl, C<sub>2</sub>H<sub>5</sub>OH, 86-94%; (x) KOH, 72-86%.

Prout *et al.* obtained a sample of the methyl ester of TBSA (isolated from *M.tb*) from Anderson's lab. This was saponified and the resulting acid was recrystallized from acetone; this material was hereafter referred to as 'natural TBSA'. With synthetic antipodes in hand, they set about to determine their relationship to natural TBSA. The optical rotations of each enantiomer were compared with 'natural TBSA' leading to the conclusion that (*R*)-TBSA, with an optical rotation of  $[\alpha]_D -0.05$  to  $-0.09$ , was the naturally occurring form.<sup>81</sup> The stereochemical relationship of natural TBSA to the synthetic

materials was deduced by chemical correlation to D-(+)-glyceraldehyde as shown in Figure 2.4. The absolute configuration of D-(+)-glyceraldehyde was resolved in 1951 by the work of Bijvoet *et al.*<sup>82</sup> who determined the absolute stereochemistry of tartaric acid.

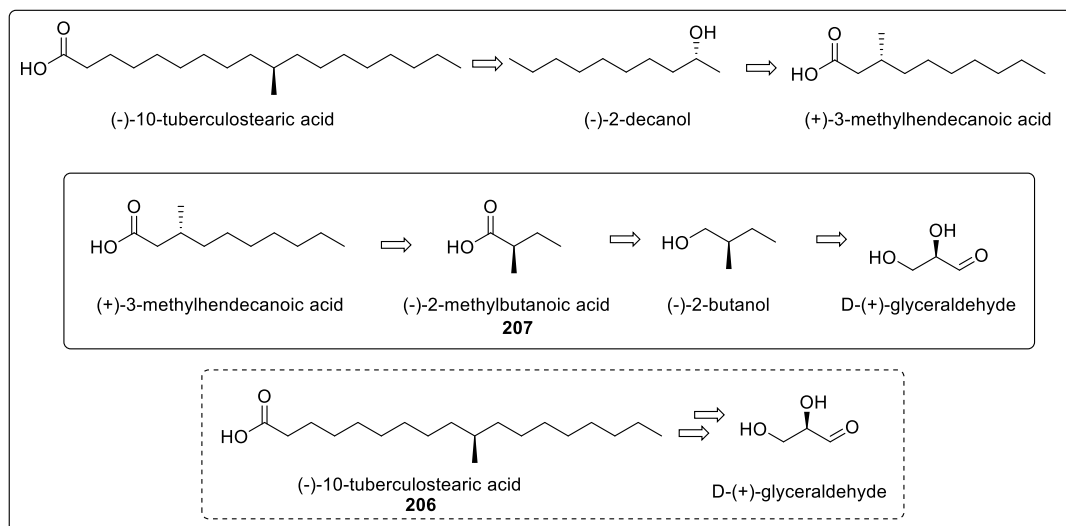
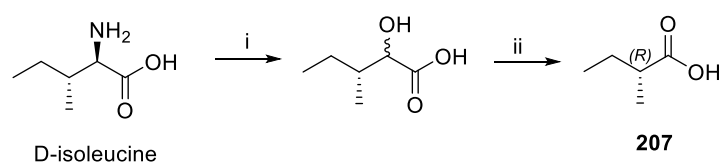


**Figure 2.4** Chemical correlation of (*R*)-TBSA to D-(+)-glyceraldehyde.<sup>81</sup>

However in their work Prout mentioned a possible ambiguity in the stereochemical correlation of (-)-2-methylbutanoic acid **207** to D-(+)-glyceraldehyde. In 1985 Henrick *et al.* synthesized and ascertained the stereochemistry of **207** as a part of their synthesis of 8-methyl decanol esters (Scheme 2.2).<sup>83</sup> They have synthesized **207** by oxidative degradation of D-isoleucine.<sup>83</sup> Deamination followed by oxidation with acidic potassium permanganate afforded **207** in 96% ee. This work confirms the stereochemistry of (-)-2-methylbutanoic acid as *R*, and the conclusion that (-)-10-tuberculostearic acid **206** can be chemically correlated to (-)-2-methylbutanoic acid.



**Scheme 2.2** Synthesis of **207**. Reagents and conditions: (i) HNO<sub>3</sub>, (ii) KMnO<sub>4</sub>.<sup>83</sup>

This conclusion based on optical rotation was supported by mixed melting point tests. A mixture of naturally occurring, recrystallized tuberculostearic acid and synthetic

levorotary (*R*)-acid **206** melted at 11.0-12.4 °C, and a mixture with synthetic dextrorotatory (*S*)-acid melted at 19.4-20.1 °C. A mixture of the two synthetic acids melted at 21.0-25.8 °C.<sup>81</sup> Since this time the stereochemistry of TBSA has never been revisited to independently confirm the stereochemistry of the natural TBSA enantiomer. For compounds with such low optical rotation values, it remains possible for errors in stereochemistry determination. As well, while the mixed melting point analyses, which are supportive of the absolute stereochemistry, do not provide insight into the optical purity, a problem compounded by the fact that the natural TBSA was purified by recrystallization prior to analysis, which may have led to enantiomeric enrichment. Thus it is possible that natural TBSA is not present entirely as a single enantiomer.

## **2.2 TBSA is present in a wide range of mycobacterial lipid-like species**

*Phosphatidylinositol mannosides, lipomannan, and lipoarabinomannan:* PIMs are glycolipids composed of fatty acids attached to a glycerol unit, linked to mannosylated *myo*-inositol by a phosphodiester bond (Figure 2.5). In mycobacteria, palmitic (C<sub>16:0</sub>) and tuberculostearic acid (C<sub>19:0</sub>) are the predominant fatty acids attached to the 1- and 2-positions of the glycerol unit.<sup>84</sup> PIMs in the mycobacterial cell wall are precursors of LM and LAM, which are also believed to share identical phosphatidyl anchors bearing TBSA.

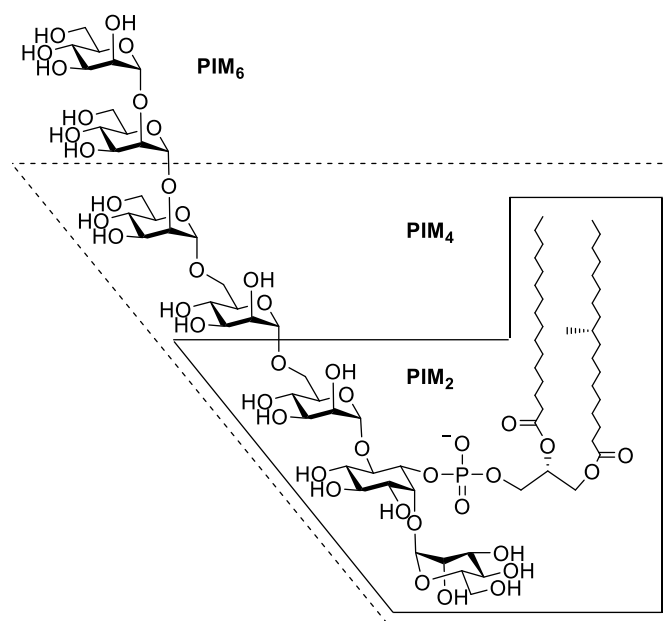


**Figure 2.5** Structure of phosphatidylinositol mannoside (PIM) bearing (*R*)-tuberculostearic acid at sn-1 position of the glycerol backbone.

*Glucuronosyl diacylglycerides*: In 1993, Brennan and co-workers isolated  $\alpha$ -glucuronosyl diacylglyceride (GlcAGroAc<sub>2</sub>; Gl-A) from *M. smegmatis*. Two major lipofoms were identified, each of which contained one palmitic acid residue; the second fatty acid was either TBSA or oleic acid.<sup>85</sup> Studies by Williams and co-workers showed that presence of TBSA at the sn-1 position and stearic acid at the sn-2 position is the natural form and is immunologically active by activating NK-T cells to produce a T<sub>H</sub>2-biased response (Figure 2.6).<sup>86</sup>

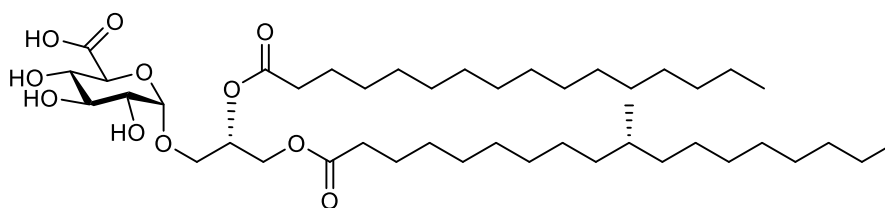


**Figure 2.6** Structure of glucuronosyl diacylglyceride (GlcAGroAc<sub>2</sub>; Gl-A) from *M. smegmatis* bearing (*R*)-TBSA at the sn-1 position of the glycerol backbone.

*Phosphatidylethanolamine (PE)*: PE is an *M.tb* glycerophospholipid that is considered to be a potential biomarker for detection of TB.<sup>87</sup> Minnaard and his group



synthesized PE and confirmed the lipid orientation of the naturally occurring form as 1-*O*-tuberculostearoyl-2-*O*-palmitoyl-*sn*-glycero-3-phosphoethanolamine (Figure 2.7).<sup>88</sup>

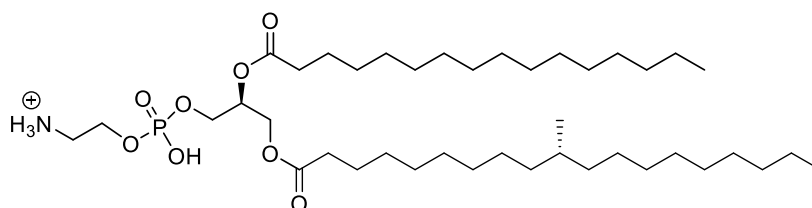


**Figure 2.7** Structure of phosphatidylethanolamine from *M. tuberculosis*.

*Phosphatidylglycerol (PG)*: PG is a minor metabolite produced by *M.tb* and is converted to cardiolipin and lysine esters.<sup>89-90</sup> It is assumed to possess (*R*)-TBSA at the *sn*-1 position, and palmitic acid at the *sn*-2 position based on a similar biosynthetic starting material as PIMs and LM (Figure 2.8).

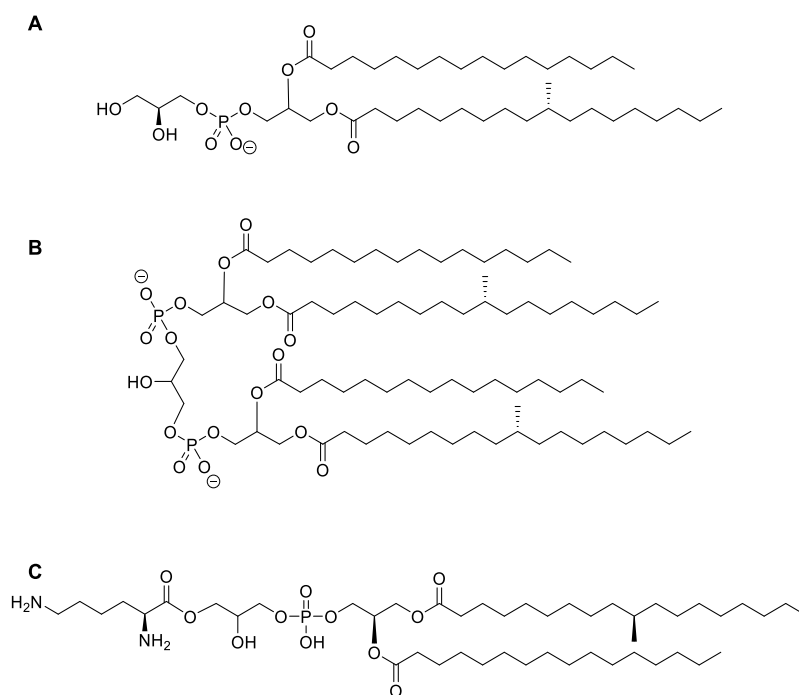


**Figure 2.8** Structures of (A) phosphatidyl glycerol, (B) cardiolipin and (C) lysine ester of PG all bearing (*R*)-TBSA at *sn*-1 position of the glycerol backbone.

*Lipoaminoacids*: Prome *et al.* identified a non-phosphorylated lipoamino acid from *M. phlei*, an ester of lysine and diglyceride. FAB-MS analysis revealed the molecule

to contain palmitic acid and TBSA as the most abundant lipid residues.<sup>91</sup> Ornithine lipids are found in Gram negative and positive bacteria, including *M. tuberculosis* and *M. bovis*. Laneelle and co-workers isolated ornithine and lysine lipids in which a  $\beta$ -hydroxy fatty acid amide is acylated with TBSA (Figure 2.9).<sup>92</sup>

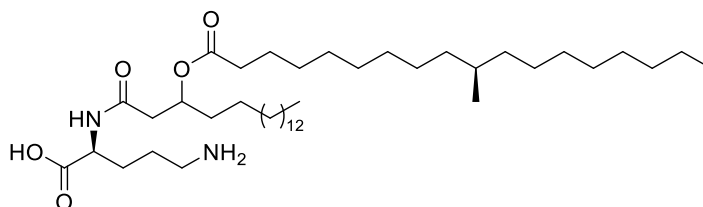


**Figure 2.9** Structure of ornithine lipoaminoacid from *M. tuberculosis*.

*Lipoproteins:* Mycobacterial lipoproteins are immunodominant antigens that activate TLR-1 and TLR-2. Sander and co-workers revealed that mycobacterial lipoproteins are triacylated and carry mycobacteria-specific fatty acids (Figure 2.10).<sup>93</sup> By FAB/MS analysis, TBSA was identified as a component fatty acid and is characteristic of mycobacteria species.

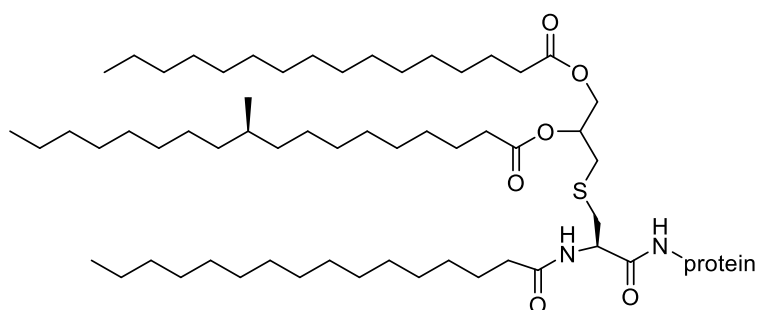
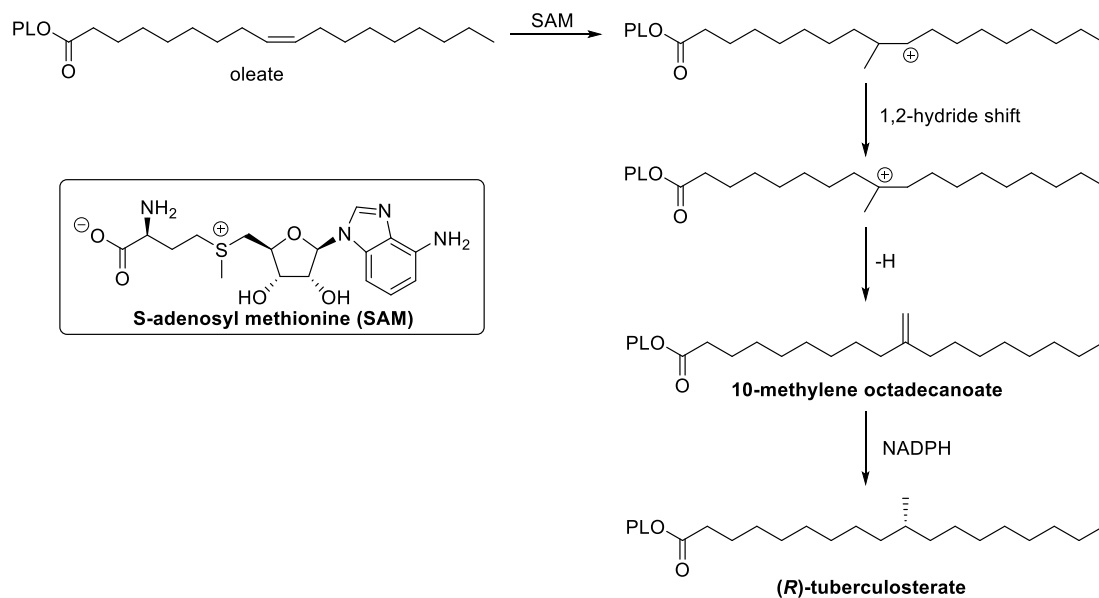


**Figure 2.10** Structure of triacylated lipoprotein identified in *M. tuberculosis*.

### 2.3 Biosynthesis of TBSA

Bloch and Scheuerbrandt studied the biosynthesis of TBSA in *M. phlei*.<sup>94</sup> Their studies established that stearic acid is directly converted to oleic acid, which is then metabolized to 10-methyl stearic acid by *S*-adenosyl methionine (SAM). This reaction is accompanied by a shift of the olefinic proton at the carbon-10 of oleate to carbon-9.<sup>95</sup> A Wagner-Meerwein rearrangement affords a stable tertiary carbocation, which upon

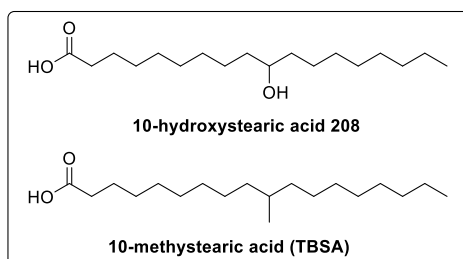
deprotonation affords an olefin. The olefin is stereoselectively reduced to produce *R*-TBSA (Scheme 2.3).



**Scheme 2.3** Biosynthesis of (*R*)-tuberculostearate occurs on phospholipid (PL) substrates.

## 2.4 10-Hydroxy stearate: a case study

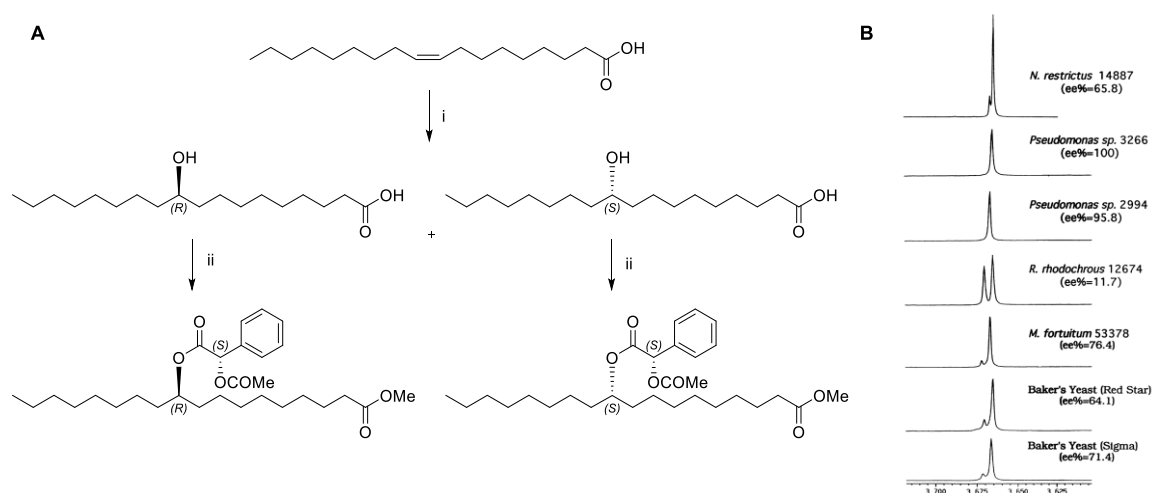
10-Hydroxystearic acid (HSA) is a naturally occurring fatty acid with similarity to TBSA in that it possesses a remote stereogenic centre. Like TBSA, (*R*)-HSA possesses a low optical rotation of -0.03, meaning that assignment of stereochemistry based on optical rotation measurements is risky (Figure 2.11).



**Figure 2.11** Comparison of the structures of 10-hydroxy stearic acid **208** and TBSA.

In 1999, Rosazza and co-workers studied the bioconversion of oleic acid to 10-hydroxy stearic acid **208** in six different micro-organisms.<sup>96-97</sup> In order to assess the

stereochemistry, they converted the fatty acid to the corresponding methyl esters with diazomethane, and then to diastereomeric *O*-*S*-(+)-acetylmandelate esters. It was shown that the chemical shifts of the fatty acid methyl esters could be distinguished in the proton NMR spectra (Figure 2.12). Using this method of chiral discrimination, the authors showed that while *Pseudomonas* species 3266 produces only one optical isomer, (the (*R*)-HAS), other microorganisms produce mixtures of the (*R*)- and (*S*)-isomers, in different ratios.

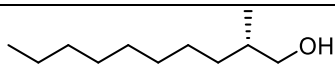
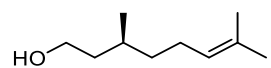
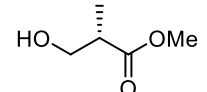
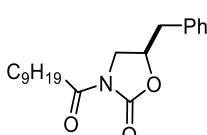
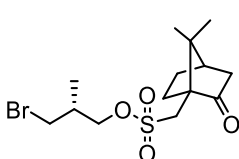
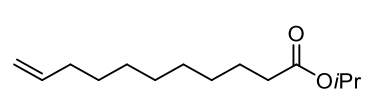
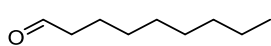
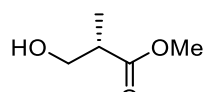
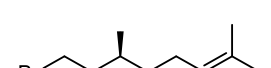


**Figure 2.12** A) Synthesis of *O*-*S*-(+)-acetylmandelate esters of 10-hydroxystearic acid. Reagents: (i) microbial hydration; (ii) 1. CH<sub>2</sub>N<sub>2</sub>, 2. (*S*)-acetylmandelic acid; B) <sup>1</sup>H NMR signals for the terminal methoxy group of the diastereoisomeric esters.<sup>96</sup>

## 2.5 Summary of enantioselective syntheses of (*R*)-TBSA.

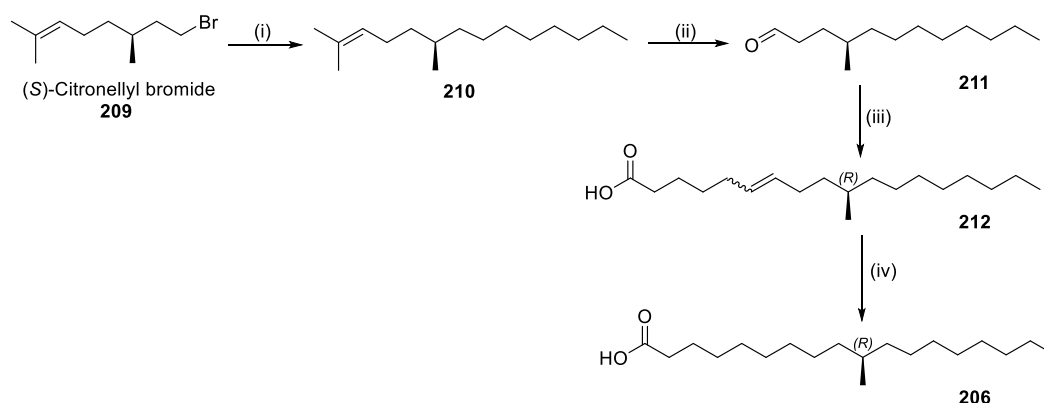
(*R*)-TBSA has been synthesized numerous times. As outlined earlier, Prout and co-workers achieved the first enantioselective synthesis of (*R*)-TBSA **206** from 2-decanol (Scheme 2.1).<sup>81</sup> The majority of approaches have origins in the chiral pool, including chiral pool substrates such as citronellol, citronellyl bromide, or Roche ester, a chiral Evans' auxiliary, or chiral resolutions using brucine salts or bromocasylates (Table 2.1). Two syntheses from the Minnaard and Minnaard-Feringa groups utilized asymmetric induction strategies.<sup>32, 86, 88, 98-100</sup>

**Table 2.1** Enantioselective syntheses of (*R*)-tuberculoheptanoic acid.

Starting material/key substrate	Approach	Steps	Ref.
 <b>(<i>R</i>)-2-methyldecanol</b>	Chiral resolution	10 <sup>a</sup>	Prout, 1948 <sup>81</sup>
 <b>(<i>S</i>)-citronellol</b>	Chiral pool	8	Larsen, 2007 <sup>101</sup>
 <b>Roche ester</b>	Chiral pool	7	Seeberger, 2006 <sup>102</sup>
 <b>(<i>R</i>)-oxazolidinone</b>	Chiral auxiliary	7	Williams, 2013 <sup>86</sup>
 <b>bromocasylate</b>	Chiral resolution	7	Hahn, 2015 <sup>98</sup>
 <b>isopropyl 10-undecenoate</b>	Catalytic enantioselective induction	6 <sup>b</sup>	Feringa, Minnaard, 2010 <sup>88</sup>
 <b>nonanal</b>	Catalytic enantioselective induction	5	Minnaard, 2013 <sup>32</sup>
 <b>Roche ester</b>	Chiral pool	5	Hung, 2015 <sup>99</sup>
 <b>(<i>S</i>)-citronellyl bromide</b>	Chiral pool	4	Baird, 2006 <sup>100</sup>

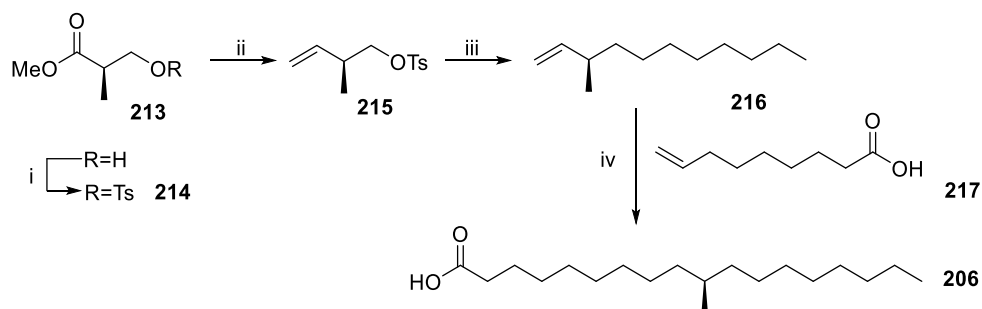
<sup>a</sup> (*R*)-2-methyldecanol was synthesized from bromooctane in 5 steps by resolution of an intermediate brucine salt. <sup>b</sup> Isopropyl 10-undecenoate can be synthesized in one step from commercially available undecylenic acid.

Among the most efficient schemes for the synthesis of (*R*)-TBSA, those of the Baird and Hung groups constitute highly efficient approaches that are of relevance.<sup>99-100</sup> Baird and Roberts reported the synthesis of both enantiomers of TBSA from commercially-available (*S*)- and (*R*)-citronellyl bromides. Copper-catalyzed cross-coupling of hexylmagnesium bromide with citronellyl bromide gave 2,6-dimethyltetradec-2-ene, which upon ozonolysis formed an aldehyde. This aldehyde was coupled in a Wittig reaction to an acid-functionalized phosphonium salt, thereby forming the carbon skeleton of the TBSA. Hydrogenation of the acid and treatment with diazomethane afforded the methyl ester of TBSA. This synthesis was achieved in four linear steps and five total synthetic steps (Scheme 2.4).<sup>100</sup>



**Scheme 2.4** Baird and Roberts' synthesis of *R*-TBSA from citronellyl bromide.<sup>100</sup>  
 Reagents and conditions: (i)  $\text{CH}_3(\text{CH}_2)_5\text{MgBr}$ ,  $\text{Li}_2\text{CuCl}_4$ ,  $-78\text{ }^\circ\text{C}$ , THF; (ii)  $\text{O}_3$ ,  $\text{CH}_2\text{Cl}_2$ , ( $-78\text{ }^\circ\text{C}$ ),  $\text{PPh}_3$ ; (iii)  $\text{BrPPh}_3(\text{CH}_2)_5\text{COOH}$ , LIHDMS, toluene; (iv) Pd (10% on carbon),  $\text{H}_2$ , MeOH.

Hung *et al.* synthesized TBSA starting from the Roche ester.<sup>99</sup> The hydroxyl group of the Roche ester was protected as a tosylate and the methyl ester was reduced to an aldehyde, which was methylenated by a Wittig reaction. Copper-mediated cross-coupling of the alkene with heptyl magnesium bromide afforded an 11-carbon terminal alkene, which was elongated with nonano-8-enic acid by tandem Grubbs metathesis/hydrogenation to afford TBSA in four steps overall (Scheme 2.5).<sup>99</sup>



**Scheme 2.5** Hung's synthesis of *R*-TBSA from Roche ester.<sup>99</sup> Reagents and conditions: (i). TsCl, Et<sub>3</sub>N, DMAP, 94%; (ii) 1. diisobutylaluminium hydride, -78° C, 2. Ph<sub>3</sub>P=CH<sub>2</sub> 72% (over 2 steps); (iii) C<sub>7</sub>H<sub>15</sub>MgBr, Li<sub>2</sub>CuCl<sub>4</sub>, -78 to 0 °C, 92%; (iv) 1. Grubbs II catalyst, reflux, 2. H<sub>2</sub>, Pd/C, 75%.

## 2.6 Aims of this chapter

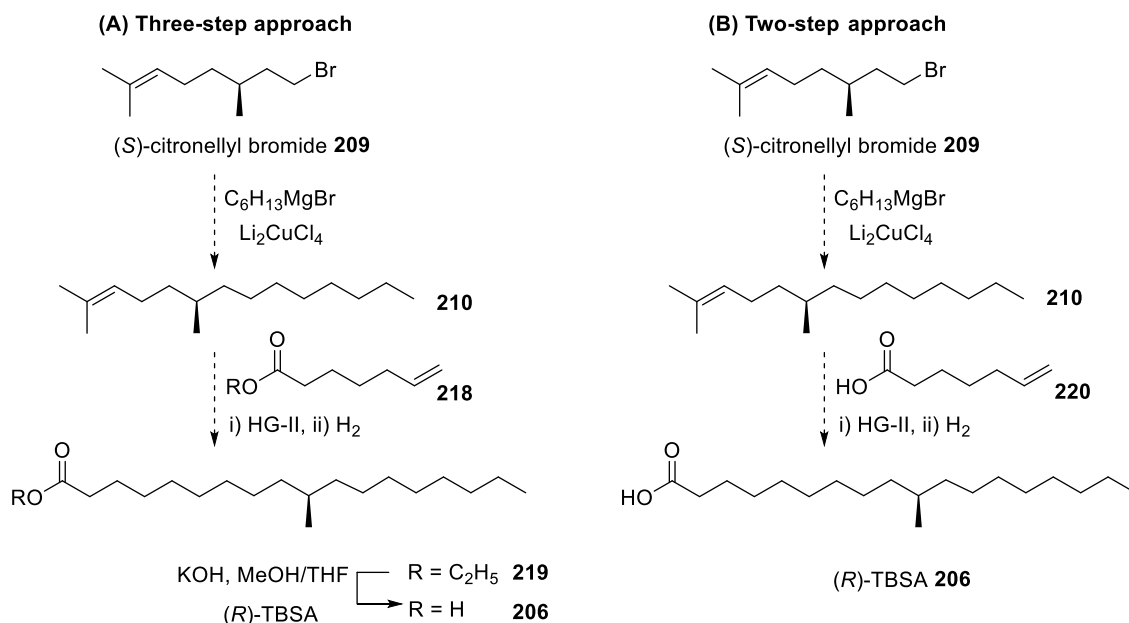
Tuberculostearic acid is a characteristic fatty acid of mycobacteria, whose absolute stereochemistry was assigned based on its very small intrinsic optical rotation.<sup>81</sup> Further, the fact that HSA **208** has been found to occur in varying levels of enantiomeric purity, depending on its source, led us to consider approaches to revisit the stereochemical assignment of natural TBSA. Therefore the aims of this chapter is to:

1. Develop a new efficient, approach allowing the synthesis of both enantiomers of TBSA starting from commercially available citronellyl bromide
2. Develop a method allowing chiral discrimination of TBSA enantiomers to unequivocally ascertain the stereochemistry of natural tuberculostearic acid.

## 2.7 Results and Discussion

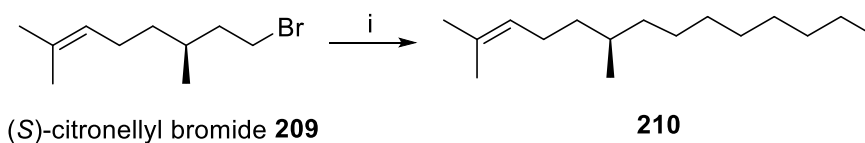
We proposed to synthesize TBSA enantiomers in a short two- or three-step sequence starting from commercially available (*S*)-citronellyl bromide and (*R*)-citronellyl bromide (Scheme 2.6). (*S*)-Citronellyl bromide would be subjected to a copper-catalyzed cross-coupling with hexylmagnesium bromide to afford (*R*)-2,3-dimethyltetradecene, exactly as described by Roberts and Baird,<sup>100</sup> which could be subjected to tandem cross metathesis/hydrogenation with ethyl heptenoate, or heptenoic acid, using Hoveyda

Grubbs 2<sup>nd</sup> generation catalyst. In the case of the ethyl ester, saponification would afford the acid in overall three steps. In the case of the acid, TBSA would be generated directly.



**Scheme 2.6** Our strategy for the synthesis of TBSA enantiomers.

We started the synthesis of (R)-TBSA **206** from commercially available (S)-citronellyl bromide. Copper-mediated cross coupling of (S)-citronellyl bromide with hexylmagnesium bromide afforded the (R)-2,6-dimethyltetradecene **210** in 90% yield (Scheme 2.7), similar to the results obtained by Baird (95%).<sup>100</sup> The spectroscopic data in agreement with Baird's.



**Scheme 2.7** Synthesis of (R)-2,6-dimethyltetradecene **210**. Reagents and conditions: (i)  $\text{Li}_2\text{CuCl}_4$ ,  $\text{Et}_2\text{O}$ ,  $\text{C}_{16}\text{H}_{13}\text{MgBr}$ ,  $-78^\circ\text{C}$  to r.t, 36 h, 90%.

### 2.7.1 Cross metathesis concept and optimization

Historically, carbon-carbon bond formations at unsaturated carbon have utilized either a carbon nucleophile that undergoes a nucleophilic attack on the carbonyl (e.g. Wittig, Horner-Wadsworth-Emmons, Julia-Koschenski reactions) or metal-catalyzed



reactions (e.g. Suzuki, Stille, Heck reactions) in which the intact multiple bond is functionalized. Olefin metathesis is a conceptually distinct olefination method, discovered in the 1950s that has transformed synthetic chemistry by allowing a fundamentally different approach to olefin synthesis.<sup>103</sup>

There are several types of olefin metathesis such as ring closure metathesis, ring opening metathesis polymerization, enyne metathesis and cross metathesis. Of these, cross metathesis is an intensively studied area that oftentimes suffers from low yields, unpredictable reaction scope, poor stereoselectivity, and poor product selectivity.

#### **2.7.1.1 Mechanism**

Olefin metathesis is a transalkylidenation reaction. A widely accepted mechanism for the reaction was proposed by Herison and Chauvin in 1971.<sup>103</sup> They proposed that the reaction begins with a [2+2] cycloaddition of an alkene to the metal alkylidene multiple-bond to form a metallocyclobutane intermediate, which undergoes a [2+2] cycloreversion to generate ethylene and a substrate-loaded metal carbene. This intermediate reacts with the second olefin to form a new metallocyclobutane intermediate, which upon cycloreversion releases the product, regenerating the catalyst and closing the cycle (Figure 2.13). It is believed that the reaction is thermodynamically-controlled and is driven forward by release of ethylene gas.

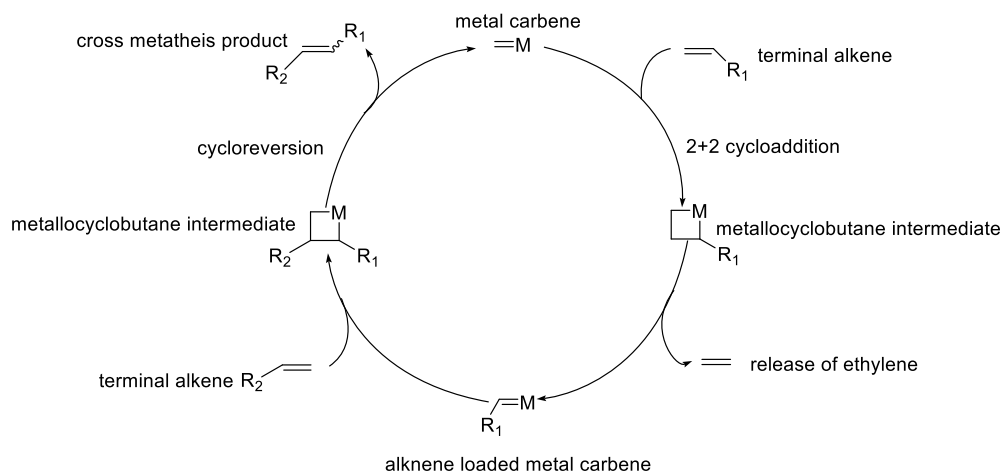


**Figure 2.13** Mechanism of Grubbs cross-metathesis of two terminal alkenes.

### 2.7.1.2 Reactivity selectivity

Steric bulk and electron deficiency are both deactivating factors for olefin metathesis. Grubbs categorized olefins into four groups (types I-IV) in order to rationalize their olefin reactivity selectivity.<sup>104</sup> Sterically unhindered, electron-rich olefins are the most reactive and are categorized as type I. Increasingly sterically hindered and/or electron-deficient olefins fall into types II through IV (Figure 2.14). Because of their high reactivity, type I olefins undergo rapid homodimerization and the resulting homodimers are sufficiently reactive to participate in secondary metathesis reactions. Type II olefins homodimerize, but these dimers are less reactive. Type III olefins do not homodimerize but are active towards metathesis. Type IV olefins are unreactive towards metathesis.

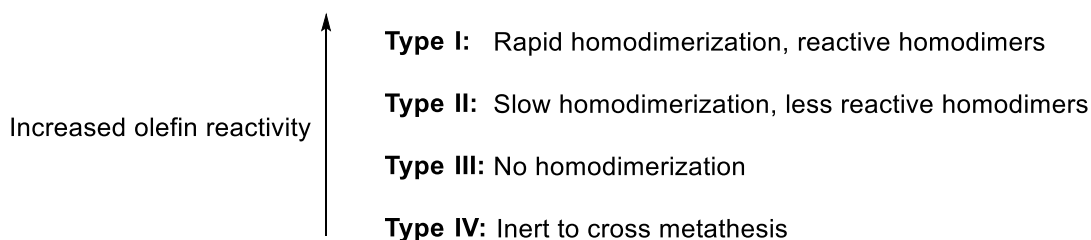


**Figure 2.14** Classification of olefins based on reactivity.

Several rules have been adopted that can aid in the choice of appropriate cross-metathesis partners.<sup>104</sup> Generally, any two olefins of the same type will give rise to

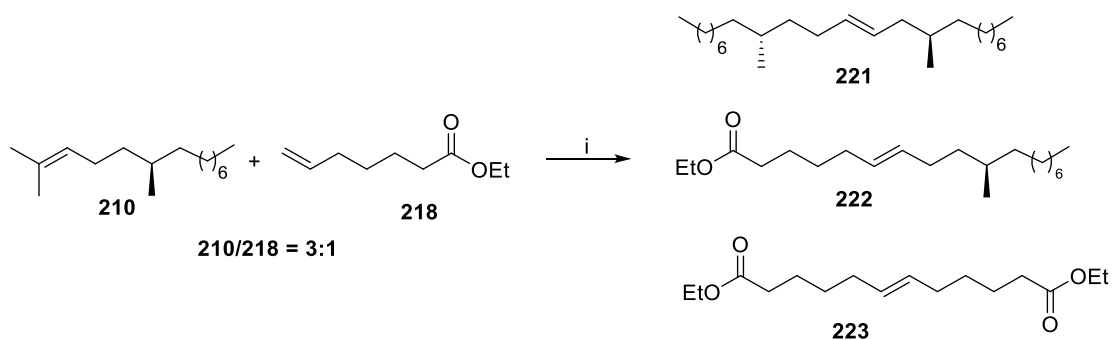
statistical mixtures, and olefins further apart in reactivity provide better cross-metathesis selectivity. For example, a reaction between two type I olefins usually results in statistical yield of the heterodimer and both homodimers. However, a reaction between a type I and a type III olefin is more selective, resulting in higher yield of the heterodimer. In case of a statistical cross-metathesis (e.g. reaction between two type I olefins), increasing the stoichiometric ratio of olefins to about 20 equivalents can afford close to theoretical yields of the heterodimer (Figure 2.15).

$$R^1-CH=CH_2 + CH_2=CH-R^2 \xrightarrow{CM} R^1-CH=CH-R^1 + R^1-CH=CH-R^2 + R^2-CH=CH-R^2$$

	Type I	Type II	Type III	Type IV	entry	R <sup>1</sup> :R <sup>2</sup>	R <sup>1</sup> -CH=CH-R <sup>1</sup> yield (%)	R <sup>1</sup> -CH=CH-R <sup>2</sup> yield (%)	R <sup>2</sup> -CH=CH-R <sup>2</sup> yield (%)
Type IV	No reaction	No reaction	No reaction	No reaction	1	1:1	25	50	25
Type III	Selective	Slow reaction	Non-selective		2	2:1		66	33
					3	4:1		80	20
Type II	Selective	Non-selective			4	10:1		91	9
Type I	Statistical				5	20:1		95	5

**Figure 2.15** General principles of selectivity and statistical distribution of products in a statistical cross metathesis (Yield quoted based on R<sup>2</sup> olefin).

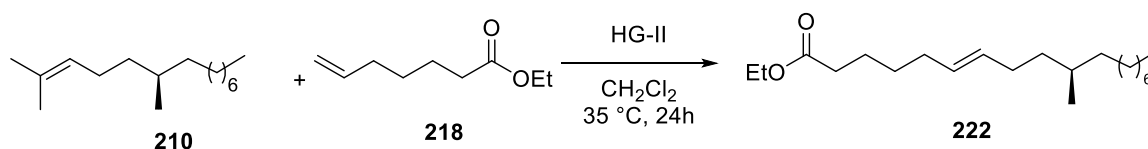
In our case, based on the 1,1-disubstituted structure of **210** we expected its reactivity to be similar to a type III olefin and the terminal olefin, ethyl heptenoate **218** to be a type I olefin. CM reactions between a type I and type III olefin are selective and usually use an excess of the type III olefin. With these generalizations in mind, we started our attempts with a 3:1 ratio of **210** and **218** (Scheme 2.8). The ester group in **218** provides better chromatographic conditions, enabling easy separation of the products.



**Scheme 2.8** Cross-metathesis reaction conditions and products. Reagents and conditions: (i) HG-II (2 x 2 mol%), CH<sub>2</sub>Cl<sub>2</sub>, 35 °C, 48 h, 87% of **222** (based on **218**).

These reaction conditions afforded good yield of the heterodimer **222**; however, we also observed 10% of homodimer **221** (yield based on **218**), suggesting that tetradecene **210** is not a typical type III olefin. Also, as the tetradecene must be synthesized from citronellyl bromide, it is not optimal to use it in a high stoichiometric ratio. Hence, we next examined use of a 1:1 ratio of the olefins under different catalyst loadings (Table 2.2). The optimal yield of the heterodimer **222** (58%) was obtained using 4% catalyst loading (entry 3). A close to statistical yield of the heterodimer **222** indicates that these two alkenes are not significantly different in their reactivity, suggesting that the tetradecene **210** displays type II or type I reactivity.

**Table 2.2** Yields of heterodimer under different catalyst loading.



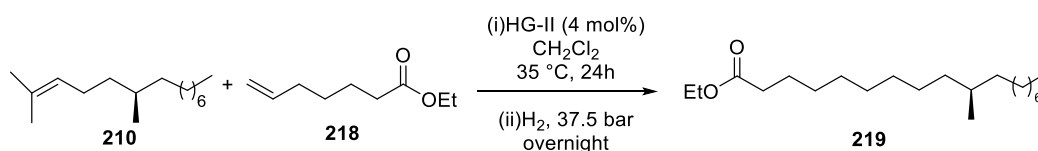
entry	210	218	mol%	yield (%)
1	1	1	1	43
2	1	1	2	39
3	1	1	4	58
4	1	1	8	58

While the 58% yield appears lower than for the example in Scheme 2.8 (using 3:1 ratio of **210/218**) it is more efficient when considering the 1:1 ratio of **210/218**. The

heterodimer alkene was subjected to hydrogenation using Pd/carbon as catalyst, affording ethyl (*R*)-TBSA **219** in 98% yield. However, as ruthenium catalysts including HG-II can be used as homogeneous hydrogenation catalysts, we explored the potential for a tandem cross-metathesis/hydrogenation.<sup>105</sup> However, unlike Pd-catalyzed reactions, hydrogenations catalyzed by HG-II require a high pressure of hydrogen.<sup>106</sup> Thus, a CM reaction was performed in CH<sub>2</sub>Cl<sub>2</sub>, and subsequently the solvent was evaporated and replaced with EtOAc. The solution was subjected to 37 bar H<sub>2</sub> overnight, affording **219** in 76% yield.

As similar yields were obtained for the cross-metathesis and tandem cross-metathesis/hydrogenation approaches, in subsequent work we sought to optimize the tandem cross-metathesis/hydrogenation process. Table 2.3 shows additional experiments in which the ratio of **210** and **218** were varied to utilize an excess of the type I olefin **218**, using a 4% catalyst loading. An optimum yield of 72% ethyl (*R*)-TBSA **219** was obtained using 1:3 ratio of **210**:**218** (entry 3).

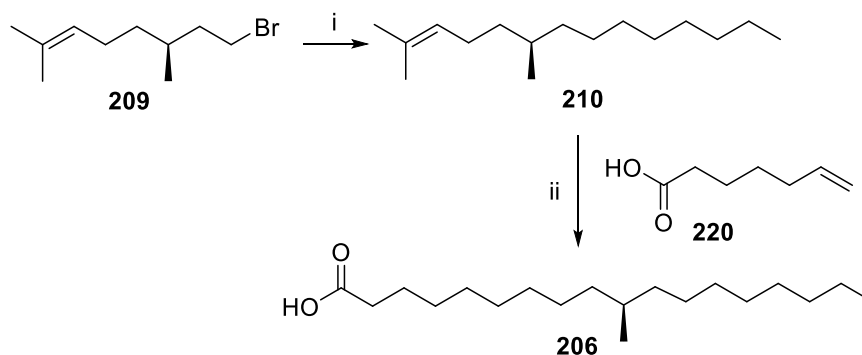
**Table 2.3** Yields of heterodimer under different stoichiometric ratios of the alkenes.



entry	210	218	yield (%)
1	1	1	48
2	1	2	41
3	1	3	72

Finally, ethyl (*R*)-TBSA **219** was saponified using KOH in MeOH/THF under reflux overnight to afford (*R*)-TBSA **206** in 95% yield (Scheme 2.9).





**Scheme 2.11** Two-step synthesis of (*R*)-TBSA. Reagents and conditions: (i)  $\text{Li}_2\text{CuCl}_4$ ,  $\text{Et}_2\text{O}$ ,  $\text{C}_{16}\text{H}_{13}\text{MgBr}$ ,  $-78\text{ }^\circ\text{C}$  to room temperature, 36 h, 92%; (ii) HG-II (2 x 2 mol%),  $\text{CH}_2\text{Cl}_2$ ,  $35\text{ }^\circ\text{C}$ , 48h, followed by  $\text{H}_2$ , 30 bar, 24 h, 73%.

## 2.8 Aim 2: NMR discrimination of TBSA enantiomers using a chiral derivatizing agent

The study of configuration of chiral molecules faces a range of issues. For a pure sample of a single enantiomer, the central challenge is the determination of the absolute configuration. Two main approaches are employed for the direct determination of absolute configuration: vibrational circular dichroism using the Cotton effect and X-ray crystallography using anomalous dispersion. The latter technique relies upon crystalline samples, and recent advances in use of coordination frameworks to entrap an analyte (the crystalline sponge method) provides a new approach to deal with non-crystalline compounds.<sup>107</sup>

A range of indirect methods are available for determination of absolute configuration. One of the most commonly applied is the use of a chiral derivatizing reagent to convert molecules to diastereomers and then to analyze these by NMR spectroscopy.<sup>108</sup> Reaction of the substrate with an ideal chiral derivatizing agent confers conformational rigidity on the diastereomer, which in turn produces predictable differences in the NMR spectra of the diastereomers. A commonly applied group of chiral derivatizing agents that have proved useful in this regard are esters of Mosher's acid ( $\alpha$ -

methoxy- $\alpha$ -trifluoromethylphenylacetic acid) **228** and MNTA acid (methoxytrifluoromethylnaphthylacetic acid) **229**.<sup>109-110</sup> Assignment of the absolute configuration is achieved by applying a mnemonic that relies upon an assumed conformation of the resulting ester and anisotropic shielding/deshielding effects induced by the reagent (Figure 2.16).

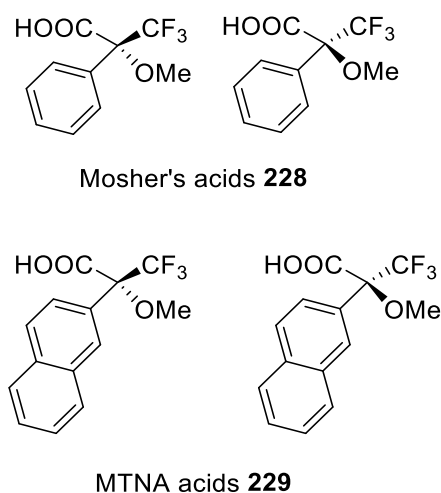


**Figure 2.16** Structures of commonly used chiral derivatizing agents.

Once the absolute stereochemistry of a compound has been determined, an important analytical problem is that of discrimination of enantiomers; that is, how to determine the chirality of a given sample, or if it is a mixture, the optical purity (often measured as the enantiomeric excess). A large number of techniques have been devised to discriminate enantiomers. Most commonly used techniques are chiroptical methods such as circular dichroism, optical rotatory dispersion, and specific optical rotation.<sup>108</sup> However, the use of many of these techniques is limited in molecules with a very small optical rotation (often arising in compounds with a remote chiral center), and can be challenging or impossible to apply to mixtures of unequal amounts of enantiomers.

An alternative strategy for the discrimination of enantiomers involves diastereomeric methods, which can be classified as direct and indirect methods.<sup>111</sup> *Direct*



*methods* include those based on diastereomeric separations on a chiral stationary phase (CSP), or diastereomeric spectral differences of NMR spectra induced by use of a chiral solvent, chiral liquid crystal, or a chiral shift reagent. *Indirect methods* include those based on the formation of diastereomers by reaction with a chiral derivatizing agent (CDA), and the subsequent analysis of the resulting diastereomeric derivatives (using for example NMR spectroscopy, or GC/HPLC on an achiral stationary phase). However, in most cases these methods are ineffective for compounds bearing stereogenic centers remote from polar functional groups.

In 1995 Tanaka *et al.* reported the synthesis and use of (*R*)- and (*S*)-1-methyl-2-naphthalimidoethyl trifluoromethanesulfonate ((*S*)-(+)-MNE-OTf) as CDAs to discriminate carboxylic acids such as mandelic acid.<sup>112</sup> Ohri *et al.* reported the synthesis and chiral discrimination ability of (*S*)-(+)-2-(2,3-anthracenedicarboximido)-1-propanol [(*S*)-1AP-OH], 1-(2,3-anthracenedicarboximido)-2-propanol [(*S*)-(+)-1A2P-OH] and (1*S*,2*S*)-2-(2,3-anthracenedicarboximido)cyclohexanol **222** (Figure 2.17).<sup>112</sup>

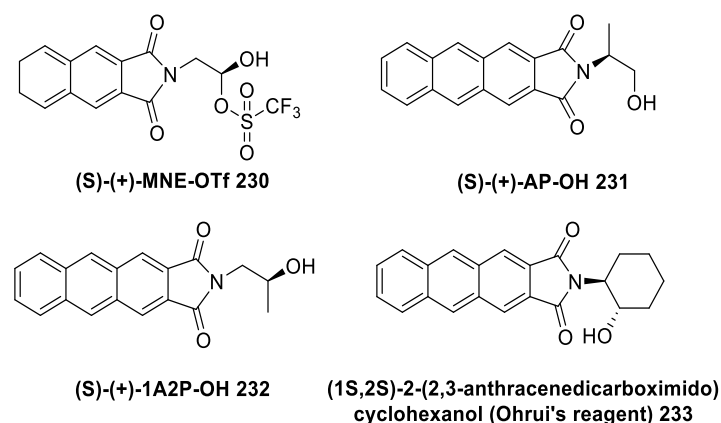


**Figure 2.17** Structures of chiral derivatizing reagents for HPLC resolution of chiral carboxylic acids with remote stereogenic centres.

Studies by Ohri *et al.* demonstrated that the CDA **233** (Ohri's reagent) forms esters with branched fatty acids that can be resolved by HPLC even when the stereocenter is remotely located up to carbon 12.<sup>113</sup> For example, diastereomeric esters of 12-

methyltetradecanoic acid and 2-(2,3-anthracenedicarboximido)cyclohexanol **233** could be separated by reverse phase HPLC at -40 °C using **233** as the chiral derivatizing reagent. Ohri argued that not only is the 2,3-anthracenedicarboximido moiety a strong fluorophore resulting in high detection sensitivity, but when appended to a *trans*-cyclohexane can induce strong intramolecular CH- $\pi$  interactions that influence the preferred conformation and thus chromatographic mobility. Ohri *et al.* also showed that this CDA provides strong chiral anisotropy in  $^1\text{H-NMR}$  spectra. In the case of a series of homologous *anteiso*-fatty acid esters with *trans*-2-(2,3-anthracenedicarboximido)cyclohexanol, the terminal methyl protons of the fatty acid shifted to a higher field compared to their corresponding methyl esters. The chemical shift difference peaked for the *anteiso*-pentanoate ( $\delta$  0.394 ppm) and this difference decreased with further increase in carbon chain length (Figure 2.18). A greater shift difference was observed using **233** as CDA, compared to the other reagents without the cyclohexanol appendage (**231**, **232**).<sup>113</sup> In the  $^1\text{H-NMR}$  analysis of (*S*)-11-methyltridecanoic acid esters of (1*R*,2*R*)-2-(2,3-anthracenedicarboximido)cyclohexanol and (1*S*,2*S*)-2-(2,3-anthracenedicarboximido)cyclohexanol, the difference in the chemical shift of the branched methyl group was 0.003 ppm, when observed in deuterated chloroform at -20 °C.<sup>113</sup>

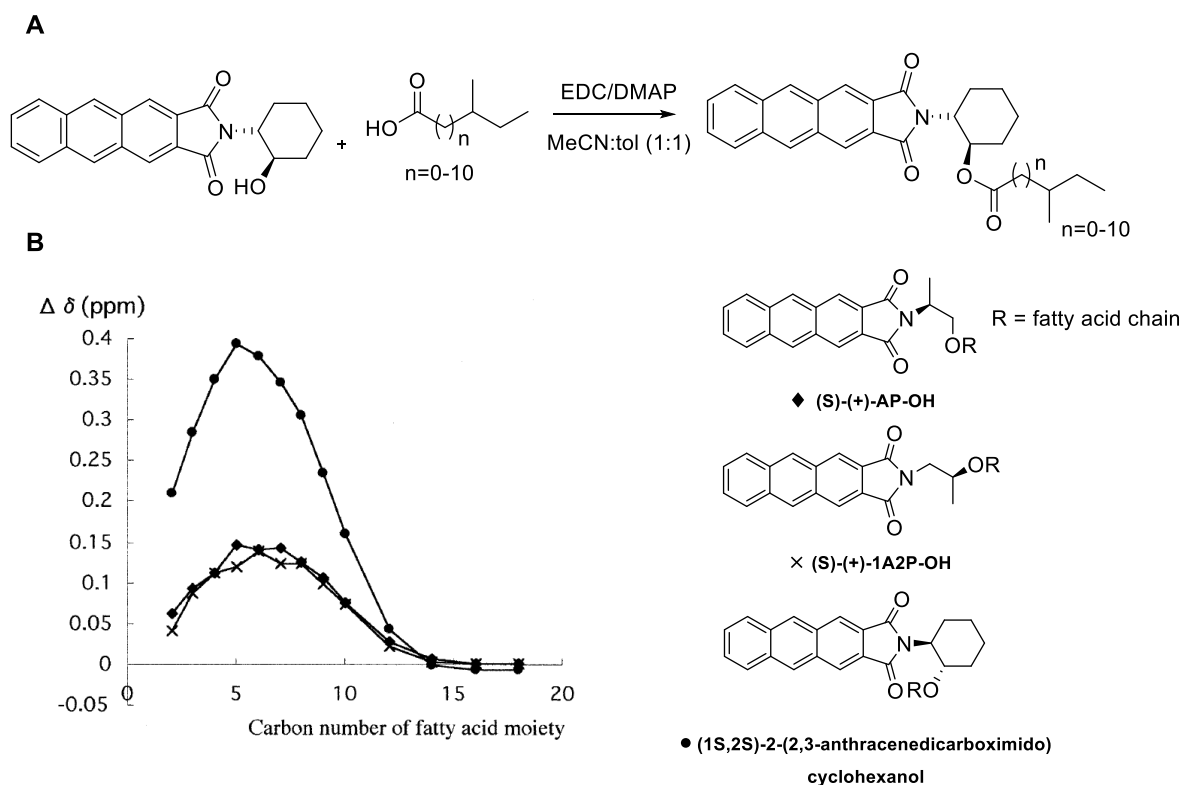


**Figure 2.18** A) Synthesis of *trans*-2-(2,3-anthracenedicarboximido)cyclohexanol esters of anteiso fatty acids; B) Graph showing the  $^1\text{H}$  NMR shift differences ( $\delta$  ppm of the terminal methyl of anteiso-fatty acids for the anthracene-based esters versus the corresponding methyl esters).

Recently, Vederas *et al.* utilized Ohri's reagent **233** to ascertain the stereochemistry of the lipid chain of tridecaptin B. They synthesized both enantiomers of 6-methyl octanoic acid (**234** and **236**) and prepared the corresponding esters with **233** (**235** and **237**) (Figure 2.19). A  $\Delta\delta$  of 0.04 ppm for the branched methyl protons was observed and supported the conclusion that the naturally occurring form is the (6*S*)-methyloctanoic acid.<sup>114</sup>

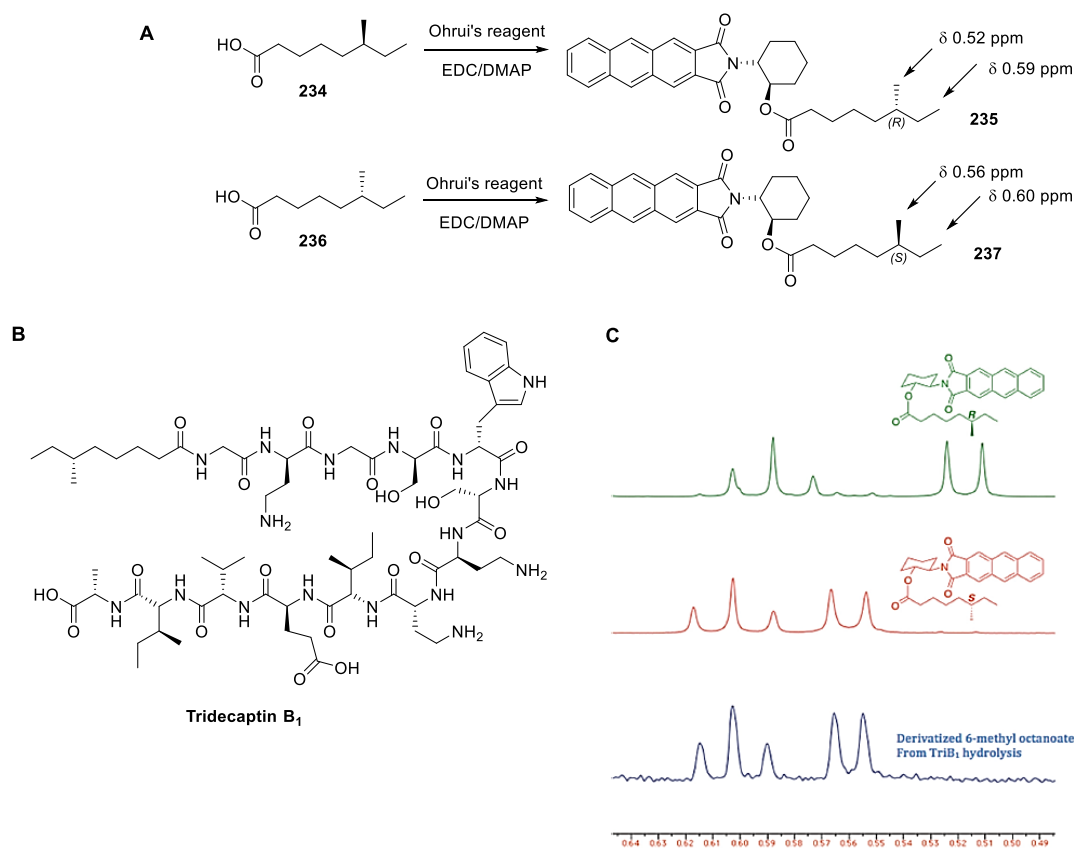
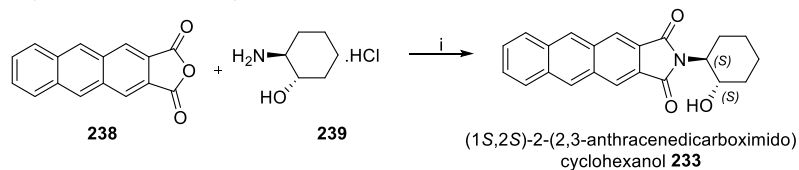


**Figure 2.19** A) Synthesis of cyclohexanol esters of both the enantiomers of 6-methyloctanoic acid; B) Structure of tridecaptin B<sub>1</sub>; C) <sup>1</sup>H NMR analysis of the diastereomers.<sup>114</sup>

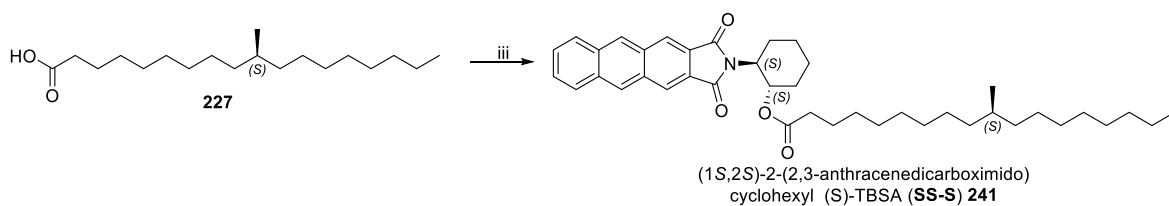
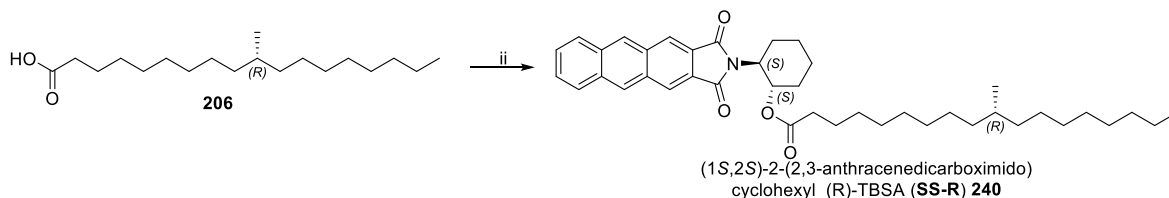
## 2.9 Results and discussion

We proposed to synthesize the (*R*)- and (*S*)-TBSA esters of (1*S*,2*S*)-2-(2,3-anthracenedicarboximido)cyclohexanol and study the <sup>1</sup>H-NMR shift of the branched methyl group protons for the two diastereoisomers, to establish whether this reagent allows their chiral discrimination by <sup>1</sup>H NMR spectroscopy. (1*S*,2*S*)-2-(2,3-Anthracenedicarboximido)cyclohexanol was prepared by reaction of (1*S*,2*S*)-*trans*-aminocyclohexanol with 2,3-anthracenedicarboxylic anhydride in the presence of trimethylamine, as reported by Ohruí *et al.* (Scheme 2.12, A).<sup>113</sup> (1*S*,2*S*)-2-(2,3-anthracenedicarboximido)cyclohexanol esters of TBSA enantiomers were synthesized using EDC/DMAP esterification (Scheme 2.12, B).

### 1. Synthesis of Ohruí's reagent



### 2. Synthesis of corresponding TBSA diastereomers



**Scheme 2.12** Synthesis of (1*S*, 2*S*)-2-(2,3-anthracenedicarboximido) cyclohexanol and the corresponding TBSA diastereomers **240** and **241**. Reagents and conditions: (i) toluene, DMF, Et<sub>3</sub>N, reflux, overnight, 95%; (ii) **233**, EDC/DMAP, overnight, CH<sub>2</sub>Cl<sub>2</sub> 65%; (iii) **233**, EDC/DMAP, overnight, CH<sub>2</sub>Cl<sub>2</sub>, 63%.

#### 2.9.1 <sup>1</sup>H NMR analysis of the cyclohexanol esters of TBSA

**240** and **241** were mixed in a 2:1 ratio and the <sup>1</sup>H NMR spectra were acquired in a range of deuterated solvents: d-chloroform, d<sub>4</sub>-methanol, d<sub>6</sub>-benzene, and DMSO-d<sub>6</sub>. NMR spectra were obtained at room temperature. The most promising result was obtained in CDCl<sub>3</sub>, for which we observed a slight splitting of the branched methyl signal at 0.73 ppm. We next investigated variable temperature NMR in this solvent. At -4.5 °C we observed a difference in chemical shift of Δδ 0.0042 ppm for the branched methyl group protons of **240** and **241** (Figure 2.20). By way of comparison, Ohruí's group observed a Δδ 0.003 ppm for the methyl groups of the pair of diastereoisomeric esters of (*S*)-11-methyltridecanoic acid ester with (1*R*,2*R*)-2-(2,3-anthracenedicarboximido)cyclohexanol

or (1*S*,2*S*)-2-(2,3-anthracenedicarboximido)cyclohexanol, in deuterated chloroform at -20 °C.

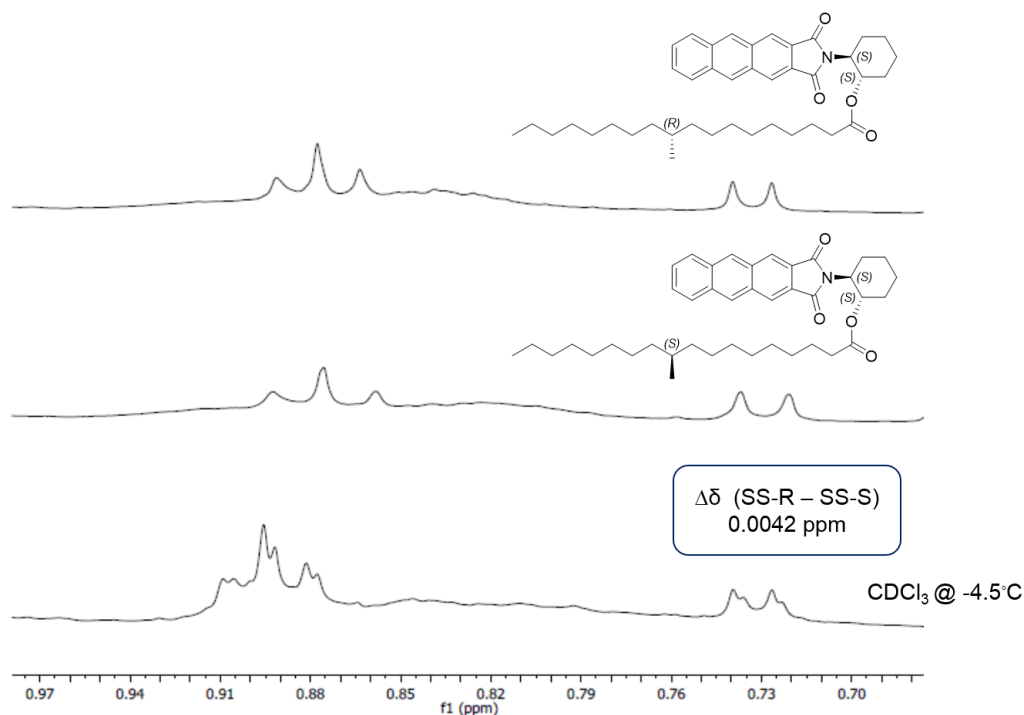


**Figure 2.20** <sup>1</sup>H-NMR analysis of TBSA esters of (1*S*,2*S*)-2-(2,3-anthracenedicarboximido) cyclohexanol **240** and **241** in deuterated chloroform at -4.5°C.

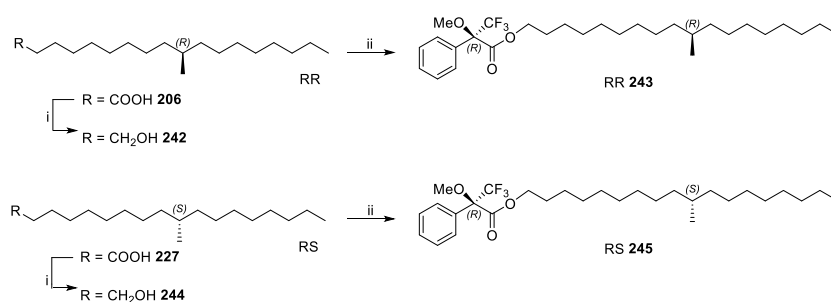
As can be seen in Figure 2.20, the observed  $\Delta\delta$  of 0.0042 ppm is sufficient to be observed, however, the separation was insufficient to allow baseline separation of the two peaks. Moreover, the separation was so small as to not allow convincing discrimination of the two diastereomers on the basis of chemical shift difference alone, as independently prepared samples had much greater chemical shift variation, presumably as a result of concentration effects. Accordingly, these results were not deemed to be sufficient to merit further studies of natural TBSA using this particular CDA.

## 2.9.2 Mosher's ester synthesis and NMR analysis

We wanted to explore if another commonly used CDA, namely esters of Mosher's acid, could provide better resolution of the TBSA enantiomers. Thus, we reduced the fatty

acids to the corresponding alcohols and coupled them with Mosher's acid. The resulting esters were combined and the proton spectra acquired for a non-equal mixture of the diastereomers in various solvents (Figure 2.21). Of the various solvent examined, the best results were obtained with DMSO-d<sub>6</sub>, wherein a  $\Delta\delta$  of 0.004 ppm was observed for the branched methyl protons of the esters. However, like the situation with the Ohruí's esters discussed earlier, this did not provide baseline separation between the peaks. The <sup>1</sup>H NMR analysis was further complicated by the presence of unresolvable impurity (indicated with an \* in Figure 2.21). As the <sup>19</sup>F NMR chemical shift range is greater than that of <sup>1</sup>H, we also acquired a fluorine spectrum of the mixture of the esters; however no chemical shift difference was observed (Figure 2.21).

#### A. Synthesis of Mosher's esters



#### B. NMR analysis

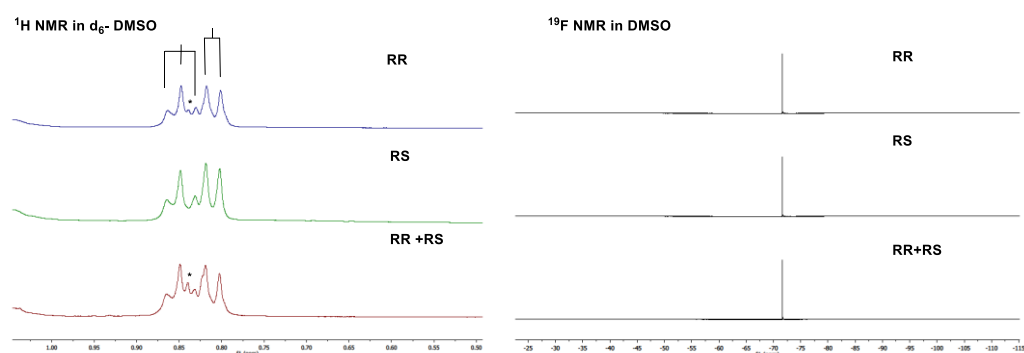


**Figure 2.21** A) Synthesis of Mosher's esters of TBSA derived alcohols; B) <sup>1</sup>H and <sup>19</sup>F NMR analysis of Mosher's esters of TBSA-derived alcohols in DMSO-d<sub>6</sub>. Reagents and conditions. (i) BH<sub>3</sub>.Me<sub>2</sub>S, 5h, 95%, (ii) *R*-242, DCC, DMAP, 63-65%.

## 2.10 Summary

TBSA is one of the simplest methyl branched fatty acids found in *M.tb*. The stereochemistry of recrystallized natural TBSA was assigned in the 1940s based on a small intrinsic optical rotation value and mixed melting point analysis and has never been revisited since then. Herein we report a very short and efficient route to access both the enantiomers of TBSA from commercially available chiral pool starting materials: (*R*) and (*S*)-citronellyl bromide. (*R*)-Citronellyl bromide was subjected to copper mediated cross-coupling with hexyl magnesium bromide and the resulting alkene was further elongated using ethyl heptenoate/heptenoic acid in presence of Hoveyda Grubbs II generation catalyst, which also acts as a catalyst for hydrogenation, facilitating tandem cross metathesis/hydrogenation in the same pot.

With the synthetic antipodes in hand, we attempted chiral discrimination of the enantiomers using NMR methods. Towards this end, we synthesized TBSA esters of Ohruí's reagent (an anthracene-based chiral derivatizing reagent) and could detect a very small chemical shift difference of  $\Delta\delta$  0.0042 ppm in the branched methyl protons of the diastereomers, which was insufficient to allow baseline separation. We next examined NMR discrimination using Mosher's acid. Here too only a very small chemical shift difference in the methyl peaks could be observed, again without baseline separation, in the  $^1\text{H}$  NMR but not in the  $^{19}\text{F}$  NMR spectra. While disappointing, future work could examine the use of NMR shift reagent or chiral solvents.



## 2.11 Experimental

### General methods

Proton ( $^1\text{H}$  NMR, 400 or 500 MHz), proton-decoupled carbon-13 ( $^{13}\text{C}$  NMR, 100 or 125 MHz) nuclear magnetic resonance spectra were obtained in deuteriochloroform, methanol- $d_4$  ( $\text{CD}_3\text{OD}$ ) or  $\text{DMSO-}d_6$  with residual protonated solvent or solvent carbon signals as internal standards. Proton peak assignments were performed using two-dimensional NMR techniques ( $1\text{H-}1\text{H}$  COSY and HMQC). Abbreviations for multiplicity are s, singlet; d, doublet; t, triplet; q, quartet; m, multiplet. Flash chromatography was carried out on silica gel 60 according to the procedure of Still *et al.*<sup>115</sup> Analytical thin layer chromatography (t.l.c.) was conducted on aluminium-backed 2 mm thick silica gel 60 F<sub>254</sub> and chromatograms were visualized with ceric ammonium molybdate (Hanessian's stain), potassium permanganate or 5%  $\text{H}_2\text{SO}_4/\text{MeOH}$ , with charring as necessary. High resolution mass spectra (HRMS) were obtained using an ESI-TOF-MS; all samples were run using 0.1% formic acid. Dry  $\text{CH}_2\text{Cl}_2$ , THF, and  $\text{Et}_2\text{O}$  were obtained from a dry solvent apparatus (Glass Contour of SG Water, Nashua, U.S.A.) as per the procedure of Pangborn *et al.*<sup>116</sup> Dry DMF was dried over 4 Å molecular sieves. Pet. spirits refers to petroleum ether, boiling range 40-60 °C.

#### **(R)-2,6-Dimethyltetradecene (210)**<sup>100</sup>

Hexylmagnesium bromide (3.14 ml, 4.56 mmol) (2.0 M in  $\text{Et}_2\text{O}$ ) was added to a solution of (*S*)-citronellyl bromide (0.23 ml, 1.14 mmol) in dry  $\text{Et}_2\text{O}$  (2.3 ml) at  $-78$  °C followed by dilithium tetrachlorocuprate ( $\text{Li}_2\text{CuCl}_4$ ) (0.1 M in THF) (1.94 ml, 0.12 mmol). The solution was allowed to warm to room temperature and stirred for 36 h. The reaction mixture was quenched with sat aq.  $\text{NH}_4\text{Cl}$ , extracted with  $\text{Et}_2\text{O}$ , and the organic phase washed with brine, dried ( $\text{MgSO}_4$ ) and concentrated under reduced pressure. Flash

chromatography (0.5% Et<sub>2</sub>O:petroleum ether) of the residue afforded **210** as a colorless oil (0.24 g, 95%); [ $\alpha$ ]<sub>D</sub><sup>22</sup> +0.75 (*c* 0.5 in CHCl<sub>3</sub>) (lit.<sup>117</sup> [ $\alpha$ ]<sub>D</sub><sup>25</sup> 1.5 in CHCl<sub>3</sub>); <sup>1</sup>H NMR (400 MHz, CDCl<sub>3</sub>)  $\delta$  0.88–0.83 (6 H, m, 2  $\times$  CH<sub>3</sub>), 1.15–1.06 (2 H, m, CH<sub>2</sub>), 1.31–1.22 (15 H, m, 7  $\times$  CH<sub>2</sub>, 1  $\times$  CH), 1.60 (3 H, s, CH<sub>3</sub>), 1.68 (3 H, s, CH<sub>3</sub>), 1.95 (2 H, m, CHCH<sub>2</sub>), 5.10 (1 H, t, *J* 7.0 Hz, CH=C); <sup>13</sup>C NMR (101 MHz, CDCl<sub>3</sub>)  $\delta$  14.2, 17.7, 19.2, 22.8, 25.7, 27.1, 29.5, 29.8, 30.1, 32.0, 32.5, 37.1, 37.3, 125.2, 131.0; HRMS calcd for C<sub>16</sub>H<sub>32</sub> [M+H]<sup>+</sup> 225.2538, found 225.2534.

#### **Ethyl (*R*)-10-methyloctadecanoate (219)**<sup>81</sup>

Hoveyda Grubbs 2<sup>nd</sup> generation catalyst (HG-II) (2.79 mg, 4 mol%) was added to a solution of **210** (0.025 g, 0.11 mmol) and ethyl heptenoate (0.059 g, 0.33 mmol) in dry dichloromethane (1.14 ml) and stirred for 24 h under reflux. Upon consumption of starting material, the reaction mixture was concentrated under reduced pressure. EtOAc (5.0 ml) was added to the residue and the solution was subjected to hydrogenation under high pressure (37.5 bar) in a Buchi® hydrogenator overnight at room temp after which the solvent was removed under reduced pressure. Flash chromatography (2% Et<sub>2</sub>O/petroleum spirits) of the crude mixture afforded the title compound as a colourless oil (0.028 g, 76%); [ $\alpha$ ]<sub>D</sub><sup>22</sup> -0.14 (*c* 0.5 in CHCl<sub>3</sub>) (lit.<sup>81</sup> [ $\alpha$ ]<sub>D</sub><sup>25</sup> -0.16 in CHCl<sub>3</sub>); <sup>1</sup>H NMR (400 MHz, CDCl<sub>3</sub>)  $\delta$  0.82 (3 H, d, *J* 6.5 Hz, CHCH<sub>3</sub>), 0.87 (3 H, t, *J* 6.8 Hz, CH<sub>3</sub>), 1.10–1.03 (2 H, m, CH<sub>2</sub>), 1.31–1.20 (28 H, m, 12  $\times$  CH<sub>2</sub>, 1  $\times$  CH, COOCH<sub>2</sub>CH<sub>3</sub>), 1.61 (2 H, m, COCH<sub>2</sub>CH<sub>2</sub>), 2.27 (2 H, t, *J* 7.6 Hz, COCH<sub>2</sub>), 4.11 (2 H, q, *J* 7.1 Hz, C=OOCH<sub>2</sub>); <sup>13</sup>C NMR (101 MHz, CDCl<sub>3</sub>)  $\delta$  14.2, 14.4, 19.8, 22.8, 25.1, 27.1, 27.2, 29.3, 29.4, 29.5, 29.6, 29.8, 30.0, 30.1, 32.0, 32.8, 32.8, 34.5, 37.2, 60.2, 174.0 (C=O); HRMS calcd for C<sub>21</sub>H<sub>42</sub>O<sub>2</sub> [M+H]<sup>+</sup> 327.3218, found 327.3220.

#### **(*R*)-10-Methyloctadecanoic acid (206)**<sup>81</sup>

**(a) From ethyl (*R*)-10-methyloctadecanoate (219):** 2 M KOH (0.085 g, 1.53 mmol) was added to a solution of the ethyl ester (0.050 g, 0.153 mmol) in MeOH/THF (1:1, 0.8 ml) and stirred under reflux overnight. The solution was acidified with aq citric acid (1 M), extracted with EtOAc, and the organic phase washed with brine, dried (MgSO<sub>4</sub>) and concentrated under reduced pressure to afford **206** as a colorless oil (0.044 g, 97%); [ $\alpha$ ]<sup>25</sup><sub>D</sub> -0.9 (*c* 1.0 in CHCl<sub>3</sub>) (lit.<sup>117</sup> [ $\alpha$ ]<sup>25</sup><sub>D</sub> -0.34 in CHCl<sub>3</sub>); <sup>1</sup>H NMR (400 MHz, CDCl<sub>3</sub>)  $\delta$  0.83 (3 H, d, *J* 6.5 Hz, CHCH<sub>3</sub>), 0.88 (3 H, t, *J* 6.8 Hz, CH<sub>2</sub>CH<sub>3</sub>), 1.12–1.04 (2 H, m, CH<sub>2</sub>), 1.36–1.21 (25 H, m, 12  $\times$  CH<sub>2</sub>, 1  $\times$  CH), 1.67–1.59 (2 H, m, OCOCH<sub>2</sub>CH<sub>2</sub>), 2.35 (2 H, t, *J* 7.5 Hz, COCH<sub>2</sub>); <sup>13</sup>C NMR (101 MHz, CDCl<sub>3</sub>)  $\delta$  14.2, 19.8, 22.8, 24.8, 27.1, 27.2, 29.2, 29.4, 29.5, 29.6, 29.8, 30.0, 30.1, 32.0, 32.8, 34.0, 37.2, 179.5 (C=O; HRMS calcd for C<sub>19</sub>H<sub>38</sub>O<sub>2</sub> [M+H]<sup>+</sup> 298.5110, found 298.5113.

**(b) From 210:** Hoveyda Grubbs 2<sup>nd</sup> generation catalyst (HG-II) (2.80mg, 4 mol%) was added to a solution of **210** (0.025 g, 0.114 mmol) and heptenoic acid **220** (0.059 g, 0.334 mmol) in dry CH<sub>2</sub>Cl<sub>2</sub> (1.14 ml) and stirred for 24 h under reflux. The reaction mixture was concentrated under reduced pressure. EtOAc (5.0 ml) was added to the residue and the solution was subjected to hydrogenation under high pressure (37.5 bar) in a Buchi@ hydrogenator overnight at room temperature after which solvent was removed under reduced pressure. Flash chromatography (2% Et<sub>2</sub>O/petroleum spirits) of the crude mixture afforded **206** as a colorless oil (0.025 g, 73%).

**(*S*)-2,6-Dimethyltetradecene (225)<sup>100</sup>**

Hexylmagnesium bromide (3.13 ml, 4.56 mmol) (2.0 M in Et<sub>2</sub>O) was added to a solution of (*R*)-citronellyl bromide **224** (0.23 ml, 1.14 mmol) in dry diethyl ether (2.3 ml) at -78 °C followed by dilithium tetrachlorocuprate (Li<sub>2</sub>CuCl<sub>4</sub>) (0.1 M in THF) (1.94 ml, 0.12 mmol). The solution was allowed to warm to room temperature and stirred for 36 h. The

reaction mixture was quenched with sat aq.NH<sub>4</sub>Cl, extracted with diethyl ether and the organic phase washed with brine, dried (MgSO<sub>4</sub>) and concentrated under reduced pressure. Flash chromatography (0.5% Et<sub>2</sub>O:petroleum ether) of the residue afforded **225** as a colorless oil (0.23 g, 95%); [ $\alpha$ ]<sup>25</sup><sub>D</sub> -1.5 (*c* 0.5 in CHCl<sub>3</sub>) (lit.<sup>100</sup> [ $\alpha$ ]<sup>25</sup><sub>D</sub> -2.0 in CHCl<sub>3</sub>) <sup>1</sup>H NMR (400 MHz, CDCl<sub>3</sub>):  $\delta$  0.88–0.83 (6 H, m, 2  $\times$  CH<sub>3</sub>), 1.15–1.06 (2 H, m, CH<sub>2</sub>), 1.31–1.22 (15 H, m, 7  $\times$  CH<sub>2</sub>, 1  $\times$  CH), 1.60 (3 H, s, CH<sub>3</sub>), 1.68 (3 H, s, CH<sub>3</sub>), 1.95 (2 H, m, CHCH<sub>2</sub>), 5.10 (1 H, t, *J* 7.0 Hz, CH=C); <sup>13</sup>C NMR (101 MHz, CDCl<sub>3</sub>)  $\delta$  14.2, 17.7, 19.2, 22.8, 25.7, 27.1, 29.5, 29.8, 30.1, 32.0, 32.5, 37.1, 37.3, 125.2, 131.0; C<sub>16</sub>H<sub>32</sub> [M+H]<sup>+</sup> 225.2538, found 225.2536

#### **Ethyl (*S*)-10-methyl octadecanoate (226)**<sup>81</sup>

Hoveyda Grubbs 2<sup>nd</sup> gen catalyst (H.G-II) (2.79 mg, 4.46  $\mu$ g) was added to a solution of **225** (0.025 g, 0.0114 mmol) and ethyl heptenoate (0.052 g, 0.33 mmol) in dry dichloromethane (1.14 ml) and stirred for 24 h under reflux. Upon consumption of starting material, the reaction mixture was concentrated under reduced pressure. EtOAc (5.0 ml) was added to the residue and the solution was subjected to hydrogenation under high pressure (37.5 bar) in a Buchi® hydrogenator overnight at room temp after which the solvent was removed under reduced pressure. Flash chromatography (2 % diethyl ether/petroleum spirits) of the crude mixture afforded **226** a colorless oil (0.031g, 85%); [ $\alpha$ ]<sup>25</sup><sub>D</sub> + 0.87 (*c* 0.5 in CHCl<sub>3</sub>) (lit.<sup>108</sup> [ $\alpha$ ]<sup>25</sup><sub>D</sub> +0.14 in CHCl<sub>3</sub>); <sup>1</sup>H NMR (400 MHz, CDCl<sub>3</sub>)  $\delta$  0.82 (3 H, d, *J* 6.5 Hz, CHCH<sub>3</sub>), 0.87 (3 H, t, *J* 6.8 Hz, CH<sub>3</sub>), 1.10–1.03 (2 H, m, CH<sub>2</sub>), 1.31–1.20 (28 H, m, 12  $\times$  CH<sub>2</sub>, 1  $\times$  CH, COOCH<sub>2</sub>CH<sub>3</sub>), 1.61 (2 H, m, COCH<sub>2</sub>CH<sub>2</sub>), 2.27 (2 H, t, *J* 7.6 Hz, COCH<sub>2</sub>), 4.11 (2 H, q, *J* 7.1 Hz, C=OOCH<sub>2</sub>); <sup>13</sup>C NMR (101 MHz, CDCl<sub>3</sub>)  $\delta$  14.2, 14.4, 19.8, 22.8, 25.1, 27.1, 27.2, 29.3, 29.4, 29.5, 29.6, 29.8, 30.0, 30.1,

32.0, 32.8, 32.8, 34.5, 37.2, 60.2, 174.0 (C=O); HRMS calcd for C<sub>21</sub>H<sub>42</sub>O<sub>2</sub> [M+H]<sup>+</sup> 327.3218, found 327.3216.

**(S)-10-Methyl octadecanoic acid (227)**<sup>81</sup>

2 M KOH (0.083 g, 1.47 mmol) solution was added to a solution of the ethyl ester **226** (0.032 g, 0.097 mmol) in MeOH/THF (1:1, 2 ml) and stirred under reflux overnight. The solution was acidified with citric acid (1 M), extracted with EtOAc, washed with brine, dried (MgSO<sub>4</sub>) and concentrated under reduced pressure to afford (*S*)-TBSA as colorless oil (0.028 g, 98%); [ $\alpha$ ]<sub>D</sub><sup>25</sup> + 0.43 (*c* 0.5 in CHCl<sub>3</sub>) (lit.<sup>100</sup> [ $\alpha$ ]<sub>D</sub><sup>25</sup> 0.21 in CHCl<sub>3</sub>) <sup>1</sup>H NMR (400 MHz, CDCl<sub>3</sub>)  $\delta$  0.83 (3 H, d, *J* 6.5 Hz, CHCH<sub>3</sub>), 0.88 (3 H, t, *J* 6.8 Hz, CH<sub>3</sub>), 1.12 – 1.04 (2 H, m, CH<sub>2</sub>), 1.36 – 1.21 (25 H, m, 12 x CH<sub>2</sub>, 1 x CH), 1.67 – 1.59 (2 H, m, COCH<sub>2</sub>CH<sub>2</sub>), 2.35 (2 H, t, *J* 7.5 Hz, COCH<sub>2</sub>); <sup>13</sup>C NMR (101 MHz, CDCl<sub>3</sub>)  $\delta$  14.2, 19.8, 22.8, 24.8, 27.3, 29.2, 29.4, 29.5, 29.6, 29.8, 30.0, 30.1, 32.0, 32.8, 34.0, 37.2, 179.4 (C=O); HRMS calcd for C<sub>19</sub>H<sub>38</sub>O<sub>2</sub> [M+H]<sup>+</sup> 298.5110 found 288.5111.

**(1*S*,2*S*)-2-(2,3-Anthracenedicarboximido)cyclohexanol (233)**<sup>113</sup>

2,3-Anthracenedicarboxylic acid anhydride **238** (100 mg, 0.403 mmol) was added to dry toluene (35 mL) and heated to reflux (oil bath, 140 °C). A solution of (1*S*,2*S*)-2-Aminocyclohexanol **239** (65 mg, 0.564 mmol) in dry DMF (10 mL) was added to the reaction mixture. Dry DIPEA (3 mL) was then added and the resulting solution refluxed for 16 h. Most of the solvent (35 mL) was then removed using a Dean-Stark tube and the resulting solution cooled to ambient temperature. Ethyl acetate (70 mL) was added and the resulting solution washed with 0.2 M NaOH (50 mL), 0.2 M HCl (50 mL) and saturated NaHCO<sub>3</sub> (50 mL). The organic phase was then dried over anhydrous Na<sub>2</sub>SO<sub>4</sub> and concentrated in vacuo to yield **233** as a fine yellow powder (130 mg, 95%). [ $\alpha$ ]<sub>D</sub><sup>25</sup> = –31.2 (*c* 0.5, DMSO) (lit.<sup>113</sup> [ $\alpha$ ]<sub>D</sub><sup>25</sup> –39.0 in DMF); <sup>1</sup>H NMR (500 MHz, CDCl<sub>3</sub>)  $\delta$  1.32–

1.17 (3 H, m, H6(ax) + H5(eq) + H5(ax)), 1.64–1.73 (3 H, m, H3(ax) + H4(eq) + H4(ax)), 1.90–1.96 (1 H, m, H6(eq)), 2.06–2.14 (1 H, m, H3(eq)), 3.84 (1 H, ddd,  $J$  12.8, 9.7, 3.4 Hz, H2), 4.06–4.12 (1 H, m, H1), 4.93 (1 H, d,  $J$  4.7 Hz, OH), 7.63–7.64 (2 H, m, H9), 8.13–8.15 (2 H, m, H10), 8.59 (2 H, s, H7), 8.87 (2 H, s, H8);  $^{13}\text{C}$  NMR (DMSO- $d_6$ , 125 MHz):  $\delta$  24.2, 25.0, 28.2, 34.7, 57.3, 67.6, 125.0, 126.6, 127.5, 128.3, 129.9, 131.6, 132.6, 167.5; HRMS calcd for  $\text{C}_{22}\text{H}_{19}\text{NO}_3$   $[\text{M} + \text{H}]^+$  346.1438, found 346.1437.

**(1*S*,2*S*)-1-((10*R*)-Tuberculostearyl)-2-(2,3-anthracenedicarboximido)  
cyclohexanoate (240)**

10-(*R*)-Methyloctadecanoic acid **206** (10.0 mg, 76  $\mu\text{mol}$ ) and EDCI·HCl (24.0 mg, 124  $\mu\text{mol}$ ) were dissolved in a 1: 1: 1 mixture of dry  $\text{CH}_2\text{Cl}_2$ , toluene and DMF (1.5 mL). Alcohol **233** (25 mg, 82  $\mu\text{mol}$ ) was added, followed by DMAP (3.1 mg, 24  $\mu\text{mol}$ ). The resulting cloudy yellow solution was stirred at ambient temperature for 16 h. The reaction mixture was diluted with EtOAc (15 mL) and washed with sat.  $\text{NaHCO}_3$  (10 mL), 10% citric acid (10 mL), water (5 mL) and brine (10 mL), dried over anhydrous  $\text{Na}_2\text{SO}_4$  and concentrated in vacuo. The crude product was subjected to column chromatography (25% EtOAc: pet.spirits) to afford the product as yellow solid (23 mg, 65%).  $[\alpha]_D^{25} = -35$  ( $c$  0.5, DMSO);  $^1\text{H}$  NMR ( $\text{CDCl}_3$ , 500 MHz):  $\delta$  0.83 (3 H, d,  $J$  6.5 Hz,  $\text{CHCH}_3$ ), 0.89 (3 H, t,  $J$  7.4 Hz,  $\text{CH}_3$ ), 1.21–1.26 (26 H, m, 13 x  $\text{CH}_2$ ), 1.59–1.20 (5 H, m,  $\text{NCHCH(ax)} + \text{NCHCH}_2\text{CH(eq)} + \text{OCHCH}_2\text{CH(ax)} + \text{COCH}_2\text{CH}_2$ ), 1.82–1.91 (3 H, m,  $\text{OCHCH(ax)} + \text{OCHCH}_2\text{CH(eq)} + \text{NCHCH}_2\text{CH(eq)}$ ), 2.04–2.14 (2 H, m,  $\text{COCH}_2$ ), 2.21–2.25 (1 H, m,  $\text{NCHCH(eq)}$ ), 2.48 (1 H, m,  $\text{OCHCH(eq)}$ ), 4.31 (1 H, ddd,  $J$  12.6, 10.5, 4.2 Hz, OCH), 5.57 (1 H, ddd,  $J$  10.7, 4.7, 4.7 Hz, NCH), 7.60–7.62 (2 H, m, H9), 8.06–8.08 (2 H, m, H10), 8.48 (2 H, s, H7), 8.61 (2 H, s, H8);  $^{13}\text{C}$  NMR ( $\text{CDCl}_3$ , 125 MHz):  $\delta$  11.3, 19.0, 24.1, 25.3, 25.5, 26.5, 26.8, 27.3, 27.5, 28.1, 28.3, 38.2, 28.7, 29.4, 31.9, 34.1, 34.7, 36.2,

54.3, 71.7, 125.9, 126.5, 127.6, 128.6, 130.2, 132.2, 133.4, 167.8, 173.2; HRMS calcd for  $C_{41}H_{54}NO_4Na$   $[M + Na]^+$  648.4023, found 648.4025.

**(1*S*,2*S*)-1-((10-*S*)-Tuberculostearyl)-2-(2,3**

**anthracenedicarboximido)cyclohexanoate (241)**

Same protocol as above. Product isolated as a yellow solid (22 mg, 63%).  $[\alpha]_D^{25} = -35$  (*c* 0.5, DMSO);  $^1H$  NMR ( $CDCl_3$ , 500 MHz):  $\delta$  0.83 (3 H, d, *J* 6.5 Hz,  $CHCH_3$ ), 0.89 (3 H, t, *J* 7.4 Hz,  $CH_3$ ), 1.21–1.26 (26 H, m, 13 x  $CH_2$ ), 1.59–1.20 (5 H, m,  $NCHCH(ax) + NCHCH_2CH(eq) + OCHCH_2CH(ax) + COCH_2CH_2$ ), 1.82–1.91 (3 H, m,  $OCHCH(ax) + OCHCH_2CH(eq) + NCHCH_2CH(eq)$ ), 2.04–2.14 (2 H, m,  $COCH_2$ ), 2.21–2.25 (1 H, m,  $NCHCH(eq)$ ), 2.48 (1 H, m,  $OCHCH(eq)$ ), 4.31 (1 H, ddd, *J* 12.6, 10.5, 4.2 Hz, OCH), 5.57 (1 H, ddd, *J* 10.7, 4.7, 4.7 Hz, NCH), 7.60–7.62 (2 H, m, H9), 8.06–8.08 (2 H, m, H10), 8.48 (2 H, s, H7), 8.61 (2 H, s, H8);  $^{13}C$  NMR ( $CDCl_3$ , 125 MHz):  $\delta$  11.3, 14.2, 19.8, 22.8, 24.8, 27.3, 29.2, 29.4, 29.5, 29.6, 29.8, 30.0, 30.1, 32.0, 32.8, 34.0, 37.2, 62.8, 54.3, 71.7, 125.9, 126.5, 127.6, 128.6, 130.2, 132.2, 133.4, 167.8, 173.2; HRMS calcd for  $C_{41}H_{54}NO_4Na$   $[M + Na]^+$  648.4023, found 648.4026.

**10-(*R*)-Methyloctadecanol (242)**

10-(*R*)-Methyloctadecnoic acid (15 mg, 50  $\mu$ mol) and  $BH_3 \cdot Me_2S$  (5.73 mg, 75  $\mu$ mol) were dissolved in THF (1 ml) and stirred at room temperature for 5 hours. The reaction mixture was quenched with methanol and solvent was evaporated under vacuum. The crude residue was subjected to chromatography (5 % methanol/ $CH_2Cl_2$ ) to afford **242** as a colorless oil (13mg, 70 %).  $^1H$  NMR ( $CDCl_3$ , 500 MHz): 0.83 (3 H, d, *J* 6.5 Hz,  $CHCH_3$ ), 0.88 (3 H, t, *J* 6.6 Hz,  $CH_3$ ), 1.08 (2 H, s, 1 x  $CH_2$ ), 1.26–1.28 (27 H, m, 13 x  $CH_2$ , 1 x CH), 1.56 (2 H, m,  $\beta$ - $CH_2$ ), 3.64 (2 H, t, *J* 6.6 Hz,  $\alpha$ - $CH_2$ );  $^{13}C$  NMR ( $CDCl_3$ , 125 MHz):

$\delta$  14.2, 19.8, 22.8, 24.8, 27.3, 29.2, 29.4, 29.5, 29.6, 29.8, 30.0, 30.1, 32.0, 32.8, 34.0, 37.2, 62.8; HRMS calcd for C<sub>19</sub>H<sub>40</sub>O [M +H]<sup>+</sup> 284.3079, found 284.3076

#### **10-(S)-Methyloctadecanol (244)**

10-(S)-Methyloctadecnoic acid (15 mg, 50  $\mu$ mol) and BH<sub>3</sub>.Me<sub>2</sub>S (5.73 mg, 75  $\mu$ mol) were dissolved in THF (1 ml) and stirred at room temperature for 5 hours. The reaction mixture was quenched with methanol and solvent was evaporated under vacuum. The crude residue was subjected to chromatography (5 % methanol/CH<sub>2</sub>Cl<sub>2</sub>) to afford colorless oil (10 mg, 68 %). <sup>1</sup>H NMR (CDCl<sub>3</sub>, 500 MHz): 0.83 (3 H, d, *J* 6.5 Hz, CHCH<sub>3</sub>), 0.88 (3 H, t, *J* 6.6 Hz, CH<sub>3</sub>), 1.08 (2 H, s, 1 x CH<sub>2</sub>), 1.26-1.28 (27 H, m, 13 x CH<sub>2</sub>, 1 x CH), 1.56 (2 H, m,  $\beta$ -CH<sub>2</sub>), 3.64 (2 H, t, *J* 6.6 Hz,  $\alpha$ -CH<sub>2</sub>); <sup>13</sup>C NMR (CDCl<sub>3</sub>, 125 MHz):  $\delta$  14.2, 19.8, 22.8, 24.8, 27.3, 29.2, 29.4, 29.5, 29.6, 29.8, 30.0, 30.1, 32.0, 32.8, 34.0, 37.2, 62.8; HRMS calcd for C<sub>19</sub>H<sub>40</sub>O [M +H]<sup>+</sup> 284.3079, found 284.3076

#### **(R)-(+)- $\alpha$ -Methoxy- $\alpha$ -trifluoromethylphenylacetate esters of (R)-10-methyloctadecanoate (243)**

A solution of (R)-(+)- $\alpha$ -Methoxy- $\alpha$ -trifluoromethylphenylacetic acid (31.9 mg, 0.136 mmol) and DMAP (16.6 mg, 0.136 mmol) in 2 ml of dry CH<sub>2</sub>Cl<sub>2</sub> was stirred, and cooled in an ice bath. A solution of **242** (12.7 mg, 0.044 mmol) and DCC (28.12 mg, 0.136 mmol) in 3 ml of CH<sub>2</sub>Cl<sub>2</sub> was added to the reaction mixture and stirred overnight. The reaction mixture was diluted with CH<sub>2</sub>Cl<sub>2</sub>, washed with water, dried (MgSO<sub>4</sub>) and concentrated in vacuo. The resulting residue was subjected to flash chromatography (10% EtOAc: Pet. spirits) to afford **243** as a colorless oil. (15.4 mg, 65%); <sup>1</sup>H NMR (DMSO-d<sub>6</sub>, 500 MHz):  $\delta$  0.83 (3 H, d, *J* 6.5 Hz, CHCH<sub>3</sub>), 0.88 (3 H, t, *J* 6.6 Hz, CH<sub>3</sub>), 1.08 (2 H, s, 1 x CH<sub>2</sub>), 1.26-1.28 (27 H, m, 14 x CH<sub>2</sub>, 1 x CH), 1.64-1.73 (2 H, m,  $\beta$ -CH<sub>2</sub>), 3.56 (3 H, s, OCH<sub>3</sub>), 4.25-4.37 (2 H, m,  $\alpha$ -CH<sub>2</sub>), 7.37-7.43 (3 H, m, aromatic), 7.50-7.54 (2 H, m,



aromatic);  $^{13}\text{C}$  NMR (DMSO- $d_6$ , 125 MHz):  $\delta$  14.2, 19.8, 22.8, 24.8, 27.3, 29.2, 29.4, 29.5, 29.6, 29.8, 30.0, 30.1, 32.0, 32.8, 34.0, 37.2, 55.3, 92.5, 124.1, 127.5, 128.1, 129.1, 129.1, 128.1, 131.9, 166.4; HRMS calcd for  $\text{C}_{29}\text{H}_{47}\text{F}_3\text{O}_3$   $[\text{M} + \text{H}]^+$  500.3477, found 500.3475

**(R)-(+)- $\alpha$ -Methoxy- $\alpha$ -trifluoromethylphenylacetate esters of (S)-10-methyl octadecanoate (245)**

Protocol same as above for **243**. Product isolated as colorless oil (13.5 mg, 63%);  $^1\text{H}$  NMR (DMSO- $d_6$ , 500 MHz):  $\delta$  0.83 (3 H, d,  $J$  6.5 Hz,  $\text{CHCH}_3$ ), 0.88 (3 H, t,  $J$  6.6 Hz,  $\text{CH}_3$ ), 1.08 (2 H, s, 1 x  $\text{CH}_2$ ), 1.26-1.28 (27 H, m, 12 x  $\text{CH}_2$ , 1 x  $\text{CH}$ ), 1.64-1.73 (2 H, m,  $\beta$ - $\text{CH}_2$ ), 3.56 (3 H, s,  $\text{OCH}_3$ ), 4.25-4.37 (2 H, m,  $\alpha$ - $\text{CH}_2$ ), 7.37-7.43 (3 H, m, aromatic), 7.50-7.54 (2 H, m, aromatic);  $^{13}\text{C}$  NMR ( $\text{CDCl}_3$ , 125 MHz):  $\delta$  14.2, 19.8, 22.8, 24.8, 27.3, 29.2, 29.4, 29.5, 29.6, 29.8, 30.0, 30.1, 32.0, 32.8, 34.0, 37.2, 55.3, 92.5, 124.1, 127.5, 128.1, 129.1, 129.1, 128.1, 131.9, 166.4; HRMS calcd for  $\text{C}_{29}\text{H}_{47}\text{F}_3\text{O}_3$   $[\text{M} + \text{H}]^+$  500.3477, found 500.3475



## **Chapter 3**

### **Synthesis of *Mycobacterium. tuberculosis* phosphatidylglycerol**

### 3.1 Introduction

Phospholipids (PLs) are anionic lipids found within biological membranes. Glycerophospholipids are characterized by a glycerol scaffold, with one or two acyl chains esterified at sn-1 and sn-2 carbons and a polar phosphate head group at the sn-3 carbon of the glycerol backbone. Modification of the polar head group distinguishes the type of PL (Figure 3.1). Plants have larger amounts of phosphatidylglycerols (PG), whereas animals have larger amounts of phosphatidylethanolamine (PE).<sup>118</sup> Other PLs include phosphatidylcholine (PC), phosphatidylinositol (PI), phosphatidylserine (PS), and diphosphatidylglycerol (cardiolipin).<sup>119</sup> For the purpose of this chapter, we are interested in PGs, particularly those from *M.tb*.

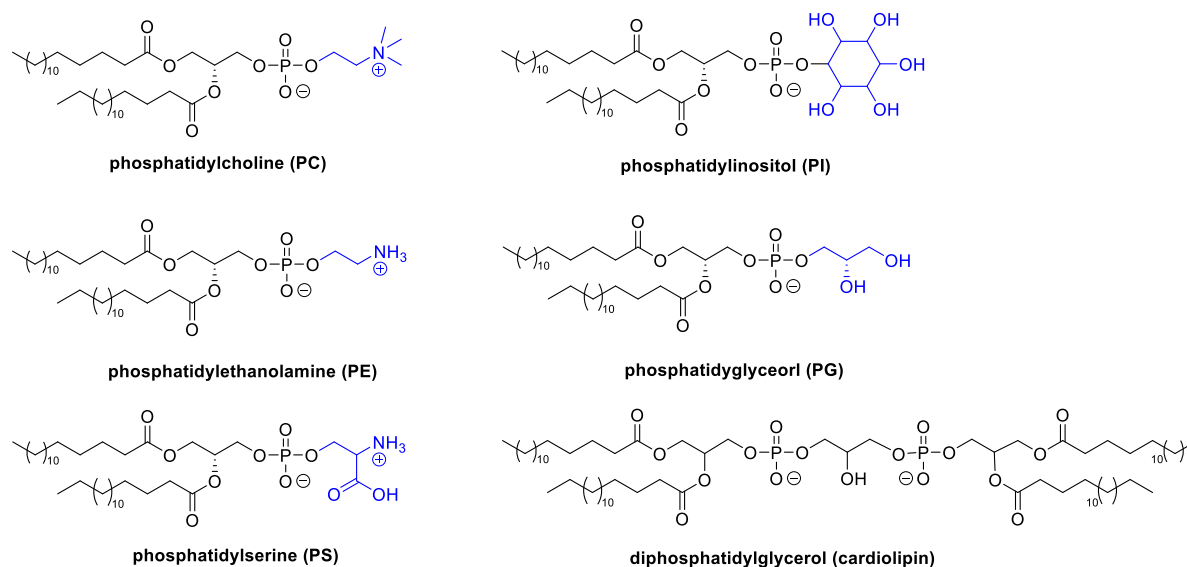


**Figure 3.1** Various classes of phospholipids found in nature. Arbitrarily, a C<sub>16</sub> fatty acyl group has been drawn for illustrative purposes.

#### 3.1.1 Discovery of PG

In 1955, Andrew Benson performed radiolabeling studies of plant and algal extracts using phosphorus-32 and discovered a novel phosphorus-containing compound using radiographs, which he identified as phosphatidylglycerol.<sup>120-121</sup> Indeed, they were quite surprised that this ubiquitous phospholipid was not identified before. In his commentary,

Andrew Benson says “*It is hard to believe that nature has kept such a simple secret for a long time*”.<sup>121</sup> In photosynthetic cyanobacteria and plants, PG is concentrated in the thylakoid membrane, a membrane that surrounds specialized photosynthetic organelles within the chloroplast, where it is usually the most abundant PL. Levels of PL are reciprocally related to those of another anionic thylakoid lipid, sulfoquinovosyldiacylglycerol under conditions of sulfur and phosphorus limitation, yet it has been found that a minimum level of PG is essential for photosynthesis and growth.<sup>119, 122</sup> In the years following its initial discovery in algae and plants, PG was discovered in a wide variety of bacteria and vertebrates.<sup>123</sup>

### 3.2 The mycobacterial cell wall is rich in PLs

A range of PLs have been isolated from mycobacteria including PG, cardiolipin, PE, PI and various mannosylated derivatives such as the PIMs, lipomannan and lipoarabinomannan.<sup>124</sup> Most of the PG in *M. tuberculosis* exists as a lysine ester (lysinylated PG) (Figure 3.2); free PG is found in very low abundance and appears to be formed mostly as an intermediate in the biosynthesis of lysinylated PG, PI, and cardiolipin.<sup>90</sup>

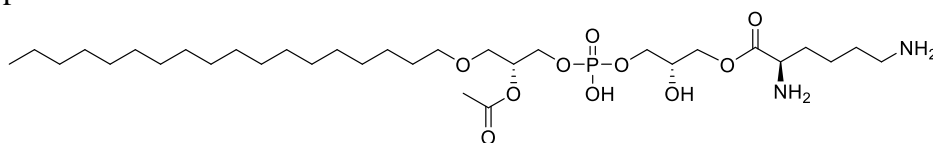


**Figure 3.2** Structure of lysinylated PG.

### 3.3 Biosynthesis and metabolism of PG

The biosynthesis of PG is reasonably well understood. Glycerol 3-phosphate is converted to phosphatidic acid through a two-step acylation with the fatty acids. Condensation of phosphatidic acid and cytidine triphosphate, catalyzed by CDP-diacylglycerol synthase, affords CDP-diacylglycerol. CDP-diacylglycerol reacts with

glycerol-3-phosphate, catalyzed by phosphatidylglycerophosphate synthase (PgsA3),<sup>90</sup> to form 3-sn-phosphatidyl-1'-sn-glycerol-3'-phosphate, accompanied by the release of cytidine monophosphate (CMP).<sup>125</sup> Finally, phosphatidylglycerophosphatase catalyzes the dephosphorylation of phosphatidylglycerophosphate to afford PG (Figure 3.3). Other minor biosynthetic routes to PG include the phospholipase-D catalyzed catabolism of cardiolipin or by glycerolysis of other phospholipids.<sup>126</sup>

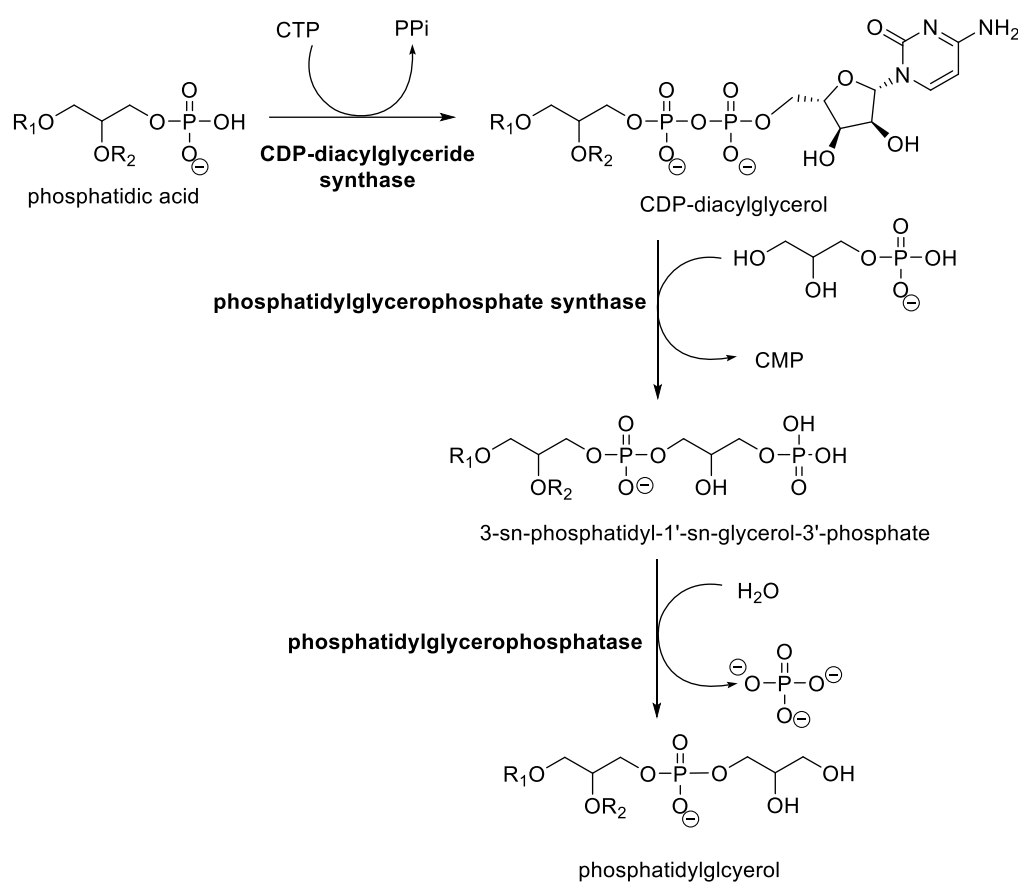


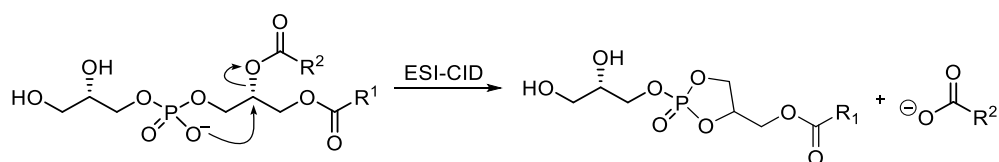
**Figure 3.3** Biosynthesis of PG.

### 3.4 Structural characterization of PG

Smith *et al.* utilized a negative ion electrospray ionization tandem mass spectrometric technique for the analysis of glycerophospholipids in chloroform/methanol extracts of four different bacterial species.<sup>127</sup> Utilizing this technique, they could identify the class of glycerophospholipid, and the molecular weights of the two fatty acid moieties.

The principal bacterial phospholipids detected by this technique were phosphatidylglycerols and diphosphatidylglycerols. Though they could determine the fatty acid composition of the phosphatidylglycerols for each bacteria by tandem mass spectrometry, the acylation pattern could not be confirmed.<sup>127</sup>

Hsu and Turk reported that negative-ion fast-atom bombardment or electrospray-ionization with collision-induced dissociation/tandem mass spectrometry of PE and PG results in fragmentation to provide high abundance fatty acid carboxylate ( $\text{RCO}_2^-$ ) fragment ions.<sup>128-129</sup> These studies revealed similar fragmentation pathways for PE and PG, and showed that regioisomeric PEs fragment in a characteristic way to produce  $\text{RCO}_2^-$  ions for which those derived from the sn-2 position are of greater intensity, thereby allowing structural characterization of fatty acyl regiochemistry. Subsequently, it was shown that CID/MS-MS of PG occurs with similar results, producing  $\text{RCO}_2^-$  ions in which those from the sn-2 position are more abundant, in what has been described as a ‘charge-driven’ process. They have proposed a mechanistic rationale for the fatty acid cleavage of phosphoglycerolipids (Scheme 3.1), which involved a nucleophilic attack by the anionic phosphate group on the sn-1 and sn-2 carbons of the glycerol. It was observed that fragments derived from the sn-2 fatty acid were more intense, indicating that attack at the sn-2 carbon was preferred.



**Scheme 3.1** Mechanism of fatty acid cleavage.

However, CID-MS of PGs differ from those for the structurally-related PI and PIMs, which under similar conditions fragment by neutral loss of fatty acids and fatty acid ketenes in a diagnostic way. While these systems also yield  $\text{RCO}_2^-$  fragment ions,

their relative intensities do not reflect the regiochemistry of their location on the phosphatidyl group because other pathways also yield these ions in abundances that are sensitive to the applied collision energy.<sup>86, 101</sup>

### **3.5 PG and cardiolipin can modulate host immune system**

#### **3.5.1 CD1d-dependent activation**

In 2013, Brenner *et al.* showed that phosphatidylglycerol (PG) and diphosphatidylglycerol (DPG) from *M.tb/C. glutamicum* and mammals were antigens that could stimulate a subset of natural killer T (NKT) cells known as diverse NKT cells (dNKTs or type II NKTs) in a CD1d-restricted manner.<sup>58</sup> *C. glutamicum* PG is an easily purified compound and its structure was well-defined. However, *M.tb* PG is a low abundance phospholipid and was isolated as a complex mixture of compounds. Brenner and co-workers published an ESI-mass spectrum that showed the mixture to contain a range of different acyl compounds. This analysis allowed identification of the fatty acyl pairs found on each PG molecule, but no data was reported that could allow determination of the individual regioisomers. Particularly abundant were species that were assigned structures of C18:1\_C16:0, C19:0\_C16:0 (Figure 3.4). While this work did not allow unambiguous assignment of the acyl regiochemistry, as various studies employing CID-MS/MS have shown that *M.tb* produces PLs bearing C<sub>18:1</sub>/C<sub>16:0</sub> and C<sub>19:0</sub>/C<sub>16:0</sub> for compounds including PI, PIMs,<sup>101</sup> and PE<sup>32</sup> and since these molecules are formed from a common pool of phosphatidyl-CDP, it can be presumed that these acylation patterns are shared by PG. Moreover, as (*R*)-tuberculostearic acid is an abundant lipid of *M.tb*, it is assumed to be the identity of the C19:0 acyl chain.



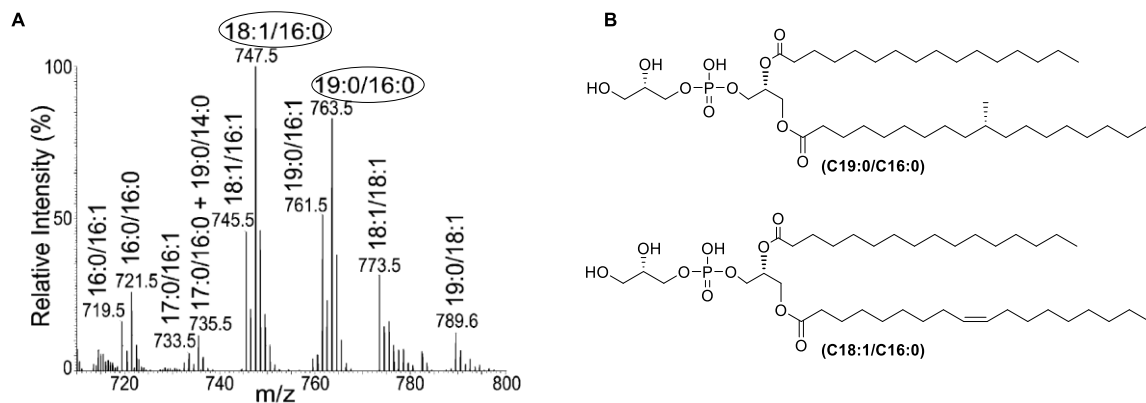


**Figure 3.4** A) Mass spec analysis of PG fraction isolated from *M.tb*; B) Tentative structures of the most abundant PG species in the isolated fraction.<sup>58</sup>

dNKT cells use diverse TCR  $\alpha$  and  $\beta$  chains and have distinct antigen specificities compared to iNKT cells, typically leading to weak or no recognition of the archetypal glycolipid  $\alpha$ -GalCer. Limited structural studies have shown that dNKT TCRs adopt alternative orientations relative to iNKT TCRs when binding. It was observed that both mammalian PG and DPG (cardiolipin) could weakly stimulate dNKT cells despite structural differences in the fatty acid chain (Figure 3.5). It is postulated that this difference in the fatty acid chains could either alter the binding affinity to CD1d, or alternatively its efficiency of loading, leading to enhanced potency.<sup>58-59</sup>

Subsequently, the Brenner group identified PG and cardiolipin from *Listeria monocytogenes* to be a more potent CD1d-restricted antigen than mammalian PG (Figure 3.5).<sup>59</sup> The acyl chains of *L. monocytogenes* PG differ from *C. glutamicum* PG through *anteiso* branching, lack of unsaturation, and shorter tail lengths. The higher potency of listerial PG was suggested to arise from either its increased CD1d loading efficiency over *C. glutamicum* PG or because it is more stably bound to CD1d over time.<sup>59</sup>

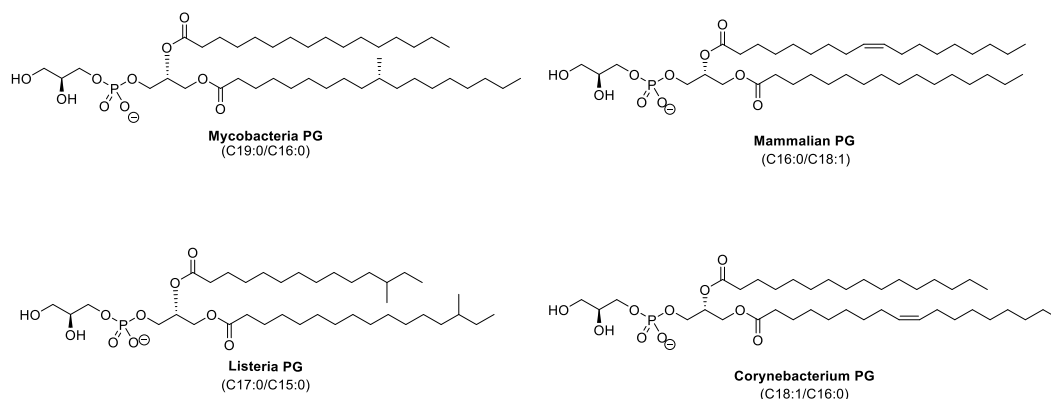


**Figure 3.5** Structures of CD1d ligands from listeria, mycobacteria, Corynebacterium and mammals.

The acylation pattern of the *L. monocytogenes* PGs were assigned by linear ion trap multi stage mass spectrometric approaches.<sup>130</sup> Fragmentation of the ion at  $[M-H]^-$  at  $m/z$  721 gave rise to ions at  $m/z$  497 and 479 (arising from loss of C15:0 acid and corresponding ketene) and ions at  $m/z$  469 and 451 (arising from loss of C17:0 fatty acid and corresponding ketene). The ions at  $m/z$  479 and 497 are more abundant than the ions at  $m/z$  469 and 451, indicating that the 17:0 fatty acid is located at sn-2 and the 15:0 fatty acid located at sn-1 (Figure 3.6).<sup>130</sup>

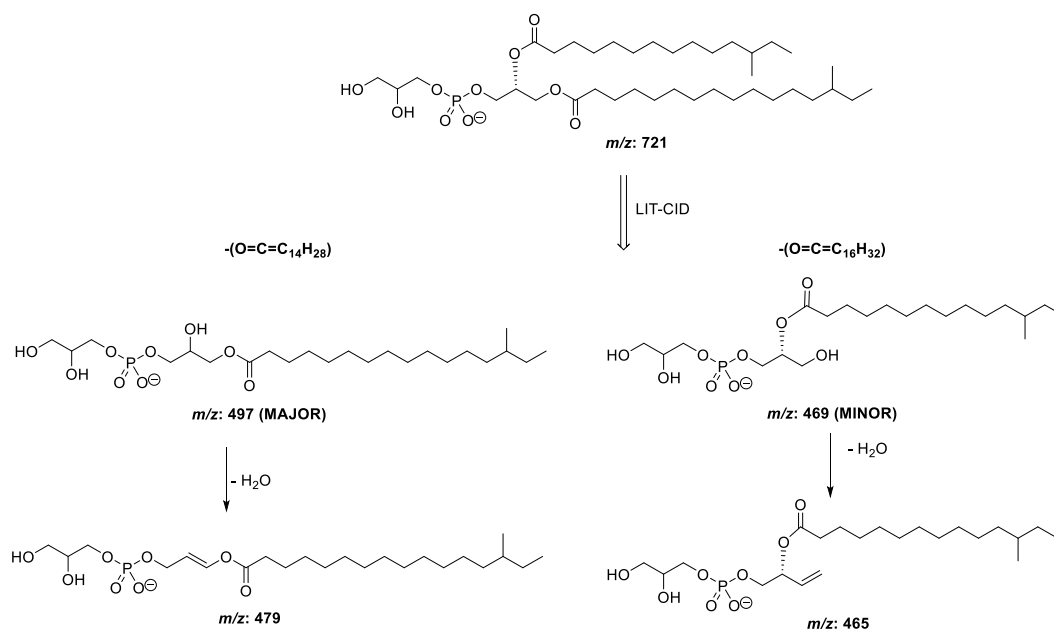


**Figure 3.6** Fragmentation of *Listeria* PG by LIT-CID.

### 3.5.2 CD1b-dependent activation

In 2016, Brenner *et al.* reported that structurally diverse PGs from bacteria including *L. monocytogenes*, *C. glutamicum*, *Escherichia coli*, *Staphylococcus typhimurium* and *Staphylococcus aureus* are CD1b-restricted antigens (Figure 3.7).<sup>76</sup> In particular, CD1b autoreactive T cells had the capacity to recognize self and foreign PG. Generally, most bacteria contain higher levels of PG than mammalian cells, and in mammalian cells, PG is mostly concentrated in mitochondrial membranes and is not present in cellular membranes carrying CD1b proteins.<sup>126</sup> However, mitochondrial stress can lead to release of PG, suggesting that the ability of mammalian PG to be recognized by T cells when presented by CD1b is an immune response to cellular stress.<sup>76</sup> Given the ability of CD1b to present a wide range of structurally-diverse PGs from assorted sources, it would be interesting to study if mycobacterial PG could also be detected by CD1b.

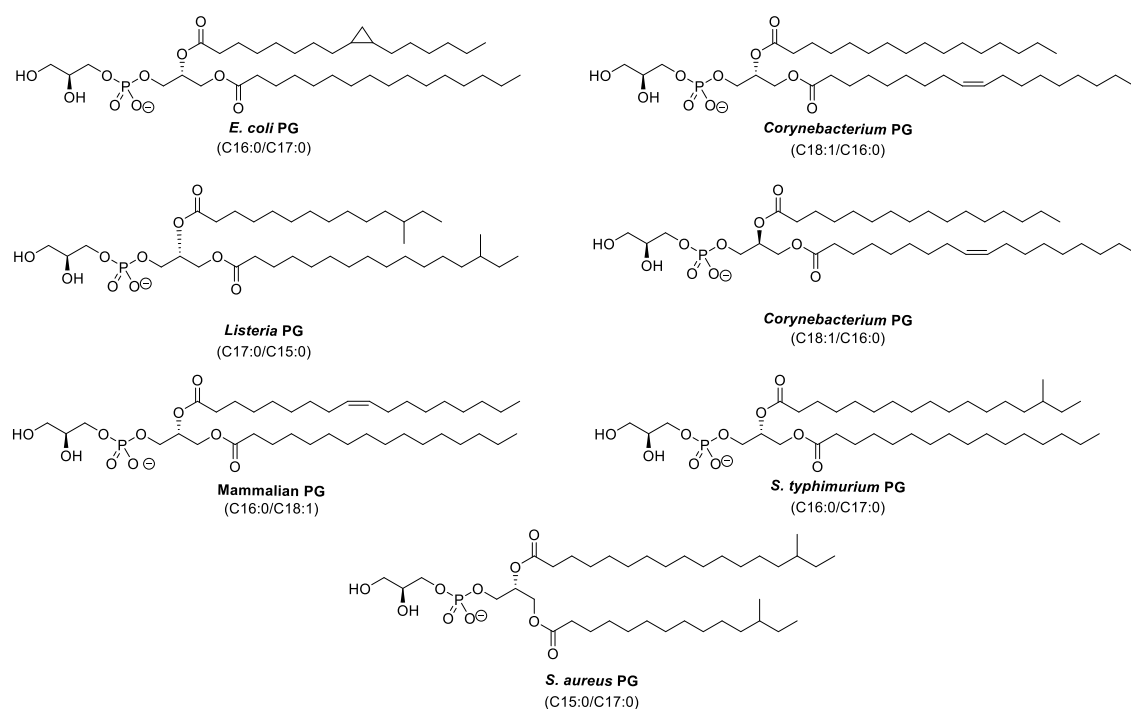
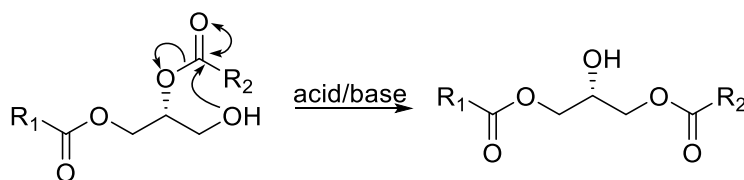


**Figure 3.7** Structures of PG presented by CD1b to T cells.

### 3.6 Synthesis of PG and related PLs

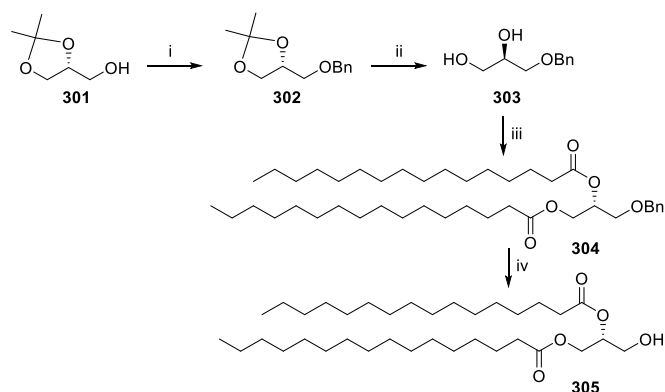
#### 3.6.1 Synthesis of 1,2-diacylglycerols

Despite their apparent structural simplicity, the stereoselective synthesis of 1,2-diacylglycerols is challenging. A critical issue in the chemical synthesis of these compounds is ensuring that the glycerol is regioselectively acylated with high fidelity. Generally, installation of two different acyl chains is performed sequentially through a  $\beta$ -hydroxy-ester intermediate in which acyl group migration is facile (Scheme 3.2), occurring under both acidic and basic conditions, and even during chromatography on silica gel.



**Scheme 3.2** Acyl group migration, releasing steric strain.

Sowden and Fisher were the first to exploit the availability of 1,2-*O*-isopropylidene-*sn*-glycerol **301** to prepare an optically active simple 1,2-diacyl-*sn*-glycerol in 1941.<sup>131</sup> The 3-hydroxyl of **301** was protected with a benzyl group, and acid hydrolysis of the isopropylidene group afforded a diol **303**, which was acylated with palmitic acid. Removal of the benzyl group by hydrogenolysis afforded 1,2-dipalmitoyl-*sn*-glycerol **305** (Scheme 3.3).<sup>131</sup> Subsequent variations of this method including changes of the benzyl group for alternative protecting groups, and strategies to allow sequential installation of different fatty acids, has allowed its use for the preparation of mixed diacylglycerols.



**Scheme 3.3** Sowden and Fisher's synthesis of diacylglycerol.<sup>131</sup> Reagents and conditions: (i) Na, BnBr (ii) H<sub>2</sub>SO<sub>4</sub>, H<sub>2</sub>O (iii) palmitic acid, pyridine (iv) H<sub>2</sub>, Pd/C.

Although widely used, this general approach has a range of shortcomings including the length of the sequence (although the commercial availability of 1,2-*O*-isopropylidene-glycerol has simplified the approach), the need for removal of a protecting group on the primary alcohol, and the sensitivity to acyl migration during purification of intermediates.

### 3.6.2 Regioselective glycidol opening reactions

An alternative approach to the synthesis of diacylglycerols seeks to exploit epoxide ring opening of glycidol derivatives. As this approach reduces the number of manipulations prior to introduction of the ester, and because the esterification itself is performed using the fatty acid rather than an activated derivative, it can be considered an atom economic option for the synthesis of diacylglycerols. This strategy has been pursued by several groups (Figure 3.8). Burgos *et al.* obtained a monoacylglycerol **307** in 25% yield starting from enantiopure glycidol **306** by applying an excess of stearic acid and Ti(OiPr)<sub>4</sub>.<sup>132</sup> Unfortunately, only a low yield (25%) was obtained, and 86% ee was observed, as a result of acyl migration leading to racemization. Ali and Bittman used BF<sub>3</sub>·Et<sub>2</sub>O for ring-opening of tosyl glycidol **308** with a fatty acid anhydride.<sup>133</sup> Although the reaction afforded the protected diacylglycerol in a good yield, it is limited to the

synthesis of simple diacylglycerols. Stawinski and Stamatov described a 3 step procedure starting from TBDMS protected glycidol.<sup>134</sup> The epoxide was first treated with an excess of  $n\text{Bu}_4\text{NI}$  and the resulting iodohydrin was treated with an excess of acid chloride to afford the monoacylated species **311**. The iodide prevented acyl migration and was substituted in the final step with an excess of the tetrabutylammonium salt of the fatty acid affording the diacyl glycerol in an excellent 92% over 3 steps. Lok *et al.* performed a direct epoxide ring opening with a fatty acid, isolated the hydroxy-ester intermediate, and then subjected this to esterification using DCC/DMAP.<sup>135</sup>

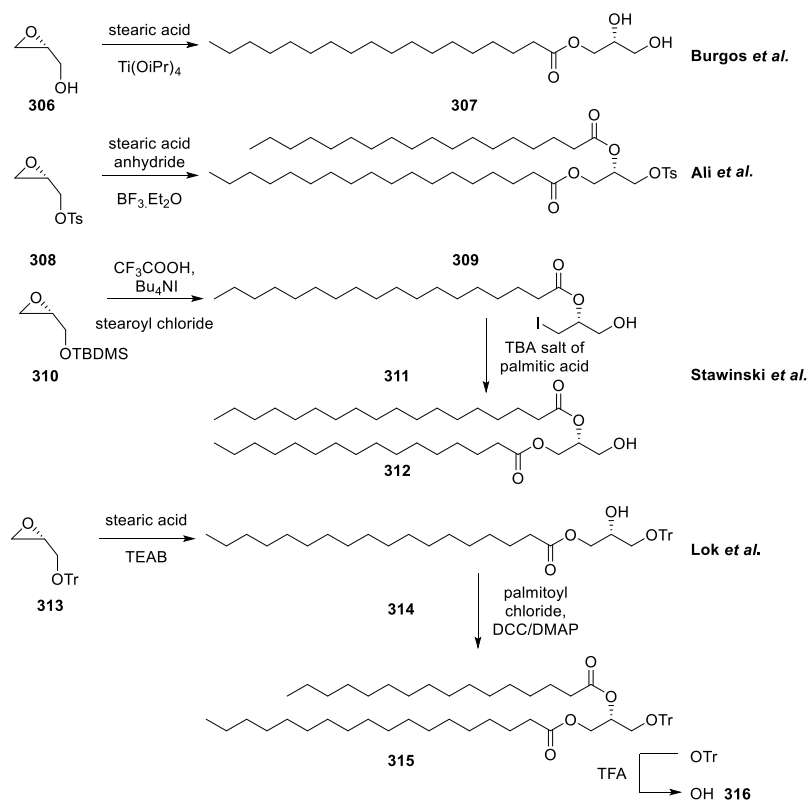
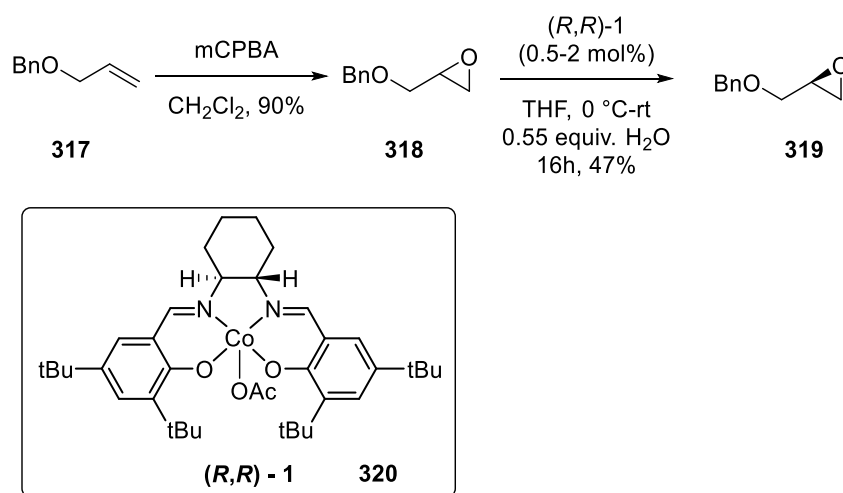


**Figure 3.8** Various approaches for the synthesis of diacylglycerol from glycidol.

All of these approaches require access to optically pure glycidols, which historically were obtained from D-mannitol. A breakthrough in access to chiral glycidols came about through the invention of the Jacobsen hydrolytic kinetic resolution of epoxides. Jacobsen *et al.* reported that chiral cobalt (III) (CoIII) salen complexes catalyze

the enantiospecific ring opening of chiral epoxides.<sup>136</sup> In this reaction a CoIII complex catalyzes the highly regioselective hydrolysis of terminal epoxides to generate diols. For the epoxide that is matched to the substrate, the reaction occurs speedily. However, for the unmatched enantiomer, the rate of hydrolysis is markedly reduced, sometimes by >100-fold.<sup>136-137</sup> By starting with a racemic mixture and including only half an equivalent of water, this reaction allows the selective transformation of just one enantiomer to the corresponding diol, providing a kinetic resolution. In practice this reaction can be run in two ways: either to access the diol or the unreacted epoxide. To provide high levels of enantiopurity of the diol, slightly less than half of one equivalent of water is used, in which cases yields of the diol are slightly less than 50% but are obtained in high ee. To obtain high levels of enantiopurity of the epoxide, slightly more than one half of an equivalent of water is used, providing the epoxide in slightly less than 50% yield, and again in high enantiopurity. By oxidation of allyl benzyl ether **317** to the racemic epoxide, and then application of the Jacobsen HKR using each enantiomer of the catalyst, both antipodes of benzyl glycidol can be directly obtained in 99% ee (Scheme 3.4).<sup>138</sup>



**Scheme 3.4** Synthesis of enantiopure epoxide by from benzyl allyl ether by hydrolytic kinetic resolution using Jacobsen's catalyst.

Mechanistic studies of the Jacobsen HKR have revealed that the reaction proceeds through a cobalt(III) complex, which is formed by autooxidation of CoII salen in the presence of acetic acid. This affords the cobalt(III) complex as the acetate salt. Jacobsen demonstrated that counter-ion addition to the epoxide can occur and is complete and irreversible when using Co(salen)-OAc, which decreases reaction rates in the late stages of HKR reactions. In contrast, the Co(salen)-OTs precatalyst undergoes a reversible addition of counterion to the epoxide, thus maintaining an approximately 1:1 mixture of Lewis acid and the nucleophilic species, allowing high reaction rates throughout the course of the reaction (Figure 3.9).<sup>139</sup>

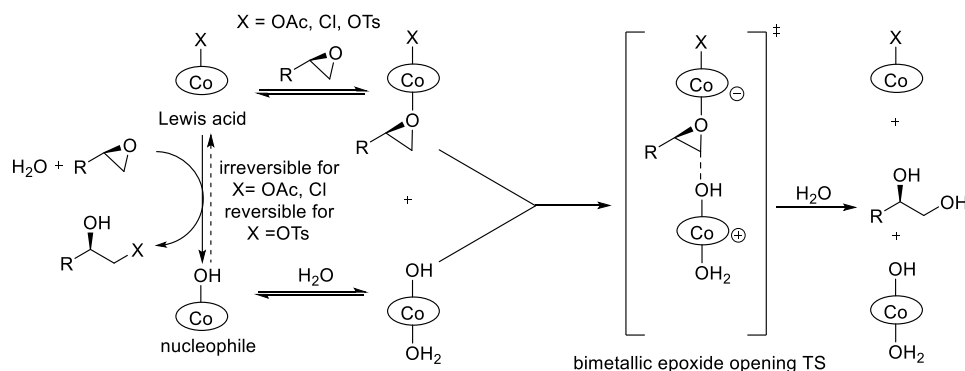
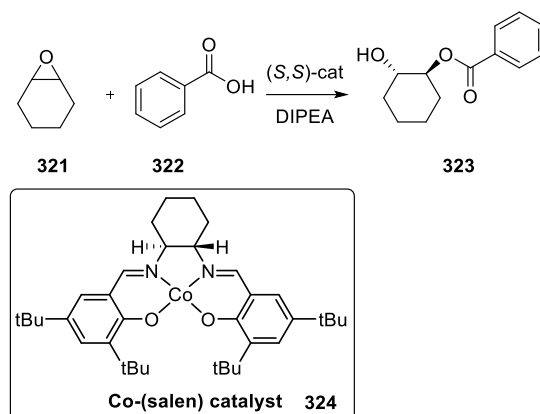


**Figure 3.9** HKR mechanism.<sup>137</sup>

Jacobsen used this unwanted side reaction to great effect to develop Co-salen complexes as catalysts for epoxide ring-opening esterifications. Auto-oxidation of a mixture of the CoII-salen complex with a carboxylic acid affords a CoIII-salen complex that catalyzes the addition of the carboxylic acid to an epoxide (Scheme 3.5).<sup>140</sup> Like the Jacobsen HKR, this reaction is highly selective for opening at the primary position of an epoxide.





**Scheme 3.5** Meso-epoxide opening with benzoic acid using Jacobsen's Co-salen catalyst.<sup>140</sup>

In 2012, Minnaard *et al.* revisited glycidol epoxide ring opening by carboxylic acids to develop a new approach for the synthesis of mixed diacylglycerols. In their approach, reaction of enantiopure TBDMS glycidol with stearic acid, in the presence of Co-salen catalyst and Hünig's base afforded the monoacylglycerol as a single regioisomer. They then esterified the 2-hydroxyl with the second fatty acid using DCC/DMAP in the same pot. Utilizing this methodology, they synthesized DAG containing ether/ester type structures.<sup>32</sup> Using chiral HPLC the products were shown to not undergo acyl migration and maintain stereochemical integrity.

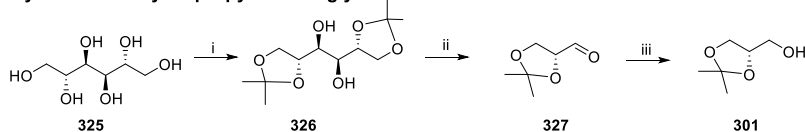
### 3.7 Previous syntheses of PG and related phospholipids

The importance of phosphatidylglycerol has inspired many chemical syntheses. Early approaches by Baer<sup>141</sup> and Schwartz were limited by the inability to incorporate different acyl chains on the glycerol fragment. A more recent approach by Servi utilized a chemo-enzymatic approach facilitated by phospholipase-D to synthesize PG from phosphatidylcholine.<sup>142-143</sup> Although, this method enables the synthesis of PG on a large scale (> 50 g), it also suffers from the inability to incorporate different acyl chains on the glycerol fragment, requiring that they already be installed on PC. Thus in spite of its limitations, Baer's route is significant and remains widely used.

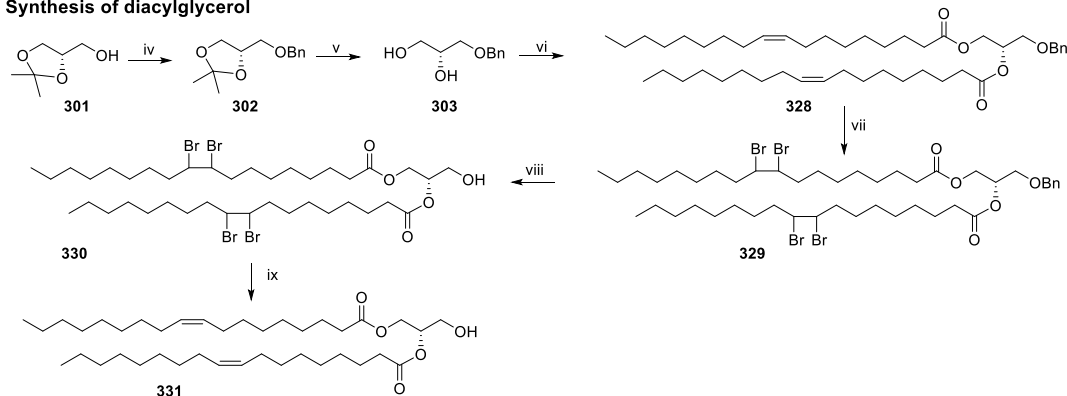
### 3.7.1 Baer's total synthesis of PG

Baer and Buchnea synthesized four PG variants, comprising the pairs of enantiomers of the bis-oleic acid and bis-stearic acid PGs. They used a historically important method for the synthesis of diacylglycerol by oxidative cleavage of a protected mannitol diol, first reported by Baer and Fischer.<sup>144-146</sup> Thus, D-mannitol was converted to **326** by treatment with 2,2-dimethoxypropane. **326** was oxidatively cleaved to afford isopropylidene-D-glyceraldehyde, and then reduced to the alcohol **301** using sodium borohydride. **301** was benzylated, and the acetonide hydrolyzed with HCl to afford the benzyl glycerol. The hydroxyls of the glycerols were acylated with oleic acid, and the double bond of oleic acid was masked by bromination, followed by hydrogenolysis to remove the benzyl group. The unsaturation was recovered by reduction of the vicinal dibromide with Zn dust (ostensibly to return the cis-alkene). Reaction of the dioleyl glycerol with excess POCl<sub>3</sub> and isopropylidene glycerol in presence of pyridine afforded the phosphochloridate **333**, which was not isolated. Instead, the chloride was hydrolyzed along with the isopropylidene protecting group to afford dioleyl PG **334** (Scheme 3.6). Reduction of dioleyl PG afforded distearoyl-L- $\alpha$ -glycerylphosphoryl-L- $\alpha$ -glycerol. The other stereoisomers were synthesized starting from L-mannitol.<sup>141</sup>

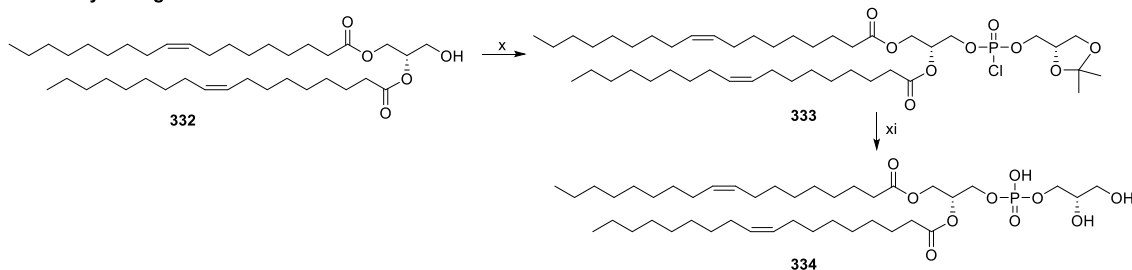
### Synthesis of key isopropylidene-D-glycerol



### Synthesis of diacylglycerol



### Assembly of fragments

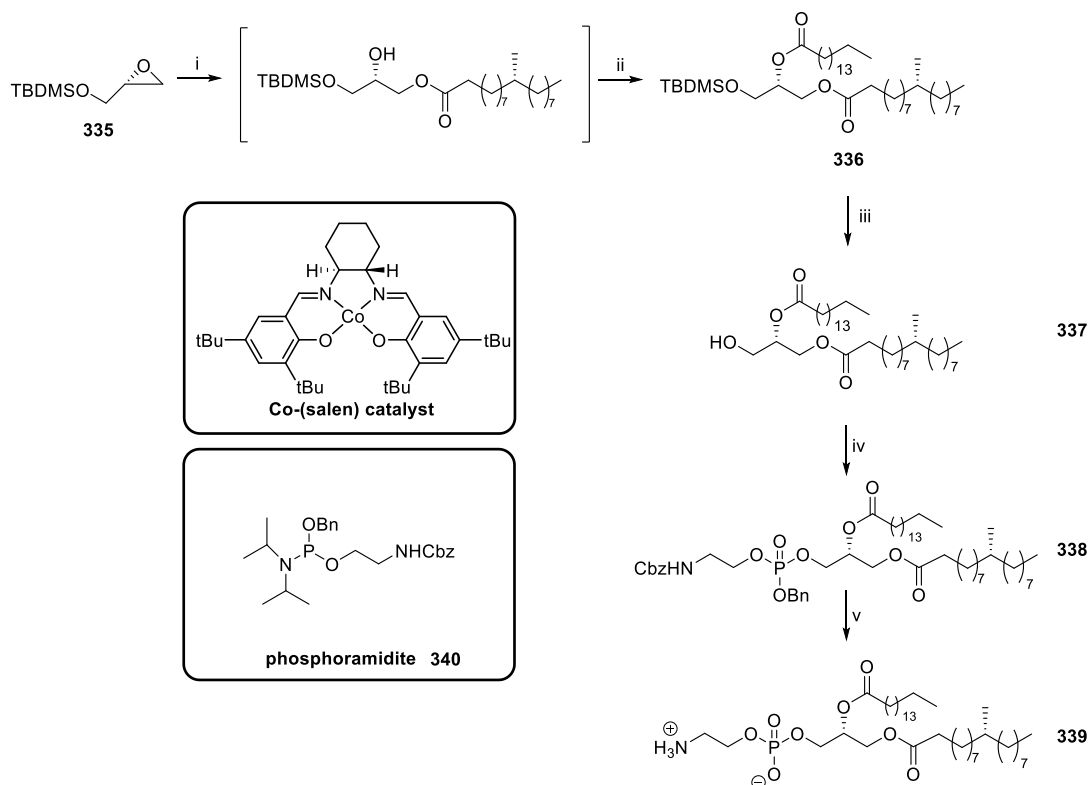


**Scheme 3.6** Baer's synthesis of phosphatidylglycerol. Reagents and conditions: (i) DMP; (ii) AcOH, NaIO<sub>4</sub>; (iii) NaBH<sub>4</sub>; (iv) BnBr; (v) HCl; (vi) oleic acid, pyridine; (vii) Br<sub>2</sub>, pet. ether; (viii) H<sub>2</sub>, Pd, AcOH; (ix) Zn, ether; (x) POCl<sub>3</sub>, isopropylidene glycerol, pyridine; (xi) 1. H<sub>2</sub>O, 2. HCl.

### 3.7.2 Minnaard's synthesis of phosphatidylethanolamine

Recently Minnaard and co-workers synthesized a TBSA-containing PE found in *M.tb*. A key step involved the epoxide ring opening esterification of TBDMS-protected enantiopure glycidol **335** by (*R*)-tuberculostearic acid in the presence of Jacobsen's catalyst, followed by acylation of the secondary alcohol with palmitic acid and DCC/DMAP to afford TBDMS-protected diacylglycerol **336**. While this procedure goes via an intermediate vicinal hydroxy ester, which are known to suffer from acyl migration,<sup>147</sup> HPLC with a chiral stationary phase supported the reaction occurring without acyl migration. The TBDMS-protecting group was removed by treatment with boron trifluoride-acetonitrile or etherate complex. The phosphate ester was installed using

a benzyl phosphoramidite, catalyzed by 4,5-dicyanoimidazole, followed by oxidation using *t*-BuOOH. Finally, the benzyl group was removed by hydrogenolysis to afford PE **339** (Scheme 3.7).<sup>32</sup>

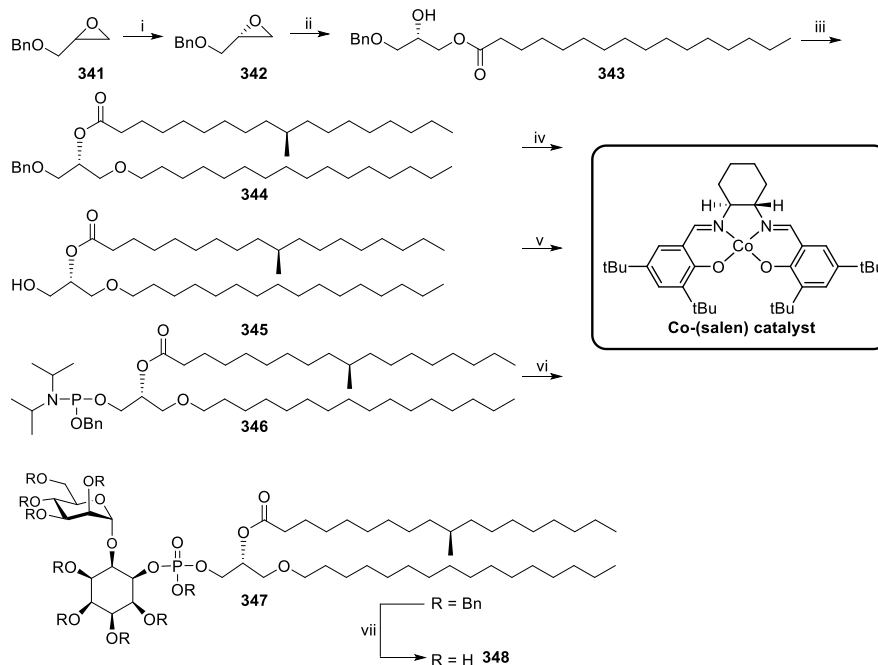


**Scheme 3.7** Minnaard's synthesis of *M.tb* PE.<sup>32</sup> Reagents and conditions: (i) Co-(salen) cat., TBSA, DIPEA, 21 °C, 16 h; (ii) palmitic acid, DCC/DMAP, 21 °C, heptane, 16 h, 90%; (iii)  $\text{BF}_3 \cdot \text{CH}_3\text{CN}$ ,  $\text{CH}_2\text{Cl}_2$ , 21 °C, 5 min; (iv) (a) phosphoramidite **306**, 4,5-dicyanoimidazole,  $\text{CH}_2\text{Cl}_2$ , 15 min; (b) *t*-BuOOH, 10 min; (v)  $\text{H}_2$ , Pd/C, MeOH-THF, AcOH, 21 °C.

### 3.7.3 Painter's synthesis of PIM<sub>2</sub>

Painter's synthesis of PIMs started with racemic benzyl glycidol **341** (Scheme 3.8).<sup>101</sup> Hydrolytic kinetic resolution of the epoxide using Jacobsen's catalyst afforded the pure epoxide **342**, which was subjected to ring opening with palmitic acid in the presence of triethylammoniumbromide. A second acylation with (*R*)-TBSA using DCC/DMAP, followed by debenzoylation afforded the diacylglycerol **345**. The DAG was subjected to phosphitylation with benzyl *N,N*-diisopropyl phosphordiamidite, to afford

the monoamidite species, which was subjected to a second coupling with benzyl mannose inositol, and subsequently oxidized and deprotected to afford PIM<sub>1</sub>.



**Scheme 3.8** Painter's synthesis of PIM. Reagents and conditions: (i) (*S,S*)-cat. AcOH, THF, H<sub>2</sub>O; (ii) palmitic acid, Et<sub>4</sub>NBr; (iii) *R*-TBSA, DCC/DMAP; (iv) 10% Pd/C, H<sub>2</sub>, AcOH, EtOH; (v) BnOP(N*i*Pr<sub>2</sub>)<sub>2</sub>, 1*H*-tetrazole, CH<sub>2</sub>Cl<sub>2</sub>; (vi) perbenzyl mannose-inositol, 1*H*-tetrazole, *m*-CPBA; (vii) 10% Pd/C, H<sub>2</sub>, AcOH, EtOH.

### 3.8 Aim

We planned to synthesize a specific *M.tb* PG bearing (*R*)-tuberculostearic acid (TBSA) at sn-1 and palmitic acid at sn-2, which is the proposed structure of the major branched species detected in Brenner's study.<sup>58</sup> Brenner's work that detailed the ability of *M.tb* PG to stimulate type 2 NKTs in a CD1d-restricted manner used a mixture of PG as a range of acylated species. Access to pure, synthetic PG should allow more detailed study of its ability to activate (NK)T cells through the CD1b and CD1d axes. As part of this work we also planned to synthesize analogues bearing stearic acid and palmitic acid at the sn-1/sn-2 positions, both as simplified model compounds upon which to develop our synthetic approach, as well as analogues of our target *M.tb* PG to allow exploration

of the importance of the distinguishing branched methyl group in the immunological properties of this molecule.

### 3.9 Results and discussion

Our route to *M.tb* PG was inspired by Minnaard's route for the synthesis of PE to assemble the diacylglycerol,<sup>32</sup> and incorporated Painter's approach for synthesizing the phosphate diester linkage using a phosphordiamidite linchpin<sup>101</sup> (Figure 3.10). TBSA is available through the approach detailed in the previous chapter employing (*S*)-citronellyl bromide (discussed in Chapter 2).

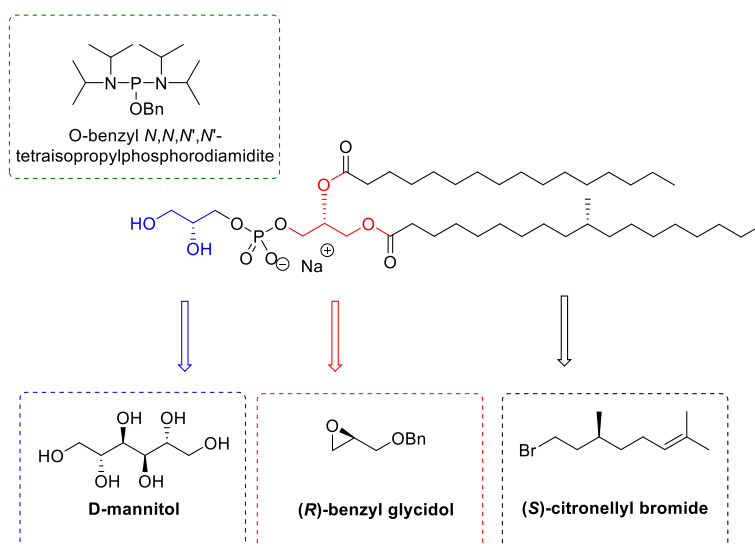
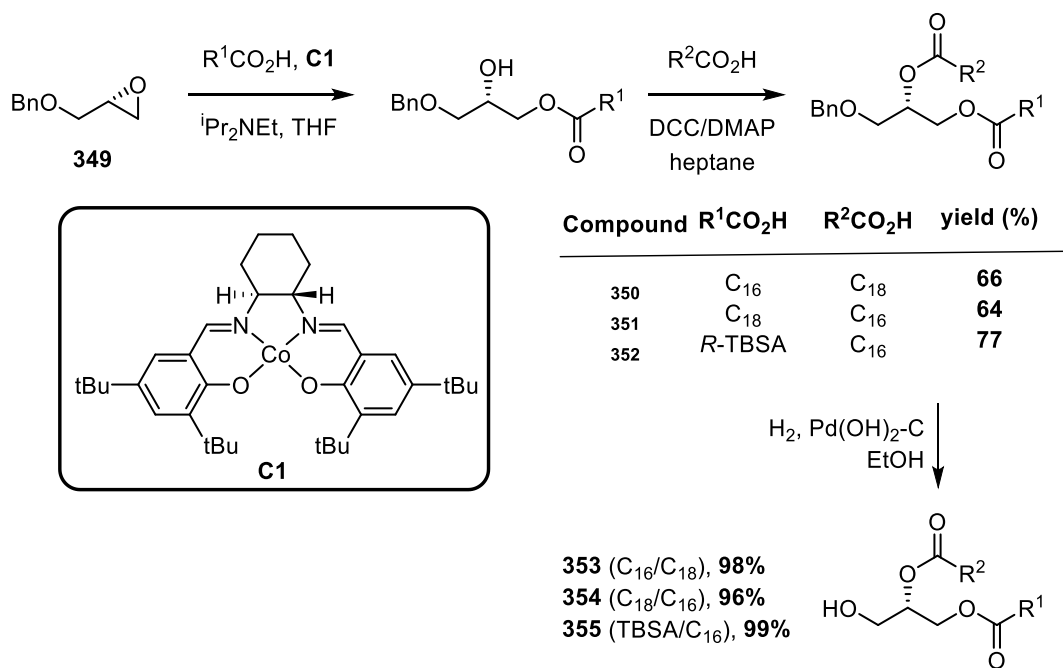


**Figure 3.10** Proposed disconnections for the synthesis of *M.tb* PG.

Using Minnaard's methodology, three different analogues of diacylglycerol were synthesized: C16/C18, C18/C16 and TBSA/C16 diacylglycerols. Regioselective epoxide ring opening of commercially-available (*R*)-benzyl glycidol **349** with *R*-TBSA **206** and Co-(*R,R*)-salen in the presence of Hünig's base in THF afforded the monoacylated intermediate, which was subjected to esterification with palmitic acid using DCC/DMAP to afford benzylated diacylglycerols **350-352** in 65-80% yield. In this procedure the monoacyl glycerol is not purified or isolated so as to minimize acyl group migration; a solution of acyl halide in heptane is added directly to the reaction mixture after removing

THF under reduced pressure. As mentioned earlier, Minnaard has shown that this approach does not lead to any detectable acyl group migration.<sup>32</sup>

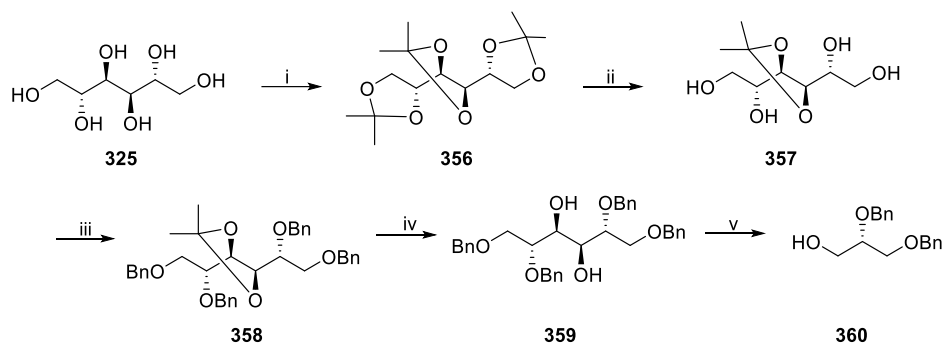
The benzyl group of compounds **350-353** were removed under H<sub>2</sub>, using Pearlman's catalyst. This material was used immediately in the next step to minimize the risk of acyl migration. The other two analogues were synthesized in a similar fashion.



**Scheme 3.9** Synthesis of diacylglycerol analogues **353-355**.

### 3.9.1 Synthesis of dibenzyl glycerol

The dibenzyl glycerol fragment **360** was synthesized from D-mannitol **325** in six steps, according to van Boom *et al.*<sup>148-149</sup> (Scheme 3.11). D-Mannitol was converted to triacetone-D-mannitol **356** by treatment with dimethoxypropane. The terminal acetals were cleaved by careful treatment with aqueous AcOH, and the tetraol was benzylated using BnBr and NaH in the presence of catalytic imidazole. The 3,4-*O*-isopropylidene group was cleaved with AcOH to give a vicinal diol. The vicinal diol **359** was oxidatively cleaved with sodium periodate and the resulting aldehyde immediately reduced with sodium borohydride to afford dibenzyl glycerol **360**.



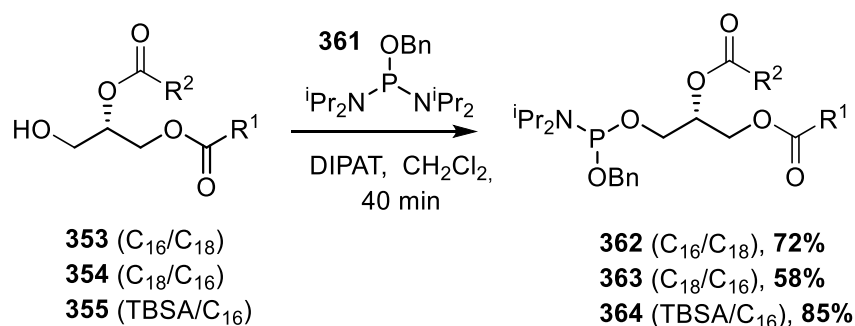
**Scheme 3.10** Synthesis of dibenzyl-*sn*-glycerol **360** from D-mannitol.<sup>149</sup> Reagents and conditions: (i) TsOH, DMP, 24 h, 65%; (ii) AcOH, 1 h, 70%; (iii) NaH, imidazole, BnBr, 24 h, 80%; (iv) AcOH, 3 h, 85%; (v) (a) NaIO<sub>4</sub>, (b) NaBH<sub>4</sub>, 1 h, 76%.

### 3.9.2 Assembly of the fragments onto the phosphorus linchpin

Early approaches to install phosphate diesters utilized POCl<sub>3</sub>, a moisture sensitive reagent that is difficult to handle. We chose to utilize contemporary phosphoramidite chemistry which has been widely applied in the synthesis of oligonucleotides and phospholipids. A phosphoramidite (RO)<sub>2</sub>PNR<sub>2</sub> is an electrophilic monoamide of a phosphite diester; nucleophilic attack displaces the NR<sub>2</sub> moiety. We were particularly attracted to the use of benzyl *bis*-(diisopropylamino) phosphordiamidite, which Painter and co-workers have applied with success in the synthesis of a PI and PIM<sub>2</sub>, using mild reaction conditions and short reaction times that minimize acyl migration of the diacylglycerol. While Painter utilized 1*H*-tetrazole as a catalyst for stepwise couplings at each diisopropylamino group, Carruthers has reported that greater selectivity can be achieved by the use of the milder catalyst diisopropylammonium tetrazolide (DIPAT) in the first phosphitylation reaction, and then the more powerful catalyst 1*H*-tetrazole in the second phosphitylation.<sup>150</sup> In these phosphatidylation reactions, the catalyst plays two roles, acting as an acidic and nucleophilic catalyst. The weaker acidity of the diisopropylammonium ion versus 1*H*-tetrazole ensures that DIPAT is a weaker catalyst, preventing activation of the second diisopropylamino group.

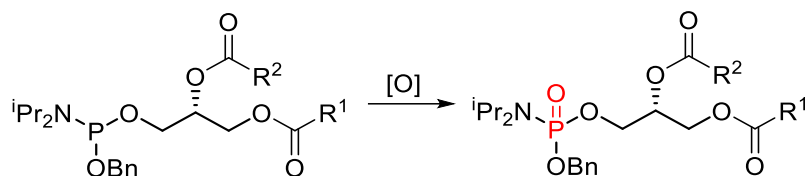


Accordingly, the diacylglycerols **353-355** obtained from hydrogenolysis were immediately treated with benzyl *bis*-(diisopropylamino)phosphordiamidite **361** and DIPAT as the activator to afford the phosphoramidites **362-364**, which could be purified by quick chromatography over alumina (Scheme 3.11). Such phosphoramidites proved to be relatively sensitive compounds and were best immediately subjected to the next reaction.



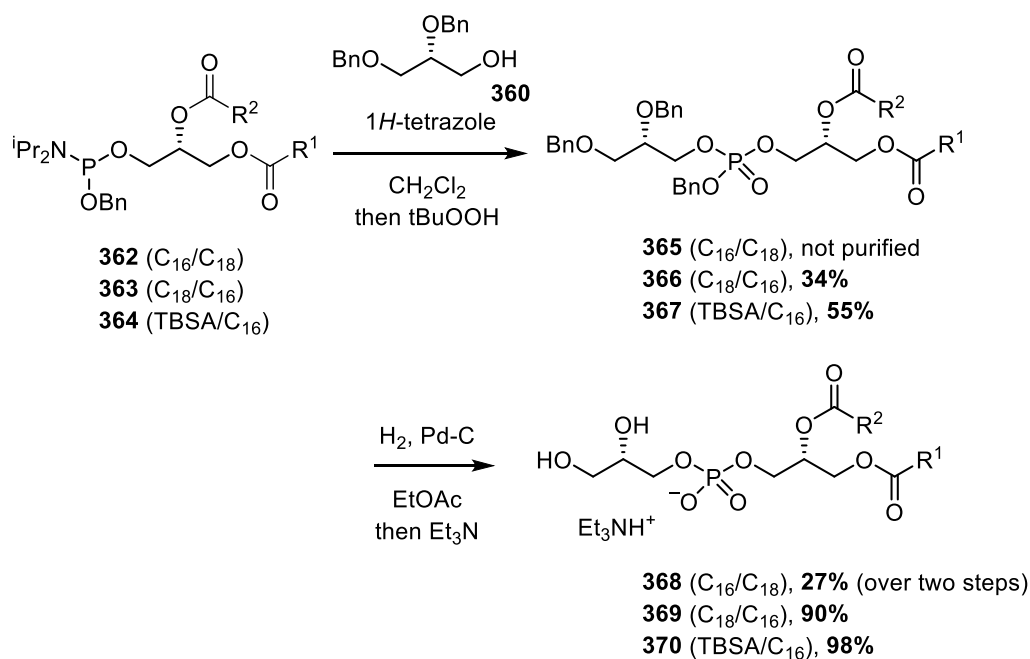
**Scheme 3.11** Synthesis of the phosphoramidites **362-364**.

The concluding steps required the coupling of dibenzyl-*sn*-glycerol **360**, oxidation of the intermediate phosphite to the phosphate ester, and hydrogenolysis to cleave the benzyl groups. One challenging issue with implementing this phosphordiamidite chemistry was difficulties arising from its auto-oxidation to a phosphoramidate (Scheme 3.12), particularly on the small scales utilized for this work. Initially, we sought to investigate whether this product could be reacted with excess dibenzyl-*sn*-glycerol in the presence of 1*H*-tetrazole, to form the protected PG. However, it proved unreactive and, moreover, we were unable to purify the protected PG from excess dibenzyl-*sn*-glycerol.



**Scheme 3.12** Auto-oxidation of phosphoramidite intermediate.

Since we were unable to avoid the loss of small amounts of the phosphoramidite to auto-oxidation, and since excess dibenzylglycerol could not be separated from the product, we chose to use a limiting amount of the dibenzylglycerol (0.8 equiv), which allowed isolation of the protected PG in excellent purity but in modest yield (Scheme 3.13). In the cases of **366** and **367**, the purified products were subjected to hydrogenolysis over Pearlman's catalyst to afford the target PGs **369** and **370**. In case of the **365** (C<sub>16</sub>/C<sub>18</sub>) analogue, we were unable to isolate the protected PG as a pure material. In this case, the isolated material comprised a 2:1 mixture of **365** and unreacted dibenzyl-sn-glycerol. This was subjected to hydrogenolysis and purification enabled separation from glycerol, affording pure PG **368**.



**Scheme 3.13** Synthesis of PG analogues **368-370**.

The <sup>1</sup>H NMR spectra of our PGs were in excellent agreement with the reported NMR data of other PGs.<sup>151</sup> The signals of the protons of the diacylglycerol backbone are slightly downfield compared to the protons of the glycerol head group. The methylene protons of glycerol C3 are non-equivalent and appear at δ 4.11 and 4.38 ppm each as

doublet of doublets, owing to germinal coupling with each other and vicinal coupling with the C2 proton. The glycerol C2 proton appears at  $\delta$  5.16 ppm as a multiplet. The C1 protons appear at 3.95 ppm. The methylene protons of C2' of the headgroup glycerol is seen characteristically at  $\delta$  3.65-3.75 ppm as a multiplet, owing to its coupling with both the C1' and C3' protons. The C1' protons are slightly downfield than the C3 protons owing to their deshielding by  $^{31}\text{P}$  of the phosphate. A  $^{31}\text{P}$  spectrum showed a phosphorus peak at 4.58 corresponding to the P(V) phosphorus

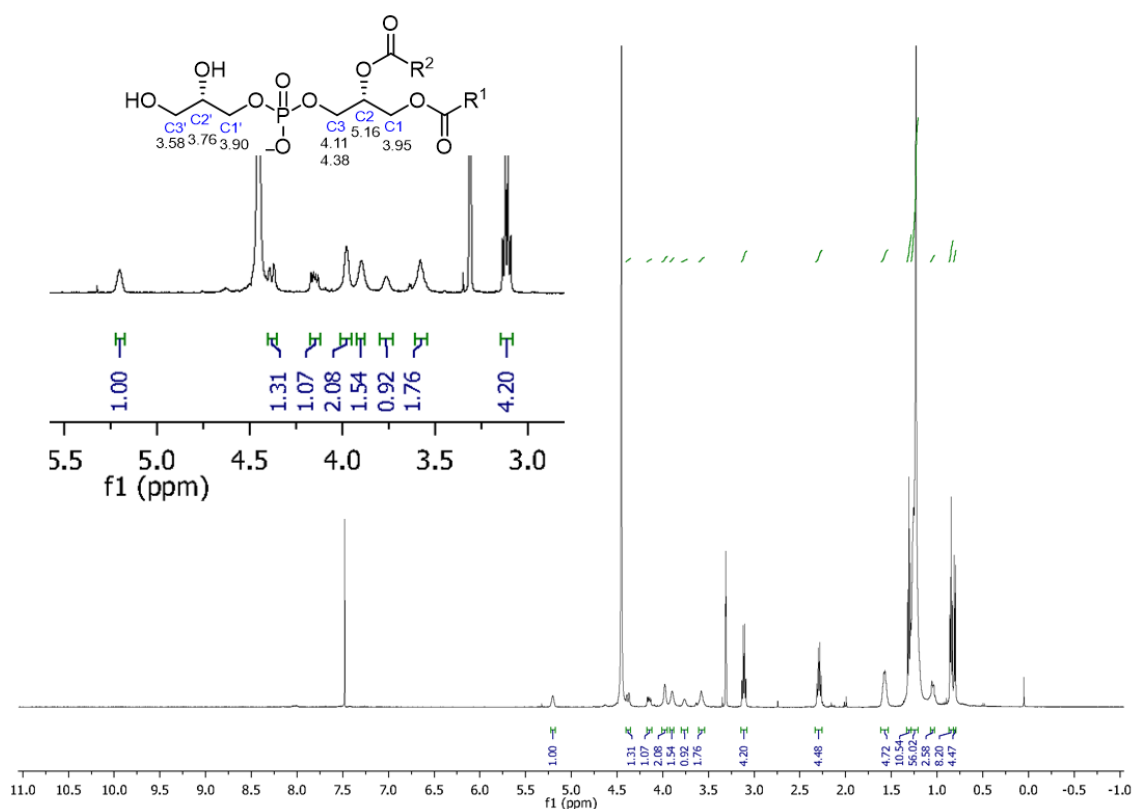


**Figure 3.11**  $^1\text{H}$  NMR spectrum of *M.tb* PG **370**.

### 3.10 ESI CID- MS/MS of PG analogues

We performed multistage mass spectrometry ( $\text{MS}^n$ ) experiments to confirm the acylation patterns of the synthesized PG. The  $\text{MS}^n$  experiments involved collision-induced dissociation of negative ions formed using electro-spray ionization. For

regioisomers **369** (C<sub>18</sub>/C<sub>16</sub>) and **368** (C<sub>16</sub>/C<sub>18</sub>), fragmentation of the parent ions [M-H]<sup>-</sup> (*m/z* 749.5) yielded characteristic fatty acid carboxylate fragment ions at *m/z* 255.2 and 283.3 (Figure 3.12 (a), (b)). In each case, the more abundant ion was that derived from the loss of fatty acid located in the sn-2 position. The CID-MS<sup>2</sup> spectrum of **370** (TBSA/C<sub>16</sub>) revealed that fragmentation of the parent ion [M-H]<sup>-</sup> (*m/z* 763.5) afforded daughter ions at *m/z* 255.2 and 297.3. Again, the most abundant fragment (*m/z* 255.2) is that derived from the palmitic acid located at the sn-2 position (Figure 3.12 (c)).

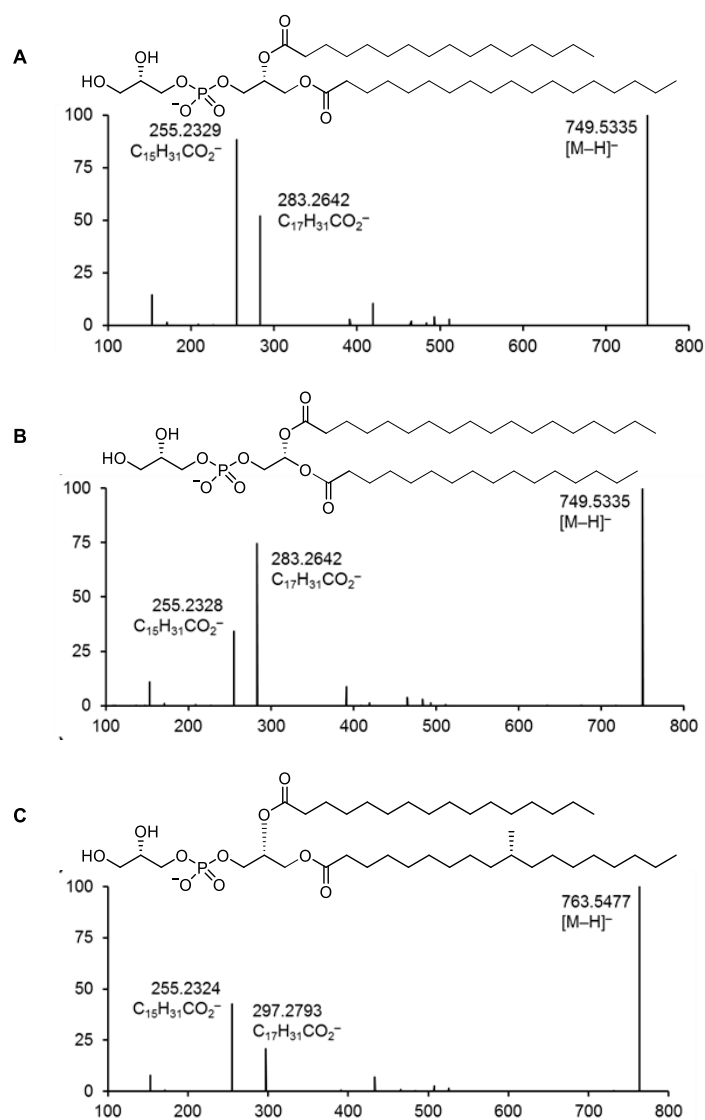


**Figure 3.12** ESI CID MS/MS spectra of A) PG **369** (C<sub>18</sub>/C<sub>16</sub>); B) PG **368** (C<sub>16</sub>/C<sub>18</sub>) and C) *M.tb* PG **370** (TBSA/C<sub>16</sub>).

### 3.11 Conclusions

We have synthesized a representative *M.tb* PG bearing TBSA and two regioisomeric analogues lacking the methyl branch of TBSA. Our approach is the first to use phosphoramidite chemistry to assemble PG, and built upon elements of various published approaches to related PGs, as well as the highly efficient synthesis of (*R*)-TBSA described in the preceding chapter. Our approach utilizes benzyl protecting groups on both the glycerol chains, and the phosphate ester, and thus is limited to the preparation of saturated PGs. However, our method could be modified to utilize different protecting groups, such as PMB groups, which could provide access to unsaturated PGs.

Mass spectrometric analysis of regioisomeric PGs confirmed previous studies of PE and PG that have shown that these classes of molecules cleave to provide abundant fragment ions derived by loss of the fatty acids, and that the most abundant fragment ions are those derived from the fatty acid ester at the sn-2 position. The distinctive fragmentation pattern observed for the characteristic *M.tb* PG could potentially be applied to develop multistage mass spectrometric methods for the identification of *M.tb*.

Finally, the synthetic *M.tb* PG obtained here represents the first homogeneous sample of this natural glycolipid, as prior studies have reported isolation of mixtures of lipofoms, and immunological studies utilized these mixtures; thus the activity of individual components is not known. Studies to date of *M.tb* PG have focused on CD1d-presentation to type 2 NKT cells. Given the recent report that assorted PGs can be detected by CD1b-restricted T cells, this synthetic material may allow broader understanding of recognition of *M.tb* PG by CD1d and CD1b restricted (NK)T cells. Towards this end, these synthetic materials have been provided to Dr. Daniel Pellici in the Department of Immunology to explore the PG-CD1b axis.

### 3.12 Experimental

For General Experimental see Chapter 2

#### **1,2:3,4:5,6-tri-*O*-Isopropylidene-D-mannitol (356)**<sup>149</sup>

A solution of TsOH (18.9 mg, 1.09 mmol) and D-mannitol **325** (2g, 10.9 mmol) in 2,2-dimethoxy propane (14 ml) was stirred at room temperature for 24 h. The reaction mixture was neutralized with triethylamine and solvent evaporated in vacuo. Resulting residue was repeatedly recrystallized from petroleum ether. The product **356** was obtained as colorless rods (2.32 g, 70%); mp 72 – 73 °C (lit.<sup>148</sup> 70-71);  $[\alpha]_{\text{D}}^{23} +13.9$  (*c* 0.5 in CHCl<sub>3</sub>) (lit. +13.4 in MeOH); <sup>1</sup>H NMR (500 MHz, CDCl<sub>3</sub>)  $\delta$  1.36 (6 H, s, 1,2:5,6-*O*-CCH<sub>3</sub>), 1.39 (6 H, s, 3,4-*O*-C(CH<sub>3</sub>)<sub>2</sub>), 1.43 (6 H, s, 1,2:5,6-*O*-CCH<sub>3</sub>), 3.94-4.01 (4 H, m, H<sub>3</sub>, H<sub>4</sub>, H<sub>1</sub>,H<sub>6</sub>), 4.06-4.10 (2 H, m, H'1, H'6), 4.19 (2 H, dd, *J* 11.2, 5.3 Hz, H<sub>2</sub>,H<sub>5</sub>); <sup>13</sup>C NMR (125 MHz, CDCl<sub>3</sub>)  $\delta$  25.5, 26.7, 27.6, 66.4, 79.5, 109.7 (C-O), 110.3 (C-O); HRMS calcd for C<sub>15</sub>H<sub>27</sub>O<sub>6</sub> [M+H]<sup>+</sup> *m/z* 303.1802, found 303.1804.

#### **3,4-*O*-Isopropylidene-D-mannitol (357)**<sup>149</sup>

A solution of compound **356** (0.50 g, 1.65 mmol) in 70% aq. AcOH (10 ml) was stirred at 40 °C for 1.5 h. Solvent was removed under vacuum immediately, residual AcOH was removed by co-evaporation with toluene. Resulting residue was dissolved in dry acetone, stirred with pot. Carbonate and filtered. The filtrate was evaporated under vacuum. The resulting solid was purified by flash chromatography and repeatedly recrystallized from acetone/ petroleum ether to afford **357** as fine white needles (0.23 g, 65%); mp 90-91 °C (lit.<sup>149</sup> 88-90 °C);  $[\alpha]_{\text{D}}^{22} +30.1$  (*c* 0.5 in MeOH) (lit.<sup>149</sup> +31.2 in MeOH); <sup>1</sup>H NMR (400 MHz, acetone (d<sub>6</sub>))  $\delta$  1.33 (6 H, s, 3,4-*O*-CCH<sub>3</sub>), 3.50-3.67 (6 H, m, 2 × CH<sub>2</sub>, 2 × OH), 3.75 (2 H, d, 2 × CH), 3.92-3.94 (2 H, dd, 2 × CH), 4.66 (2 H, s, 2 × OH); <sup>13</sup>C NMR (125

MHz, acetone-d<sub>6</sub>)  $\delta$  27.3, 64.6, 74.3, 80.8, 109.8; HRMS calcd for C<sub>9</sub>H<sub>19</sub>O<sub>6</sub> [M+H]<sup>+</sup> *m/z* 223.1176, found 223.1176.

**1,2,5,6-Tetra-*O*-benzyl-3,4,-*O*-isopropylidene-D-mannitol (358)**<sup>149</sup>

NaH in mineral oil (0.41 g, 17.2 mmol) was added to a solution of **357** (0.7 g, 3.13 mmol) in dry DMF (7 ml) and stirred at 0 °C for 30 min. BnBr (2.12 ml, 17.8 mmol) was added and the reaction mixture was stirred under N<sub>2</sub> overnight warming to room temperature. The reaction mixture was quenched with MeOH, diluted with water and extracted into diethyl ether. The organic layer was washed with brine, dried (MgSO<sub>4</sub>), filtered and concentrated in vacuo. The residue was purified by flash chromatography (toluene/acetone 5:1) affording the product **358** as colorless oil (1.33 g, 96%);  $[\alpha]_D^{23} +12.5$  (*c* 0.5 in CHCl<sub>3</sub>) (lit.<sup>152</sup> +7.0 in CHCl<sub>3</sub>); <sup>1</sup>H NMR (500 MHz, CDCl<sub>3</sub>)  $\delta$  1.36 (6 H, s, C(CH<sub>3</sub>)<sub>2</sub>), 3.6 (2 H, dd, *J* 5.5, 10.4 Hz, H1, H6), 3.7 (2 H, dd, *J* 5.5, 10.4 Hz, H1, H6), 3.7-3.8 (2 H, m, H2, H5), 4.17-4.20 (2 H, m, H3, H4), 4.44 (2 H, d, *J* 11.9 Hz, 1-CH<sub>2</sub>Ph, 6-CH<sub>2</sub>Ph), 4.46 (2 H, d, *J* 11.9 Hz, 1-OCH<sub>2</sub>Ph, 6-CH<sub>2</sub>Ph), 4.5 (2 H, d, *J* 11.9 Hz, 2-CH<sub>2</sub>Ph, 5-CH<sub>2</sub>Ph), 4.7 (2 H, d, *J* 11.9 Hz, 2-CH<sub>2</sub>Ph, 5-CH<sub>2</sub>Ph), 7.2-7.4 (20 H, m, Ph); <sup>13</sup>C NMR (125 MHz, CDCl<sub>3</sub>)  $\delta$  27.4, 70.9, 73.5, 74.2, 79.5, 80.4, 110.7, 128.6, 128.63, 128.8, 129.1, 129.3, 129.4, 139.6, 139.8 (aromatic); HRMS calcd for C<sub>37</sub>H<sub>43</sub>O<sub>6</sub> [M+H]<sup>+</sup> *m/z* 583.3055, found 583.3054.

**1,2,5,6-Tetra-*O*-benzyl-D-mannitol (359)**<sup>149</sup>

A solution of **358** (1.00 g, 1.72 mmol) in 70% AcOH (14 ml) was heated under reflux in a nitrogen atmosphere for 3 h. The solution was cooled to room temperature and concentrated under vacuum. The residue was purified by flash chromatography (20% EtOAc: pet.spirits) to afford **359** as colorless oil (0.93 g, 98%).  $[\alpha]_D^{23} -11.5$  (*c* 0.5 in CHCl<sub>3</sub>) (lit.<sup>152</sup> -15.1 in CHCl<sub>3</sub>); <sup>1</sup>H NMR (500 MHz, methanol-d<sub>4</sub>)  $\delta$  3.7 (2 H, dd, *J* 10.4,

5.3 Hz, H1, H6), 3.8 (2 H, ddd,  $J$  7.7, 5.3, 2.7 Hz, H2, H5), 3.9 (2 H, dd,  $J$  10.4, 2.7, Hz, H'1, H'6), 4.0 (2 H, d,  $J$  7.7 Hz, H3, H4), 4.52 (2 H, d,  $J$  12.0 Hz, CH<sub>2</sub>OCH<sub>2</sub>Ph), 4.54 (2 H, d,  $J$  12.0 Hz, CH<sub>2</sub>OCH<sub>2</sub>Ph), 4.6 (2 H, d,  $J$  11.3 Hz, CHOCH<sub>2</sub>Ph), 4.7 (2 H, d,  $J$  11.3 Hz, CHOCH<sub>2</sub>Ph), 7.2-7.4 (20 H, m, Ph); <sup>13</sup>C NMR (125 MHz, methanol-d<sub>4</sub>)  $\delta$  70.2, 71.3, 73.7, 74.4, 80.1, 128.51, 128.54, 128.8, 128.9, 129.2, 129.3, 139.5, 140.0; HRMS calcd for C<sub>34</sub>H<sub>38</sub>NaO<sub>6</sub> [M+H]<sup>+</sup>  $m/z$  565.2561, found 565.2561.

### **1,2-di-*O*-benzyl-*sn*-glycerol (360)**<sup>149</sup>

A solution of **359** (1.03 g, 0.0018 mmol) in dry CH<sub>2</sub>Cl<sub>2</sub> was added to a vigorously stirred suspension of silica gel-supported NaIO<sub>4</sub> reagent in CH<sub>2</sub>Cl<sub>2</sub>. The reaction mixture was stirred at room temperature under nitrogen for 1h, then filtered and evaporated to dryness. A solution of NaBH<sub>4</sub> in water was added to a solution of the residue in EtOH at 0 °C. The reaction mixture was warmed to room temperature and stirred under nitrogen for 1h. The reaction mixture was neutralized by slow addition of 50% aq.AcOH at 0 °C, diluted in to water and extracted with Et<sub>2</sub>O. The combined extracts were washed with NaHCO<sub>3</sub>, brine, dried, filtered and concentrated. Flash chromatography of the residue (30% EtOAc : pet.spirits) afforded **360** as colorless oil. [ $\alpha$ ]<sub>D</sub><sup>23</sup> -16.5 ( $c$  0.5 in CHCl<sub>3</sub>) (lit.<sup>149</sup> -15.8 in CHCl<sub>3</sub>); <sup>1</sup>H NMR (400 MHz, CDCl<sub>3</sub>)  $\delta$  3.50–3.71 (5 H, m, 2  $\times$  CH<sub>2</sub>, CH), 4.43–4.50 (2 H, m, CH<sub>2</sub>Ph), 4.54 (1 H, d,  $J$  11.7 Hz, CH<sub>2</sub>Ph), 4.64 (1 H, d,  $J$  11.8 Hz, CH<sub>2</sub>Ph), 7.18-7.30 (10 H, m, Ph); <sup>13</sup>C NMR (101 MHz, CDCl<sub>3</sub>)  $\delta$  62.9, 70.3, 72.2, 73.6, 78.1, 127.7, 127.8, 127.9, 128.5, 128.5, 128.5, 138.0, 138.3 (aromatic); HRMS calcd for C<sub>17</sub>H<sub>20</sub>O<sub>3</sub> [M+H]<sup>+</sup>  $m/z$  273.1446, found 273.1448.

### **3-*O*-Benzyl-1-*O*-((*R*)-10-methyloctadecanoyl)-2-*O*-palmitoyl-*sn*-glycerol (352)**<sup>32</sup>

A solution of (*R*)-TBSA **206** (100 mg, 335  $\mu$ mol) and Co[salen] Cl (4.0 mg, 2 mol%) in Et<sub>2</sub>O (1 ml) was stirred under an oxygen balloon for 10 min. The solvent



was evaporated under vacuum to afford a brown residue. THF (0.2 ml) and Hünig's base (58  $\mu$ l, 372  $\mu$ mol) was added to the residue, and the mixture was stirred for 5 min. (*R*)-Glycidyl benzyl ether **349** (56.7  $\mu$ l, 372  $\mu$ mol) was added and the resulting mixture was stirred overnight at room temperature followed by removal of solvents in vacuo. Heptane (800  $\mu$ l), palmitic acid (114 mg, 446  $\mu$ mol) and DMAP (2.27 mg, 18.6  $\mu$ mol, 5 mol%) were added to the resulting residue. The mixture was cooled to 0 °C, followed by addition of DCC (91.9 mg, 446  $\mu$ mol) and stirred overnight. The solvent was removed in vacuo and the residue was subjected to flash chromatography (10% Et<sub>2</sub>O:pentane) to afford the title compound as a colorless thick liquid (178 mg, 77%);  $[\alpha]_D^{23}$  lit.<sup>102</sup> +5.45 (c = 3.9, CHCl<sub>3</sub>); <sup>1</sup>H NMR (400 MHz, CDCl<sub>3</sub>)  $\delta$  0.83 (3 H, d, *J* 6.5 Hz, CCH<sub>3</sub> (TBSA)), 0.88 (6 H, t, *J* 6.8 Hz, 2  $\times$  CH<sub>3</sub>), 1.07 (2 H, m, CH<sub>2</sub> (TBSA)), 1.25 (48 H, m, 24  $\times$  CH<sub>2</sub>), 1.60 (4 H, m, 2  $\times$  COCH<sub>2</sub>CH<sub>2</sub>), 2.25–2.34 (4 H, m, 2  $\times$  COCH<sub>2</sub>), 3.59 (2 H, d, *J* 5.2 Hz, H3a, H3b), 4.19 (1 H, dd, *J* 11.9, 6.4 Hz, H1a), 4.34 (1 H, dd, *J* 11.9, 3.8 Hz, H1b), 4.50–4.58 (2 H, m, CH<sub>2</sub>Ph), 5.24 (1 H, m, H2), 7.27–7.37 (5 H, m, Ph); <sup>13</sup>C NMR (125 MHz, CDCl<sub>3</sub>)  $\delta$  14.2, 19.8, 22.8, 25.0, 25.1, 27.2, 29.2, 29.2, 29.4, 29.5, 29.6, 29.6, 29.8, 30.1, 30.1, 32.0, 32.9, 34.2, 34.4, 37.2, 62.8, 68.4, 70.1, 73.4, 127.7, 127.9, 128.5, 137.8 (Ph), 173.2, 173.5 (C=O); HRMS: calcd for C<sub>45</sub>H<sub>80</sub>O<sub>5</sub> [M + H]<sup>+</sup> 701.6039, found 701.6038.

### **3-*O*-Benzyl-1-*O*-palmitoyl-2-*O*-stearoyl-sn-glycerol (350)**

Synthesized as for **352**, 0.25 g (0.36 mmol, 66%).  $[\alpha]_D^{25}$  +5.6 (c = 0.5, CHCl<sub>3</sub>); <sup>1</sup>H NMR (400 MHz, CDCl<sub>3</sub>)  $\delta$  0.88 (6 H, t, *J* 6.8 Hz, 2  $\times$  CH<sub>3</sub>), 1.27 (48 H, m, 24  $\times$  CH<sub>2</sub>), 1.60 (4 H, m, 2  $\times$  COCH<sub>2</sub>CH<sub>2</sub>), 2.25–2.34 (4 H, m, 2  $\times$  COCH<sub>2</sub>), 3.59 (2 H, d, *J* 5.2 Hz, H3a, H3b), 4.19 (1 H, dd, *J* 11.9, 6.4 Hz, H1a), 4.34 (1 H, dd, *J* 11.9,

3.8 Hz, H1b), 4.50–4.58 (2 H, m, CH<sub>2</sub>Ph), 5.24 (1 H, m, H2), 7.28–7.37 (5 H, m, Ph); <sup>13</sup>C NMR (101 MHz, CDCl<sub>3</sub>) δ 14.2, 22.8, 25.0, 25.1, 29.2, 29.2, 29.4, 29.5, 29.6, 29.8, 29.8, 32.0, 34.2, 34.4, 62.8, 68.4, 70.1, 73.4, 127.7, 127.9, 128.5, 137.8, 173.2, 173.5 (C=O); HRMS: calcd for C<sub>44</sub>H<sub>78</sub>O<sub>5</sub> [M + H]<sup>+</sup> 687.5883, found 687.5884.

### **3-*O*-Benzyl-1-*O*-stearoyl-2-*O*-palmitoyl-sn-glycerol (351)**

Synthesized as for **352**, 0.062 g (0.093 mmol, 64%). [α]<sub>D</sub><sup>25</sup> +5.8 (c = 0.5, CHCl<sub>3</sub>), lit.<sup>153</sup> [α]<sub>D</sub><sup>23</sup> +5.4 (c = 1.63, CHCl<sub>3</sub>); <sup>1</sup>H NMR (400 MHz, CDCl<sub>3</sub>) δ 0.88 (6 H, t, *J* 6.8 Hz, 2 × CH<sub>3</sub>), 1.27 (48 H, m, 24 × CH<sub>2</sub>), 1.60 (4 H, m, 2 × COCH<sub>2</sub>CH<sub>2</sub>), 2.25–2.34 (4 H, m, 2 × COCH<sub>2</sub>), 3.59 (2 H, d, *J* 5.2 Hz, H3a, H3b), 4.19 (1 H, dd, *J* 11.9, 6.4 Hz, H1a), 4.34 (1 H, dd, *J* 11.9, 3.8 Hz, H1b), 4.50–4.58 (2 H, m, CH<sub>2</sub>Ph), 5.24 (1 H, m, H2), 7.28–7.37 (5 H, m, Ph); <sup>13</sup>C NMR (101 MHz, CDCl<sub>3</sub>) δ 14.2, 22.8, 25.0, 25.1, 29.2, 29.2, 29.4, 29.5, 29.6, 29.8, 29.8, 32.0, 34.2, 34.4, 62.8, 68.4, 70.1, 73.4, 127.7, 127.9, 128.5, 137.8 (Ph), 173.2, 173.5 (C=O); HRMS: calcd for C<sub>44</sub>H<sub>78</sub>O<sub>5</sub> [M + H]<sup>+</sup> 687.5883, found 687.5884.

### **1-*O*-((*R*)-10-Methyloctadecanoyl)-2-*O*-palmitoyl-sn-glycerol (355)<sup>32</sup>**

A mixture of **352** (65 mg, 0.089 mmol) and Pd(OH)<sub>2</sub> on carbon (20%, 40 mg, 0.285 mmol) in ethanol (3 ml) was stirred under hydrogen at 10 bar for 2 h. The reaction mixture was filtered through Celite and the solvent removed in vacuo to afford the product as a colorless liquid (61 mg, 99%). The compound was used directly without delay or purification. <sup>1</sup>H NMR (400 MHz, CDCl<sub>3</sub>) δ 0.83 (3 H, d, *J* 6.5 Hz, CCH<sub>3</sub> (TBSA)), 0.88 (6 H, t, *J* 6.8 Hz, 2 × CH<sub>3</sub>), 1.08 (2 H, m, CH<sub>2</sub> (TBSA)), 1.27 (48 H, m, 24 × CH<sub>2</sub>), 1.62 (4 H, m, 2 × COCH<sub>2</sub>CH<sub>2</sub>), 2.30–2.37 (4 H, m, 2 ×

COCH<sub>2</sub>), 3.73 (2 H, d, *J* 5.2 Hz, H3a,3b), 4.24 (1 H, dd, *J* 11.9, 5.6 Hz, H1a), 4.32 (1 H, dd, *J* 11.9, 4.6 Hz, H1b), 5.06–5.11 (1 H, m, H2).

**1-*O*-Palmitoyl-2-*O*-stearoyl-sn-glycerol (353)**

Synthesized as for **355**, 30.4 mg (98%). <sup>1</sup>H NMR (500 MHz, CDCl<sub>3</sub>) δ 0.88 (6 H, t, *J* 7.0 Hz, 2 × CH<sub>3</sub>), 1.27–1.34 (48 H, m, 24 × CH<sub>2</sub>), 1.62 (4 H, m, 2 × COCH<sub>2</sub>CH<sub>2</sub>), 2.30–2.37 (4 H, m, 2 × COCH<sub>2</sub>), 3.73 (2 H, dd, *J* 5.0, 1.4 Hz, H3a,3b), 4.23 (1 H, dd, *J* 11.9, 5.7 Hz, H1a), 4.32 (1 H, dd, *J* 11.9, 4.5 Hz, H1b), 5.06–5.11 (1 H, m, H2).

**1-*O*-Stearoyl-2-*O*-palmitoyl-sn-glycerol (354)**

Synthesized as for **355**, 40.2 mg (96%). <sup>1</sup>H NMR (500 MHz, CDCl<sub>3</sub>) δ 0.88 (6 H, t, *J* 7.0 Hz, 2 × CH<sub>3</sub>), 1.27–1.34 (48 H, m, 24 × CH<sub>2</sub>), 1.62 (4 H, m, 2 × COCH<sub>2</sub>CH<sub>2</sub>), 2.30–2.37 (4 H, m, 2 × COCH<sub>2</sub>), 3.73 (2 H, dd, *J* 5.0, 1.4 Hz, H3a,3b), 4.23 (1 H, dd, *J* 11.9, 5.7 Hz, H1a), 4.32 (1 H, dd, *J* 11.9, 4.5 Hz, H1b), 5.06–5.11 (1 H, m, H2).

***O*-Benzyl-*O*-(1-*O*-((*R*)-10-methyloctadecanoyl)-2-*O*-palmitoyl-sn-glycer-3-yl) *N,N*-diisopropylphosphoramidite (364)<sup>101</sup>**

Diisopropylammonium tetrazolide (34.1 mg, 0.199 mmol) was added to a solution of alcohol **355** (58.0 mg, 0.094 mmol) and benzyl bis(*N,N*-diisopropyl)phosphoramidite<sup>154</sup> **361** (62.3 mg, 0.189 mmol) in dry CH<sub>2</sub>Cl<sub>2</sub> at 0 °C under nitrogen. The reaction mixture was stirred for 30 min at 0 °C and 25 min at room temperature. The solvent was removed in vacuo and the residue was purified by column chromatography on alumina (5% EtOAc/petroleum ether) to afford the title compound as a colorless oil (50 mg, 85%); [α]<sub>D</sub><sup>23</sup> +5.4 (*c* 0.5, CHCl<sub>3</sub>); <sup>1</sup>H NMR (500 MHz, CDCl<sub>3</sub>) δ 0.83 (3 H, d, *J* 6.6 Hz, CCH<sub>3</sub> (TBSA)), 0.88 (6 H, t, *J*

6.9 Hz, 2 × CH<sub>3</sub>), 1.18 (2 H, m, CH<sub>2</sub>), 1.17–1.20 (12 H, m, 2 × CH(CH<sub>3</sub>)<sub>2</sub>), 1.23–1.35 (49 H, m, 24 × CH<sub>2</sub>, 1 × CH), 1.57–1.62 (4 H, m, COCH<sub>2</sub>CH<sub>2</sub>), 2.21–2.31 (4 H, m, COCH<sub>2</sub>), 3.60–3.81 (4 H, m, 2 × CH(CH<sub>3</sub>)<sub>2</sub>, H3a,3b), 4.13–4.20 (1 H, m, H1a), 4.31–4.37 (1 H, m, H1b), 4.64–4.77 (2 H, m, CH<sub>2</sub>Ph), 5.15–5.22 (1 H, m, H2), 7.30–7.41 (5 H, m, Ph); <sup>13</sup>C NMR (75 MHz, CDCl<sub>3</sub>) δ 14.2, 19.8, 22.8, 24.6, 24.7, 24.8, 25.0, 29.2, 29.4, 29.5, 29.6, 29.8, 29.8, 32.0, 34.3, 43.1, 43.2, 61.6, 61.7, 61.9, 62.6, 63.2, 65.4, 65.6, 70.9 (N-CH), 127.0, 127.4, 128.3, 139.4 (Ph), 173.1, 173.5 (C=O); <sup>31</sup>P NMR (202 MHz, CDCl<sub>3</sub>) δ 148.8; HRMS-ESI: [M + H]<sup>+</sup> calcd for C<sub>51</sub>H<sub>95</sub>O<sub>6</sub>NP 848.6897; found 848.6885.

***O*-Benzyl-*O*-(1-*O*-((*R*)-10-methyloctadecanoyl)-2-*O*-palmitoyl-*sn*-glyceryl)-*O*-(2,3-di-*O*-benzyl-*sn*-glycer-1-yl) phosphate (**367**)**

1*H*-Tetrazole (4.8 mg, 0.068 mmol) was added to a solution of phosphoramidite (42.0 mg, 0.049 mmol) and 2,3-di-*O*-benzyl-*sn*-glycerol **360** (10.7 mg, 0.0392 mmol) in dry CH<sub>2</sub>Cl<sub>2</sub> (2 ml) at 0 °C under nitrogen. The reaction mixture was stirred for 15 min at 0 °C and 2 hours at room temperature. The reaction mixture was cooled to 0 °C and *t*-BuOOH (5 M in decane) (5 μl, 0.0582 mmol) was added and stirred for 2 h warming to room temperature. Excess oxidant was quenched with sodium metabisulfite (1M, 0.1 ml), the reaction mixture was diluted with CH<sub>2</sub>Cl<sub>2</sub>, extracted, dried (MgSO<sub>4</sub>), filtered and concentrated. The residue was purified by column chromatography on silica gel (35% EtOAc/ petroleum ether, 0.5% Et<sub>3</sub>N) to afford the title compound as an oil (25 mg, 55%); [α]<sub>D</sub><sup>24</sup> 6.3 (*c* 0.25, CHCl<sub>3</sub>); <sup>1</sup>H NMR (600 MHz, CDCl<sub>3</sub>) δ 0.83 (3 H, d, *J* 6.6 Hz, CCH<sub>3</sub> (TBSA)), 0.88 (6 H, t, *J* 6.9 Hz, 2 × CH<sub>3</sub> (TBSA, palmitoyl)), 1.06–1.07 (2 H, m, CH<sub>2</sub>), 1.26 (49 H, m, 24 × CH<sub>2</sub>, 1 × CH), 1.57 (4 H, m, 2 × COCH<sub>2</sub>CH<sub>2</sub>), 2.26 (4 H, m, 2 ×

COCH<sub>2</sub>), 3.56 (2 H, t, *J* 5.6 Hz, H3'a,3'b), 3.77 (1 H, m, H2'), 4.03–4.16 (4 H, m, H3a,3b,1'a,1'b), 4.23 (2 H, m, H1a,1b), 4.51 (2 H, d, *J* 4.8 Hz, CH<sub>2</sub>Ph), 4.60–4.67 (2 H, m, CH<sub>2</sub>Ph), 5.02–5.05 (2 H, m, CH<sub>2</sub>Ph), 5.16 (1 H, m, H2'), 7.32 (15 H, m, Ph); <sup>13</sup>C NMR (126 MHz, CDCl<sub>3</sub>) δ 14.2, 19.8, 22.8, 24.9, 27.2, 29.2, 29.2, 29.4, 29.5, 29.6, 29.7, 29.8, 30.1, 30.2, 32.0, 32.9, 34.1, 34.2, 37.2, 61.8, 65.5, 67.3, 67.3, 69.1, 69.4, 69.4, 69.5, 69.6, 72.3, 73.6, 127.7, 127.8, 127.9, 128.0, 128.5, 128.5, 128.7 (Ph), 172.9, 173.3 (C=O); <sup>31</sup>P NMR (202 MHz, CDCl<sub>3</sub>) δ –1.01, –0.98; HRMS: [M + H]<sup>+</sup> calcd for C<sub>62</sub>H<sub>99</sub>O<sub>10</sub>P, 1035.7009; found 1035.7006.

**Triethylammonium *O*-(1-*O*-(*R*)-10-methyloctadecanoyl-2-*O*-palmitoyl-*sn*-glyceryl)-*O*-(*sn*-glycer-1-yl) phosphate (370)**

A mixture of Pd(OH)<sub>2</sub> on carbon (20%, 5 mg, 0.035 mmol), **367** (10 mg, 9.65 μmol) in EtOAc:methanol (5 ml, 5:1) was stirred under hydrogen (20 bar) for 4 h at room temperature. The reaction mixture is filtered through a short plug of Celite to remove the catalyst. Triethylamine (5 μl) was added to the filtrate and solvent removed under reduced pressure. The resulting residue was purified by flash chromatography (20% methanol:chloroform) to afford **370** as a colorless oil (9 mg, 98%); [α]<sub>D</sub><sup>24</sup> +5.8 (*c* 0.25, CHCl<sub>3</sub>); <sup>1</sup>H NMR (500 MHz, CD<sub>3</sub>OD:CDCl<sub>3</sub> (1:2)) δ 0.80 (3 H, d, *J* 6.6 Hz, CCH<sub>3</sub> (TBSA)), 0.85 (6 H, t, *J* 6.8 Hz, 2 × CH<sub>3</sub> (TBSA, palmitoyl)), 1.03–1.06 (2 H, m, CH<sub>2</sub>), 1.17–1.36 (62 H, m, 26 × CH<sub>2</sub>, 1 × CH, HN(CH<sub>2</sub>CH<sub>3</sub>)<sub>3</sub>), 1.57 (4 H, m, 2 × COCH<sub>2</sub>CH<sub>2</sub>), 2.29 (4 H, dd, *J* 15.6, 8.0 Hz, 2 × COCH<sub>2</sub>), 3.11 (4 H, q, *J* 7.3 Hz, NH(CH<sub>2</sub>CH<sub>3</sub>)<sub>3</sub>) 3.58 (2 H, s, H3'a,3'b), 3.76 (1 H, s, H2'), 3.90 (2 H, s, H1'a,1'b), 3.98 (2 H, s, H3a,3b), 4.15 (1 H, dd, *J* 11.8, 6.5 Hz, H1b), 4.38 (1 H, d, *J* 12.0 Hz, H1a), 5.20 (1 H, s, H2); <sup>13</sup>C NMR (126 MHz, CD<sub>3</sub>OD:CDCl<sub>3</sub> (1:2)) δ 14.2, 19.9, 23.0, 25.2, 25.2, 27.4, 29.5, 29.5, 29.7, 29.9,

29.9, 30.0, 30.3, 30.4, 32.3, 33.1, 34.4, 34.6, 37.4, 46.8, 62.9, 64.2, 67.1, 70.7, 71.4 (glycerol C), 174.0, 174.3 (C=O);  $^{31}\text{P}$  NMR (202 MHz,  $\text{CD}_3\text{OD}:\text{CDCl}_3$  (1:2))  $\delta$  4.78; HRMS:  $[\text{M} + \text{H}]^+$  calcd for  $\text{C}_{47}\text{H}_{96}\text{NO}_{10}\text{P}$  866.6805; found 866.6806.

***O*-Benzyl-*O*-(1-*O*-(palmitoyl)-2-*O*-stearoyl-*sn*-glycer-3-yl) *N,N*-diisopropylphosphoramidite (362)**

Alcohol **353** (30 mg, 0.050 mmol) was treated as for the preparation of **364** to afford **362** (30.4 mg, 72%).  $[\alpha]_{\text{D}}^{24} +5.8$  (*c* 0.5,  $\text{CHCl}_3$ );  $^1\text{H}$  NMR (600 MHz,  $\text{CDCl}_3$ )  $\delta$  0.88 (6 H, t, *J* 6.8 Hz,  $2 \times \text{CH}_3$ ), 1.17–1.20 (12 H, m,  $2 \times \text{CH}(\text{CH}_3)_2$ ), 1.23–1.35 (52 H, m,  $26 \times \text{CH}_2$ ), 1.57–1.62 (4 H, m,  $\text{COCH}_2\text{CH}_2$ ), 2.21–2.31 (4 H, m,  $\text{COCH}_2$ ), 3.60–3.67 (2 H, m,  $2 \times \text{CH}(\text{CH}_3)_2$ ), 3.69–3.75 (1 H, m, H3b), 3.76–3.81 (1 H, m, H3a), 4.13–4.20 (1 H, m, H1a), 4.34 (1 H, td, *J* 12.2, 3.8 Hz, H1b), 4.63–4.79 (2 H, m,  $\text{CH}_2\text{Ph}$ ), 5.18–5.19 (1 H, m, H2), 7.27–7.35 (5 H, m, Ph);  $^{13}\text{C}$  NMR (101 MHz,  $\text{CDCl}_3$ )  $\delta$  14.2, 22.8, 24.6, 24.7, 24.8, 25.0, 29.2, 29.4, 29.5, 29.6, 29.8, 29.8, 32.0, 34.3, 43.1, 43.2, 61.6, 61.7, 61.9, 62.6, 63.2, 65.4, 65.6, 70.9 (N-CH), 127.0, 127.4, 128.3, 139.4 (Ph), 173.1, 173.5 (C=O);  $^{31}\text{P}$  NMR (202 MHz,  $\text{CDCl}_3$ )  $\delta$  148.8; HRMS-ESI:  $[\text{M} + \text{H}]^+$  calcd for  $\text{C}_{50}\text{H}_{92}\text{NO}_6\text{P}$  834.6696; found 834.6696.

***O*-Benzyl-*O*-(1-*O*-(stearoyl)-2-*O*-palmitoyl-*sn*-glycer-3-yl) *N,N*-diisopropylphosphoramidite (363)**

Alcohol **354** (36.0 mg, 0.60 mmol) was treated as for the preparation of **364** to afford **363** (29.8 mg, 58%).  $[\alpha]_{\text{D}}^{24} +5.5$  (*c* 0.5,  $\text{CHCl}_3$ );  $^1\text{H}$  NMR (400 MHz,  $\text{CDCl}_3$ )  $\delta$  0.88 (6 H, t, *J* 6.8 Hz,  $2 \times \text{CH}_3$ ), 1.17–1.20 (12 H, m,  $2 \times \text{CH}(\text{CH}_3)_2$ ), 1.23–1.35 (52 H, m,  $26 \times \text{CH}_2$ ), 1.57–1.62 (4 H, m,  $\text{COCH}_2\text{CH}_2$ ), 2.21–2.31 (4 H, m,  $\text{COCH}_2$ ), 3.58–3.83 (4 H, m,  $2 \times \text{CH}(\text{CH}_3)_2$ , H3a, H3b), 4.12–4.19 (1 H, m, H1a), 4.30–4.38 (1 H, m, H1b), 4.62–4.80 (2 H, m,  $\text{CH}_2\text{Ph}$ ), 5.17–5.24 (1 H, m, H2), 7.27–7.35 (5

H, m, Ph);  $^{13}\text{C}$  NMR (75 MHz,  $\text{CDCl}_3$ )  $\delta$  14.2, 22.8, 24.6, 24.7, 24.8, 25.0, 29.2, 29.4, 29.5, 29.6, 29.8, 29.8, 32.0, 34.3, 43.1, 43.2, 61.6, 61.7, 61.9, 62.6, 63.2, 65.4, 65.6, 70.9 (N-CH), 127.0, 127.4, 128.3, 139.4 (Ph), 173.1, 173.5 (C=O);  $^{31}\text{P}$  NMR (202 MHz,  $\text{CDCl}_3$ )  $\delta$  148.0; HRMS-ESI:  $[\text{M} + \text{H}]^+$  calcd for  $\text{C}_{50}\text{H}_{92}\text{NO}_6\text{P}$  834.6696; found 834.6696.

***O*-Benzyl-*O*-(1-*O*-(palmitoyl)-2-*O*-stearoyl-sn-glycer-3-yl)-*O*-(2,3-di-*O*-benzyl-sn-glycer-1-yl) phosphate (365)**

1*H*-Tetrazole (2.7 mg, 0.039 mmol) was added to a solution of **362** (24.0 mg, 0.028 mmol) and **360** (9.4 mg, 0.034 mmol) in dry  $\text{CH}_2\text{Cl}_2$  (2 ml) at 0 °C under nitrogen. The reaction mixture was stirred for 15 min at 0 °C and 2 h at room temperature. The reaction mixture was cooled to 0 °C and *t*-BuOOH (5 M in decane) (4.1  $\mu\text{l}$ , 0.042 mmol) was added to the reaction mixture and stirred for 2 h with warming to room temperature. Excess oxidant was quenched with sodium metabisulfite (1 M, 0.1 ml), the reaction mixture was diluted with  $\text{CH}_2\text{Cl}_2$ , extracted, dried ( $\text{MgSO}_4$ ), filtered and concentrated. The solvent was removed in vacuo and the residue was purified by column chromatography on silica gel (35% EtOAc/petroleum ether, 0.5%  $\text{Et}_3\text{N}$ ) which resulted in a 1:1 mixture the product and unreacted dibenzyl glycerol, which was directly subjected to hydrogenolysis.

***O*-Benzyl-*O*-(1-*O*-(stearoyl)-2-*O*-palmitoyl-sn-glycer-3-yl)-*O*-(2,3-di-*O*-benzyl-sn-glycer-1-yl) phosphate (366)**

Synthesized as for **367**, 10.2 mg (34%).  $[\alpha]_{\text{D}}^{25} +6.2$  ( $c = 0.25$ ,  $\text{CHCl}_3$ );  $^1\text{H}$  NMR (600 MHz,  $\text{CDCl}_3$ )  $\delta$  0.88 (6 H, t,  $J$  6.8 Hz,  $2 \times \text{CH}_3$ ), 1.27 (56 H, m,  $28 \times \text{CH}_2$ ), 1.57 (4 H, m,  $2 \times \text{COCH}_2\text{CH}_2$ ), 2.26 (4 H, t,  $J$  7.6 Hz,  $2 \times \text{COCH}_2$ ), 3.56 (2 H, t,  $J$  5.6 Hz, H3'a,3'b), 3.75–3.79 (1 H, m, H2'), 4.03–4.29 (6 H, m,

H1'a,1'b,3a,3b,1a,1b), 4.50–4.54 (2 H, m, CH<sub>2</sub>Ph), 4.60–4.68 (2 H, m, CH<sub>2</sub>Ph), 5.04 (2 H, m, CH<sub>2</sub>Ph), 5.13–5.20 (1 H, m, H<sub>2</sub>), 7.27–7.35 (15 H, m, Ph); <sup>13</sup>C NMR (126 MHz, CDCl<sub>3</sub>) δ 14.2, 22.8, 24.9, 27.2, 29.2, 29.2, 29.4, 29.5, 29.6, 29.7, 29.8, 30.1, 30.2, 32.0, 32.9, 34.1, 34.2, 37.2, 61.8, 65.5, 67.3, 67.3, 69.1, 69.4, 69.4, 69.5, 69.6, 72.3, 73.6, 127.7, 127.8, 127.9, 128.0, 128.5, 128.5, 128.7 (Ph), 172.9, 173.3 (C=O); <sup>31</sup>P NMR (202 MHz, CDCl<sub>3</sub>) δ –1.01, –0.98; HRMS: [M + H]<sup>+</sup> calcd for C<sub>61</sub>H<sub>97</sub>O<sub>10</sub>P 1021.6853; found 1021.6852.

**Triethylammonium *O*-(1-*O*-palmitoyl-2-*O*-stearoyl-*sn*-glyceryl)-*O*-(*sn*-glycer-1-yl) phosphate (368)**

Synthesized as for **370**, 6.2 mg (27% over 2 steps). [α]<sub>D</sub><sup>25</sup> +5.6 (*c* 0.25, CHCl<sub>3</sub>); <sup>1</sup>H NMR (400 MHz, CD<sub>3</sub>OD:CDCl<sub>3</sub> (1:2)) δ 0.84 (6 H, t, *J* 6.4 Hz, 2 × CH<sub>3</sub>), 1.10–1.14 (9 H, m, HN(CH<sub>2</sub>CH<sub>3</sub>)<sub>3</sub>), 1.17–1.36 (56 H, m, 28 × CH<sub>2</sub>), 1.52 (4 H, s, 2 × COCH<sub>2</sub>CH<sub>2</sub>), 2.23 (4 H, dd, *J* 14.5, 7.2 Hz, 2 × COCH<sub>2</sub>), 3.46–3.61 (6 H, s, H3'a,3'b, HN(CH<sub>2</sub>CH<sub>3</sub>)<sub>3</sub>), 3.65–3.73 (1 H, m, H<sub>2</sub>'), 3.83–3.90 (4 H, m, H1'a,1'b,3a,3b), 3.95 (2 H, m, H3a,3b), 4.11 (1 H, dd, *J* 12.0, 6.6 Hz, H1b), 5.16 (1 H, s, H<sub>2</sub>); <sup>13</sup>C NMR (126 MHz, CD<sub>3</sub>OD:CDCl<sub>3</sub> (1:2)) δ 14.2, 23.0, 25.2, 25.2, 29.5, 29.5, 29.7, 29.7, 29.9, 30.0, 30.0, 32.3, 34.4, 34.6, 46.5, 62.8, 63.0, 63.7, 66.8, 70.8, 70.9, 71.5, 72.7, 174.0, 174.4 (C=O); <sup>31</sup>P NMR (202 MHz, CDCl<sub>3</sub>) δ 4.78; HRMS: [M + H]<sup>+</sup> calcd for C<sub>40</sub>H<sub>79</sub>O<sub>10</sub>P 751.5444; found 751.5444.

***O*-(1-*O*-Stearoyl-2-*O*-palmitoyl-*sn*-glyceryl)-*O*-(*sn*-glycer-1-yl) phosphate (369)**

Synthesized as for **370**, 9.1 mg (90%). [α]<sub>D</sub><sup>25</sup> +4.8 (*c* 0.25, CHCl<sub>3</sub>); <sup>1</sup>H NMR (400 MHz, CD<sub>3</sub>OD:CDCl<sub>3</sub> (1:2)) δ 0.84 (6 H, t, *J* 6.4 Hz, 2 × CH<sub>3</sub>), 1.17–1.36 (56 H, m, 28 × CH<sub>2</sub>), 1.57 (4 H, s, 2 × COCH<sub>2</sub>CH<sub>2</sub>), 2.29 (4 H, dd, *J* 14.5, 7.2 Hz, 2 × COCH<sub>2</sub>), 3.57 (2 H, s, H3'a,3'b), 3.70–3.78 (1 H, m, H<sub>2</sub>'), 3.84–3.90 (2 H, s, H1'a,



H1'b), 3.95 (2 H, m, H3a,3b), 4.15 (1 H, dd,  $J$  11.9, 6.7 Hz, H1b), 4.37 (1 H, m, H1a), 5.20 (1 H, s, H2);  $^{13}\text{C}$  NMR (126 MHz,  $\text{CD}_3\text{OD}:\text{CDCl}_3$  (1:2))  $\delta$  14.2, 23.0, 25.2, 25.2, 29.5, 29.5, 29.7, 29.7, 29.9, 30.0, 30.0, 32.3, 34.4, 34.6, 46.5, 62.8, 63.0, 63.7, 66.8, 70.8, 70.9, 71.5, 72.7, 174.0, 174.4;  $^{31}\text{P}$  NMR (202 MHz,  $\text{CDCl}_3$ )  $\delta$  5.25; HRMS:  $[\text{M} + \text{H}]^+$  calcd for  $\text{C}_{40}\text{H}_{79}\text{O}_{10}\text{P}$  751.5444; found 751.5444.

### **Collision-induced dissociation mass spectrometry of phosphatidylglycerols**

Characterization of lipid ions, introduced to a Q Exactive Plus Orbitrap mass spectrometer (Thermo Fisher Scientific, Bremen, Germany) via nanoESI (nESI) using an Advion Triversa Nanomate (Advion, Ithaca, NY), was performed in negative ionization mode by higher-energy collision induced dissociation (HCD)-tandem mass spectrometry (MS/MS). Deprotonated precursor ions were mono-isotopically isolated using a window of  $\pm 0.5$   $m/z$ . Product ion spectra were acquired using a mass resolving power of 70,000. Spectra shown are the average of 100 scans.



## **Chapter 4**

**A second generation synthesis of Gl-A, a  
GlcA-DAG from *M. smegmatis***

## 4.1 Introduction

Glycosyl diacylglycerols are ubiquitous membranous components present in higher plants and gram positive bacteria.<sup>155-156</sup> Yet, glucuronosyl diacylglycerols are comparatively rare and so are of special interest. Wilkinson *et al.* reported  $\alpha$ -D-glucuronosyl diglyceride and a glucosyl- $\alpha$ -glucuronosyl diglyceride as major glycolipids in *Pseudomonas diminuta*<sup>157</sup> and a few others were isolated from *Bacillus cereus* and various halotolerant bacteria.<sup>156</sup> Also,  $\alpha$ -glucuronosyl diglycerides have been described in a range of plants, with its expression linked to phosphorus starvation.<sup>19</sup> Of relevance to this chapter, several glycosyl diglycerols have been reported in mycobacteria, including glucosyl diglycerols and  $\alpha$ -glucuronosyl diglycerols.<sup>85, 158</sup>

## 4.2 Mycobacterial glycosyl diacylglycerols

### 4.2.1 Gentiobiosides

Early work showed that neutral mono and diglucosyl diacylglycerols would be formed by cellular extracts of *M. smegmatis*.<sup>159</sup> However no glycosyl DAGs were isolated from mycobacteria until the discovery of a diglucosyl diacylglycerol from the avirulent H37Ra strain of *M.tb* by Hunter *et al* in 1986.<sup>160</sup> After extensive extraction and purification, a family of  $\beta$ -gentiobiosyl diacylglycerides were characterized that existed in at least 5 different lipofoms. The major fatty acids were identified as iso-pentadecanoic acid, anteiso-pentadecanoic acid, hexadecanoic acid, iso-hexadecanoic acid, iso-heptadecanoic acid and anteiso-heptadecanoic acid (Figure 4.1).<sup>160</sup> Our group recently reported the first total synthesis of representatives of this class of compounds.<sup>161</sup> They were shown to be able to signal through mouse MinCLE, but not human MinCLE. Additionally, monoglucosyl diglycerides, the putative biosynthetic precursors to the gentiobiosides, were also synthesized. These were shown to signal more potently through

mouse Mincle and also through human Mincle.<sup>161</sup> Mincle is a transmembrane CLR that recognizes a broad range of self and foreign molecules as a part of innate sensing (See section 1.4.1). Ligand binding occurs at carbohydrate recognition domain (CRD). Studies performed using the  $\beta$ -gentiobiosyl glycerides shown in Figure 4.1 and other synthetic analogues suggest that human and mouse Mincle can preferentially recognize  $\beta$ -glycosyl diglycerides rather than their extended derivatives.

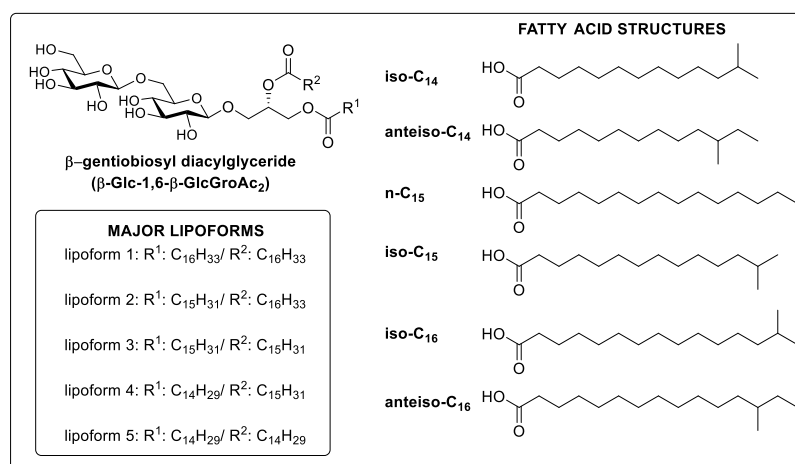


**Figure 4.1** Structure of  $\beta$ -gentiobiosyl diacylglycerides from *M. tuberculosis*. The major lipoforms and the structure of the lipids are shown.

#### 4.2.2 $\alpha$ -Glucuronides

In 1993, Brennan and co-workers isolated  $\alpha$ -glucuronosyl diacylglyceride (GlcAGroAc<sub>2</sub>; GI-A) from *M. smegmatis* MNC strain 13. It was shown that this material was comprised of two lipoforms, both of which contained palmitic acid residues and the second fatty acid was either TBSA or oleic acid (Figure 4.3).<sup>85</sup> The proposed structures of these glycolipids were confirmed by total synthesis and mass spectrometric fragmentation experiments (see below). The oleic acid containing lipoform has also been isolated from *Corynebacterium glutamicum*, as well as a mannosylated variant bearing an  $\alpha$ -mannosyl group at O4.<sup>162</sup>

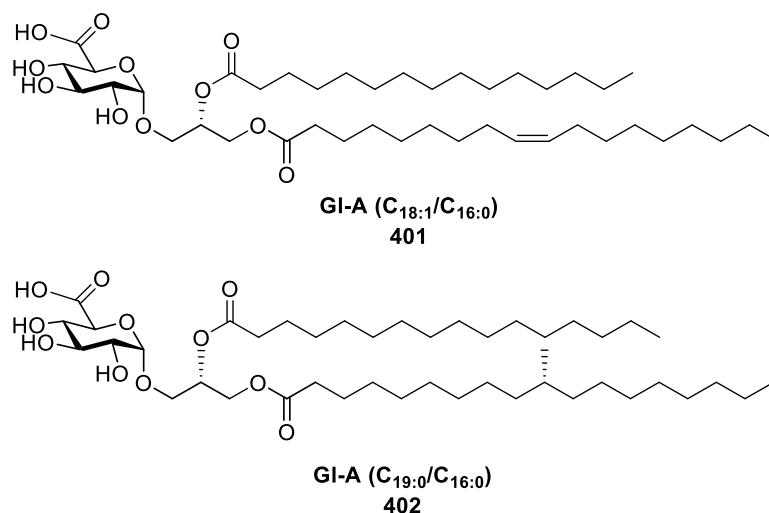


**Figure 4.2** Two GI-A lipoforms isolated from *M. smegmatis*.

### 4.3 Determination of the structure of GI-A lipoforms

Brennan *et al.* studied the GI-A isolated from *M. smegmatis* by mass spectrometry and detected two molecular species of  $m/z$  755 and 785 (**401**, **402**). Upon FAB/MS fragmentation, both these molecular ions fragmented to afford a major peak at  $m/z$  255 corresponding to palmitic acid. For one of the lipoforms, the second peak was that at  $m/z$  297 corresponding to TBSA while for the other lipoform a fragment was observed at  $m/z$  289 corresponding to oleic acid (Figure 4.3).<sup>85</sup> The negative ion FAB-MS/MS spectrum of native GI-A  $m/z$  785 corresponding to TBSA also revealed fragment ions at  $m/z$  547 and 505, corresponding to the cleavage of palmitic acid and tuberculostearic acid, respectively, in an intensity ratio of 3:1.

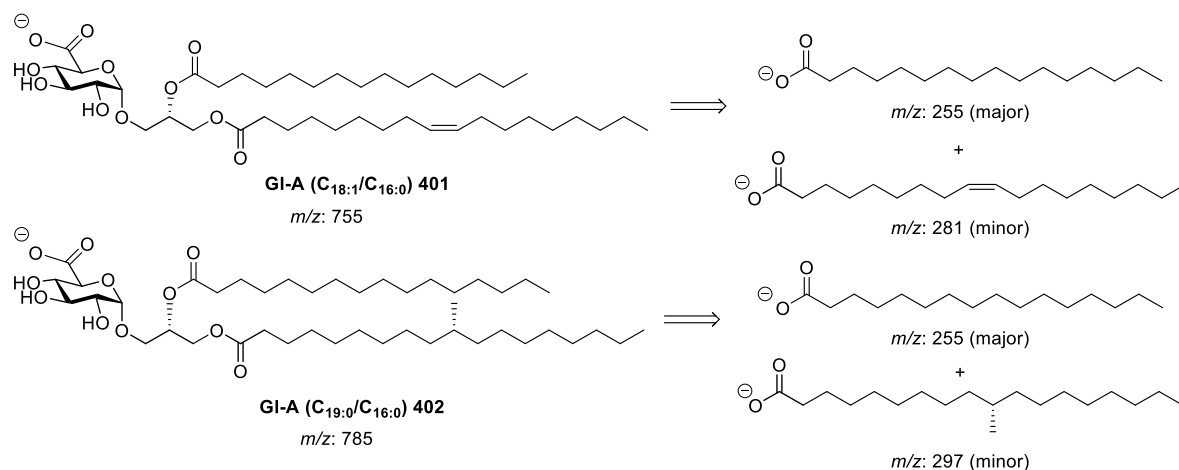


**Figure 4.3** FAB/MS fragmentation of the isolated isoforms of GI-A.

In 2011, Cao *et al.* synthesized the proposed structure of GI-A and a regioisomer variant, iso-GI-A, with the reverse acylation pattern at sn-1 and sn-2 of the glycerol fragment (Figure 4.4).<sup>86</sup> Cao *et al.* performed ESI CID-MS/MS of the deprotonated isomers and observed fragment ions with clear differences in the relative intensities.<sup>86</sup>

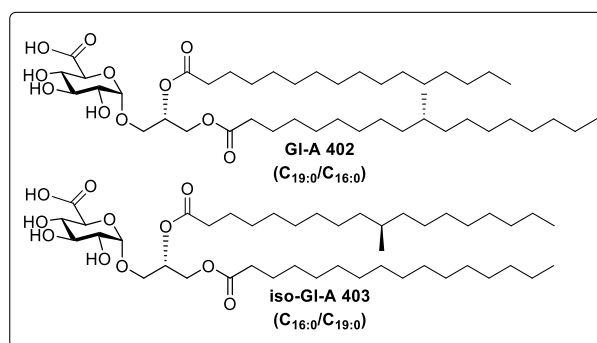


**Figure 4.4** Structures of synthetic GI-A and the regioisomeric variant: iso-GI-A.

For example, fragmentation of the  $[M-H]^-$  pseudomolecular ion of GI-A (C<sub>19:0</sub>/C<sub>16:0</sub>) **402** gave rise to ions at *m/z* 547 and 505 in a ratio of 3:1, via loss of palmitic acid and tuberculostearic acid in the form of ketenes, respectively (Figure 4.5). For iso-GI-A (C<sub>16:0</sub>/C<sub>19:0</sub>) **403** the ion at *m/z* 547 was one third the intensity of the ion at *m/z* 505. This reversal of intensities of fragment ions indicated that fragmentation at sn-2 position is the preferred pathway. The relative intensity of the *m/z* 547/505 fragment ions of **402** matched that observed for the natural material, and differed to that of synthetic iso-

GI-A **403**, which has the intensities in the opposite ratio. Therefore, this work confirmed that the structure originally proposed by Brennan was correct.

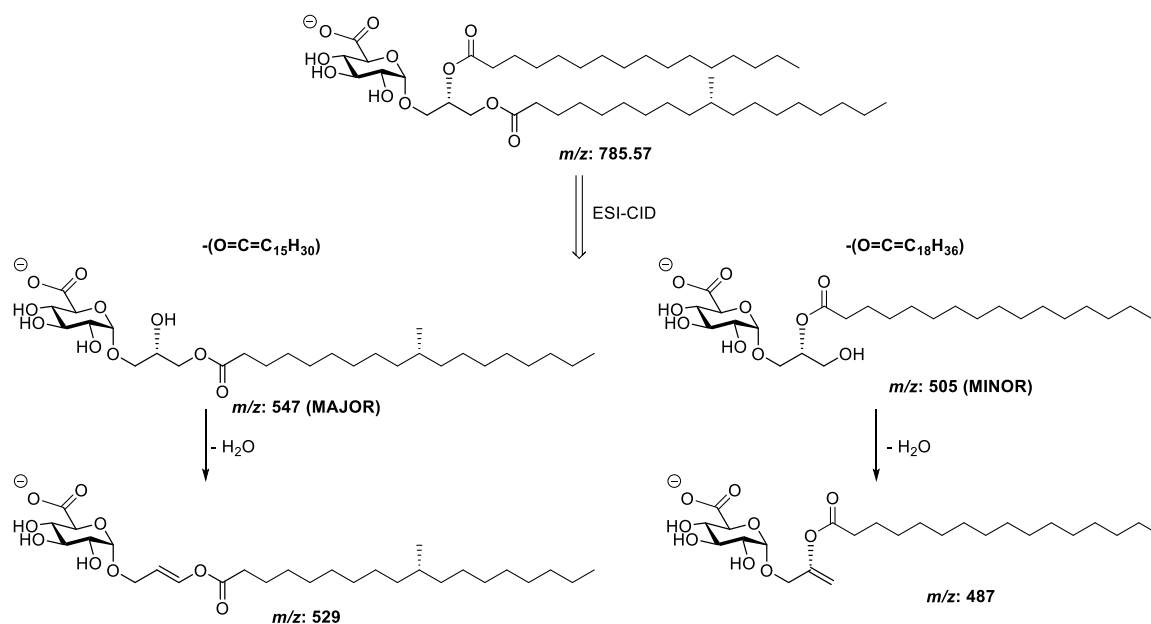


**Figure 4.5** Fragment ions formed in the CID spectra of deprotonated GlcAGroAc<sub>2</sub> **402**.

#### 4.4 Structural role of GI-A in the biosynthesis of corynebacterial lipomannan

Mycobacteria and the related Corynebacteria possess a lipid-rich cell wall comprising a mycolyl-arabinogalactan-peptidoglycan macromolecule and an array of cell wall associated glycolipids such as PIMs, and two major lipopolysaccharides: lipoarabinomannan (LAM) and lipomannan (LM)<sup>17</sup> which share a common PI anchor core. By utilizing pulse-chase analysis, which examine a cellular process by successively exposing the cells to the labelled compound (pulse) and the unlabeled compound (chase),<sup>163</sup> it has been found that there is a biosynthetic connection between PIMs, LAM and LM in mycobacteria.

The biosynthesis of LM and LAM is a complex process involving a suite of intermediates and enzymes. The early stages involving the construction and incorporation of the PI anchor are shown in Figure 4.6. Condensation of CDP-diacylglycerol with





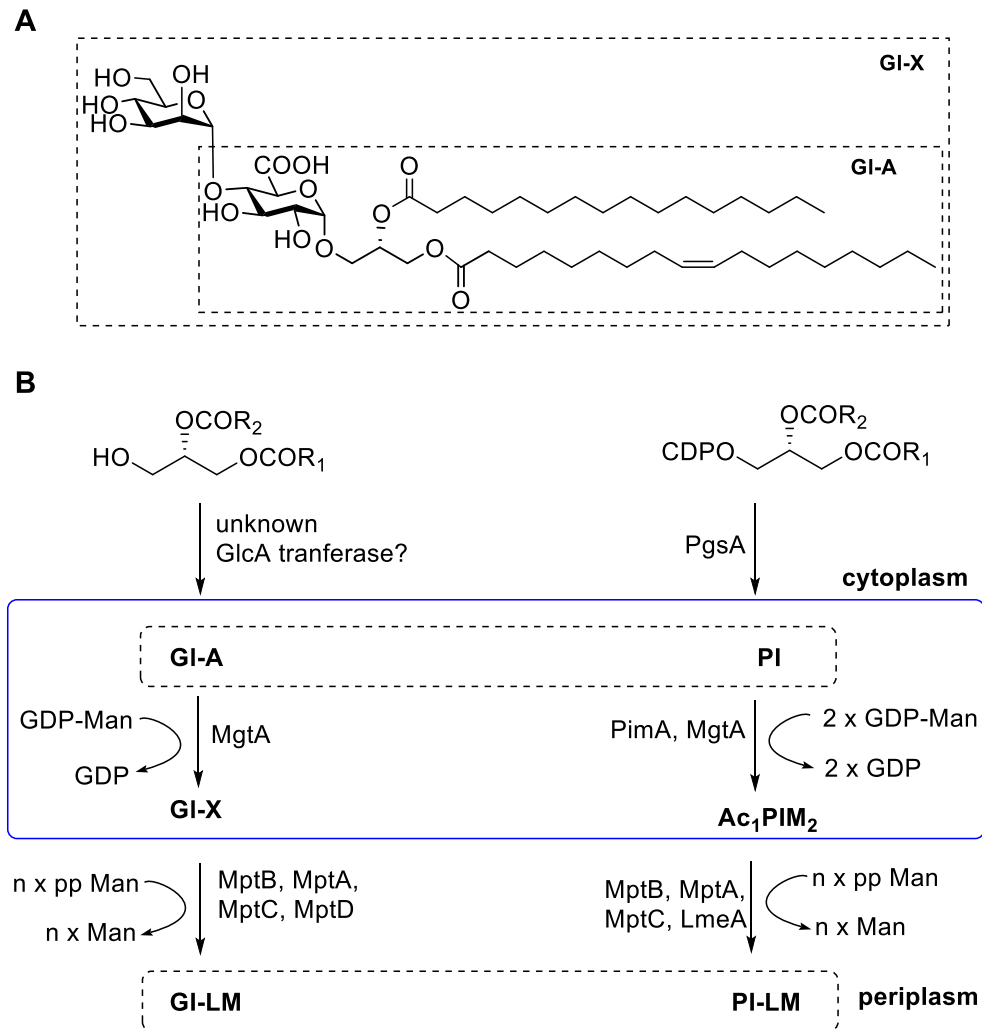


**Figure 4.7** A) Chemical structures of GI-A and Man-GI-A from *C. glutamicum*; B) Outline of involvement of GI-A in the biosynthesis of *C. glutamicum* GI-LM and comparison with PI-LM biosynthesis.

As mentioned in the earlier section, although there are reports of isolation of GI-A in *M. smegmatis*, there is no evidence for such species in *Mtb*. However it has been shown that *Mtb* orthologues of the *mgtA* gene can complement the production of GI-LM in *C. glutamicum*. It is curious that despite the presence of the orthologous genes *mgtA*, *mptA* and *mptB* in *M. tuberculosis*, no GlcAGroAc<sub>2</sub>-based glycolipids have been reported from this organism, perhaps because of a lack of the orthologous GlcA transferase. Knockout of the orthologue of *mgtA* in *M. tuberculosis* Erdman (Rv0557) resulted in a

moderate decrease in Man-LAM and LM content, but did not abolish either of these glycolipids.<sup>162</sup> Possibly, MgtA is redundant with PimB'.

#### 4.5 Gl-A can act a selective agonist for V $\alpha$ 10 NKT cells

Uldrich *et al.* showed that Gl-A is a selective agonist for atypical type Ia NKT cells, when presented by CD1d. Type Ia NKT cells are characterized by the presence of V $\alpha$ 10  $\alpha$  TCRs.<sup>63</sup> Of the assortment of  $\alpha$ -glycolipid ligands screened for their activity against V $\alpha$ 10 NKT cells a 1:1:1 mixture of Gl-A analogues **402**, **403**, **404** (bearing C<sub>19:0</sub>/C<sub>16:0</sub>, C<sub>16:0</sub>/C<sub>19:0</sub>, and C<sub>16:0</sub>/C<sub>18:0</sub>) (Figure 4.8 A) showed a distinct preference towards V $\alpha$ 10 NKT cells, generating about 2-4 fold greater cytokine proliferation than /for type I NKTs. The mixture of three lipids released ILs at levels 10-100 fold times greater than type I NKTs, showing this glycolipid is able to selectively activate V $\alpha$ 10 NKT cells.

Of the three components of the Gl-A mixture, only Gl-A **402** (C<sub>19:0</sub>/ C<sub>16:0</sub>), the natural form found in *M. smegmatis*, could stimulate V $\alpha$ 10 NKT cells (Figure 4.8 B). The fact that the other isoforms did not stimulate a response indicates the importance of the methyl group of TBSA and the acylation pattern. It was suggested that as a consequence of the reversal of the fatty acids, the presentation of the glucuronic acid head group towards the TCRs presented on the NKT cells is altered.<sup>165</sup> Gl-A induces a strong immune response by activating V $\alpha$ 10 NKT cells in a dose range of 0.6-10  $\mu$ g/ml producing about 100-fold greater abundance of IFN- $\gamma$  than for type I NKTs (Figure 4.8 C). The ability of Gl-A to elicit a strong immune response, indicates its immunotherapeutic potential.

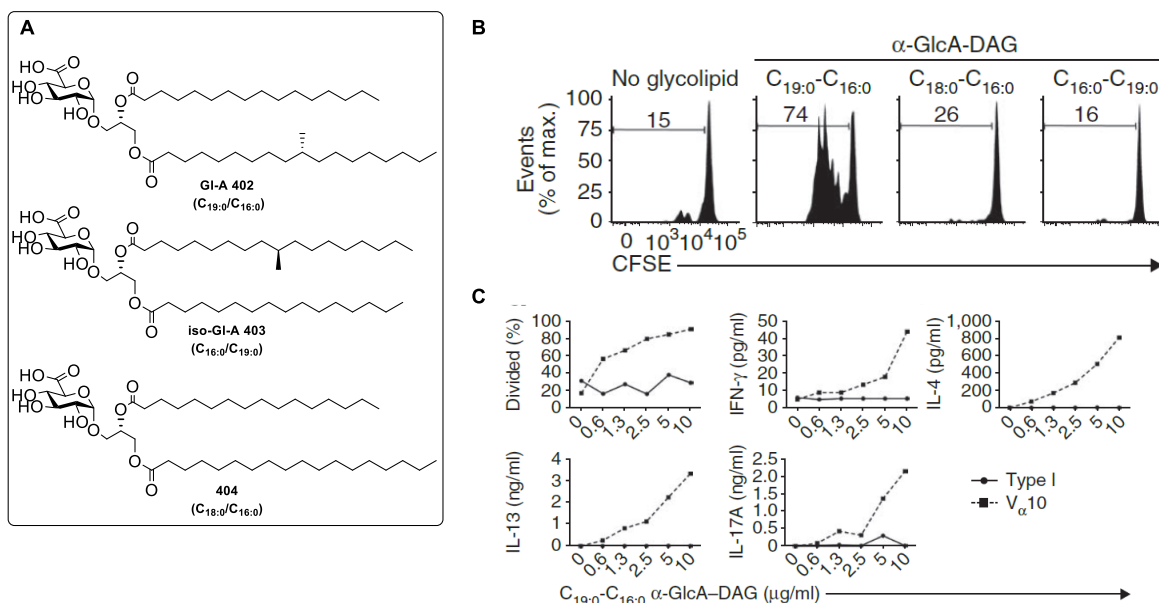


**Figure 4.8** A) Structures of the three GI-A analogues: **402**, **403**, **404**; B) Proliferation of gated V $\alpha$ 10 NKT cells positive for the CD1d- $\alpha$ -GalCer tetramer, for different analogues (10  $\mu$ g/ml); C) Proliferation and cytokine concentrations in supernatants of NKT cells positive for the CD1d- $\alpha$ -GalCer tetramer and 2-fold dilutions of  $\alpha$ -GlcA-DAG (C<sub>19:0</sub>-C<sub>16:0</sub>).

#### 4.6 Previous synthesis of GI-A

GI-A has previously been synthesized in our group. The approach involved assembly of the three main components: (i) the  $\alpha$ -D-glucosyl group, and its oxidation, (ii) the chiral glycerol fragment, and (iii) (*R*)-TBSA (Figure 4.9).<sup>86</sup>

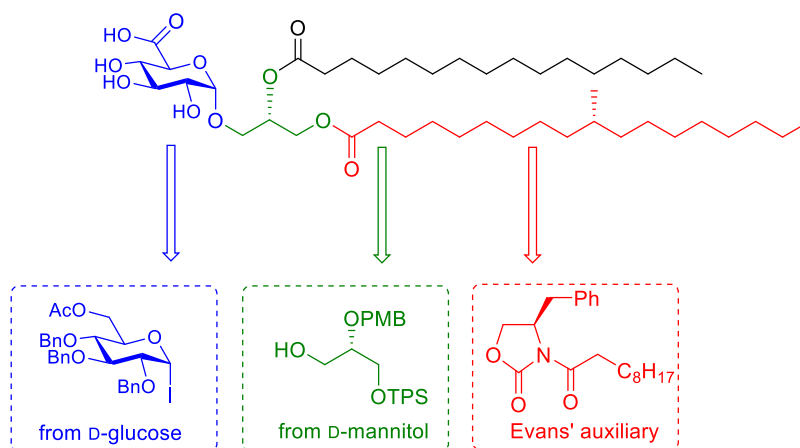
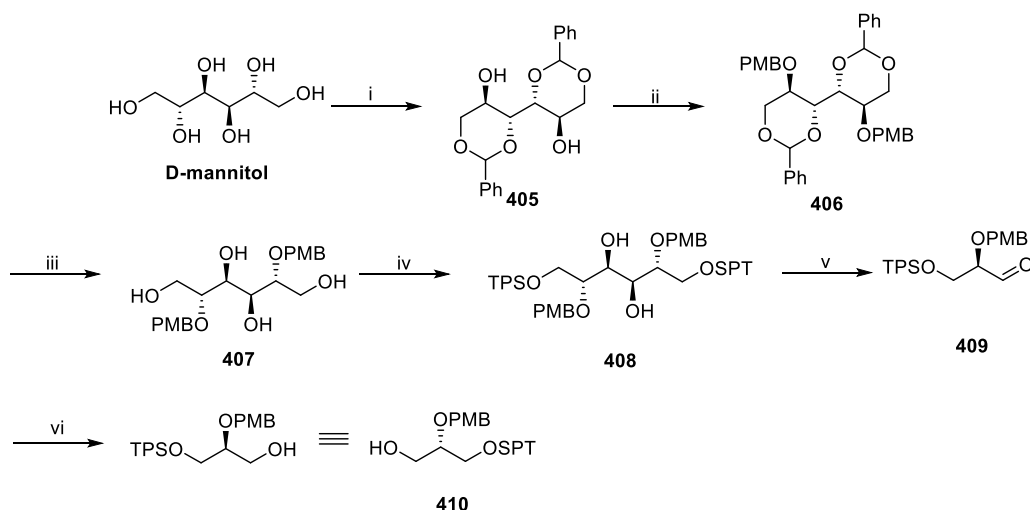


**Figure 4.9** Disconnections for the synthesis of GI-A.<sup>86</sup>

#### 4.6.1 Chiral glycerol fragment synthesized from D-mannitol

A selectively-protected glycerol **401** with TPS ether at sn-1 and PMB ether at sn-2 **410** was chosen as a precursor for step-wise installation of the fatty acid chains late in the synthesis (Scheme 4.1). D-Mannitol was dibenzylidenated by treating with benzaldehyde and sulfuric acid **405**. The diol was converted to the di-PMB ether **406**, the benzylidene groups were removed by acid catalyzed methanolysis **407**, and the primary hydroxyls of the resulting tetraol were silylated using TPSCl to afford the vicinal diol **408**. The vicinal diol was cleaved by NaIO<sub>4</sub> and the resultant aldehyde **409** reduced with NaBH<sub>4</sub> to afford the selectively protected chiral glycerol **410**.

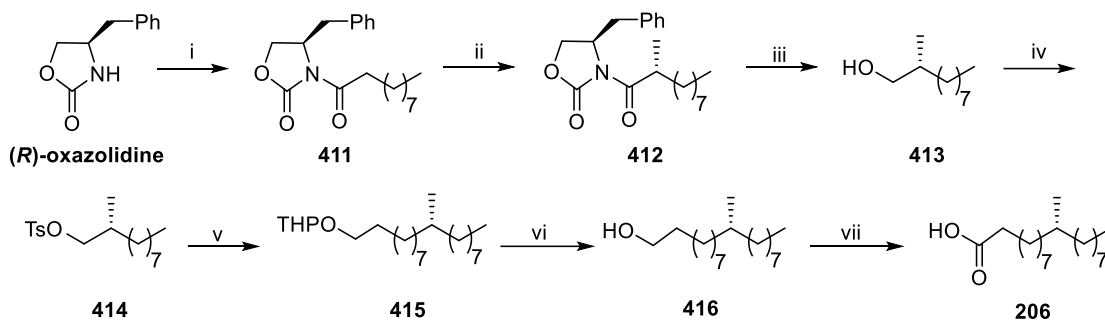


**Scheme 4.1** Synthesis of the sn-glycerol fragment from D-mannitol **410**. Reagents and conditions: (i) benzaldehyde, H<sub>2</sub>SO<sub>4</sub>, DMF, rt, 3 d 28%; (ii) PMBCl, NaH, DMF, 0 °C-rt, 91%; (iii) aq. HCl, hexane/MeOH, 39%; (iv) TPSCl, imidazole, DMF, 94%; (v) NaIO<sub>4</sub>, THF/H<sub>2</sub>O; NaBH<sub>4</sub>, EtOH/H<sub>2</sub>O, 91%.

#### 4.6.2 Chiral auxiliary approach to (R)-TBSA

The *N*-decyl-oxazolidinone **411** was prepared from the D-phenylalanine-derived (*R*)-oxazolidine, and then stereoselectively  $\alpha$ -methylated **412** (Scheme 4.2). The chiral auxiliary was cleaved by treatment with NaBH<sub>4</sub> to yield 2-methyldecanol **413**, which was tosylated to give **414** and then underwent a copper-mediated cross-coupling with 8-THP-

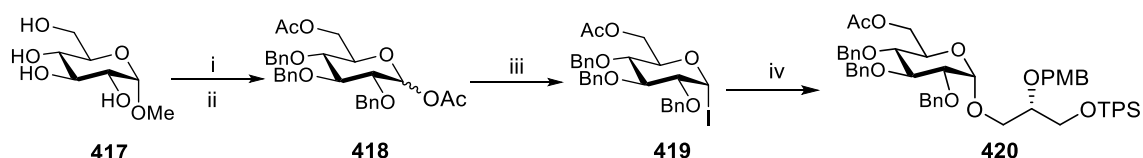
octylmagnesium bromide **415**. Deprotection, and oxidation under phase transfer conditions using  $\text{KMnO}_4$ , afforded (*R*)-TBSA.



**Scheme 4.2** Synthesis of (*R*)-TBSA using a chiral auxiliary. Reagents and conditions: (i)  $n\text{-BuLi}$ ,  $\text{CH}_3(\text{CH}_2)_8\text{COCl}$ , THF,  $-78$  to  $0$  °C, 1 h; (ii)  $\text{NaHMDS}$ , THF,  $-78$  °C, MeI,  $-78$  °C, 2 h; (iii)  $\text{NaBH}_4$ , THF/ $\text{H}_2\text{O}$ , 93% ; (iv)  $\text{TsCl}$ , pyridine  $0$  °C; (v)  $\text{THPOC}_8\text{H}_{16}\text{MgBr}$ ,  $\text{Li}_2\text{CuCl}_4$ , THF,  $0$  °C; (vi)  $\text{TsOH}$ , MeOH/hexane; (vii)  $\text{KMnO}_4$ ,  $\text{Bu}_4\text{NBr}$ ,  $\text{CH}_2\text{Cl}_2/\text{H}_2\text{O}/\text{AcOH}$ .

#### 4.6.3 Formation of the challenging 1,2-*cis* glucosidic bond by halide-ion catalysis

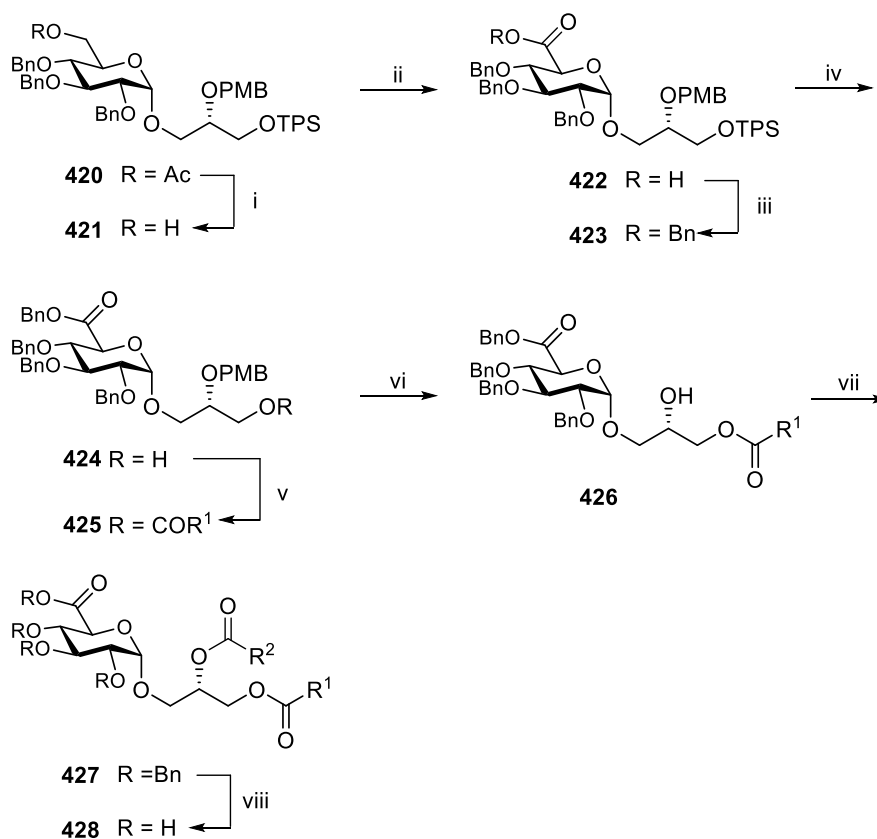
A halide-ion catalysed glycosylation was used to form the 1,2-*cis* glycosidic bond using a glycosyl iodide. Methyl  $\alpha$ -D-glucopyranoside **417** was benzylated, subjected to acetylation to afford the diacetate **418**, which was treated with TMSI to afford glucosyl iodide **419**. The *sn*-glycerol fragment **410** was treated with glycosyl iodide in the presence of  $\text{Bu}_4\text{NI}$  and the hindered base 2,6-di-*tert*-butyl pyridine (TTBP) to afford the  $\alpha$ -glucoside **420** in 63% yield (Scheme 4.3).  $\alpha$ -D-glycosyl iodides, that possess a 2-*O*-benzyl protecting group, rapidly equilibrate with the  $\beta$ -D-anomer in the presence of tetraalkylammonium iodide catalyst. The highly reactive  $\beta$ -D-anomer undergoes nucleophilic attack in an  $\text{S}_{\text{N}}2$  manner to give the  $\alpha$ -glucoside.



**Scheme 4.3** Synthesis of  $\alpha$ -glucoside **420**. Reagents and conditions: (i)  $\text{BnBr}$ ,  $\text{NaH}$ , DMF,  $0$  °C to r.t.; (ii)  $\text{TsOH}$ ,  $\text{Ac}_2\text{O}$ ,  $70$  °C, 2 h; (iii)  $\text{TMSI}$ ,  $\text{CH}_2\text{Cl}_2$ ,  $0$  °C, 1 h; (iv) **410**,  $\text{Bu}_4\text{NI}$ , TTBP,  $\text{CH}_2\text{Cl}_2$ , 6 d, 63%.

#### 4.6.4 Assembly of the fragments

The acetate group of **420** was cleaved and the alcohol **421** was oxidized with TEMPO/PhI(OAc)<sub>2</sub> to afford D-glucuronic acid **422**, which was benzylated using benzyl alcohol and HBTU to afford the benzyl glucuronate **423**. The silyl ether was cleaved using HF.pyridine in THF to give **424**. The alcohol intermediate was treated with *R*-TBSA, COMU, DIPEA and catalytic DMAP to afford the monoacylated product **425**. The PMB protecting group was cleaved using CAN to afford the secondary alcohol **426**, which was subjected to another COMU coupling reaction with palmitic acid **427**. Removal of the benzyl groups afforded the final compound **428** (Scheme 4.4).



**Scheme 4.4** Assembly of the fragments. Reagents and conditions: (i) NaOMe, MeOH, CH<sub>2</sub>Cl<sub>2</sub>, 75%; (ii) cat. TEMPO, PhI(OAc)<sub>2</sub>, CH<sub>2</sub>Cl<sub>2</sub>/H<sub>2</sub>O, 87%; (iii) BnOH, HBTU, DIPEA, cat. DMAP, CH<sub>2</sub>Cl<sub>2</sub>, 84%; (iv) HF.pyr, THF, 94%; (v) two portions of (*R*)-TBSA, COMU, DIPEA, cat. DMAP, DMF, 50 °C, 24 h, 87%, (vi) CAN, MeCN/H<sub>2</sub>O (vii) two portions of palmitic acid, COMU, DIPEA, DMAP, DMF, rt, 2 d, 75%; (viii) H<sub>2</sub>, Pd(OH)<sub>2</sub>, MeOH/THF/AcOH.

#### 4.6.5 Shortcomings of the synthesis

The synthetic strategy for GI-A was convergent and involved synthesis and assembly of a range of fragments. A selectively protected glycerol was synthesized in five steps, TBSA was synthesized in 8 steps, and the glycosyl iodide donor was synthesized in three steps. These fragments were assembled in another 8 steps to provide the target. Five protecting groups were utilized in the synthesis, resulting in 10 installation and removal steps alone. Use of benzyl as a protecting group prevents the installation of unsaturated fatty acids. In summary the synthesis of GI-A required 27 total steps with a longest linear route of 23 steps.

#### 4.7 Strategies for the synthesis of glycosyl diglycerides and limitations

A widely used strategy for the synthesis of complex glycosyl diglycerides involves glycosylation of protected glycerol (or glycidol) derivatives, and subsequent acylation with the fatty acids either simultaneously (for a simple diglyceride) or sequentially via a hydroxy ester intermediate (for complex diglycerides) (Figure 4.10). These approaches require separate protecting groups to mask the hydroxyl groups on the sugar residue and tune the stereoselectivity of the glycosylation, and to mask the glycerol.<sup>27</sup> For example, ester protecting groups on the sugar promote the formation of a 1,2-*trans* glycoside. However, it is difficult to remove these protecting groups, especially in the presence of ester groups in the diacylglyceride. These challenges have in the past required the use of multiple protecting groups, often with protecting group exchanges, leading to cumbersome syntheses. Additionally, for targets bearing unsaturated fatty acids, it is essential to identify suitable protecting group combinations that can be removed under conditions compatible with the double bond. For example, hydrogenolysis to remove the benzyl groups leads to reduction of the double bond in the fatty acid; although this can be



sometimes avoided by careful use of transfer hydrogenation conditions. In case of complex glycosyl glycerides, stepwise regioselective acylation proceeds via a hydroxy ester intermediate, which is susceptible to acyl migration leading to formation of inseparable and typically undetected regioisomers. Although use of preformed mixed diacylglycerides appears a promising option, they are also hydroxy esters that can suffer from acyl migration or could have traces of regioisomeric impurities.

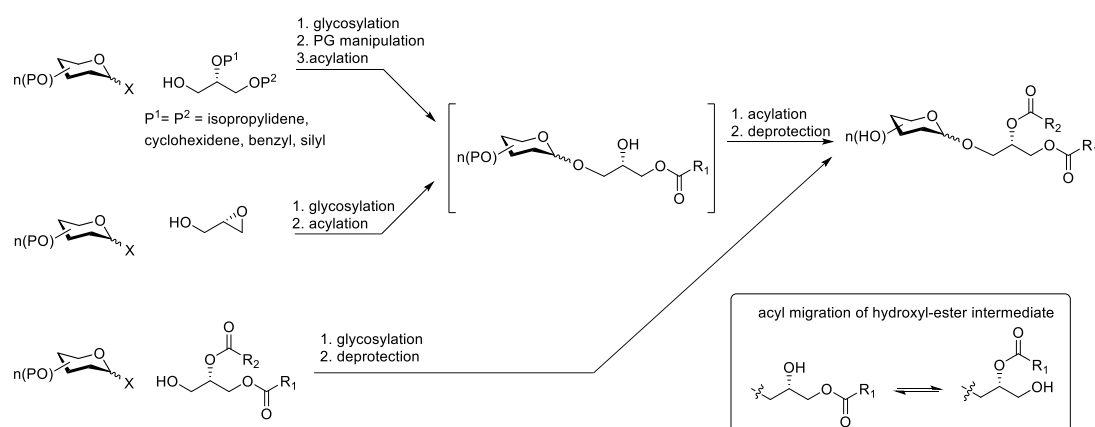


**Figure 4.10** General synthetic strategies for the synthesis of glycosyl diacylglycerols involving a  $\beta$ -hydroxyl ester intermediate.

#### 4.8 Allyl glycosides: masked precursors for glycosyl diglyceride synthesis

Allyl glycosides are an alternative for assembly of glycosyl glycerides that avoid the requirement for glycosylation of glycerols required in the previously described approaches. There are two main approaches to access glycosyl diacylglycerides from allyl glycosides (Figure 4.11). The first approach involves dihydroxylation of the terminal alkene using oxidizing agents such as hydrogen peroxide,  $\text{KMnO}_4$ , or  $\text{OsO}_4$ , or AD-mix<sup>166-167</sup> which affords a glycosyl glycerol, which can be acylated with fatty acids. However, the major drawback is the lack of stereoselectivity obtained in oxidation to the glycerol. Typically, asymmetric dihydroxylation of terminal alkenes occurs with relatively poor stereoselectivity. Stick *et al.* reported that AD-mix- $\beta$  stereoselectively dihydroxylates allyl  $\beta$ -glucoside to afford the diols in 19:1 ratio; recrystallization gave

the major compound as a pure diastereoisomer.<sup>168</sup> However this appears to be a special case; AD-mix  $\alpha$  or  $\beta$  gave poor diastereoselectivity for  $\alpha$ -xylosides.<sup>169</sup> The second approach involves epoxidation of the allyl group using oxidizing agents such as mCPBA, followed by ring opening of the oxirane to afford the glycerol. Here again the major drawback is lack of stereoselectivity as most enantioselective epoxidation catalysts (Shi catalyst, Jacobsen's catalyst) exhibit poor stereoselectivity on terminal alkenes.<sup>170</sup>

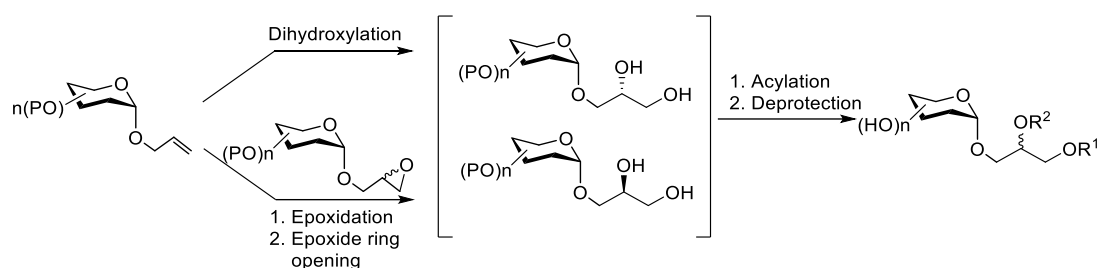
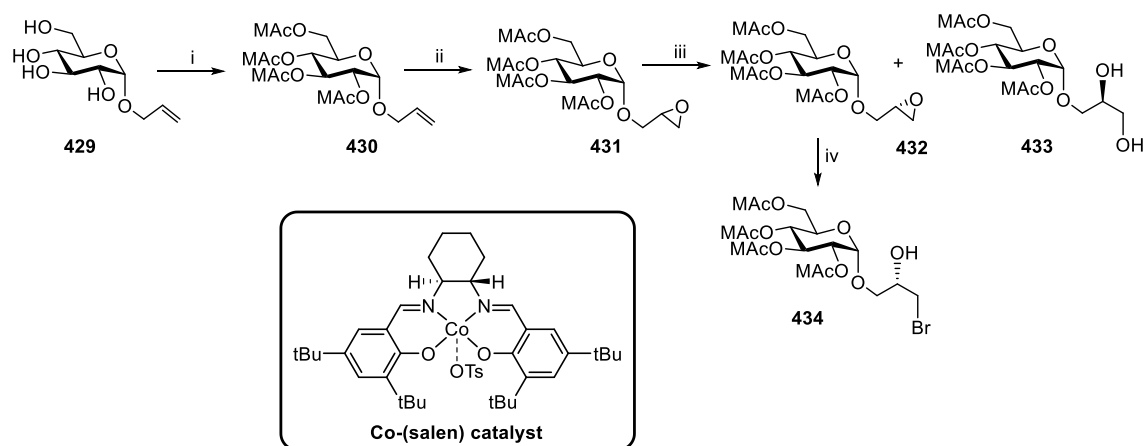


**Figure 4.11** Synthetic strategies for the synthesis of glycosyl diacylglycerols using  $\alpha$ -allyl glycosides.

#### 4.9 A new approach to access glycosyl diacylglycerols via a bromohydrin intermediate

Our group recently developed a new approach that provides efficient access to mixed glycosyl diglycerides, and which avoids all of the aforementioned problems. It is a linear, simplified approach that minimizes the need for protecting groups, and avoid the glycosylation step.<sup>27</sup> Commercially available allyl  $\alpha$ -D-glucopyranoside was chosen as the starting material, which already possesses the  $\alpha$ -glucosidic linkage required in the product. A sole protecting group was used, the methoxyacetyl group, which was chosen owing to its reasonable stability and the mild conditions required for removal ( $t\text{-BuNH}_2$  in  $\text{MeOH}/\text{CH}_2\text{Cl}_2$ ) which can be achieved in the presence of fatty acids, and is compatible with fatty acid unsaturation. Protection of allyl  $\alpha$ -D-glucopyranoside was achieved using  $\text{MeOAcCl}/\text{pyridine}$ . The protected allyl glucoside was treated with mCPBA to afford the epoxide as a 1:0.95 ( $2'R/2'S$ ) mixture of diastereomers. Hydrolytic kinetic resolution of

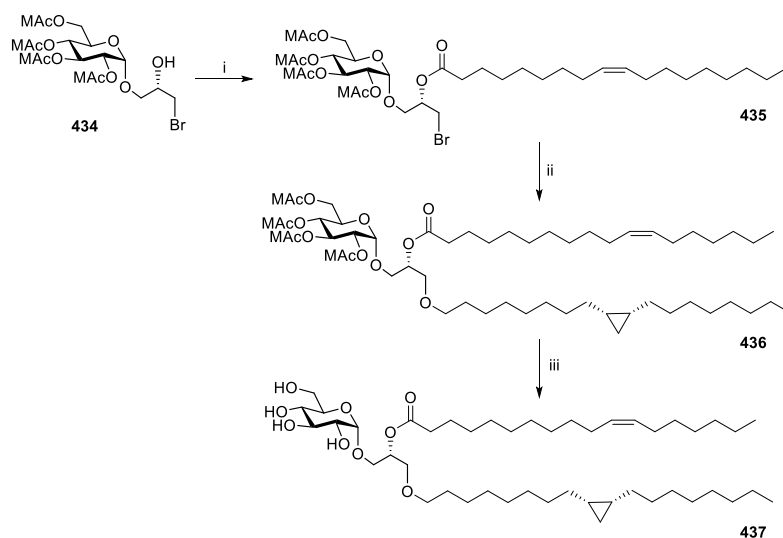
the mixture of epoxides with *S,S*-Co[salen].OTs catalyst (C1.OTs) afforded enantiopure 2'*R* epoxide in 48% yield. Dilithium tetrabromonickelate ( $\text{Li}_2\text{NiBr}_4$ ) was used to open the epoxide to afford the bromohydrin.  $\text{Li}_2\text{NiBr}_4$  serves as a source of soft nucleophilic bromide with a hard but mild electrophilic Lewis acidic  $\text{Li}^+$  (Scheme 4.5). This combination ensures that the other acid/ base sensitive groups remain intact and epoxide ring opening occurs with high regioselectivity.<sup>171</sup>



**Scheme 4.5** Synthesis of bromohydrin intermediate **434**. Reagents and conditions: (i) MeOAcCl, pyridine, 90%; (ii) *m*-CPBA,  $\text{CH}_2\text{Cl}_2$ , 90%; (iii) *S,S*-1.OTs Jacobsen's catalyst,  $\text{H}_2\text{O}$  (0.55 eq.), THF, 48%; (iv)  $\text{Li}_2\text{NiBr}_4$ , THF, 87%.

#### 4.9.1 Synthesis of glycolipids utilizing the bromohydrin intermediate.

Synthesis of GL-1 **437**, a glycolipid from *Lactobacillus plantarum* possessing a cyclopropane fatty acid at sn-1 and oleic acid at sn-2 is shown below (Scheme 4.6). The 2-OH of the bromohydrin **434** was acylated with oleoyl group using oleoyl chloride and pyridine **435**. Nucleophilic substitution of the bromide with the tetrabutylammonium salt of 9*S*,10*R*-dihydrosterculeic acid afforded the protected glyceride **436**. Removal of the MeOAc groups with *tert*-butylamine afforded GL-1 **437** in seven steps.<sup>27</sup>



**Scheme 4.6** Synthesis of GL-1 from *Lactobacillus plantarum*. Reagents and conditions: (i) oleoyl chloride, pyridine, CH<sub>2</sub>Cl<sub>2</sub>, overnight, 93%; (ii) tetrabutylammonium 9S,10S-dihydrostercolate, toluene, 85 °C, 55%; (iii) <sup>1</sup>BuNH<sub>2</sub>, MeOH, CHCl<sub>3</sub>, 84%.

Utilizing the same methodology, SPN-GlcDAG **438** was synthesized. This glycolipid is a glucosyl diglyceride from *Streptococcus pneumoniae* and is characterized by the presence a *cis*-vaccenoyl group at the sn-2 position (Figure 4.12).<sup>9</sup>

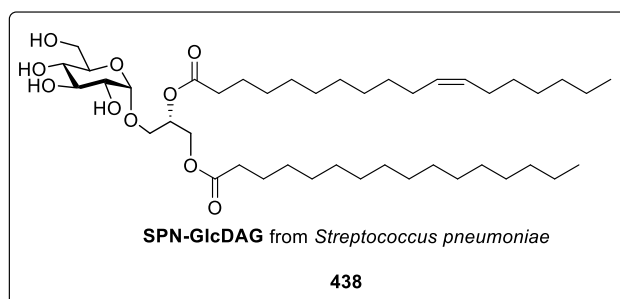


**Figure 4.12** Structure of SPN-GlcDAG from *S. pneumoniae*, containing palmitic acid at sn-1 and *cis*-vaccenic acid at sn-2.

Using quantitative <sup>13</sup>C NMR (in the presence of a paramagnetic relaxation enhancement reagent) and a <sup>13</sup>C labelled fatty acid it was shown that GlcDAGs synthesized via a bromohydrin intermediate (and which avoided a β-hydroxyl ester intermediate), possess exquisite regioselective acylation fidelity (*R* = 99%), which surpassed that for other well-established methods that involve a β-hydroxyl ester

intermediate.<sup>9</sup> In summary, this HKR-bromohydrin strategy represents a highly efficient strategy to access glycosyl diglycerides with high fidelity acylation regioselectivity.

#### 4.10 Aim of this project

We aimed to develop a second generation synthesis of GlcADAG that is dramatically shortened using the HKR-bromohydrin approach from allyl  $\alpha$ -D-glucopyranoside. Using this new route we planned to synthesize a variant containing the unnatural lipid isomer (*S*)-TBSA to explore the importance of its stereochemistry in its immunological activity. Additionally, we planned to synthesize the glucosyl variants of GlcDAG (Figure 4.13). As this approach avoids the use of benzyl protecting groups, it will potentially allow the synthesis of the unsaturated lipiform, GlcADAG (C<sub>18:1</sub>/C<sub>16:0</sub>).

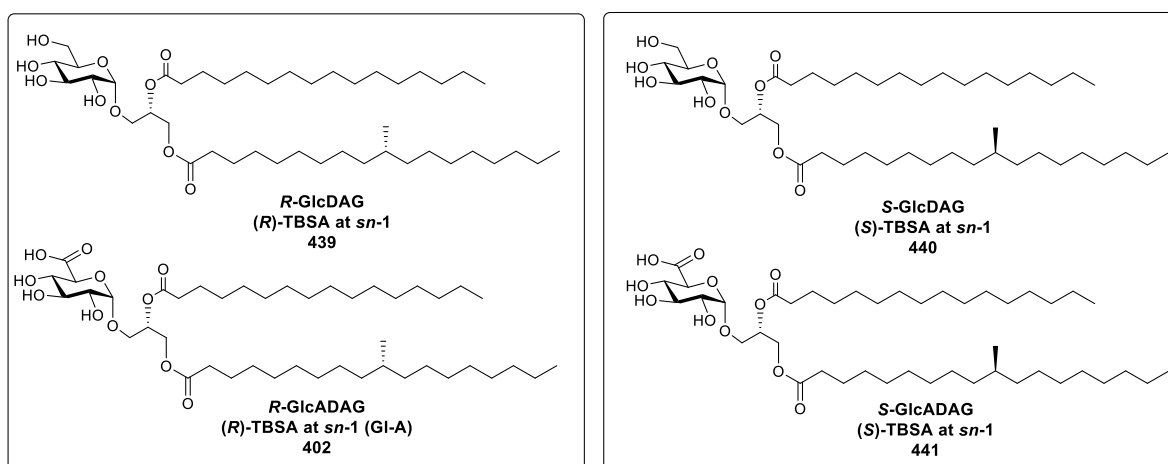


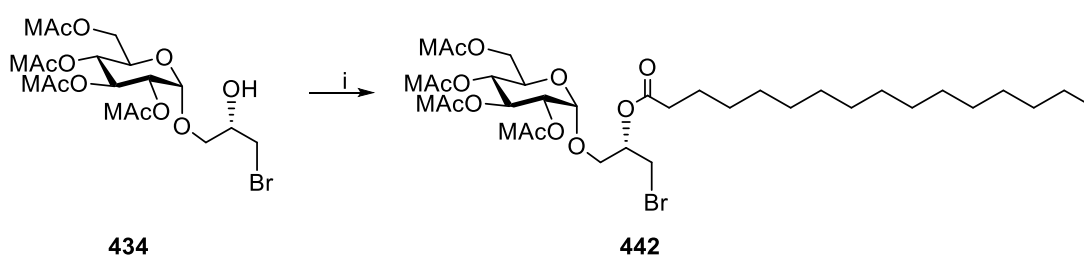
**Figure 4.13** Proposed synthetic targets. GlcADAG and GlcDAG lipids containing (*R*)-TBSA and (*S*)-TBSA.

These synthetic compounds will allow study of their immunological properties on an assortment of NKT cells. The analogues will be used to probe the importance of the glucuronic acid head group for activity, and also to understand if the stereochemistry of the methyl group in the TBSA chain is important for activity.

## 4.11 Results and discussion

### 4.11.1 Synthesis of glucosyl diacylglycerols (GlcDAGs)

I was fortunate to obtain several hundred milligrams of the bromohydrin intermediate **434** from Dr. Sayali Shah, a previous lab member. With this key intermediate in hand, it allowed me to proceed directly with the next steps (Scheme 4.7). The palmitoyl group at the sn-2 position was installed uneventfully using palmitoyl chloride and pyridine, affording the bromo-ester **442** in 90% yield.

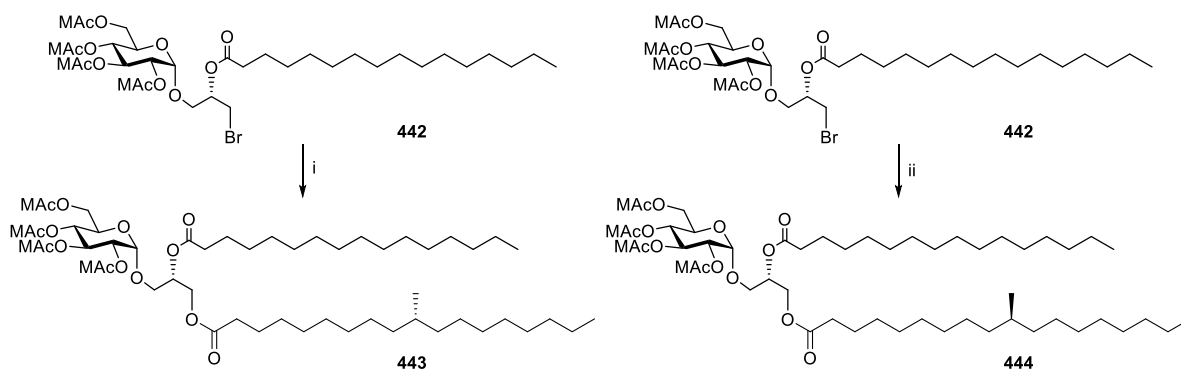


**Scheme 4.7** Installation of the palmitoyl group. Reagents and conditions: (i) palmitoyl chloride, pyridine, CH<sub>2</sub>Cl<sub>2</sub>, overnight, 90%.

Next, the TBSA chains were installed by nucleophilic substitution of the primary bromide **442**. Although not often used, nucleophilic carboxylate substitution reactions have nonetheless fairly extensive precedent. Two main approaches can be used, using either cesium carboxylates, or tetrabutylammonium carboxylates.<sup>135, 172-173</sup> Kellogg *et al.* have shown that cesium carboxylates, formed by reaction of cesium carbonate or hydrogencarbonate with acids, are good nucleophiles, as a result of the cesium effect, which involves weak ion-pairing as a result of the large size of cesium. Owing to the low solubility of cesium salts in non-polar solvents, these reactions are typically performed in the polar, aprotic solvent DMF, which adds some complexity to isolation of the products because of its low volatility. On the other hand, tetrabutylammonium carboxylates have been employed by Stawinski *et al.*<sup>173</sup> and Lok *et al.*<sup>174</sup> They are readily prepared by treatment of the carboxylic acid with tetrabutylammonium hydroxide in toluene. Owing

to their more lipophilic nature, they are soluble in non-polar solvents such as toluene, allowing for the formation of nucleophilic ‘naked’ carboxylate ions that perform well in substitution reactions of primary alkyl bromides and iodides.

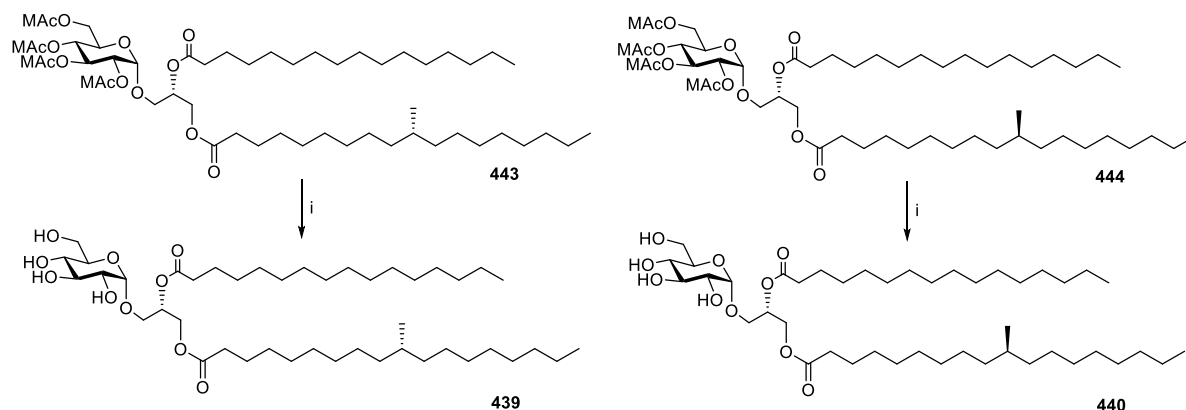
The tetrabutylammonium salt of *R*- and *S*-TBSA were individually prepared by stirring the parent acids and tetrabutylammonium hydroxide in water overnight, and then removing the excess solvent under reduced pressure, by co-evaporation with toluene. The TBSA esters were installed by substitution of the bromide **442** by the two enantiomeric tetrabutylammonium TBSA salts, by reaction in toluene at 85 °C. It was discovered that it was important to run this substitution reaction for only a limited time, as prolonged reaction time resulted in loss of the MeOAc groups, as observed by formation of more polar material by TLC, which could be isolated and deprotected (as described below) to afford the deprotected glucoside. The protected GlcDAGs containing *R*-TBSA **443** or *S*-TBSA **444** were isolated in yields of 75 and 67%, respectively.



**Scheme 4.8** Substitution of the bromide **442** by tertabutylammonium salt of *R*-TBSA. Reagents and conditons: (i) tetrabutylammonium 10*R*-tuberculostearate, toluene, 85 °C, 75%; (ii) tetrabutylammonium 10*S*-tuberculostearate, toluene, 85 °C, 67%.

Next, the methoxyacetyl esters needed to be removed. While it has been shown that MeOAc groups can be selectively removed in the presence of other esters using ytterbium(III) triflate in MeOH,<sup>175</sup> a comparative study reported higher yields using *t*-

BuNH<sub>2</sub> in MeOH/CHCl<sub>3</sub>.<sup>176</sup> This reaction is believed to proceed via a base-catalysed methanolysis, rather than aminolysis, as shown by a lack of reactivity in pure CHCl<sub>3</sub>.<sup>176</sup> Treatment of the protected *R*-GlcDAG **443** or *S*-GlcDAG **444** with *t*-BuNH<sub>2</sub> in MeOH/CHCl<sub>3</sub> afforded the *R*-GlcDAG **439** or *S*-GlcDAG **440** in 80 and 78%, respectively.



**Scheme 4.9** Synthesis of *R*-GlcDAG **439**. Reagents and conditions: (i) <sup>t</sup>BuNH<sub>2</sub>, MeOH, CHCl<sub>3</sub>, 82% for **439**, 89% for **440**.

#### 4.11.2 Synthesis of glucuronosyl diacylglycerols (GlcADAGs)

The final task to obtain the GlcADAGs was to selectively oxidize the primary alcohol of the GlcDAG glycolipids. We chose to employ catalytic TEMPO and BAIB, a reagent combination developed by Epp and Widlanski, owing to its selectivity for primary hydroxyls and mild reaction conditions.<sup>177</sup> In this reaction AcOH catalyzes bismutation of TEMPO to the oxoammonium salt and the hydroxylamine (Figure 4.15). The oxoammonium salt operates as the primary oxidant to oxidize the alcohol to the corresponding aldehyde, and results in reduction of the oxoammonium salt to the hydroxylamine. The hydroxylamine is oxidized back into the TEMPO radical by BAIB, thus completing the catalytic cycle. Oxidation of the aldehyde to the acid is achieved by hydration of the aldehyde to a geminal diol (aldehyde hydrate), which is oxidized through a similar mechanism to the acid (Figure 4.14).<sup>177-178</sup> While a range of co-oxidants can be



used, BAIB is especially mild and simply generates acetic acid and iodobenzene as byproducts avoiding inorganic salt contaminants.

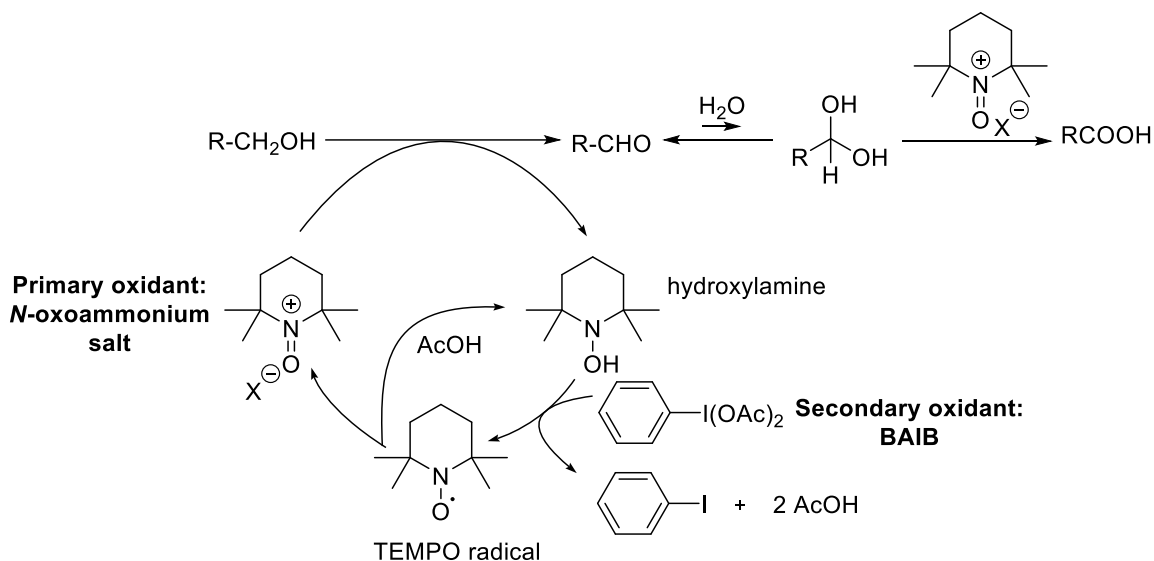


**Figure 4.14** Mechanism of TEMPO/BAIB oxidation of primary alcohol to a carboxylic acid.

While TEMPO/co-oxidant has been widely used for the selective oxidation of the primary hydroxyl of a range of unprotected glycosides<sup>179-181</sup> there is scarce literature precedent for oxidation of unprotected glucose diacylglycerol, of which we were concerned owing to the amphiphilic nature of both the glucoside and glucuronoside. Epp and Widlanski utilized a 1:1 acetonitrile–water solvent system in which all components were soluble. They reported improved yields by using NaHCO<sub>3</sub> to maintain a basic pH of the system, which otherwise becomes more acidic as the carboxylic acid and acetic acid is generated during the reaction.<sup>177</sup> It has been shown that oxidation under basic conditions is faster and proceeds with greater selectivity for primary alcohols.<sup>178</sup> It has been proposed that under basic conditions, the transition state of the key oxidation step, which leads from the alcohol adduct of the oxoammonium ion, involves a unimolecular reaction in a compact five membered ring, whereas under acidic conditions an extended ‘linear’ bimolecular transition state is invoked (Figure 4.15).

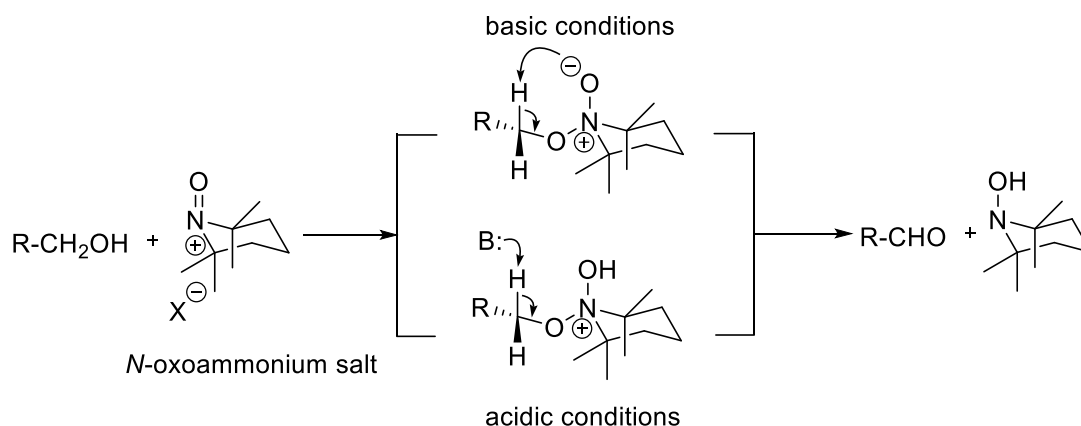
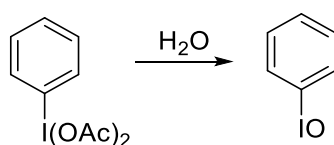


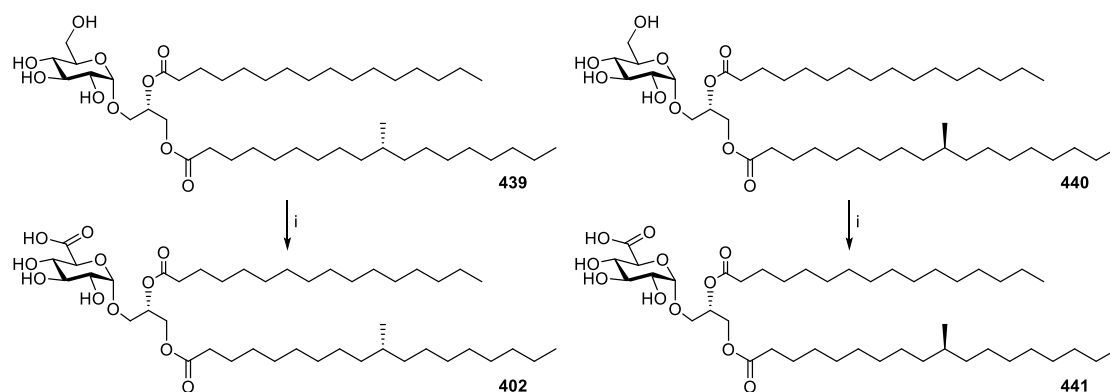
**Figure 4.15** Proposed mechanisms for TEMPO oxidation under acidic and basic conditions.

We started our TEMPO oxidations by treating **439** with catalytic TEMPO and 1.1 equiv. of BAIB in a 1:1 acetonitrile/water system, containing 5 equiv. of  $\text{NaHCO}_3$ , a protocol used by Epp and Widlanski. TLC and mass spec analysis revealed the presence of starting material after running the reaction over 24 h indicating insufficient oxidant. So, the quantity of BAIB was increased to 2.2 equiv. of BAIB, but starting material was still evident after 24 h. These results led us to suspect that BAIB was hydrolyzing to iodosylbenzene, which does not act as a co-oxidant and precipitates as yellow solid (Scheme 4.10).<sup>182</sup>



**Scheme 4.10** Hydrolysis of BAIB to produce insoluble iodosylbenzene.

In order to drive the reaction forward, a second dose of TEMPO/BAIB was added after 24 h and stirring continued for another 24 h, with occasional sonication. This protocol afforded *R*-GlcADAG **402** in 85% yield. The  $^1\text{H}$  NMR spectrum of the isolated compound matched that of the previously reported spectra.<sup>85-86</sup> By the same approach *S*-GlcADAG **441** was synthesized from **440** in 70% yield.



**Scheme 4.11** Oxidation of *R*-GlcDAG to afford *R*-GlcADAG **402** and *S*-GlcDAG **440** to *S*-GlcADAG **441**. Reagents and conditions: (i) TEMPO, PhI(OAc)<sub>2</sub>, NaHCO<sub>3</sub>, MeCN: H<sub>2</sub>O (1:1), 48 h, 0 °C-rt, 85% for **402** and 70% for **441**

#### 4.12 Summary

Using the bromohydrin route for the synthesis of glycosyl glycerides developed in our lab, we synthesized two GlcDAGs containing either (*R*)-TBSA or (*S*)-TBSA. By application of TEMPO/BAIB oxidation, these were converted to the corresponding GlcADAGs in one step. While previous approach to GI-A included 27 overall synthetic steps and 5 different protecting groups, this new approach delivered GI-A in 9 steps, utilizing only one protecting group. Including our new approach to TBSA, the total step-count is 11 steps. Another key feature is that this route allows the installation of unsaturated fatty acids, while it was not possible in the previous approach as it utilizes benzyl protecting groups, which are not compatible with unsaturated fatty acids. A colleague in my lab, Mr. Dylan Smith, has applied this approach to synthesize GlcADAG (C<sub>18:1</sub>/C<sub>16:0</sub>) (unpublished)

#### 4.13 Biological activity of $\alpha$ -glucosyl and $\alpha$ -glucuronosyl diacylglycerides

It has previously been established that GI-A is presented by CD1d and activates V $\alpha$ 10 NKTs to induce a T<sub>H</sub>2 biased response.<sup>86</sup> With the structural analogues synthesized herein

and others prepared in our laboratory, we wished to understand how variation in the structure of GlcADAG would affect its immunological activity. Specifically:

1. Is the D-glucuronic acid carboxylate group essential or can a glucose head-group produce a similar effect?
2. Does the stereochemistry of the methyl group in the chain influence the activity?
3. Does an alkene in the lipid chains alter biological activity?

The structural analogues we had available to study these questions are shown in Figure 4.16. Aside from the compounds synthesized in this thesis, the additional compounds were synthesized by Mr Dylan Smith in our laboratory. The immunological evaluations were conducted by Dr. Catarina Almeida in the laboratory of Prof. Dale Godfrey (Department of Microbiology and Immunology, University of Melbourne)

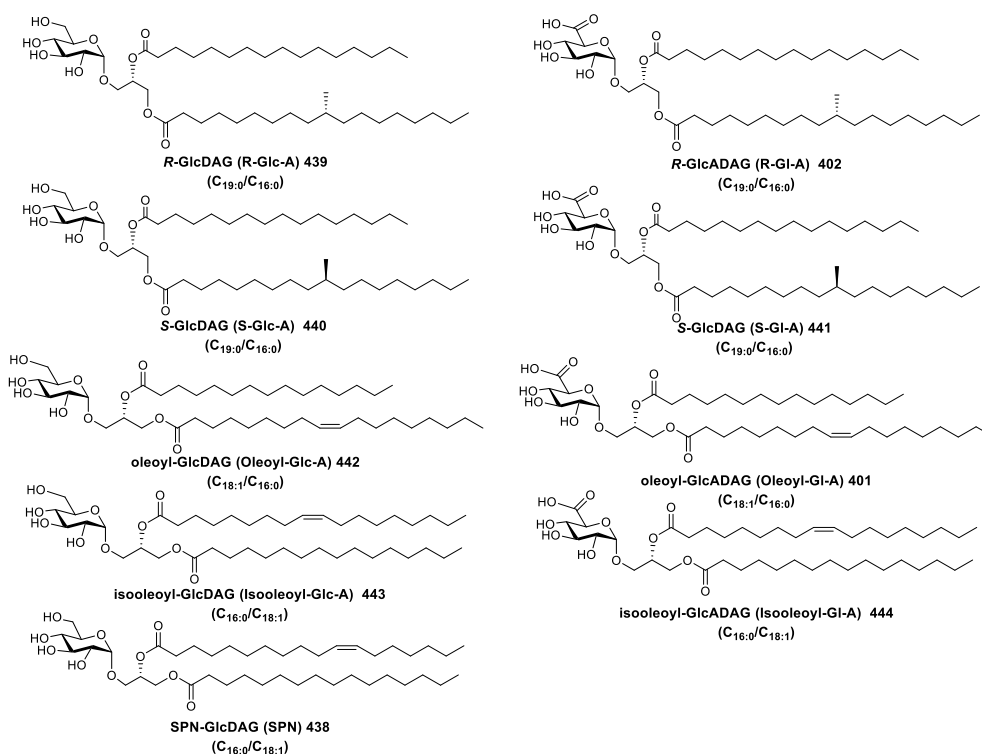


**Figure 4.16** Structures of GlcDAGs and GlcADAGs examined for their activity against NKT cells.

#### 4.13.1 Activation of NKT cells

The ability of the GlcDAGs and GlcADAGs to bind to CD1d and interact with a conventional Type 1 TCR ( $V\alpha 10$ - $V\beta 8$ ), two atypical Type 1a TCRs ( $V\alpha 10$ - $V\beta 8.1$  and  $V\alpha 10$ - $V\beta 8.3$ ), and a Type II NKT TCRs was studied. These studies were performed using assays that directly measure the ability of the antigen to mediate cellular activation (by measuring CD1d-glycolipid induced CD69 expression by cells expressing an appropriate TCR).

For Jurkat cells expressing a type I NKT cell  $V\beta 8$  TCR, the greatest activation of around 3-fold that of endogenous lipids was achieved by co-culturing with C1R cells that expressed CD1d and *R*-GlcADAG and oleoyl-GlcADAG. These two glycolipids correspond to the naturally occurring species from *M. smegmatis* and *C. glutamicum*. For the  $\alpha$ -glucosyl diacylglycerides, the induction of CD69 expression upon co-culture with CR1 cells was generally low, comparable with that produced by endo (referring to endogenously loaded lipids) (Figure 4.17). At odds with previously reported data,<sup>41</sup> the *S. pneumoniae*  $\alpha$ -glucosyl diacylglyceride (SPN-GlcDAG) did not activate cells expressing this type I TCR.

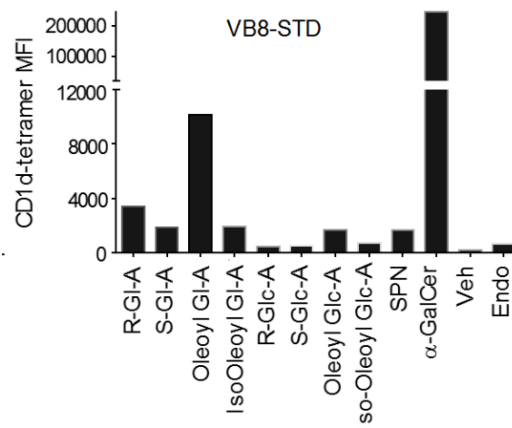


**Figure 4.17** Activation of Jurkat cells expressing a type 1 ( $V\alpha 10$ - $V\beta 8$ ) TCR by C1R cells transduced to express CD1d, measured by expression of the activation marker CD69. TCR<sup>+</sup> cells were co-cultured overnight with CD1d-expressing C1R cells in the presence of glycolipids.

Figure 4.18 shows data for Jurkat cells expressing two Type Ia TCRs. V $\beta$ 8.1 TCR<sup>+</sup> Jurkat cells did not exhibit CD69 induction by any of the glycolipids studied, except  $\alpha$ -GalCer (Figure 4.18). However, Jurkat cells expressing the V $\beta$ 8.3 TCR displayed varying reactivity to a range of the studied glycolipids. While the strongest reactivity was observed for  $\alpha$ -GalCer, strong activation was seen for SPN-GlcDAG, intermediate levels of staining was observed for *R*- and *S*-GlcDAG and the oleoyl- and isooleoyl-GlcDAGs.

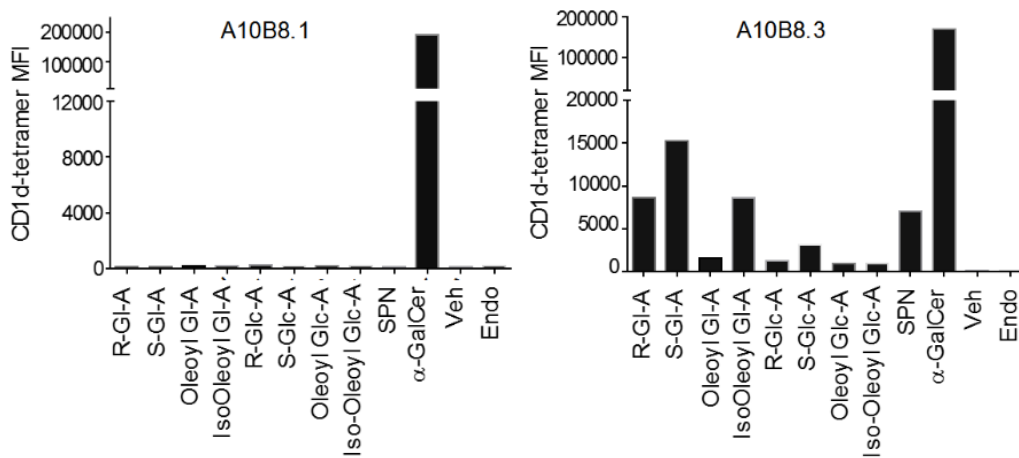


**Figure 4.18** Activation of Jurkat cells expressing type Ia (V $\alpha$ 10-V $\beta$ 8.3 and V $\alpha$ 10-V $\beta$ 8.1) TCR by C1R cells transduced to express CD1d, measured by expression of the activation marker CD69. TCR<sup>+</sup> cells were co-cultured overnight with CD1d-expressing C1R cells in the presence of glycolipids.

In summary, this data suggests that the V $\alpha$ 10-V $\beta$ 8.3 TCR, in addition to an ability to recognize  $\alpha$ -GalCer, has the ability to recognize a broad range of  $\alpha$ -glucuronosyl and  $\alpha$ -glucosyl diglycerides, with the specificity determined by the nature of the lipids, and their order of presentation on the glycerol, with a preference for the naturally occurring isomers from *M. smegmatis* and *C. glutamicum*. Notably, the  $\alpha$ -glucosyl diacylglyceride (SPN-GlcDAG) from *S. pneumoniae* also activated the type Ia V $\beta$ 8.3 TCR.

For Jurkat cells expressing a Type II NKT TCR (Trav 410) *R*-GlcADAG and the oleoyl-GlcADAG showed about three fold greater staining of this cell line while the *S*-

GlcADAG showed a lower activity (Figure 4.19). The Type II NKTs showed no reactivity towards the GlcDAGs indicating that the glucuronic head group is essential for cellular activation through this type II NKT TCR. This data suggests that the glucuronic head group, stereochemistry of methyl group of TBSA, and the acylation pattern are important for recognition by type II NKTs

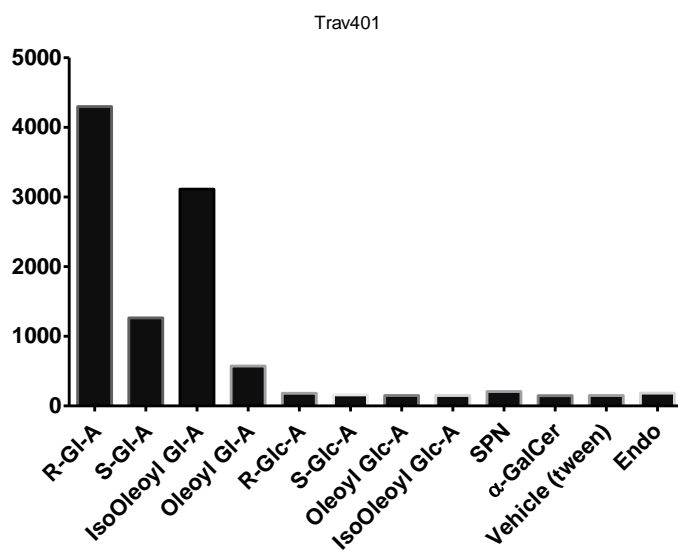


**Figure 4.19** Activation of Jurkat cells expressing type II NKT TCR by C1R cells transduced to express CD1d, measured by expression of the activation marker CD69. TCR<sup>+</sup> cells were co-cultured overnight with CD1d-expressing C1R cells in the presence of glycolipids.

#### 4.14 Summary and conclusions

In this chapter we disclose a new approach to  $\alpha$ -glucuronosyl diacylglycerides that is dramatically shorter than the previously reported approach to *M. smegmatis* Gl-A, enabling the resynthesis of this compound and a diastereoisomer varied in the stereochemistry of the TBSA chain. This new approach provides greater acylation fidelity at the glycerol, providing the diglyceride as a single regioisomer. Moreover, this new approach is compatible with lipid unsaturation, allowing synthesis of the oleic acid-containing GlcADAG isolated from *M. smegmatis* and *C. glutamicum*, and its regioisomer.

These synthetic  $\alpha$ -glucosyl and  $\alpha$ -glucuronosyl diacylglycerides were used to establish glycolipid recognition preferences for type I, Ia and II NKT TCRs. While GlcADAGs can weakly activate cells expressing a type I NKT TCR, much more potent activation is seen for a type Ia (V $\beta$ 8.3) and type II NKT TCR. The type Ia V $\beta$ 8.3 possesses an ability to recognize a range of  $\alpha$ -glucosyl and  $\alpha$ -glucuronosyl diacylglycerides, in particular the naturally occurring species from *C. glutamicum*, *M. smegmatis*, and *S. pneumoniae*, and thus can be considered to have a preference for this lipid class. By contrast, the type II NKT TCR was highly specific for  $\alpha$ -glucuronosyl diacylglycerides, with a marked preference for the *R*-TBSA and oleic acid containing GlcADAGs from *M. smegmatis* and *C. glutamicum*.



#### 4.15 Experimental

For General Experimental see Chapter 2

##### **(2'R)-3'-Bromo-2'-hydroxypropyl 2,3,4,6-tetra-O-methoxyacetyl- $\alpha$ -D-glucopyranoside (434)<sup>27</sup>**

<sup>1</sup>H NMR (CDCl<sub>3</sub>, 400 MHz)  $\delta$  3.39, 3.41, 3.43, 3.45 (4  $\times$  3 H, 4s, CH<sub>3</sub>OCH<sub>2</sub>), 3.45–3.54 (1 H, m, H<sub>2'</sub>), 3.60 (1 H, dd,  $J_{1',1'}$  10.4,  $J_{1',2'}$  6 Hz, H<sub>1a'</sub>), 3.87 (1 H, dd,  $J_{1',1'}$  10.4,  $J_{1',2'}$  6 Hz, H<sub>1b'</sub>), 3.96, 4.00, 4.02, 4.00 (4  $\times$  2 H, 4s, CH<sub>3</sub>OCH<sub>2</sub>), 3.96–4.23 (4 H, m, H<sub>5,6,3'a,3'b</sub>), 4.37 (1 H, dd,  $J_{5,6}$  4,  $J_{6,6}$  12 Hz, H<sub>6</sub>), 5.01 (1 H, dd,  $J_{1,2}$  4,  $J_{2,3}$  10 Hz, H<sub>2</sub>), 5.11–5.16 (2 H, m, H<sub>1,4</sub>), 5.54 (1 H, t,  $J_{2,3} = J_{3,4}$  10 Hz, H<sub>3</sub>); <sup>13</sup>C NMR (CDCl<sub>3</sub>, 100 MHz)  $\delta$  34.5 (C<sub>1'</sub>), 59.5, 59.59, 59.61, 59.7 (4 C, CH<sub>3</sub>), 62.0, 67.4, 68.6, 69.5, 69.6, 69.68, 69.71, 70.6, 70.8 (9 C, C<sub>2,3,4,5,6,CH<sub>2</sub>OCH<sub>3</sub></sub>), 70.9 (C<sub>2'</sub>), 96.6 (C<sub>1</sub>), 169.3, 169.5, 169.7, 170.0 (4 C, C=O); HRMS (ESI<sup>+</sup>) calcd for C<sub>21</sub>H<sub>33</sub>BrO<sub>15</sub>Na (M+Na) 627.0895. Found 627.0896.

##### **(2'S)-3'-Bromo-2'-palmitoyloxypropyl 2,3,4,6-tetra-O-methoxyacetyl- $\alpha$ -D-glucopyranoside (442)<sup>27</sup>**

Palmitoyl chloride (0.1 ml, 0.331 mmol) was added to a stirred solution of (2'S)-3'-bromo-2'-hydroxypropyl-2,3,4,6-tetra-O-methoxyacetyl- $\alpha$ -D-glucopyranoside **434** (0.102 g, 0.165 mmol) in dry CH<sub>2</sub>Cl<sub>2</sub> (3 ml) and pyridine (0.266 ml, 3.30 mmol) at 0 °C. The reaction mixture was allowed to warm to room temperature and stirring was continued overnight. The reaction mixture was diluted with CH<sub>2</sub>Cl<sub>2</sub>, washed with water, sat aq. CuSO<sub>4</sub>, followed by sat. aq. NaHCO<sub>3</sub>. The combined organic layers were dried (MgSO<sub>4</sub>), filtered and concentrated under reduced pressure. Flash chromatography of the residue (50% EtOAc /petroleum ether) afforded **442** as colorless oil (0.132 g, 95%). [ $\alpha$ ]<sub>D</sub><sup>26</sup> = +55.9 (*c* 0.5, CHCl<sub>3</sub>). <sup>1</sup>H NMR (CDCl<sub>3</sub>, 400 MHz)  $\delta$  0.87 (3 H, t,  $J$  6.7 Hz, CH<sub>3</sub>), 1.24–

1.31 (24 H, m,  $12 \times \text{CH}_2$ ), 1.56–1.63 (2 H, m,  $\beta\text{-CH}_2$ ), 2.32–2.37 (2 H, m,  $\alpha\text{-CH}_2$ ), 3.37, 3.38, 3.40, 3.42 (12 H, 4s,  $4 \times \text{OCH}_3$ ), 3.52 (1H, dd,  $J_{1',2'}$  6,  $J_{1',1'}$  10.8 Hz, H1a'), 3.60 (1 H, dd,  $J_{1',2'}$  6.0,  $J_{1',1'}$  10.8 Hz, H1b'), 3.72 (1 H, dd,  $J_{2',3'}$  4.8,  $J_{3',3'}$  10.8 Hz, H3a'), 3.89 (1 H, dd,  $J_{2',3'}$  4.8,  $J_{3',3'}$  10.8 Hz, H3b'), 3.96, 4.00, 4.10 (6 H, 3s,  $3 \times \text{CH}_3\text{OCH}_2$ ), 4.02 (2 H, m,  $\text{CH}_3\text{OCH}_2$ ), 4.06–4.13 (1 H, m, H6), 4.17–4.20 (1 H, m, H5), 4.36 (1 H, dd,  $J_{5,6\text{eq}}$  4.2,  $J_{6,6}$  12.4 Hz, H6), 4.97 (1 H, dd,  $J_{1,2}$  3.7,  $J_{2,3}$  10.2 Hz, H2), 5.10–5.14 (3 H, m, H2', H1, H4), 5.50 (1 H, t,  $J_{2,3} = J_{3,4}$  9.6 Hz, H3);  $^{13}\text{C}$  NMR ( $\text{CDCl}_3$ , 100 MHz)  $\delta$  14.2 ( $\text{CH}_2\text{CH}_3$ ), 22.7, 25.0, 29.2, 29.3, 29.4, 29.58, 29.7, 29.7, 29.7, 29.9, 32.0, 34.3 ( $\text{CH}_2$ ), 59.4, 59.5, 59.5, 59.5 (4 C,  $\text{OCH}_3$ ), 61.7, 67.4, 67.4, 68.4, 69.4, 69.5, 69.6, 70.4, 70.5, 70.7, 96.2 (C1), 169.2, 169.5, 169.6, 170.0 (4 C,  $\text{MeOCH}_2\text{C}=\text{O}$ ), 172.8 (sn2-C=O); HRMS (ESI<sup>+</sup>) calcd for  $\text{C}_{37}\text{H}_{63}\text{BrO}_{16}$  (M+H)<sup>+</sup> 842.3299. Found 842.3296. The downfield shift of H2' upon converting 434 to 442 from from  $\delta$  3.45–3.54 ppm (1H, m, H2') to  $\delta$  5.09–5.17 ppm (3 H, m, H1,2',4) provided evidence for the regiochemistry of the brominolysis of the epoxide of 434.

**1'-O-((R)-10-tuberculostearyl)-2'-O-palmitoyl-sn-glycerol 2,3,4,6-tetra-O-methoxyacetyl- $\alpha$ -D-glucopyranoside (443)**

Tetrabutylammonium hydroxide (60 % w/w in  $\text{H}_2\text{O}$ ) (0.058 ml, 0.092 mmol) was added to a suspension of (R)-tuberculostearic acid **206** (0.030 g, 0.103 mmol) in  $\text{H}_2\text{O}$  (1.5 ml). The resulting mixture was vigorously stirred at room temperature overnight. The solvent was evaporated under reduced pressure and the crude residue was co-evaporated with toluene several times to afford tetrabutylammonium salt of tuberculostearic acid. Tetrabutylammonium tuberculostearte (0.054 g, 0.101 mmol) was added to a solution of **442** (0.043 g, 0.050 mmol) in toluene (0.5 ml) and the resulting mixture was heated to 85 °C and stirred vigorously for 25 min. The solvents were evaporated under reduced

pressure. Flash chromatography of the residue (40% EtOAc/petroleum ether) afforded **443** as a colourless oil (0.038 g, 70%).  $[\alpha]_D^{25} = +29.6$  (*c* 0.25, CHCl<sub>3</sub>). <sup>1</sup>H NMR (CDCl<sub>3</sub>, 400 MHz)  $\delta$  0.83 (3 H, d, *J* 6.4 Hz, CHCH<sub>3</sub>), 0.87 (6 H, t, *J* 6.8 Hz, 2 × CH<sub>3</sub>), 1.10–1.14 (2 H, m, tuberculostearyl CH<sub>2</sub>), 1.25–1.42 (49 H, m, 24 × CH<sub>2</sub>, 1 × CH), 1.61 (4 H, m, 2 ×  $\beta$ -CH<sub>2</sub>), 2.31 (4 H, q, *J* 7.7 Hz, 2 ×  $\alpha$ -CH<sub>2</sub>), 3.39, 3.41, 3.43, 3.45 (12 H, 4s, 4 × OCH<sub>3</sub>), 3.63 (1 H, dd, *J*<sub>2',3'</sub> 4.8, *J*<sub>3',3'</sub> 10.8 Hz, H3a'), 3.81 (1 H, dd, *J*<sub>2',3'</sub> 4.8, *J*<sub>3',3'</sub> 10.8 Hz, H3b'), 3.95, 4.00, 4.02, 4.08 (8 H, 4s, 4 × OCOCH<sub>2</sub>), 4.06–4.08 (1 H, m, H5), 4.11–4.20 (2 H, m, H1a', H6), 4.31–4.41 (2 H, m, H1b' H6), 4.97 (1 H, dd, *J*<sub>1,2</sub> 3.7, *J*<sub>2,3</sub> 10.1 Hz, H2), 5.12–5.23 (3 H, m, H1, H4, H2'), 5.52 (1 H, t, *J*<sub>2,3</sub> = *J*<sub>3,4</sub> 9.7 Hz, H3); <sup>13</sup>C NMR (CDCl<sub>3</sub>, 100 MHz)  $\delta$  14.2 (2 × CH<sub>2</sub>CH<sub>3</sub>), 19.7 (CHCH<sub>3</sub> (tuberculostearyl)), 22.7, 24.9, 24.95, 27.1, 29.2, 29.2, 29.3, 29.4, 29.6, 29.6, 29.7, 29.7, 30.0, 30.1, 32.0, 32.8, 34.1, 34.2 (fatty acyl), 59.4, 59.48, 59.55, 59.57, 67.3, 68.4, 69.2, 69.3, 69.4, 69.5, 69.7, 70.4, 70.6, 76.7, 77.1, 77.4, 96.2 (C1), 170.0 (MeOCH<sub>2</sub>C=O), 173.0 (sn-1-C=O), 173.3 (sn-2-C=O); HRMS (ESI<sup>+</sup>) calcd for C<sub>56</sub>H<sub>100</sub>O<sub>18</sub>Na (M+Na)<sup>+</sup> 1083.6802. Found 1083.6801.

**1'-O-((S)-10-tuberculostearyl)-2'-O-palmitoyl-sn-glyceryl 2,3,4,6-tetra-O-methoxyacetyl- $\alpha$ -D-glucopyranoside (444)**

Tetrabutylammonium hydroxide (60 % w/w in H<sub>2</sub>O) (0.041 ml, 0.064 mmol) was added to a suspension of 10-(S)-tuberculostearic acid (0.021 g, 0.071 mmol) in H<sub>2</sub>O (1 ml). The resulting mixture was vigorously stirred at room temperature overnight. The solvent was evaporated under reduced pressure and the crude residue was co-evaporated with toluene several times to afford tetrabutylammonium salt of tuberculostearic acid. Tetrabutylammonium tuberculostearte (0.038 g, 0.712 mmol) was added to a solution of **442** (0.030 g, 0.036 mmol) in toluene (0.5 ml) and the resulting mixture was heated to 85 °C and stirred vigorously for 25 min. The solvents were evaporated under reduced

pressure. Flash chromatography of the residue (40% EtOAc/petroleum ether) afforded **444** as a colourless oil (0.019 g, 50%).  $[\alpha]_D^{25} = +29.5$  (*c* 0.5, CHCl<sub>3</sub>). <sup>1</sup>H NMR (CDCl<sub>3</sub>, 400 MHz)  $\delta$  0.83 (3 H, d, *J* 6.4 Hz, CHCH<sub>3</sub>), 0.87 (6 H, t, *J* 6.8 Hz, 2 × CH<sub>3</sub>), 1.10–1.14 (2 H, m, tuberculostearyl CH<sub>2</sub>), 1.25–1.42 (49 H, m, 24 × CH<sub>2</sub>, 1 × CH), 1.61 (4 H, m, 2 × β-CH<sub>2</sub>), 2.31 (4 H, q, *J* 7.7 Hz, 2 × α-CH<sub>2</sub>), 3.39, 3.41, 3.43, 3.45 (12 H, 4s, 4 × OCH<sub>3</sub>), 3.63 (1 H, dd, *J*<sub>2',3'</sub> 4.8, *J*<sub>3',3'</sub> 10.8 Hz, H3a'), 3.81 (1 H, dd, *J*<sub>2',3'</sub> 4.8, *J*<sub>3',3'</sub> 10.8 Hz, H3b'), 3.95, 4.00, 4.02, 4.08 (8 H, 4s, 4 × OCOCH<sub>2</sub>), 4.06–4.08 (1 H, m, H5), 4.11–4.20 (2 H, m, H1a', H6), 4.31–4.41 (2 H, m, H1b' H6), 4.97 (1 H, dd, *J*<sub>1,2</sub> 3.7, *J*<sub>2,3</sub> 10.1 Hz, H2), 5.12–5.23 (3 H, m, H1, H4, H2'), 5.52 (1 H, t, *J*<sub>2,3</sub> = *J*<sub>3,4</sub> 9.7 Hz, H3); <sup>13</sup>C NMR (CDCl<sub>3</sub>, 100 MHz)  $\delta$  14.2 (2 × CH<sub>2</sub>CH<sub>3</sub>), 19.7 (CHCH<sub>3</sub> (tuberculostearyl)), 22.7, 24.9, 24.96, 27.1, 29.2, 29.2, 29.3, 29.4, 29.6, 29.6, 29.7, 29.7, 30.0, 30.1, 32.0, 32.8, 34.1, 34.2, (fatty acyl), 59.4, 59.48, 59.55, 59.57, 67.3, 68.4, 69.2, 69.3, 69.4, 69.5, 69.7, 70.4, 70.6, 76.7, 77.1, 77.4, 96.2 (C1), 170.0 (MeOCH<sub>2</sub>C=O), 173.0 (sn-1-C=O), 173.3 (sn-2-C=O); HRMS (ESI<sup>+</sup>) calcd for C<sub>58</sub>H<sub>100</sub>O<sub>18</sub>Na (M+Na)<sup>+</sup> 1083.6802. Found 1083.6803.

**1'-O-((R)-10-tuberculostearyl)-2'-O-palmitoyl-sn-glycerol α-D-glucopyranoside (439)**

A solution of *tert*-butylamine (0.109 ml, 1.05 mmol) and **443** (0.023 g, 0.021 mmol) in CHCl<sub>3</sub> (0.165 ml) and MeOH (0.385 ml) was stirred at 0 °C for 10 min and then at 10 °C for an hour. The solvents were evaporated under reduced pressure at 10-15 °C. Flash chromatography of the residue (5% MeOH/CHCl<sub>3</sub>) afforded **439** as a white semisolid (0.013 g, 82%).  $[\alpha]_D^{26} = +45.1$  (*c* 0.5, CHCl<sub>3</sub>). <sup>1</sup>H NMR (DMSO-d<sub>6</sub>, 400 MHz)  $\delta$  0.80 (3 H, d, *J* 6.4 Hz, CHCH<sub>3</sub>), 0.84 (6 H, t, *J* 6.7 Hz, 2 × CH<sub>2</sub>CH<sub>3</sub>), 1.06 (2 H, m, CH<sub>2</sub> (tuberculostearyl)), 1.23–1.42 (49 H, m, 24 × CH<sub>2</sub>, 1 × CH), 1.38–1.48 (4 H, m, 2 × β-CH<sub>2</sub>), 2.25 (4 H, q, *J* 7.3 Hz, 2 × α-CH<sub>2</sub>), 3.07 (1 H, td, *J*<sub>2,3</sub> 5.4, *J*<sub>3,4</sub> 9.3 Hz, H3), 3.17 (1

H, dd,  $J_{1,2}$  3.7,  $J_{2,3}$  6.5, H2), 3.43–3.51 (4 H, m, H3'a, H4, H6, H6), 3.57 (1 H, m, H5), 3.69 (1 H, dd,  $J_{2,3}$  5.7,  $J_{3,3'}$  10.8 Hz, H3'b), 4.14 (1 H, dd,  $J_{1,2'}$  7.0,  $J_{1',1'}$  12 Hz, H1'a), 4.31 (1 H, dd,  $J_{1,2'}$  7.0,  $J_{1',1'}$  12 Hz, H1'b), 4.40 (1 H, t,  $J$  5.8 Hz, OH), 4.64 (1 H, d,  $J_{1,2}$  3.6 Hz, H1), 4.66 (1 H, d,  $J$  6.5 Hz, OH), 4.77 (1 H, d,  $J$  4.8 Hz, OH), 4.86 (1 H, d,  $J$  5.3 Hz, OH), 5.12 (1 H, m, H2');  $^{13}\text{C}$  NMR (DMSO- $d_6$ , 150 MHz)  $\delta$  13.8, 19.5, 22.1, 23.5, 24.4, 26.5, 28.7, 29.1, 31.3, 32.1, 33.3, 33.5, 36.4 (fatty acyl), 60.7 (C6), 62.3, 64.9, 65.0, 68.5, 69.6, 69.9, 71.7, 72.9, 73.0, 98.9 (C1), 172.3 (sn-2-C=O), 172.5 (sn-2-C=O); HRMS (ESI $^+$ ) calcd for  $\text{C}_{44}\text{H}_{88}\text{NO}_{10}$  ( $\text{M}+\text{NH}_4$ ) $^+$  790.6403. Found 790.6403

**1'-O-((S)-10-tuberculostearyl)-2'-O-palmitoyl-sn-glyceryl  $\alpha$ -D-glucopyranoside (440)**

A solution of *tert*-butylamine (0.085 ml, 0.815 mmol) and **444** (0.017 g, 0.016 mmol) in  $\text{CHCl}_3$  (0.165 ml) and MeOH (0.385 ml) was stirred at 0 °C for 10 min and then at 10 °C for an hour. The solvents were evaporated under reduced pressure at 10-15 °C. Flash chromatography of the residue (5% MeOH/ $\text{CHCl}_3$ ) afforded **440** as a white semisolid (0.011 g, 89%).  $[\alpha]_{\text{D}}^{25} = +44.4$  ( $c$  0.5,  $\text{CHCl}_3$ ).  $^1\text{H}$  NMR (DMSO- $d_6$ , 400 MHz)  $\delta$  0.80 (3 H, d,  $J$  6.4 Hz,  $\text{CHCH}_3$ ), 0.84 (6 H, t,  $J$  6.7 Hz,  $2 \times \text{CH}_2\text{CH}_3$ ), 1.06 (2 H, m,  $\text{CH}_2$  (tuberculostearyl)), 1.23–1.42 (49 H, m,  $24 \times \text{CH}_2$ ,  $1 \times \text{CH}$ ), 1.38–1.48 (4 H, m,  $2 \times \beta\text{-CH}_2$ ), 2.25 (4 H, q,  $J$  7.3 Hz,  $2 \times \alpha\text{-CH}_2$ ), 3.07 (1 H, td,  $J_{2,3}$  5.4,  $J_{3,4}$  9.3 Hz, H3), 3.17 (1 H, dd,  $J_{1,2}$  3.7,  $J_{2,3}$  6.5, H2), 3.43–3.51 (4 H, m, H3'a, H4, H6, H6), 3.57 (1 H, m, H5), 3.69 (1 H, dd,  $J_{2,3}$  5.7,  $J_{3,3'}$  10.8 Hz, H3'b), 4.14 (1 H, dd,  $J_{1,2'}$  7.0,  $J_{1',1'}$  12 Hz, H1'a), 4.31 (1 H, dd,  $J_{1,2'}$  7.0,  $J_{1',1'}$  12 Hz, H1'b), 4.40 (1 H, t,  $J$  5.8 Hz, OH), 4.64 (1 H, d,  $J_{1,2}$  3.6 Hz, H1), 4.66 (1 H, d,  $J$  6.5 Hz, OH), 4.77 (1 H, d,  $J$  4.8 Hz, OH), 4.86 (1 H, d,  $J$  5.3 Hz, OH), 5.12 (1 H, m, H2');  $^{13}\text{C}$  NMR (DMSO- $d_6$ , 150 MHz)  $\delta$  13.9, 19.5, 22.0, 23.5, 24.4, 26.3, 28.4, 28.7, 29.0, 29.3, 31.3, 32.1, 33.3, 33.5, 36.4 (fatty acyl), 60.7, 62.3, 64.9, 65.0, 68.5,

69.6, 69.9, 71.7, 72.9, 73.0, 98.9 (C1), 172.3 (sn-2-C=O), 172.5 (sn-2-C=O); HRMS (ESI<sup>+</sup>) calcd for C<sub>44</sub>H<sub>88</sub>NO<sub>10</sub> (M+NH<sub>4</sub>)<sup>+</sup> 790.6403. Found 790.6402

**1'-O-((R)-10-tuberculostearyl)-2-O-palmitoyl-sn-glycerol  $\alpha$ -D-glucopyranosiduronic acid (402)<sup>86</sup>**

(2,2,6,6-Tetramethylpiperidin-1-yl)oxyl (TEMPO) (0.53 mg, 3.42  $\mu$ mol), BAIB (12.17 mg, 0.037 mmol) and NaHCO<sub>3</sub> (7.18 mg, 0.0855 mmol) were added to a solution of **439** (13.2 mg, 0.017 mmol) in acetonitrile: water (1:1, 1.0 ml) at 0 °C and stirred vigorously for 24 h. Another batch of TEMPO (0.53 mg, 3.42  $\mu$ mol) and BAIB (12.17 mg, 0.037 mmol) were added after 24 h and stirring continued overnight. The reaction mixture was quenched with 2M sodium thiosulphate, acidified with HCl and extracted with diethyl ether. The organic portion was dried over (Na<sub>2</sub>SO<sub>4</sub>), filtered and concentrated under reduced pressure. Flash chromatography of the residue (70:20:1 MeOH/ CHCl<sub>3</sub>/ H<sub>2</sub>O and 1% acetic acid) afforded **402** as a colorless semisolid (13.2 mg, 85%). [ $\alpha$ ]<sub>D</sub><sup>26</sup> = +35.8 (c 0.25, DMSO). <sup>1</sup>H NMR (DMSO-d<sub>6</sub>, 500 MHz)  $\delta$  0.79 (3 H, d, *J* 6.4 Hz, CHCH<sub>3</sub>), 0.83 (6 H, t, *J* 6.7 Hz, 2  $\times$  CH<sub>2</sub>CH<sub>3</sub>), 1.04 (2 H, m, CH<sub>2</sub> (tuberculostearyl)), 1.21–1.35 (49 H, m, 24  $\times$  CH<sub>2</sub>, 1  $\times$  CH), 1.38–1.48 (4 H, m, 2  $\times$   $\beta$ -CH<sub>2</sub>), 2.21–2.27 (4 H, m, 2  $\times$   $\alpha$ -CH<sub>2</sub>), 3.22–3.24 (1 H, m, H2), 3.54 (1H, m, H3'a), 3.69 (1 H, m, H3'b), 3.76 (1 H, d, *J*<sub>4,5</sub> 10.1 Hz, H5), 4.15 (1 H, dd, *J*<sub>1'2'</sub> 7.2, *J*<sub>1',1'</sub> 12 Hz, H1'a), 4.32 (1 H, dd, *J*<sub>1'2'</sub> 7.2, *J*<sub>1',1'</sub> 12 Hz, H1'b), 4.68 (1 H, d, *J*<sub>1,2</sub> 3.6 Hz, H1), 4.76 (1 H, d, *J* 4.8 Hz, OH), 4.87 (1 H, d, *J* 5.3 Hz, OH), 5.11–5.21 (1 H, m, H2'); <sup>13</sup>C NMR (DMSO-d<sub>6</sub>, 150 MHz)  $\delta$  13.8, 19.6 (CHCH<sub>3</sub> (tuberculostearyl)), 22.1, 24.33, 24.35, 26.3, 26.33, 28.33, 28.35, 28.58, 28.6, 28.64, 28.84, 28.95, 29.2, 31.1, 31.9, 33.3, 33.4, 36.33, 36.35, 36.37, 62.1, 65.4, 69.5 (C1', C2', C3'), 71.3, 71.7, 71.8, 72.6, 99.3 (C1), 170.9 (C6), 172.2, 172.4 (C = O); HRMS (ESI<sup>+</sup>) calcd for C<sub>44</sub>H<sub>82</sub>O<sub>11</sub>Na [M+Na]<sup>+</sup> 809.5749. Found 809.5745.

**1'-O-((S)-10-tuberculostearyl)-2-O-palmitoyl-sn-glyceryl** **$\alpha$ -D-****glucopyranosiduronic acid (441)**

TEMPO (0.34 mg, 1.99  $\mu$ mol), Bis(acetoxy)iodobenzene (BAIB) (7.97 mg, 0.0219 mmol) and NaHCO<sub>3</sub> (4.72 mg, 0.0498 mmol) were added to a solution of **440** (7.7 mg, 0.001 mmol) in acetonitrile : water (1:1, 1.0 ml) at 0 °C and stirred vigorously for 24 h. TEMPO (0.34 mg, 1.99  $\mu$ mol), BAIB (7.97 mg, 0.0219 mmol) were added after 24 h and stirred overnight. The reaction was quenched with 2M sodium thisulphate, acidified with HCl and extracted with diethyl ether. The organic layer was dried over (Na<sub>2</sub>SO<sub>4</sub>), filtered and concentrated under reduced pressure. Flash chromatography of the residue (70:20:1 MeOH/ CHCl<sub>3</sub>/ H<sub>2</sub>O and 1% acetic acid) afforded **441** as a colorless semisolid (5.4 mg, 70%).  $[\alpha]_D^{26} = +45.4$  (*c* 0.6, CHCl<sub>3</sub>). <sup>1</sup>H NMR (DMSO-d<sub>6</sub>, 500 MHz)  $\delta$  0.79 (3 H, d, *J* 6.4 Hz, CHCH<sub>3</sub>), 0.83 (6 H, t, *J* 6.7 Hz, 2  $\times$  CH<sub>2</sub>CH<sub>3</sub>), 1.04 (2 H, m, CH<sub>2</sub> (tuberculostearyl)), 1.21–1.35 (49 H, m, 24  $\times$  CH<sub>2</sub>, 1  $\times$  CH), 1.38–1.48 (4 H, m, 2  $\times$   $\beta$ -CH<sub>2</sub>), 2.21–2.27 (4 H, m, 2  $\times$   $\alpha$ -CH<sub>2</sub>), 3.22–3.24 (1 H, m, H2), 3.54 (1H, m, H3'a), 3.69 (1 H, m, H3'b), 3.76 (1 H, d, *J*<sub>4,5</sub> 10.1 Hz, H5), 4.15 (1 H, dd, *J*<sub>1'2'</sub> 7.2, *J*<sub>1',1'</sub> 12 Hz, H1'a), 4.32 (1 H, dd, *J*<sub>1'2'</sub> 7.2, *J*<sub>1',1'</sub> 12 Hz, H1'b), 4.68 (1 H, d, *J*<sub>1,2</sub> 3.6 Hz, H1), 4.76 (1 H, d, *J* 4.8 Hz, OH), 4.87 (1 H, d, *J* 5.3 Hz, OH), 5.11–5.21 (1 H, m, H2'); <sup>13</sup>C NMR (DMSO-d<sub>6</sub>, 150 MHz)  $\delta$  13.8, 19.6 (CHCH<sub>3</sub> (tuberculostearyl), 22.1, 24.33, 24.35, 26.3, 26.33, 28.33, 28.35, 28.58, 28.6, 28.64, 28.84, 28.95, 29.2, 31.1, 31.9, 33.3, 33.4, 36.33, 36.35, 36.37, 62.1, 65.4, 69.5 (C1', C2', C3'), 71.3, 71.7, 71.8, 72.6, 99.3 (C1), 170.9 (C6), 172.2, 172.4 (C = O); HRMS (ESI<sup>+</sup>) calcd for C<sub>44</sub>H<sub>82</sub>O<sub>11</sub>Na [M+Na]<sup>+</sup> 809.5749. Found 809.5746.





## **PART II**

**Development of oxime-based activated esters as safer alternatives to hydroxybenzotriazoles for chemo- and regioselective benzylation.**

## Chapter 5: Development of oxime-based activated esters

### 5.1 Introduction

*“Protection is not a principle but an expedient” – Benjamin Disraeli.<sup>183</sup>*

#### 5.1.1 Hydroxyl protecting groups in carbohydrate chemistry

Protecting groups are functionalities that are temporarily installed to block reactions at a specific site while allowing chemical transformations to occur at other sites (Figure 5.1). Selective protection of functional groups is critical so as to allow selective transformations of polyfunctional molecules.<sup>184</sup>

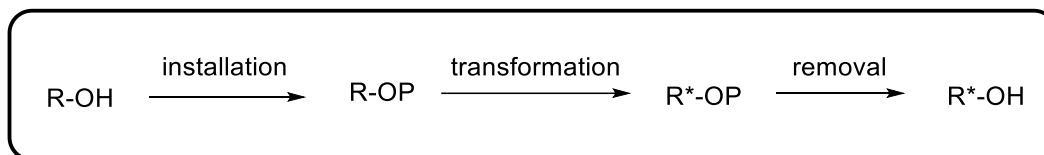


**Figure 5.1** The conceptual basis of hydroxyl protecting groups.

Temporary protection of hydroxyl groups has evolved as a significant concept in synthetic organic chemistry and especially in carbohydrate chemistry.<sup>183-184</sup> For polyhydroxylated molecules such as carbohydrates, it is critical to selectively protect the hydroxyl groups to allow reactions at a desired site (for an example see Figure 5.2). Protecting group manipulations and deprotections have evolved to be an essential part of the synthetic strategy for the preparation of oligosaccharides. As protecting groups are often unavoidable and essential, the identification of improved protecting groups and the means to selectively introduce and remove them are subjects of enduring interest.<sup>183</sup>

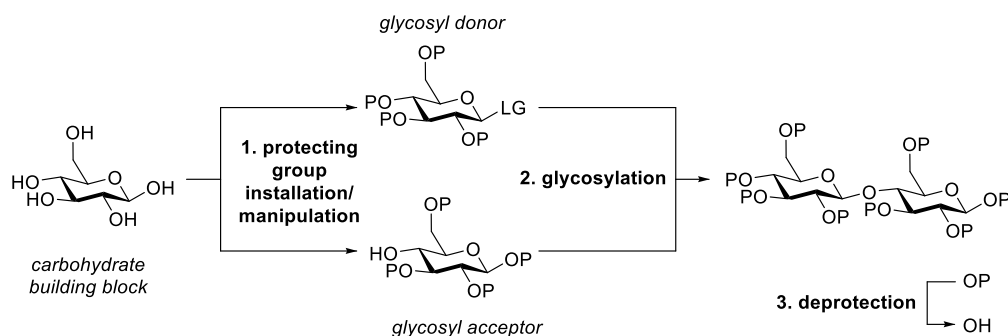


**Figure 5.2** General strategy for construction of oligosaccharides.

An ideal protecting group should:<sup>183-184</sup>

- be selectively installed using mild conditions;
- be selectively removed using mild conditions under which the deprotected molecule is stable;
- be installed and removed in good yields, and provide byproducts that are easily separated;
- be stable under a wide range of reaction conditions;
- contain a minimum number of functional groups so as to be inert to other reaction conditions;
- not contain stereogenic centers, which for chiral substrates can result in unwanted diastereomers with different reactivity and complicated spectra;
- be readily available and cost effective;
- be safe for use and transport.

## 5.2 Principles of selective hydroxyl group protection

It is highly desirable to develop approaches for selective introduction of protecting groups on polyhydroxylated substrates. Based on nucleophilicity, the selective installation of monovalent protecting groups onto hydroxyl groups follows three main principles:

1. The nucleophilicity of hydroxyl groups follows the order of  $1^\circ > 2^\circ > 3^\circ$ . Thus, a primary hydroxyl group can be selectively protected in the presence of secondary and tertiary hydroxyl groups; and a secondary hydroxyl group can be selectively protected

in the presence of tertiary hydroxyl groups. The reactivity of hydroxyls can be fine-tuned by varying the strength of base used. Under weakly basic conditions tertiary and secondary hydroxyls cannot be deprotonated. While medium basic conditions, can deprotonate primary and secondary hydroxyl stronger bases such as DBU are required to deprotonate tertiary hydroxyl making incipient alkoxide. However, such tertiary alkoxide formed is strongly basic and is less reactive compared to 1° and 2° alkoxide. Hence, the reactivity order is 1° > 2° > 3°. This order of reactivity could be reversed by employing very strong bases such as NaOH.

2. An equatorial hydroxyl group is more nucleophilic than an axial hydroxyl group. Therefore, an equatorial hydroxyl group can be protected selectively, relative to an axial hydroxyl group.
3. An equatorial hydroxyl with a *cis* vicinal oxygen is more reactive than an isolated hydroxyl without a vicinal oxygen and thus can be selectively protected. This reactivity difference is believed to arise due to intramolecular hydrogen bond formation between the hydroxyl group and the adjacent oxygen.

There are several protecting groups used for hydroxyl group protection such as esters, ethers and acetals. For the purpose of this chapter, we would focus on ester protecting groups, especially benzoates.

### 5.3 Esters as hydroxyl protecting groups

Esters satisfy many of the ideal characteristics of a protecting group in terms of cost, availability, installation, removal and stability (Figure 5.3). Commonly used esters include those of acetic acid (acetate, Ac), benzoic acid (benzoate, Bz), and pivalic acid (pivalate, Piv). However, ester protecting groups can also influence the reactivity and stereoselectivity of reactions of the substrate.

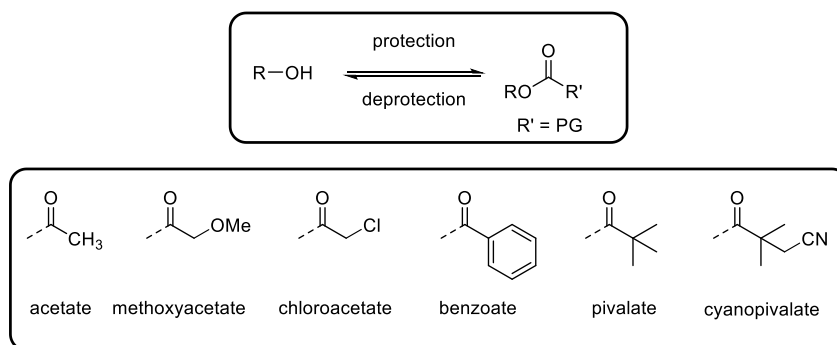
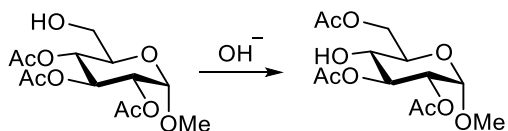


**Figure 5.3** Common ester protecting groups.

### 5.3.1 Intramolecular migration

Ester protecting groups especially acetates can undergo intramolecular migration to a neighboring hydroxyl group. The propensity for intramolecular migration can be overcome by use of bulkier protecting groups such as benzoates or pivalates. However, intramolecular migration can be advantageous in allowing the synthesis of otherwise difficult-to-prepare derivatives. In the example below (Scheme 5.1), the acetate group at the 4-OH has migrated to the 6-OH position thus giving access to this useful alcohol.



**Scheme 5.1** Intramolecular migration of acetate group from 4-OH to the 6-OH under basic conditions.

### 5.3.2 Neighboring group participation

Ester groups can influence the course of reactions. In glycosylation reactions, esters at the 2-OH of the donor “participate” with the intermediate oxocarbenium-ion to generate a cyclic dioxolenium ion, which undergoes substitution with inversion to afford a 1,2-*trans*-glycoside, usually with very high selectivity (Figure 5.4).<sup>183, 185</sup>

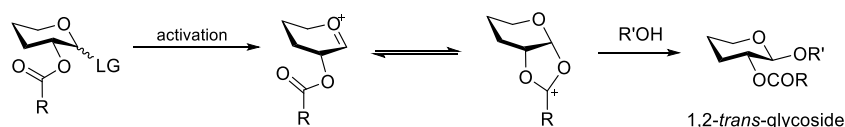


**Figure 5.4** Neighboring group participation.

### 5.3.3 “Armed/disarmed” principle

Ester functional groups can enable chemoselective glycosylations. In 1988, Fraser-Reid *et al.* espoused the “armed-disarmed effect” to describe the differences in reactivity between glycosyl donors based on their protecting groups.<sup>186</sup> The glycosyl donor forms positively charged oxocarbenium or dioxolenium intermediates upon reaction with a suitable electrophile. The presence of an electron-withdrawing group such as an ester at 2-OH destabilizes (disarms) the intermediate, while the presence of an electron-donating group such as an ether stabilizes (arms) the intermediate. This allows a selective coupling of the armed pentenyl glycoside with the disarmed pentenyl glycoside carrying a free hydroxyl group (Figure 5.5).

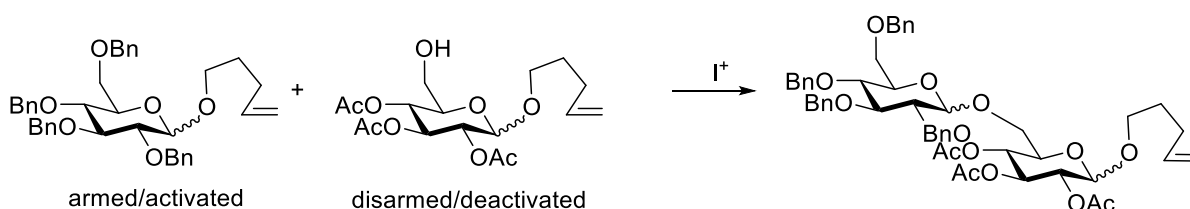


**Figure 5.5** Selective glycosylation of armed and disarmed pentenyl glycosides.

## 5.4 Use of benzoates in carbohydrate chemistry

Benzoic acid esters (benzoates) are a widely-used protecting group. Benzoates are relatively resistant to acid-catalyzed hydrolysis, reasonably immune to acyl migration, and the phenyl group provides a useful chromophore for monitoring reactions.<sup>184</sup> Commonly used benzoylating reagents include BzCl in pyridine, benzoic anhydride with triethylamine, and *N*-benzoylimidazole (BzIm),<sup>187-188</sup> tin oxides (e.g. dibutyltin oxide, bis(tributyltin) oxide) with BzCl,<sup>189</sup> and benzoyloxybenzotriazole (BBTZ).<sup>190</sup> Other less

commonly used benzoylating agents include benzoyl cyanide,<sup>191</sup> triphenylphosphine-benzoyl-peroxide,<sup>192</sup> *N*-benzoyltetrazole,<sup>193</sup> heptafluoro-1-methylethyl phenyl ketone,<sup>194</sup> and benzoyl trifluoromethanesulfonate (BzOTf) (Figure 5.6).<sup>195</sup> Benzoates are stable to a wide range of reaction conditions and can be cleaved under mild conditions that do not affect the rest of the molecule. Commonly used methods for removal are saponification using NaOH, anion exchange resin (OH<sup>-</sup> form), or transesterification using catalytic NaOMe or K<sub>2</sub>CO<sub>3</sub> in MeOH.

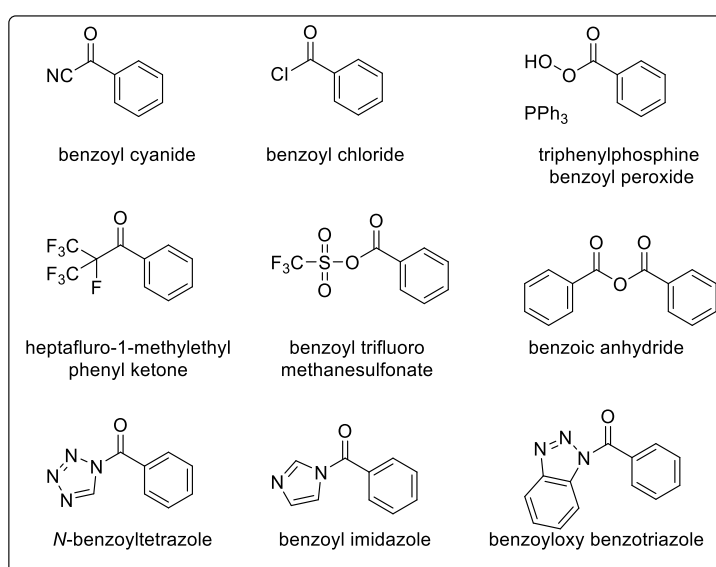
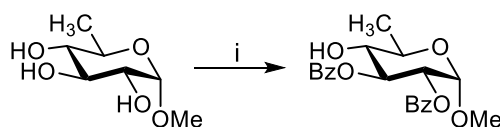


**Figure 5.6** An array of various benzoylating reagents.

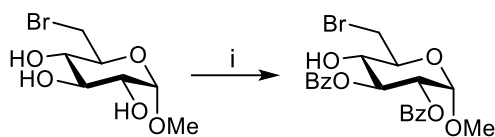
#### 5.4.1 Selective installation of benzoyl groups

Benzoates can be selectively installed onto hydroxyl groups by the use of appropriate reagents and reaction conditions. For example, BzCl in pyridine can be used to selectively protect the 2- and 3-hydroxyl groups in methyl 6-deoxy- $\alpha$ -D-glucopyranoside.<sup>188</sup>



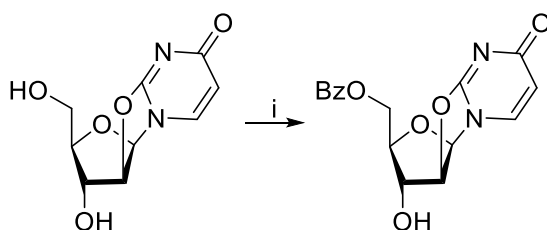
**Scheme 5.2** Selective benzoylation of 2- and 3-OH using BzCl. Reagents and conditions: (i) BzCl, pyridine, 3 d, -40 °C, 61%.

BzIm can be used to selectively benzoylate the 2- and 3-positions of 6-bromo-methyl  $\alpha$ -D-glucopyranoside (Scheme 5.3).<sup>187</sup>



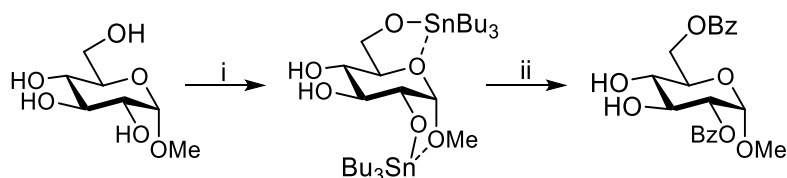
**Scheme 5.3** Selective benzoylation of 2- and 3- OH using BzIm. Reagents and conditions: (i) BzIm,  $\text{CH}_2\text{Cl}_2$ , 24 h, reflux, 75%.

Holy and Soucek utilized BzCN for benzoylation of the 3- and 5-OH of 2,2'-anhydro-(1- $\beta$ -D-arabinofuranosyl)uracil using tributylamine as base (Scheme 5.4).<sup>191</sup>



**Scheme 5.4** Reagents and conditions: (i) BzCN,  $\text{Bu}_3\text{N}$ , 88%.

Organotin reagents in combination with acylating agents are commonly used for installing benzoyl groups. Bis(trialkyltin) oxides  $[(\text{R}_3\text{Sn})_2\text{O}]$  and dialkyl tin oxides  $(\text{R}_2\text{SnO})$  react with hydroxyl groups to form stannyl ethers or stannylene acetals respectively, which upon treatment with BzCl afford the benzoate esters. For example, bis(tributyltin)oxide can be used to selectively stannylate methyl  $\alpha$ -D-glucopyranoside; upon treatment with BzCl the 2,6-di-benzoate can be isolated in 82% yield (Scheme 5.5).<sup>189</sup>



**Scheme 5.5** Reagents and conditions: (i)  $(\text{Bu}_2\text{Sn})_2\text{O}$ ; (ii) BzCl, 82%.

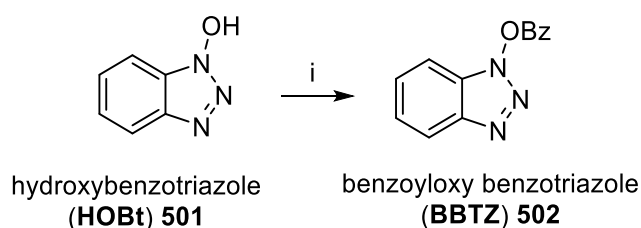
While many of the reagents discussed thus far are effective for selective benzoylations, they possess various shortcomings that include:



- the need for low temperature conditions, as in case of BzCl in pyridine, which is not possible for many polar substrates owing to poor solubility;
- release of toxic HCN as byproduct in case of BzCN;
- poor regioselectivity;
- harsh reaction conditions are required for derivatization of hindered alcohols, leading to undesired side reactions;
- prolonged reaction times (often several days in case of BzCl in pyridine);
- the use of stoichiometric quantities of toxic reagents and associated waste streams in the case of organotin reagents.

### 5.5 An introduction to HOBt and BBTZ

Standing apart from the aforementioned reagents is benzoyloxybenzotriazole (BBTZ), first introduced by Kim *et al.* for the selective benzylation of diols in 1984.<sup>196</sup> BBTZ is a benzoate ester of *N*-hydroxybenzotriazole (HOBt), prepared by treating HOBt with BzCl (Scheme 5.6).



**Scheme 5.6** Synthesis of BBTZ. Reagents and conditions: (i) BzCl, Et<sub>3</sub>N, CH<sub>2</sub>Cl<sub>2</sub>, o/n, 85%.

Wolfgang Kiinig *et al.* introduced HOBt **501** as an additive to suppress racemization and decrease the formation of unwanted byproducts during peptide couplings using dicyclocarbodiimide (DCC).<sup>197-198</sup> It has been reported that HOBt assists as a nucleophilic catalyst, as shown in the following mechanism, which involves the formation of an active HOBt-ester intermediate (Figure 5.7).

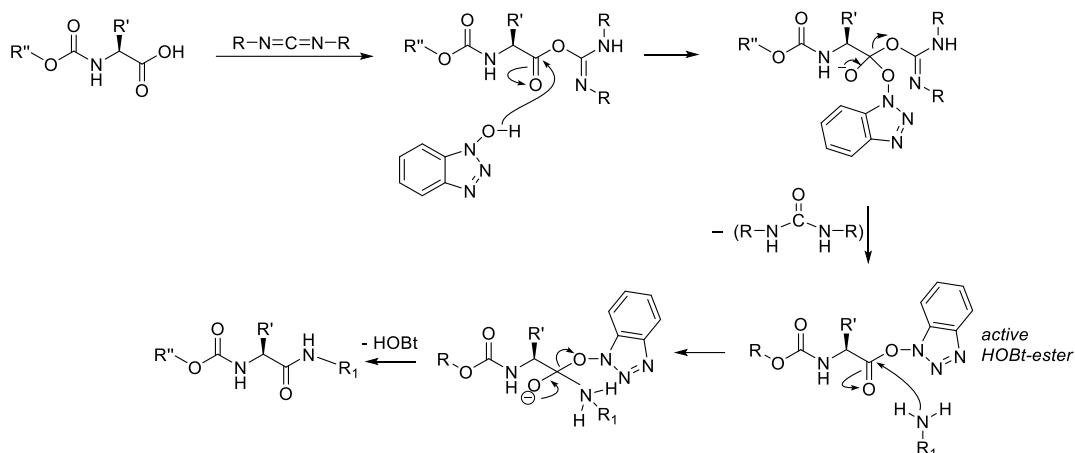


**Figure 5.7** Mechanism of action of HOBt via an active HOBt-ester.

Uronium salts (HBTU, HDMB; **503** and **504**) and tetrafluoroborate salts (TBTU, **505**) of HOBt, **501** (Figure 5.8) are reported to be even more effective in suppressing racemization in peptide couplings. They can be used either as additives or as standalone reagents.

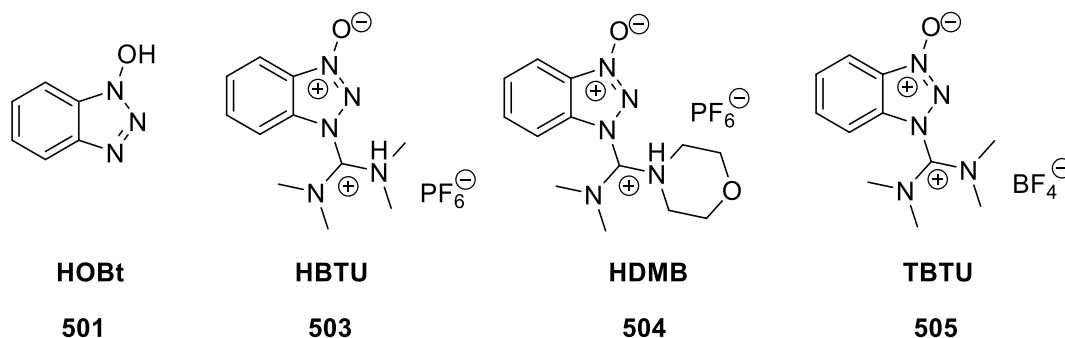


**Figure 5.8.** Structures of HOBt and HOBt-derived salts used in peptide coupling.

Use of HOBt and its derivatives has also been explored for esterification reactions (Figure 5.9). Osaki *et al.* used HOBt as an additive in DCC/DMAP mediated esterification of a primary alcohol in the synthesis of conagenin.<sup>199</sup> Williams *et al.* used HBTU for esterification of primary alcohol with oleuropeic acid in the synthesis of cuniloside and cypellocarpin.<sup>200</sup> Rosul and co-workers reported the use of TBTU as a standalone reagent in esterifications of a wide array of alcohols with benzoic acid.<sup>201</sup>

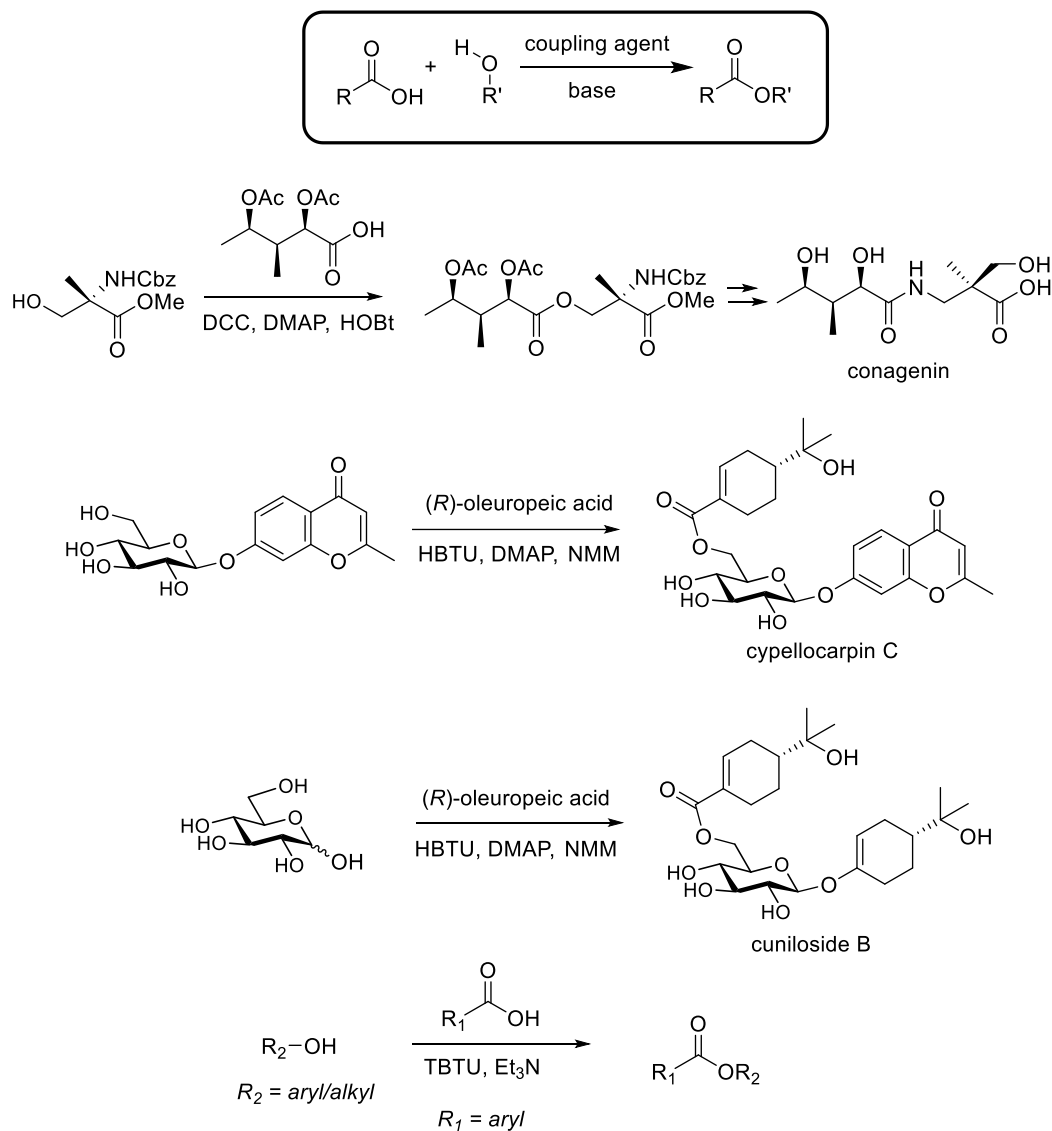


**Figure 5.9** Esterification examples using HOBt and HOBt-based reagents.

BBTZ (**502**), the benzoate ester of *N*-hydroxybenzotriazole (HOBt) has been used for selective benzoylations in carbohydrate chemistry. BBTZ reacts under mild conditions with outstanding regio- and chemo-selectivity that surpasses that of most other benzoylating reagents. For example, BBTZ selectively benzoylates the 2-hydroxyl group in methyl 4,6-*O*-benzylidene- $\alpha$ -D-glucopyranoside **506** giving the 2-benzoate **507** in 90% yield.<sup>196</sup> BBTZ can selectively benzoylate the 2-hydroxyl group of methyl 4,6-*O*-benzylidene- $\alpha$ -D-mannopyranoside **508** to afford the 2-benzoate **509** in 90% yield. Wang

*et al.* utilized the selective benzoylating ability of BBTZ to selectively protect the 2- and 6-OH of a methoxyphenyl  $\beta$ -D-glucopyranoside **510** in the total synthesis of biotinylated chacotriose.<sup>202</sup>

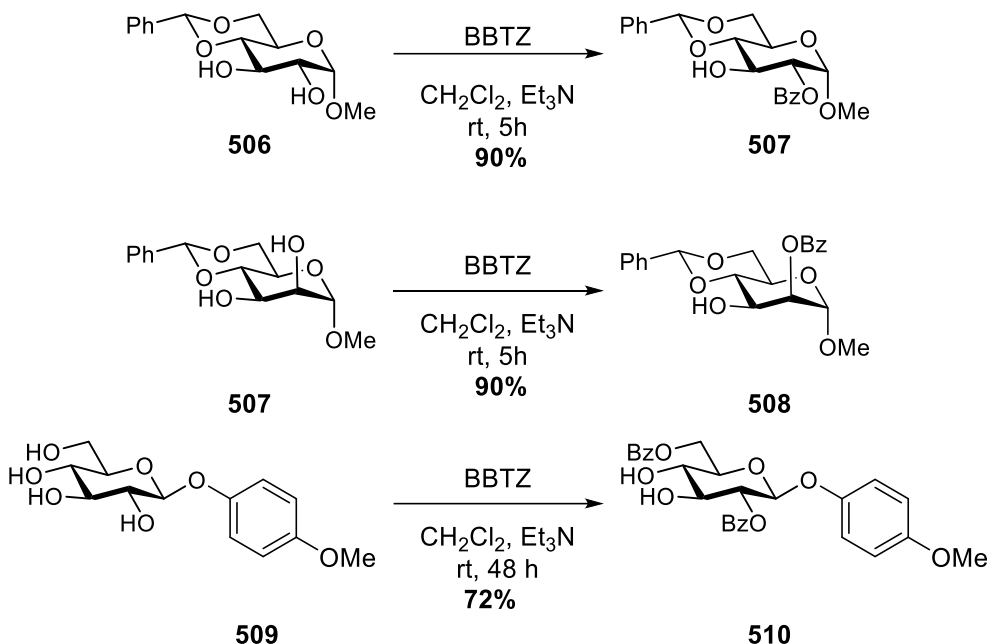


**Figure 5.10** Examples of selective benzoylation using BBTZ **502**.

### 5.5.1 Safety considerations

In 2005, the safety of HOBt was called into question. Wehrstedt *et al.* studied the safety profile of HOBt and HOBt-based coupling reagents using differential scanning calorimetry (DSC) and accelerating rate calorimetry (ARC) experiments.<sup>203-204</sup>

DSC experiments measure the amount of heat released by a test compound under thermal treatment. When HOBt hydrate **501** was heated in a closed crucible under nitrogen flow from 30 to 300 °C, at a constant heating rate, it was observed to decompose at 190 °C releasing 234 kJ/mol. HOBt-based coupling reagents such as HDMB **504** also exhibited explosive behavior similar to HOBt ( $\Delta H = 209$  kJ/mol) and decomposed at 180 °C.

Safety profile studies using ARC enable the study of decomposition of a compound under adiabatic conditions. Upon decomposition of the sample the associated pressure rise and

onset of decomposition temperatures can be accurately measured. ARC analysis revealed that HOBt hydrate releases 178 bar pressure and decomposition began at 145 °C. The HOBt-based coupling reagent HDMB released 24 bar pressure with the onset of decomposition occurring at 180 °C. Moreover, the decomposition kinetic profile of HOBt and HOBt-based coupling reagents showed sharp rises in temperature and sudden decomposition, posing a risk of thermal runaway explosions. As a result of these studies HOBt was classified as a Class I explosive. Since its classification as an explosive, transport of HOBt and related reagents has become difficult and is at the discretion of the transport companies. In light of the safety issues of HOBt and HOBt-based reagents, the need for new selective esterification reagents has been revisited and new alternatives have been proposed.

## 5.6 Oxime based reagents

Itoh first introduced ethyl 2-hydroximino-2-cyanoacetate (Oxya, OxyaPure **511**) in 1973.<sup>205</sup> Oxya is an oxime bearing electron-withdrawing ethyl-ester and cyano groups at the  $\alpha$ -positions. Oxya was shown to be a better racemization suppressant in peptide synthesis than HOBt. The uronium type Oxya-based coupling reagents COMU **512** and HOTU **513** (Figure 5.11) were shown to be superior to the HOBt-based coupling agent HBTU **503** in terms of yield, reaction rate and racemization suppression.<sup>16</sup>

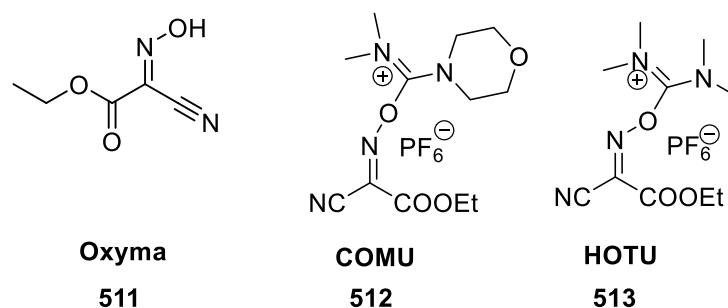


**Figure 5.11** Structures of Oxya and corresponding uronium salts.

Grindley *et al.* compared the esterification properties of COMU and HOBt-based analogues HBTU and TBTU in selective esterification reactions.<sup>206</sup> They observed that COMU is more effective than TBTU and TATU for esterification of tertiary alcohols and it is logical to suggest that in each of these applications activated esters of Oxyma are formed as reactive intermediates *in situ* (Figure 5.12).

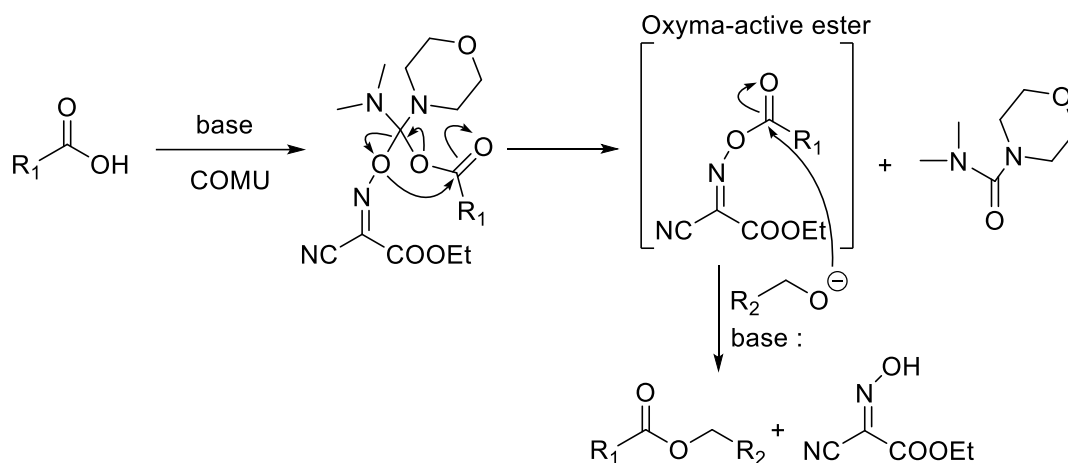


**Figure 5.12** Mechanism of esterification via the formation of an active ester of Oxyma.

### 5.6.1 Other Oxime based reagents

In 2010, Alberico *et al.* introduced uronium salts of isonitroso Meldrum's acid (HONM, **514**: referred to as Mel-Oxy in our project) named as HTMU **515**, HMMU **516**, and HDmPyMU **517** (Figure 5.13A). These authors showed that these salts outperform the corresponding Oxyma and HOBt analogues, providing excellent results when used as coupling agents, using only 1 equiv. of base, which is a key feature for reducing racemization.<sup>207</sup> However, HONM cannot be used as an additive to DCC as it forms an unreactive isourea intermediate, **518**. The same group, reported the use of Oxyma-B, **519** ((5-hydroxyimino)-1,3-dimethylpyrimidine-2,4,6 (1*H*,3*H*,5*H*)-trione).<sup>208</sup> Oxyma-B is structurally similar to HONM **514** but the oxime group is flanked by two amide carbonyl groups. This variation results in decreased reactivity compared to HONM making it suitable as an additive in carbodiimide reactions. Oxyma-B outperforms Oxyma and

HOAt in racemization suppression.<sup>208</sup> The uronium salts of Oxyma–B COMBU, **520** and TOMBU **521** (Figure 5.13 B) showed better racemization suppression compared to HBTU but did not surpass COMU.<sup>209</sup>

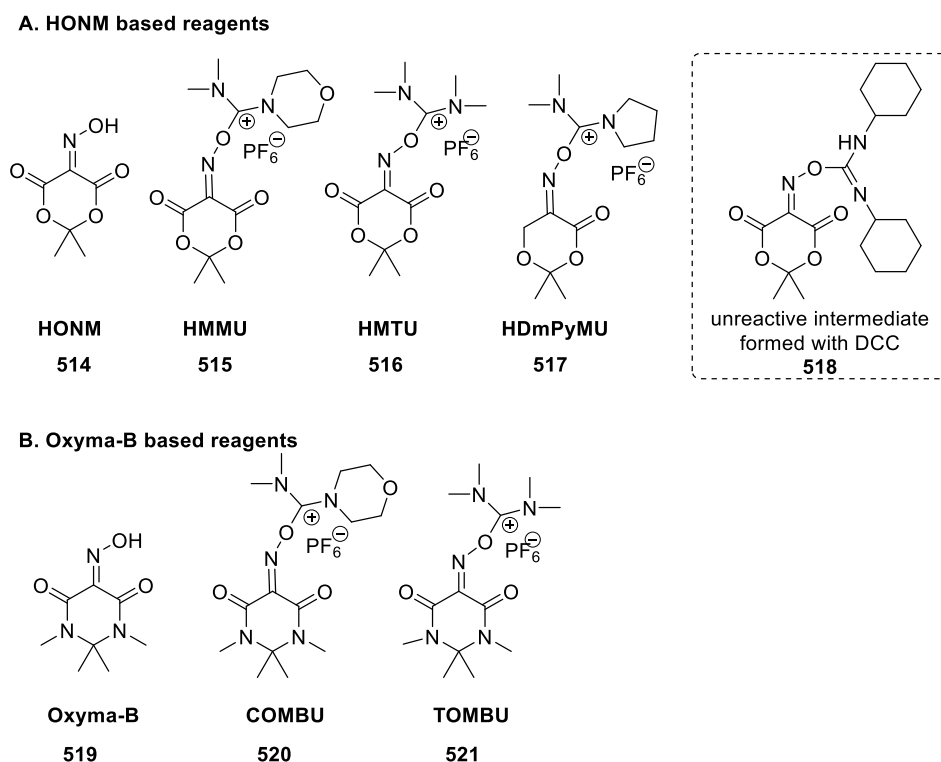


**Figure 5.13** A) Structures of HONM and corresponding uronium analogues; B) Structures of Oxyma-B and corresponding uronium analogues.

## 5.6.2 Safety

Ramon *et al.* used DSC and ARC to show that Oxyma and the Oxyma-based coupling reagent COMU exhibit a better safety profile compared to HOBt and HOBt-based coupling reagents (Table 5.1). Although the onset of decomposition temperatures for Oxyma **511** and COMU **512** are lower than for HOBt **501** and HDMB **504**, the decomposition profile showed a slower and constant decomposition in contrast to the sharp decomposition exhibited by HOBt and HOBt based coupling reagents, equating to a reduced risk of thermal runaway explosions.<sup>204</sup>

**Table 5.1** Comparison of safety profile of HOBt and Oxyma.

Safety parameter	HOBt	Oxyma
Onset of decomposition	190 °C	131°C
Heat released during decomposition ( $\Delta H$ )	234 kJ/mol	125 kJ/mol
Pressure released during decomposition	178 bar	61 bar

## 5.7 Aim and Overview

Now that HOBt and related reagents are scheduled as a Class I explosives<sup>203</sup> the need for alternative selective benzoylating agents should be revisited to replace the HOBt-derived BBTZ. Considering the improved safety profile of Oxyma, the similarity of  $pK_a$  values of HOBt ( $pK_a = 4.6$ )<sup>196</sup> and Oxyma ( $pK_a = 4.6$ ),<sup>205</sup> and the proven ability for COMU to allow selective esterification of alcohols, presumably via an active ester intermediate, we planned to investigate if benzoate esters of oximes such as Oxyma may provide safer alternatives to BBTZ for the selective protection of hydroxyl groups. In this chapter we designed and synthesized a series of oxime-based reagents, and performed structural and chemical characterization. Next, we assessed their benzoylating ability on a simple alcohol and thereafter their ability to selectively benzoylate various polyhydroxylated substrates.

## 5.8 Results and discussion

### 5.8.1 Design of oxime-based reagents

Leaving group ability correlates with the  $pK_a$  value of the conjugate acid. The  $pK_a$  value of HOBt is 4.60. By comparison, simple oximes have  $pK_a$  values of approximately 9. However, by introduction of electron-withdrawing groups, the  $pK_a$  value drops



significantly; for example the  $pK_a$  value of Oxyma is 4.60. El-Fahem, Albericio and co-workers demonstrated that Oxyma undergoes reaction at the imino and ethoxycarbonyl groups when used as an additive in peptide coupling. As well, it has been shown that the ethoxycarbonyl group of Oxyma is reactive and can lead to unwanted side reactions.<sup>204, 210</sup> Therefore, we planned to develop a series of oxime-based reagents by changing the nature of the EWG at the  $\alpha$ -position, and convert these to a series of benzoate esters (Figure 5.14).

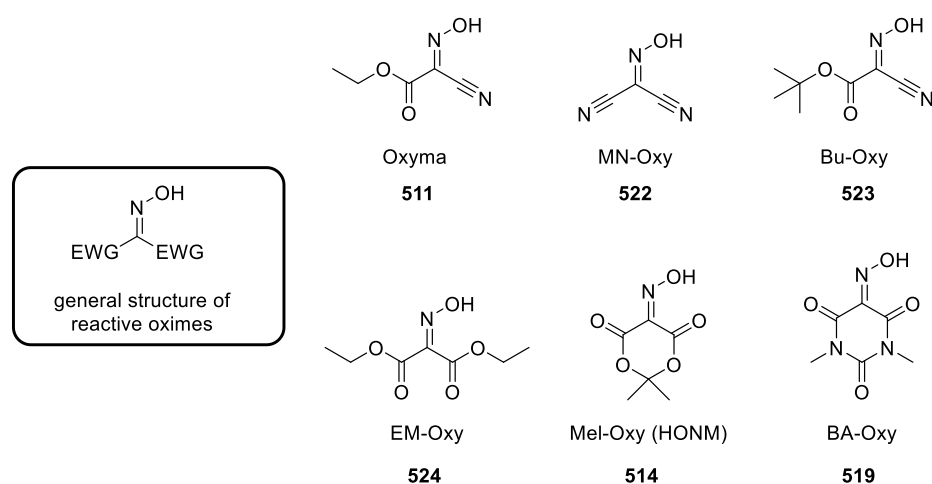


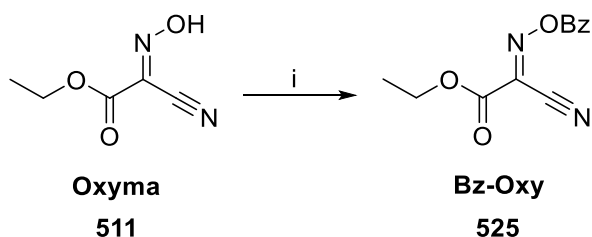
**Figure 5.14** Structures of oxime-based reagents.

## 5.8.2 Preparation of benzoylated oxime-based reagents

### 5.8.2.1 Benzoyl-Oxyma (Bz-Oxy, 525)

Bz-Oxy was prepared by benzoylating commercially-available Oxyma using benzoic anhydride in diethyl ether.<sup>‡</sup> Upon mixing the reagents Bz-Oxy precipitated within one minute (Scheme 5.7, Figure 5.15). We were able to obtain a single crystal X-ray structure of Bz-Oxy, which revealed that the stereochemistry about the C=N double bond is *Z*. The result also defines the stereochemistry of the precursor, Oxyma, as *Z*.

<sup>‡‡</sup> This procedure was developed by Dr. Philip van der Peet.<sup>211</sup> Burugupalli, S.; Shah, S.; van der Peet, P. L.; Arora, S.; White, J. M.; Williams, S. J., *Org Biomol Chem* **2016**, *14*, 97-104.



**Scheme 5.7** Synthesis of Benzoyl-Oxyma. Reagents and conditions: (i) Bz<sub>2</sub>O, Et<sub>2</sub>O, 90%, 1 min, r.t.

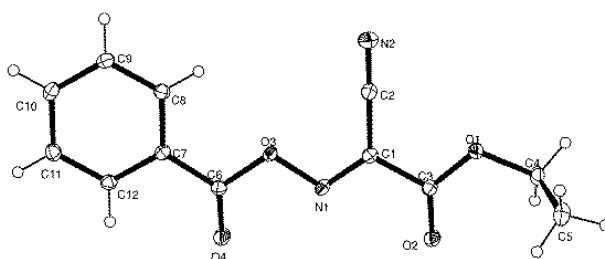
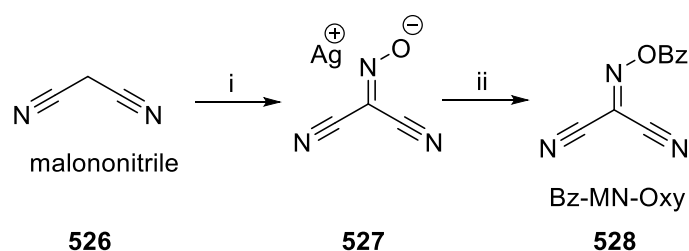


**Figure 5.15** ORTEP representation of the single molecule structure of Bz-Oxyma determined by X-ray crystallography. The X-ray structure was obtained by Prof. Jonathan White.

### 5.8.2.2 Benzoyl-malononitrileoxime (Bz-MN-Oxy, 528)

Cyano groups are slightly more electron-withdrawing (Hammett substituent constant,  $\sigma = 0.56$  for cyano) than ethoxycarbonyl groups ( $\sigma = 0.37$  for ethoxycarbonyl).<sup>212</sup> The silver salt of MN-Oxy **527** was prepared by treating malononitrile **526** with sodium nitrite and silver nitrate in acetic acid in a variant of the Knoevenagel reaction.<sup>213</sup> The silver salt **527** was treated with BzCl in pyridine to yield Bz-MN-Oxy **528** (Scheme 5.8).<sup>214</sup>

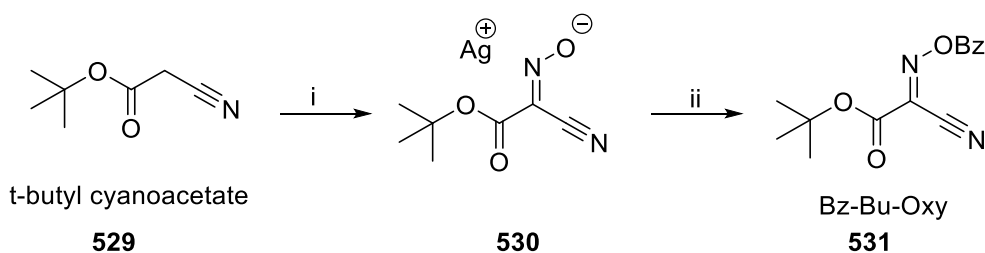


**Scheme 5.8** Synthesis of Bz-MN-Oxy. Reagents and conditions: (i) NaNO<sub>2</sub>, AgNO<sub>3</sub>, AcOH, 99%; (ii) BzCl, pyridine, 64%.

### 5.8.2.3 Benzoyl *tert*-butylcyanooxime (Bz-Bu-Oxy, 531)

Replacement of the ethyl ester of Oxyma with a *tert*-butyl ester should afford a derivative

with a less reactive carbonyl group. The silver salt of Bu-Oxy was prepared in a similar manner as **527**, by treating *tert*-butyl cyanoacetate **529** with sodium nitrite and silver nitrate to form the silver salt of *tert*-butyl cyanoacetate oxime **530**.<sup>215</sup> Bz-Bu-Oxy **531** was prepared by benzoylating **530** using BzCl and pyridine (Scheme 5.9).



**Scheme 5.9** Synthesis of Bz-Bu-Oxy. Reagents and conditions: (i) NaNO<sub>2</sub>, AgNO<sub>3</sub>, AcOH, 70%; (ii) BzCl, pyridine, 65%.

The crystal structure of Bz-Bu-Oxy (Figure 5.16) shows that the stereochemistry about the C=N double bond is *Z*, matching that of Bz-Oxy.

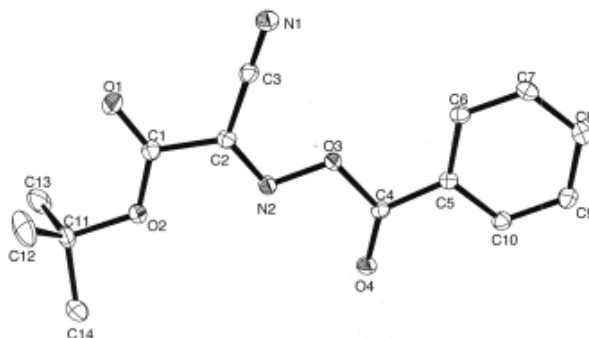
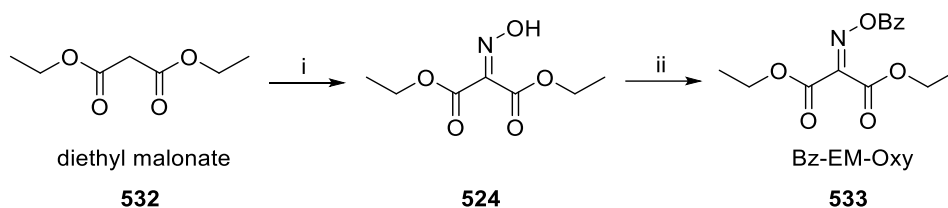


**Figure 5.16** ORTEP representation of the single molecule structure of Bz-Bu-Oxy determined by X-ray crystallography. The X-ray structure was obtained by Prof. Jonathan White.

#### 5.8.2.4 Benzoyl diethyl-malonateoxime (Bz-EM-Oxy) **533**

The cyano group in Oxyma was replaced with an ethoxycarbonyl moiety. EM-Oxy **524** was prepared by reacting diethyl malonate with sodium nitrite in acetic acid. Treatment of **524** with BzCl in triethylamine afforded Bz-EM-Oxy<sup>§</sup> **533** (Scheme 5.10).<sup>216</sup>

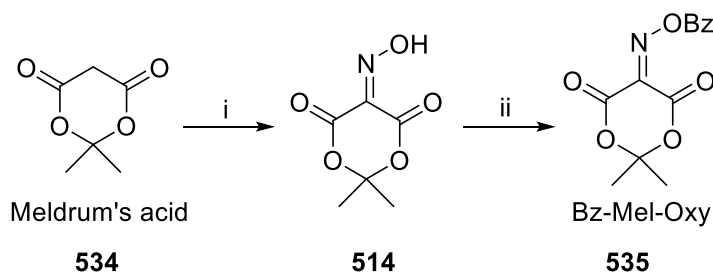
<sup>§</sup> This sequence was performed by Seep Arora.



**Scheme 5.10.** Synthesis of of Bz-EM-Oxy. Reagents and conditions: (i)  $\text{NaNO}_2$ ,  $\text{AcOH}$ , 84%; (ii)  $\text{BzCl}$ ,  $\text{Et}_3\text{N}$ , 78%.

#### 5.8.2.5 Benzoyl-Meldrum's acid oxime (Bz-Mel-Oxy, 535)

An oxime of Meldrum's acid would represent a cyclic oxime with two carbonyl groups as EWGs. Mel-Oxy **514** was prepared by treating Meldrum's acid **534** with sodium nitrite and methanol.<sup>207</sup> Oxime **514** was benzoylated using benzoic anhydride to give **535**\*\* (Scheme 5.11).



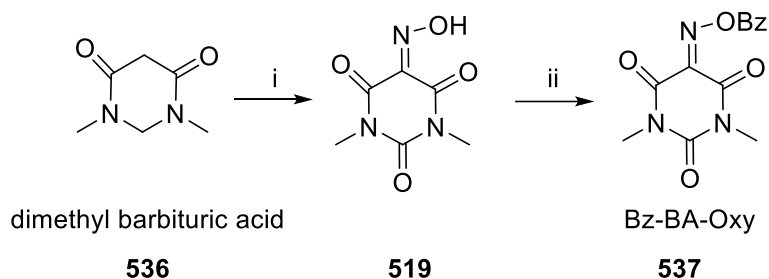
**Scheme 5.11** Preparation of Bz-Mel-Oxy. Reagents and conditions: (i)  $\text{NaNO}_2$ ,  $\text{MeOH}$ , 85%; (ii)  $\text{Bz}_2\text{O}$ ,  $\text{Et}_2\text{O}$ , 80%.

#### 5.8.2.6 Benzoyl-dimethyl barbituric acid oxime (Bz-BA-Oxy, 537)

BA-Oxy was prepared by treating dimethyl barbituric acid **536** with a solution of sodium hydroxide in methanol, followed by sodium nitrite and acetic acid (Scheme 5.12). Oxime **519** was benzoylated using benzoic anhydride in dry diethyl ether to afford **537**.<sup>208</sup>

---

\*\* This sequence was performed by Seep Arora.



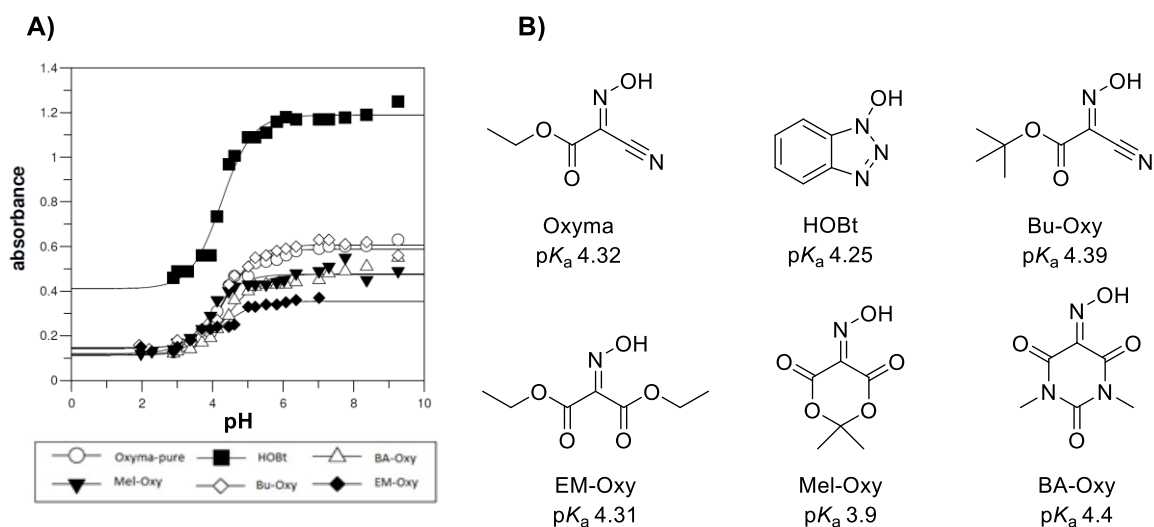
**Scheme 5.12** Preparation of Bz-BA-Oxy. Reagents and conditions: (i) (a) NaOH, MeOH; (b) NaNO<sub>2</sub>, MeOH, 66%; (ii) Bz<sub>2</sub>O, Et<sub>2</sub>O, 83%.

### 5.8.3 p*K*<sub>a</sub> values of the oximes

Acid dissociation constants indicate the extent of ionization of molecules in solution at different pH values and correlate to nucleofugacity: the weaker the conjugate base, the better the leaving group. While simple oximes possess p*K*<sub>a</sub> values of 8.3-11.8,<sup>217</sup> Oxyma is characterized by the presence of strongly electron-withdrawing cyano and ethoxycarbonyl groups. The p*K*<sub>a</sub> value of Oxyma is reported to be 4.6, matching that reported for HOBT.<sup>205</sup>

The p*K*<sub>a</sub> values of some of these oximes have been reported. However, owing to the range of different solvents used for these studies we were unable to directly compare the values of various oximes, and for comparison purposes, we required values for several compounds that had not previously been reported. Consequently, we measured the p*K*<sub>a</sub> values for the series of compounds by spectrophotometric titration of the oximes in a solution in 95% MeCN in water (Figure 5.18) in wavelength range of 220 to 330 nm. A plot of variation of absorbance against the pH values at a specific wavelength range of 220-320 nm resulted in a sigmoid curve. The inflection point of the sigmoid curve gave the p*K*<sub>a</sub> of the compound under investigation. The p*K*<sub>a</sub> values for the series of oximes fell within the range 3.96-4.39, and under these conditions the p*K*<sub>a</sub> value of HOBT was determined to be 4.25. The narrow range of these results was surprising. Based solely on these measured p*K*<sub>a</sub> values, it would be expected that the oximes should possess similar

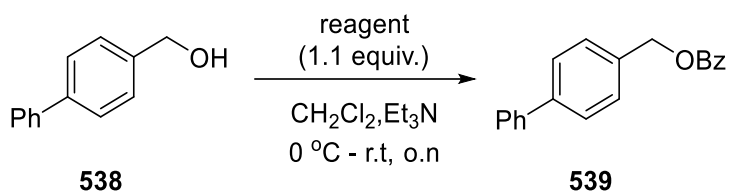
intrinsic leaving group ability, and thus that the benzoylated oximes should display similar reactivity.



**Figure 5.17** A) Spectrophotometric titration curves for the series of oximes; B)  $pK_a$  values of the reagents.

#### 5.8.4 Initial screening of the reagents with a primary alcohol

The benzoylating efficiency of the oxime based reagents was investigated by studying their reaction with 4-phenylbenzyl alcohol **538**, a simple primary alcohol. Alcohol **538** was chosen as a model substrate owing to its crystallinity, easy detectability due to the presence of a chromophore, and its availability in dry form. The alcohol was treated with 1.1 equivalents of the reagent in the presence of triethylamine as base. The reagents were added at 0 °C and the solution was stirred overnight, with warming to room temperature. Workup, followed by flash chromatography afforded the benzoate **539** as a white crystalline solid. These results are shown in table 5.2.

**Table 5.2** Yields of the benzoate esters with BBTZ and oxime-based reagents.

entry	reagent	yield (%) <sup>a</sup>
1	BBTZ <b>502</b>	100
2	Bz-Oxy <b>525</b>	80 (95) <sup>b</sup>
3	Bz-Bu-Oxy <b>531</b>	98
4	Bz-MN-Oxy <b>528</b>	95
5	Bz-EM-Oxy <b>533</b>	50 <sup>c</sup>
6	Bz-Mel-Oxy <b>535</b>	2
7	Bz-BA-Oxy <b>537</b>	15

<sup>a</sup> Reactions performed using Et<sub>3</sub>N as received. <sup>b</sup> Reaction using Et<sub>3</sub>N dried by distillation over CaH<sub>2</sub>. <sup>c</sup>Yield after 5 days. At this time the reaction still contained unreacted starting materials.

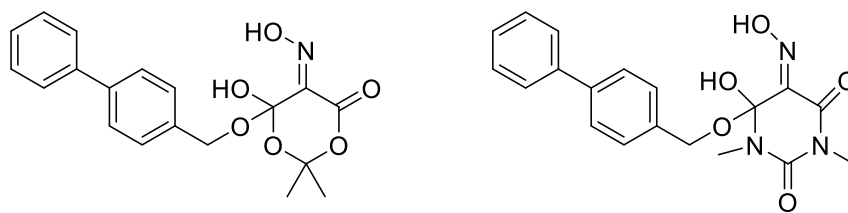
BBTZ resulted in a quantitative yield of the benzoate **539**, highlighting the impressive reactivity of the reagent (Table 5.2, entry 1). Treatment with Bz-Oxy afforded the product in 80% yield (entry 2). However, a better yield (95%) could be obtained by using dry Et<sub>3</sub>N. Hence, we suspect that this reagent is highly sensitive to water and may lead to unwanted side reactions. While traces of byproducts were isolated, the NMR spectra were deceptively simple and unrevealing of their structures; unsuccessful efforts were made to obtain a crystal structure of the byproducts in an attempt to better

understand the reaction.

Despite the formation of by-products (as detected by tlc), Bz-MN-Oxy and Bz-Bu-Oxy formed the benzoate in excellent yields of 95% and 98%, respectively (entries 3, 4). The reaction with Bz-EM-Oxy was very slow and afforded the product in only 50% yield after 5 days at room temperature (entry 5). The poor reactivity is at odds with the  $pK_a$  value of the conjugate acid of the leaving group; however, we highlight that Bz-EM-Oxy is the only non-crystalline compound of the series and we speculate that the two ethoxycarbonyl groups  $\alpha$ - to the oxime cause steric distortion of the system, affecting its conjugation and possibly attenuating its reactivity. In the case of the Meldrum's acid derived Bz-Mel-Oxy, tlc analysis revealed rapid consumption of the reagent yet little product formation (2%, entry 6); it appears likely that nucleophilic attack at the dioxanedione carbonyl groups results in fragmentation of the reagent

Bz-BA-Oxy afforded the benzoate, **539** in 15% yield (entry 7). The byproduct was tentatively assigned the structure shown in Figure 5.18 based on  $^1\text{H}$  NMR and mass spectrometric analysis.  $^1\text{H}$  NMR spectroscopy showed characteristic peaks at  $\delta$  3.01 and 3.05 ppm corresponding to the two methyl groups and singlets at  $\delta$  5.29 and 5.41 ppm, corresponding to the  $\text{CH}_2$  of the biphenyl alcohol and the benzyl protons at  $\delta$  7.42–7.85 ppm. Additionally, a peak at  $m/z$  383.14, on the ESI-TOF mass spectrum led us to propose the structure of adduct as shown below in Figure 5.18. Though we could not derive a conclusive structure of the byproducts of Bz-Mel-Oxy **535**, we propose that it could be similar to that with the BA-Bz-Oxy derivative

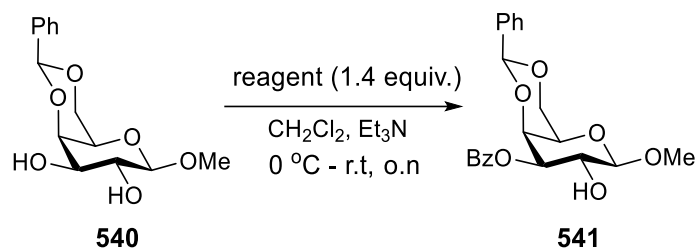




**Figure 5.18** Proposed structures of the byproduct formed from the reaction of Bz-BA-Oxy with **538** and Bz-Mel-Oxy with **538**.

### 5.8.5 Selective benzylation of carbohydrate alcohols

Having identified Bz-Oxy, Bz-MN-Oxy and Bz-Bu-Oxy as the most promising reagents, we next sought to investigate the selective acylation of carbohydrate diols. We started our exploration with methyl 4,6-*O*-benzylidene- $\beta$ -D-galactopyranoside **540**. Typically, good acylation selectivity is observed for its 3-hydroxyl owing to its *cis*-disposed vicinal oxygen, which is believed to result from the presence of an intramolecular hydrogen bond that enhances its reactivity.<sup>211</sup> Using the optimum protocol identified from the above simple benzylation, the benzylation of this galactoside was studied. Consistent with literature yields treatment of galactoside with BBTZ provided a quantitative yield of the 3-benzoate **541** (Table 5.3, entry 1). The oxime based reagents gave yields ranging from 68–90% (entries 2-7). Tlc showed unconsumed starting material, hence we increased the amount of reagent from 1.1 equivalents to 1.4 equivalents, which resulted in improved yields, Bz-Oxy and Bz-Bu-Oxy (entries 3,7) performing on par with BBTZ. Use of dry Et<sub>3</sub>N also enhanced the yields, again emphasizing the moisture sensitivity of not just Bz-Oxy but also other reagents as well. These results indicate that these oxime-based reagents can selectively protect the hydroxyl groups in a polyhydroxylated molecule in yields comparable to BBTZ, but require a greater excess of reagent.

**Table 5.3** Yields of the selective benzylation with BBTZ and oxime-based reagents.

entry	Reagent	Equiv.	yield (%) <sup>a</sup>
1	BBTZ <b>502</b>	1.1	100
2	Bz-Oxy <b>525</b>	1.1	90
3	Bz-Oxy <b>525</b>	1.4	100/ 89 <sup>a</sup>
4	Bz-MN-Oxy <b>528</b>	1.1	72/ 68 <sup>a</sup>
5	Bz-MN-Oxy <b>528</b>	1.4	90 <sup>a</sup>
6	Bz-Bu-Oxy <b>531</b>	1.1	90
7	Bz-Bu-Oxy <b>531</b>	1.4	100 <sup>a</sup>

a: used  $\text{Et}_3\text{N}$  from bottle without drying

We next explored acylation of methyl 4,6-O-benzylidene- $\alpha$ -D-glucopyranoside **542**. Kim *et al.* reported that treatment of **542** with 1.0 equivalents of BBTZ for five hours at room temperature afforded the 2-benzoate **543** in 90% yield.<sup>196</sup> When we repeated the same protocol, we obtained the 2-benzoate in a yield of only 75%. Using our optimized protocol from above using 1.1 equiv of BBTZ, we obtained an 87% yield. Under the same protocol, the three nitrile-containing oximes gave marginally lower yields (75-83%) (Table 5.4,

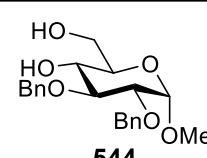
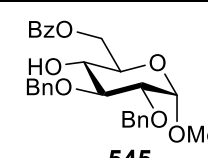
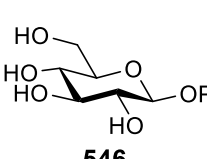
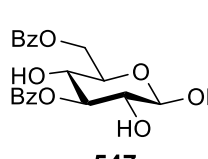
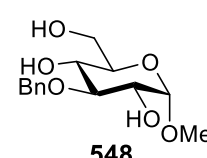
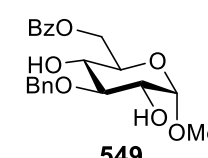
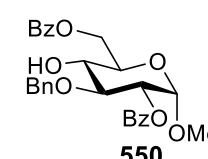
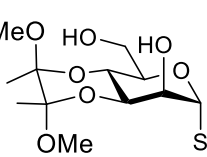
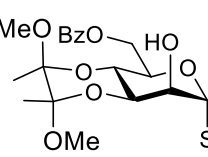
entry 2-7), with the best result obtained for the Oxyma-derived reagent, Bz-Oxy (83%, entry 2). Increasing the amount of Bz-Oxy to 1.4 equivalents afforded the 2-benzoate in 89% yield (entry 3), commensurate with that obtained using 1.1 equivalents of BBTZ. Bz-MN-Oxy and Bz-Bu-Oxy (entries 5 and 7) afforded yields slightly better than BBTZ when 1.4 equiv. was used. We therefore conclude that the nitrile-based reagents are effective for selective acylation of diols, with the Oxyma-derived reagent Bz-Oxy the most promising owing to its lower cost and ease of preparation.

**Table 5.4** Yields of the selective benzylation with BBTZ and oxime-based reagents.

Entry	Reagent	equiv	yield (%)
1	BBTZ <b>502</b>	1.1	87
2	Bz-Oxy <b>525</b>	1.1	83
3	Bz-Oxy <b>525</b>	1.4	89
4	Bz-MN-Oxy <b>528</b>	1.1	80
5	Bz-MN-Oxy <b>528</b>	1.4	93
6	Bz-Bu-Oxy <b>531</b>	1.1	75
7	Bz-Bu-Oxy <b>531</b>	1.4	93

We ventured into exploring an array of polyhydroxylated carbohydrate examples using Bz-Oxyma. We studied the selectivity for a primary versus a secondary alcohol using the polyhydroxylated substrates shown in Table 5.5. Benzoylation of methyl 2,3 di-*O*-benzyl- $\alpha$ -D-glucopyranoside **544**, a 4,6-diol, afforded the 6-benzoate **545** in 86% yield (entry 1). 4-methylphenyl 3,4-*O*-(2',3'-dimethoxybutan-2',3'-diyl)-1-thio- $\alpha$ -D-mannopyranoside **551** afforded the 6-benzoate **552** in 50% yield (entry 5). Treatment of methyl 3-*O*-benzyl- $\alpha$ -D-glucopyranoside **548** with 1.4 equiv. of Bz-Oxy afforded the 6-benzoate **549** in 93% yield (entry 3). However treatment with 2.8 equivalents of the reagent afforded 2,6-dibenzoate **550** in 41% (entry 4), with greater reactivity of the 2-position relative to the 4-position, a result of the *cis*-relationship with the anomeric oxygen. Disappointingly when 2.2 equiv. of the reagent was reacted with methyl  $\beta$ -D-mannopyranoside or methyl  $\beta$ -D-galactopyranoside, the di-benzoates were obtained as an inseparable mixture in poor yield (not shown in the table). Finally, treatment of a tetraol, phenyl 3,6-di-*O*-benzoyl- $\beta$ -D-glucopyranoside **546** with 2.2 equiv. of Bz-Oxyma provided the 3,6-dibenzoate **547** in 55% yield (entry 2).

**Table 5.5** Selective benzylation of carbohydrate alcohols using Bz-Oxy\*.

entry	equiv.	starting material	product	yield (%)
1	1.4	 <b>544</b>	 <b>545</b>	86
2	2.2	 <b>546</b>	 <b>547</b>	55
3	1.4	 <b>548</b>	 <b>549</b>	93
4	2.8	<b>548</b>	 <b>550</b>	41
5	1.4	 <b>551</b>	 <b>552</b>	50

\*Reactions were performed using the indicated equivalent of reagent, 1.2-fold of dry Et<sub>3</sub>N in dry CH<sub>2</sub>Cl<sub>2</sub>, 0 °C to r.t overnight.

## 5.9 Summary and Conclusions

We have developed a series of oxime-based reagents by changing the EWG at the  $\alpha$ -position. These were converted to their benzoate esters, which were screened for their benzoylating efficiency using the simple alcohol 4-phenylbenzyl alcohol. By-products were observed with all the reagents, but in only one case were we able to assign a structure to a byproduct, which revealed reaction at a site other than the oxime-ester; it seems likely

that the unidentified by-products from the other reagents also result from reaction at a remote site.

Based on the yields for benzoylating 4-phenylbenzyl alcohol, the most-promising reagents, Bz-Oxy, Bz-MN-Oxy and Bz-Bu-Oxy were investigated for their efficiency to selectively benzoylate methyl 4,6-*O*-benzylidene- $\alpha$ -D-glucopyranoside. While Bz-MN-Oxy and Bz-Bu-Oxy gave the best yields, the yield achieved with Bz-Oxy was slightly lower. However, as Bz-Oxy is comparatively easier and more cost effective to synthesize, we elected to investigate the efficiency of Bz-Oxy on a wider range of polyhydroxylated substrates. Bz-Oxy exhibited good selectivity between a primary and secondary hydroxyl group; between an equatorial and axial hydroxyl; and for equatorial hydroxyls with a *cis* oxygen atom. In conclusion, the oxime-based reagents represent safer alternatives to HOBt-based BBTZ, and exhibit good chemo- and regio-selectivity comparable to BBTZ but require a greater excess of the reagent to achieve equivalent results.

## 5.10 Experimental

### General

IR spectra were obtained as thin films or solids on a Fourier-transform attenuated total reflectance infrared spectrophotometer equipped with a diamond-coated zinc selenide sample accessory. High resolution mass spectra (HRMS) were obtained by ionizing samples using electro-spray ionization (ESI) and a time-of-flight mass analyzer. Oxyma (ethyl hydroximino cyanoacetate) was purchased from Sigma-Aldrich. The synthesis of various oximes and oxime benzoates has been reported previously.

### Ethyl benzoyloximino cyanoacetate (Bz-Oxy 525)

A mixture of benzoic anhydride (2.21 g, 8.44 mmol) and Oxyma **511** (1.00 g, 7.04 mmol) in dry diethyl ether (25 mL) was stirred at room temperature for 1 min. The resulting

precipitate was filtered and washed with cold petroleum ether to afford the product as a white crystalline powder (1.50 g, 90%), m.p. 99.3 °C (lit.<sup>218</sup> 100 °C); <sup>1</sup>H NMR (CDCl<sub>3</sub>, 400 MHz) δ 1.43 (3 H, t, *J* 7.1 Hz, CH<sub>3</sub>), 4.50 (2 H, q, *J* 7.1 Hz, CH<sub>2</sub>), 7.54–8.21 (5 H, m, Ph); <sup>13</sup>C NMR (CDCl<sub>3</sub>, 100 MHz) 14.1 (CH<sub>3</sub>), 64.6 (CH<sub>2</sub>), 107.1 (C=N), 125.8 (C≡N), 129.2, 130.6, 131.7, 135.2 (Ph), 157.0 (C=O), 160.7 (C=O); IR ν 2988.1, 2200.2, 1776.1, 1752.3, 1599.1, 1583.7, 1451.9, 1368.7, 1297.3, 1233.3, 1179.0, 1146.7, 1110.4, 1077.1, 1031.0, 996.2, 904.4, 837.5, 801.6, 764.9, 709.2, 666.5 cm<sup>-1</sup>; HRMS [M+Na]<sup>+</sup> calcd for C<sub>12</sub>H<sub>10</sub>N<sub>2</sub>O<sub>4</sub>Na *m/z* 269.0533, found 269.0532.

#### **(Benzoyloxy)carbonimidoyl dicyanide 528**

A solution of sodium nitrite (5.73 g, 8.30 mmol) in water (25 mL) was added to a solution of malanonitrile (5.00 g, 75.60 mmol) in acetic acid (15 mL) and water (15 mL) at 0 °C. The solution was stirred at room temperature for 12 h in the dark. A solution of AgNO<sub>3</sub> (12.91 g, 76.50 mmol) in water (25 mL) was added and stirred for 30 min. The resulting yellow precipitate was collected by filtration, washed with cold petroleum ether, and dried under vacuum (15.20g, 99%). BzCl (3.16ml, 27.23 mmol) was added to a stirred solution of the yellow precipitate (5.00 g, 25.75 mmo) in toluene (37.5 mL). A drop of pyridine was added to the solution resulting in the rapid formation of a white precipitate. Stirring was continued for another 30 min and then the precipitate was collected by filtration. The filtrate was concentrated and the residue recrystallized from ether/petroleum ether to afford **528** as a white crystalline solid (3.21 g, 64%); m.p. 102-104.3 °C, lit.<sup>218</sup> 104-106 °C ; <sup>1</sup>H NMR (CDCl<sub>3</sub>, 400 MHz) δ 7.55–8.21 (5 H, m, Ph); <sup>13</sup>C NMR (CDCl<sub>3</sub>, 100 MHz) δ 107.4, 125.7, 128.9, 130.3, 132.6, 134.8, 155.2, 160.6; HRMS [M+Na]<sup>+</sup> calcd for C<sub>10</sub>H<sub>5</sub>N<sub>3</sub>O<sub>2</sub>Na 222.0274, found 222.0276.

#### ***t*-Butyl benzoyloximino cyanoacetate 531**

A solution of sodium nitrite (2.93 g, 42.5 mmol) in water (13 mL) was added to a solution of *t*-butyl cyanoacetate **529** (2.00 g, 14.1 mmol) in acetic acid (6 mL) and water (6 mL) at 0 °C. The solution was stirred at room temperature for 12 h in the dark. A solution of AgNO<sub>3</sub> (2.40 g, 14.1 mmol) in water (13 mL) was added and stirred for 30 min. The resulting yellow precipitate was collected by filtration, washed with cold petroleum ether, and dried under vacuum (3.57 g, 70%). BzCl (0.554 g, 3.94 mmol) was added to a stirred solution of the yellow precipitate (1.00 g, 3.58 mmol) in toluene (7.5 mL). A drop of pyridine was added to the solution resulting in the rapid formation of a white precipitate. Stirring was continued for another 30 min and then the precipitate was collected by filtration. The filtrate was concentrated and the residue recrystallized to afford **531** as a white crystalline solid (0.62 g, 65%), m.p. 72.5–73.5 °C (ether/petroleum ether); <sup>1</sup>H NMR (CDCl<sub>3</sub>, 400 MHz) δ 1.63 (9 H, s), 7.55–8.21 (5 H, m, Ph); <sup>13</sup>C NMR (CDCl<sub>3</sub>, 100 MHz) 27.0, 87.4, 107.4, 125.7, 128.9, 130.3, 132.6, 134.8, 155.2, 160.6; IR ν 3679.5, 2984.8, 2938.9, 2844.3, 2238.0, 1978.2, 1928.0, 1841.7, 1778.1, 1730.8, 1598.1, 1449.1, 1347.5, 1259.5, 1224.9, 1175.7, 1141.2, 1028.8, 989.8, 901.6, 843.0, 701.9, 665.7 cm<sup>-1</sup>; HRMS [M+Na]<sup>+</sup> calcd for C<sub>14</sub>H<sub>14</sub>N<sub>2</sub>O<sub>4</sub>Na *m/z* 297.0846, found 297.0847.

#### **Benzoate ester of isonitroso Meldrum's acid 535**

Isonitroso Meldrum's acid **534** was synthesized according to literature.<sup>207</sup> **534** (0.500 g, 2.89 mmol) was dissolved in CH<sub>2</sub>Cl<sub>2</sub> (7 mL) and Et<sub>3</sub>N (0.44 mL, 3.16 mmol) was added, followed by addition of BzCl (0.34 mL, 2.9 mmol). The solution was stirred for 1 h, then diluted with CH<sub>2</sub>Cl<sub>2</sub> (35 mL) and stirred for another 5 min. The solution was washed with water (2 × 20 mL), dried (MgSO<sub>4</sub>), filtered and concentrated under reduced pressure. Flash chromatography (5-10% EtOAc/petroleum ether) afforded **535** as a brown solid (1.50 g, 70%), m.p. 108.5–109 °C; <sup>1</sup>H NMR (CDCl<sub>3</sub>, 400 MHz) δ 1.87 (6 H, s, CH<sub>3</sub>),



7.55–8.27 (5 H, m, Ph);  $^{13}\text{C}$  NMR ( $\text{CDCl}_3$ , 100 MHz) 28.4, 46.0, 106.8, 126.2, 129.0, 129.2, 130.7, 131.0, 134.6, 135.1, 139.2, 150.9, 155.7, 161.3, 162.5; IR  $\nu$  3750.7, 2943.4, 1778.5, 1749.4, 1589.9, 1556.2, 1493.8, 1453.1, 1396.4, 1384.2, 1293.3, 1264.7, 1230.0, 1198.3, 1181.8, 1159.3, 1055.4, 1032.0, 1011.9, 982.3, 969.9, 949.0, 930.9, 891.0, 864.9, 798.8, 739.0, 701.8, 677.7, 667.1  $\text{cm}^{-1}$ ; HRMS  $[\text{M}+\text{Na}]^+$  calcd for  $\text{C}_{13}\text{H}_{11}\text{NO}_6\text{Na}$   $m/z$  300.0479, found 297.0478.

### **Benzoate ester of isonitroso dimethylbarbituric acid 537**

Isonitroso dimethyl barbituric acid **536** was synthesized according to literature.<sup>208</sup> Benzoic anhydride (0.70 g, 2.97 mmol) was added to a solution of **536** (0.500 g, 2.70 mmol) in dry  $\text{Et}_2\text{O}$  (12.5 mL) and the solution was stirred overnight at room temperature. The resulting precipitate was filtered and washed with cold petroleum ether. The product was obtained as a green solid (0.65 g, 83%), m.p. 218.5–219 °C;  $^1\text{H}$  NMR ( $\text{CDCl}_3$ , 400 MHz)  $\delta$  3.45 (3 H, s,  $\text{CH}_3$ ), 3.47 (3 H, s,  $\text{CH}_3$ ), 7.54–8.33 (5 H, m, Ph);  $^{13}\text{C}$  NMR ( $\text{CDCl}_3$ , 100 MHz) 29.0, 29.5, 31.0, 126.5, 129.1, 130.9, 134.9, 161.7; IR  $\nu$  3000.1, 1949.2, 1773.7, 1686.0, 1447.8, 1367.7, 1283.3, 1234.9, 1070.9, 1014.7, 994.2, 970.3, 924.2, 866.2, 793.4, 746.3, 716.5  $\text{cm}^{-1}$ ; HRMS  $[\text{M}+\text{Na}]^+$  calcd for  $\text{C}_{13}\text{H}_{11}\text{N}_3\text{O}_5\text{Na}$   $m/z$  312.0591, found 312.0595.

### **Protocol for benzylation of 4-phenylbenzyl alcohol**

A mixture of 4-phenylbenzyl alcohol (0.100 g, 0.542 mmol), 1.1 equivalents of the benzoylating reagent and  $\text{Et}_3\text{N}$  (0.091 mL, 0.650 mmol) in dry  $\text{CH}_2\text{Cl}_2$  (3.0 mL) at 0 °C was stirred overnight. The solution was diluted with  $\text{CH}_2\text{Cl}_2$ , washed with water ( $2 \times 20$  mL), dried ( $\text{MgSO}_4$ ), filtered and concentrated under reduced pressure. The residue was purified by flash chromatography (10–15%  $\text{EtOAc}$ /petroleum ether) to afford 4-phenylbenzyl benzoate as a white solid, m.p. 62–63 °C (lit.<sup>219</sup> 61.5–62.5 °C);  $^1\text{H}$  NMR

(CDCl<sub>3</sub>, 400 MHz)  $\delta$  5.42 (2 H, s, CH<sub>2</sub>), 7.34–8.12 (15 H, m, Ph); <sup>13</sup>C NMR (CDCl<sub>3</sub>, 100 MHz) 66.6 (CH<sub>2</sub>), 127.2, 127.5, 127.6, 128.5, 128.9, 129.8, 130.2, 133.2, 135.1, 140.8, 141.3 (Ph), 166.6 (C=O); HRMS [M+Na]<sup>+</sup> calcd for C<sub>20</sub>H<sub>16</sub>O<sub>2</sub>Na *m/z* 311.1043, found 311.1042.

**Characterization data for adduct of benzoate ester of isonitroso dimethylbarbituric acid and 4-phenylbenzyl alcohol**

<sup>1</sup>H NMR (CDCl<sub>3</sub>, 400 MHz)  $\delta$  3.01 (3 H, s, Me), 3.05 (3 H, s, Me), 5.29 (1 H, d, *J* 12 Hz, CH<sub>2</sub>), 5.41 (1 H, d, *J* 12 Hz, CH<sub>2</sub>), 7.42–7.85 (14 H, m, 2 × Ph, C<sub>6</sub>H<sub>4</sub>); <sup>13</sup>C NMR (CDCl<sub>3</sub>, 100 MHz)  $\delta$  25.54, 26.15, 69.32, 82.3, 126.4, 127.2, 127.3, 127.4, 127.6, 127.7, 128.5, 128.8, 128.9, 129.0, 129.4, 129.2, 129.4, 132.8, 134.1, 140.4, 142.2, 155.9, 162.3, 164.8, 166.3; HRMS [M+H]<sup>+</sup> calcd for C<sub>26</sub>H<sub>23</sub>N<sub>3</sub>O<sub>6</sub> *m/z* 474.1620, found 474.1659

**Methyl 3-*O*-benzoyl 4,6-*O*-benzylidene- $\beta$ -D-galactopyranoside **541**<sup>219</sup>**

A mixture of methyl 4,6-*O*-benzylidene- $\beta$ -D-galactopyranoside **540** (0.100 g, 0.354 mmol), benzoylating reagent (1.1 equivalent), and Et<sub>3</sub>N (0.060 mL, 0.42 mmol) in dry CH<sub>2</sub>Cl<sub>2</sub> (3.0 mL) at 0 °C was stirred overnight. The solution was diluted with CH<sub>2</sub>Cl<sub>2</sub>, washed with water (2 × 20 mL), dried (MgSO<sub>4</sub>), filtered and concentrated under reduced pressure. Flash chromatography (75–85 % EtOAc/petroleum ether) of the residue afforded the 3-benzoate **541** as a white solid, m.p. 163–164 °C (lit.<sup>220</sup> m.p. 166–167 °C); [ $\alpha$ ]<sub>D</sub> +94 (*c* 1.0, CHCl<sub>3</sub>; lit.<sup>220</sup> [ $\alpha$ ]<sub>D</sub> +95); <sup>1</sup>H NMR (CDCl<sub>3</sub>, 400 MHz)  $\delta$  2.34 (1 H, d, *J* 2.4 Hz, OH), 3.60–3.62 (4 H, m, H5,CH<sub>3</sub>), 4.11 (1 H, dd, *J*<sub>5,6</sub> 12.5, *J*<sub>6,6</sub> 1.7 Hz, H6), 4.18 (1 H, ddd, *J*<sub>2,3</sub> 10.1, *J*<sub>1,2</sub> 7.8, *J*<sub>2-OH</sub> 2.5 Hz, H2), 4.41–4.36 (2 H, m, H1,6), 4.51 (1 H, dd, *J*<sub>3,4</sub> 3.6 *J*<sub>4,5</sub> 10.2 Hz, H4), 5.15 (1 H, dd, *J*<sub>3,4</sub> 3.7, *J*<sub>2,3</sub> 10.1 Hz, H3), 5.53 (1 H, s, PhCH), 7.29–8.12 (10 H, m, Ph); <sup>13</sup>C NMR (CDCl<sub>3</sub>, 100 MHz) 57.4 (CH<sub>3</sub>), 66.7, 68.9, 69.1, 73.7,

74.3, 100.9, 104.2 (C1), 126.2, 128.1, 128.5, 128.9, 129.8, 130.0, 133.4, 137.7 (Ph), 166.6 (C=O); HRMS [M+H]<sup>+</sup> calcd for C<sub>21</sub>H<sub>22</sub>O<sub>7</sub>Na *m/z* 409.1254, found 409.1254.

**Methyl 2-*O*-benzoyl 4,6-*O*-benzylidene- $\alpha$ -D-glucopyranoside 543**<sup>196</sup>

A mixture of methyl 4,6-*O*-benzylidene- $\alpha$ -D-glucopyranoside **542** (0.100 g, 0.354 mmol), 1.4 equivalents of the benzoylating reagent and Et<sub>3</sub>N (0.060 mL, 0.415 mmol) in dry CH<sub>2</sub>Cl<sub>2</sub> (3.0 mL) at 0 °C was stirred overnight. The solution was diluted with CH<sub>2</sub>Cl<sub>2</sub>, washed with water (2 × 20 mL), dried (MgSO<sub>4</sub>), filtered and concentrated under reduced pressure. Flash chromatography (25–35 % EtOAc/petroleum ether) of the residue afforded the 2-benzoate **543** as a white solid, m.p. 169–170 °C (lit.<sup>196</sup> 169–170 °C); [ $\alpha$ ]<sub>D</sub> +108 (*c* 1.0, CHCl<sub>3</sub>; lit.<sup>196</sup> [ $\alpha$ ]<sub>D</sub> +107); <sup>1</sup>H NMR (CDCl<sub>3</sub>, 400 MHz)  $\delta$  2.57 (1 H, s, OH), 3.40 (3 H, s, CH<sub>3</sub>), 3.63 (1 H, t, *J*<sub>5,6a</sub> 9.8 Hz, H6), 3.80 (1 H, t, *J*<sub>6a,6b</sub> 10.3 Hz, H6), 3.91 (1 H, ddd, *J*<sub>5,6a</sub> 9.8, *J*<sub>4,5</sub> 9.8, *J*<sub>5,6b</sub> 4.7 Hz, H5), 4.34 (2 H, m, H3,4), 5.04 (1 H, dd, *J*<sub>2,3</sub> 9.5, *J*<sub>1,2</sub> 3.8 Hz, H2), 5.08 (1 H, d, *J*<sub>1,2</sub> 3.8 Hz, H1), 5.58 (1 H, s, PhCH), 7.36–8.13 (10 H, m, Ph); <sup>13</sup>C NMR (CDCl<sub>3</sub>, 100 MHz) 55.7 (CH<sub>3</sub>), 62.2, 69.0, 69.1, 74.2, 81.6, 97.9, 102.2 (C1), 126.4, 128.5, 128.6, 129.4, 130.1, 133.5, 137.1 (Ph), 166.3 (C=O); HRMS [M+H]<sup>+</sup> calcd for C<sub>21</sub>H<sub>22</sub>O<sub>7</sub>Na *m/z* 409.1257, found 409.1260.

**Methyl 2,3-di-*O*-benzyl-6-*O*-benzoyl- $\alpha$ -D-glucopyranoside 545**<sup>221</sup>

A mixture of Benzoyl-Oxyma (0.092 g, 0.374 mmol), methyl 2,3-di-*O*-benzyl- $\alpha$ -D-glucopyranoside<sup>221</sup> (0.100 g, 0.267 mmol) and Et<sub>3</sub>N (0.050 mL, 0.32 mmol) in dry CH<sub>2</sub>Cl<sub>2</sub> (3.0 mL) at 0 °C was stirred overnight. The solution was diluted with CH<sub>2</sub>Cl<sub>2</sub>, washed with water (2 × 20 mL), dried over (MgSO<sub>4</sub>), filtered and concentrated under reduced pressure. Flash chromatography (30–40% EtOAc/petroleum ether) of the residue afforded **27** (0.11 g, 86%), m.p 77–79 °C (lit.<sup>222</sup> 75–77 °C); [ $\alpha$ ]<sub>D</sub> +35 (*c* 0.25, CHCl<sub>3</sub>; lit.<sup>222</sup> [ $\alpha$ ]<sub>D</sub> +25); <sup>1</sup>H NMR (CDCl<sub>3</sub>, 400 MHz)  $\delta$  2.53 (1 H, d, *J* 2.9 Hz, OH), 3.40 (3 H, s, CH<sub>3</sub>), 3.53

(2 H, m, H4,5), 3.87 (2 H, m, H2,3), 4.51 (1 H, dd,  $J_{5,6a}$  12.1,  $J_{6a,6b}$  2.1 Hz, H6), 4.59–4.68 (3 H, m, H1,6,CH<sub>2</sub>), 4.77 (2 H, dd,  $J$  11.6, 10.3 Hz, CH<sub>2</sub>Ph), 5.01 (1 H, d,  $J$  11.3, CH<sub>2</sub>Ph), 7.28–8.02 (15 H, m, Ph); <sup>13</sup>C NMR (CDCl<sub>3</sub>, 100 MHz) 55.3, 63.8, 69.5, 70.2, 73.3, 75.7, 79.7, 81.3, 98.2 (C1), 128.0, 128.1, 128.2, 128.4, 128.6, 128.7, 129.8, 133.2, 138.0, 138.7 (Ph), 166.8 (C=O); HRMS [M+Na]<sup>+</sup> calcd for C<sub>28</sub>H<sub>30</sub>O<sub>7</sub>Na  $m/z$  501.1884, found 501.1886.

#### **Phenyl 3,6-di-*O*-benzoyl-β-D-glucopyranoside 547**

A mixture of Benzoyl-Oxyrna (0.210 g, 0.853 mmol), phenyl β-D-glucopyranoside (0.100 g, 0.390 mmol) and Et<sub>3</sub>N (0.060 mL, 0.468 mmol) in dry CH<sub>2</sub>Cl<sub>2</sub> (3.0 mL) at 0 °C was stirred overnight. The solution was diluted with CH<sub>2</sub>Cl<sub>2</sub>, washed with water (2 × 20 mL), dried (MgSO<sub>4</sub>), filtered and concentrated under reduced pressure. Flash chromatography (2–5 % acetone/CH<sub>2</sub>Cl<sub>2</sub>) of the residue afforded the product as a white solid (0.11 g, 55%), m.p 144 °C; [α]<sub>D</sub> +2.7 (*c* 0.5, CHCl<sub>3</sub>); <sup>1</sup>H NMR (CDCl<sub>3</sub>, 400 MHz) δ 2.81 (1 H, s, OH), 3.49 (1 H, s, OH), 3.83 (1 H, t,  $J$  9.3 Hz, H4), δ 2.81 (1 H, s, OH), 3.49 (1 H, s, OH), 3.83 (1 H, t,  $J_{3,4}$  9.3 Hz, H4), 3.90 (1 H, ddd,  $J_{4,5}$  9.7,  $J_{5,6a}$  6.1,  $J_{5,6b}$  2.3 Hz, H5), 4.00 (1 H, dd,  $J_{2,3}$  9.1,  $J_{1,2}$  8.0 Hz, H2), 4.63 (1 H, dd,  $J_{6a,6b}$  12.0,  $J_{5,6a}$  6.1 Hz, H6), 4.74 (1 H, dd,  $J_{6a,6b}$  12.0,  $J_{5,6b}$  2.3 Hz, H6), 5.07 (1 H, d,  $J_{1,2}$  7.7 Hz, H1), 5.33 (1 H, t,  $J_{2,3} = J_{3,4}$  9.1 Hz, H3), 7.07–8.08 (15 H, m, Ph); <sup>13</sup>C NMR (CDCl<sub>3</sub>, 100 MHz) 63.0, 69.7, 72.2, 74.6, 78.6 (C2,3,4,5), 101.0 (C1), 117.0, 123.2, 128.5, 128.6, 129.3, 129.6, 129.7, 129.9, 130.1, 133.4, 133.7, 157.0 (Ph), 166.9, 167.6 (C=O); HRMS [M+H]<sup>+</sup> calcd for C<sub>26</sub>H<sub>24</sub>O<sub>8</sub>Na  $m/z$  487.1363, found 487.1361.

#### **Methyl 3-*O*-benzyl 6-*O*-benzoyl-α-D-glucopyranoside 549**

A mixture of Benzoyl-Oxyrna (0.121 g, 0.491 mmol), methyl 3-*O*-benzyl-α-D-glucopyranoside (0.100 g, 0.351 mmol) and Et<sub>3</sub>N (0.060 mL, 0.421 mmol) in dry CH<sub>2</sub>Cl<sub>2</sub>

(3.0 mL) at 0 °C was stirred overnight. The solution was diluted with CH<sub>2</sub>Cl<sub>2</sub> washed with water (2 × 20 mL), dried over (MgSO<sub>4</sub>), filtered and concentrated under reduced pressure. Flash chromatography (40–50% EtOAc/petroleum ether) of the residue afforded as a white solid (0.13 g, 55%), m.p 70–71 °C; [ $\alpha$ ]<sub>D</sub> +88.0 (*c* 1.0, CHCl<sub>3</sub>); <sup>1</sup>H NMR (CDCl<sub>3</sub>, 400 MHz)  $\delta$  2.27 (1 H, d, *J* 8.3 Hz, OH), 2.83 (1 H, d, *J* 3.2 Hz, OH), 3.45 (3 H, s, CH<sub>3</sub>), 3.54 (1 H, dd, *J*<sub>3,4</sub> 8.4, *J*<sub>4,5</sub> 9.8 Hz, H4), 3.63 (1 H, dd, *J*<sub>3,4</sub> 8.4, *J*<sub>2,3</sub> 3.8 Hz, H3), 3.69 (1 H, ddd, *J*<sub>1,2</sub> 9.1, *J*<sub>2,3</sub> 3.8 Hz, H2), 3.87 (1 H, ddd, *J*<sub>5,6a</sub> 2.2, *J*<sub>5,6b</sub> 4.7, *J*<sub>4,5</sub> 9.8 Hz, H5), 4.52 (1 H, dd, *J*<sub>6a,6b</sub> 12.1, *J*<sub>5,6a</sub> 2.2 Hz, H6), 4.67 (1 H, dd, *J*<sub>6a,6b</sub> 12.1, *J*<sub>5,6b</sub> 4.7 Hz, H6), 4.77–4.83 (2 H, m, H1, CH<sub>2</sub>), 4.98 (1 H, d, *J* 11.4, CH<sub>2</sub>), 7.29–8.08 (10 H, m, Ph); <sup>13</sup>C NMR (CDCl<sub>3</sub>, 100 MHz) 55.4 (CH<sub>3</sub>), 63.7, 69.9, 69.9, 72.7, 75.3, 82.5, 99.6 (C1), 120.3, 128.1, 128.5, 128.7, 129.8, 129.8, 133.3, 138.5 (Ph), 167.0 (C=O); HRMS [M+H]<sup>+</sup> calcd for C<sub>21</sub>H<sub>24</sub>O<sub>7</sub> Na *m/z* 411.1414, found 411.1412.

### **Methyl 3-*O*-benzyl-2,6-di-*O*-benzoyl- $\alpha$ -D-glucopyranoside 550**

A mixture of Benzoyl-Oxyrna (0.194 g, 0.787 mmol), of methyl 3-*O*-benzyl- $\alpha$ -D-glucopyranoside <sup>223</sup> (0.080 g, 0.281 mmol) and Et<sub>3</sub>N (0.05 mL, 0.337 mmol) in dry CH<sub>2</sub>Cl<sub>2</sub> (3.0 mL) at 0 °C was stirred overnight. The solution was diluted with CH<sub>2</sub>Cl<sub>2</sub>, washed with water (2 × 20 mL), dried over (MgSO<sub>4</sub>), filtered and concentrated under reduced pressure. Flash chromatography (30–40% EtOAc/petroleum ether) of the residue afforded the product as a syrup (0.0600 g, 41%), [ $\alpha$ ]<sub>D</sub> +100.4 (*c* 0.5, CHCl<sub>3</sub>); <sup>1</sup>H NMR (CDCl<sub>3</sub>, 400 MHz)  $\delta$  3.42 (3 H, s, CH<sub>3</sub>), 3.72 (1 H, t, *J*<sub>3,4</sub> = *J*<sub>4,5</sub> 9.1 Hz, H4), 3.98 (1 H, ddd, *J*<sub>5,6a</sub> 2.2, *J*<sub>5,6b</sub> 4.4, *J*<sub>4,5</sub> 10.1 Hz, H5), 4.08 (1 H, t, *J*<sub>3,4</sub> = *J*<sub>2,3</sub> 9.0 Hz, H3), 4.56 (1 H, dd, *J*<sub>6a,6b</sub> 12.1, *J*<sub>5,6a</sub> 2.2 Hz, H6), 4.73–4.79 (2 H, m, H2,6), 4.88 (1 H, d, *J* 11.3 Hz, CH<sub>2</sub>Ph), 5.07–5.12 (2 H, m, H1, CH<sub>2</sub>Ph), 7.48–8.12 (10 H, m, Ph); <sup>13</sup>C NMR (CDCl<sub>3</sub>, 100 MHz) 55.4 (CH<sub>3</sub>), 63.6, 69.7, 70.4, 73.9, 75.5, 79.6, 82.5, 97.5, 99.6 (C1), 128.0, 128.1, 128.5,

128.6, 128.7, 129.7, 129.8, 129.9, 129.9, 130.2, 133.3, 133.4, 133.5, 138.1 (Ph), 160.0, 167.1 (C=O); HRMS [M+H]<sup>+</sup> calcd for C<sub>28</sub>H<sub>28</sub>O<sub>8</sub>Na *m/z* 515.1676 found 515.1668.

**4-Methylphenyl 3,4-*O*-(2',3'-dimethoxybutan-2',3'-diyl)-6-*O*-benzoyl-1-thio- $\alpha$ -D-mannopyranoside 552**

A mixture of Benzoyl-Oxy (0.036 g, 0.146 mmol), 3,4-di-*O*-(2,3-dimethoxybutane-2,3-diyl)- $\alpha$ -D-mannopyranoside **551** (0.042 g, 0.105 mmol), and Et<sub>3</sub>N (0.020 mL, 0.126 mmol) in dry CH<sub>2</sub>Cl<sub>2</sub> (3.0 mL) at 0 °C was stirred overnight. The solution was diluted with CH<sub>2</sub>Cl<sub>2</sub>, washed with water (2 × 20 mL), dried over (MgSO<sub>4</sub>), filtered and concentrated under reduced pressure. Flash chromatography (50–70% EtOAc/petroleum ether) of the residue afforded the product as a syrup (0.030 g, 50%), [ $\alpha$ ]<sub>D</sub> +167.8 (*c* 0.25, CHCl<sub>3</sub>); <sup>1</sup>H NMR (CDCl<sub>3</sub>, 400 MHz)  $\delta$  )  $\delta$  1.30 (3 H, s, CH<sub>3</sub>), 1.34 (3 H, s, CH<sub>3</sub>), 2.27 (3 H, s, CH<sub>3</sub>Ar), 3.17 (3 H, s, OCH<sub>3</sub>), 3.32 (3 H, s, OCH<sub>3</sub>), 4.07 (1 H, dd, *J*<sub>1,2</sub> 9.1, *J*<sub>2,3</sub> 3.0 Hz, H<sub>2</sub>), 4.18–4.22 (2 H, m, H<sub>3,6</sub>), 4.49 (1 H, ddd, *J*<sub>5,6a</sub> 11.9, *J*<sub>5,6b</sub> 6.1 Hz, H<sub>6</sub>), 4.55–4.65 (2 H, m, H<sub>4,5</sub>), 5.52 (1 H, s, H<sub>1</sub>), 6.98–8.01 (10 H, m, Ph); <sup>13</sup>C NMR (CDCl<sub>3</sub>, 100 MHz) 14.1 (CH<sub>3</sub>), 17.7 (CH<sub>3</sub>), 17.8, 21.2, 29.8, 48.1, 48.3, 63.0, 64.1, 64.7, 67.1, 69.7, 72.7, 87.1, 100.2, 100.5, 107.1, 125.8, 128.4, 128.54, 129.2, 129.7, 129.8, 130.0, 130.0, 130.7, 132.7, 133.1, 133.3, 135.3, 138.2, 157.1 (Ph), 160.7, 165.9, 166.4 (C=O); HRMS [M+H]<sup>+</sup> calcd for C<sub>26</sub>H<sub>32</sub>O<sub>8</sub>SNa *m/z* 527.1701 found 527.1705.

**X-ray crystallography (Solved by Prof. Jonathan white)**

Crystals of **Bz-Oxy** and **Bz-Bu-Oxy** were mounted in low temperature oil then flash cooled using an Oxford low temperature device. Intensity data were collected at 130 K on an Oxford SuperNova X-ray diffractometer with CCD detector using Cu-K $\alpha$  ( $\alpha$  = 1.54184 Å) radiation. Data were reduced and corrected for absorption. The structures were solved by direct methods and difference Fourier synthesis using the SHELX suite

of programs<sup>224</sup> as implemented within the WINGX software.<sup>225</sup> Thermal ellipsoid plots were generated using the program ORTEP-3.

Crystal data for **Bz-Oxy**:  $C_{12}H_{10}N_2O_4$   $M = 246.22$ ,  $T = 130.0(1)$  K,  $\lambda = 1.54184$ , monoclinic, space group  $P2_1/n$ ,  $a = 11.8867(1)$ ,  $b = 8.0556(1)$ ,  $c = 12.3853(1)$  Å,  $\beta = 99.064(1)$ ,  $V = 1171.14(2)$  Å<sup>3</sup>,  $Z = 4$ ,  $D_c = 1.396$  g cm<sup>-3</sup>,  $\mu(\text{Cu-K}\alpha) 0.904$  mm<sup>-1</sup>,  $F(000) = 512$ , crystal size  $0.49 \times 0.44 \times 0.32$  mm. 8000 reflections measured, 2434 independent reflections ( $R_{\text{int}} = 0.0170$ ), the final R was 0.0342 [ $I > 2 \sigma(I)$  2347 data] and  $wR(F^2)$  (all data) was 0.0966. CCDC deposition: 1406156.

Crystal data for **Bz-Bu-Oxy**:  $C_{14}H_{14}N_2O_4$   $M = 274.27$ ,  $T = 130.0(1)$  K,  $\lambda = 1.54184$  Å, monoclinic, space group  $P2_1/n$ ,  $a = 5.9020(1)$ ,  $b = 21.5230(3)$ ,  $c = 11.2041(2)$  Å,  $\beta = 102.073(2)^\circ$ ,  $V = 1391.76(4)$  Å<sup>3</sup>,  $Z = 4$ ,  $D_c = 1.309$  g cm<sup>-3</sup>,  $\mu(\text{Cu-K}\alpha) 0.813$  mm<sup>-1</sup>,  $F(000) = 576$ , crystal size  $0.50 \times 0.15 \times 0.06$  mm. 9619 reflections measured, 2897 independent reflections ( $R_{\text{int}} = 0.0299$ ), the final R was 0.0392 [ $I > 2 \sigma(I)$  2605 data] and  $wR(F^2)$  (all data) was 0.1018. CCDC deposition: 1406157.

### **Spectrophotometric titrations**

Dissociation constants ( $pK_a$  values) of the oximes or HOBt were measured spectrophotometrically using a Cary-50 Bio UV/Vis spectrophotometer in 95% (v/v) MeCN-water at wavelengths of 220-315 nm. Buffer solutions across the pH range of 2-10 were prepared by adding 0.2 M NaOH to a mixture of 0.04 M phosphoric acid, acetic acid, and boric acid. HOBt or oximes at 0.1 mM concentration were prepared in the buffer solutions and the absorbance measured. Each cuvette contained 50  $\mu$ l of 1 mM stock solution of oxime or HOBt in MeCN, 100  $\mu$ l of 40 mM buffer, and 1.85 mL of MeCN were used to obtain a final concentration of 0.025 mM of the reagent. Absorbances were

measured at the wavelength where the maximum difference between the absorbance of the oxime or HOBt, and its conjugate base.



## References

1. *World Health Forum* **1993**, *14*, 438.
2. *WHO Tuberculosis fact sheet No. 104* **2017**.
3. Rainczuk, A. K.; Yamaryo-Botte, Y.; Brammananth, R.; Stinear, T. P.; Seemann, T.; Coppel, R. L.; McConville, M. J.; Crellin, P. K., *J. Biol. Chem.* **2012**, *287*, 42726-38.
4. Knechel, N. A., *Crit. Care. Nurse* **2009**, *29*, 34-43.
5. Zumla, A.; Nahid, P.; Cole, S. T., *Nat. Rev. Drug Discov.* **2013**, *12*, 388-404.
6. Mangtani, P.; Abubakar, I.; Ariti, C.; Beynon, R.; Pimpin, L.; Fine, P. E. M.; Rodrigues, L. C.; Smith, P. G.; Lipman, M.; Whiting, P. F.; Sterne, J. A., *Clin. Infect. Dis.* **2014**, *58*, 470-480.
7. Uhlin, M.; Andersson, J.; Zumla, A.; Maeurer, M., *J. Infect. Dis.* **2012**, *205*, S325-34.
8. Li, L.; Bannantine, J. P.; Zhang, Q.; Amonsin, A.; May, B. J.; Alt, D.; Banerji, N.; Kanjilal, S.; Kapur, V., *Proc. Natl. Acad. Sci. USA* **2005**, *102*, 12344-9.
9. Richardson, M. B.; Smith, D. G.; Williams, S. J., *Chem. Commun.* **2017**, *53*, 1100-1103.
10. Lea-Smith, D. J.; Martin, K. L.; Pyke, J. S.; Tull, D.; McConville, M. J.; Coppel, R. L.; Crellin, P. K., *J. Biol. Chem.* **2008**, *283*, 6773-82.
11. Brosch, R.; Gordon, S. V.; Garnier, T.; Eglmeier, K.; Frigui, W.; Valenti, P.; Dos Santos, S.; Duthoy, S.; Lacroix, C.; Garcia-Pelayo, C.; Inwald, J. K.; Golby, P.; Garcia, J. N.; Hewinson, R. G.; Behr, M. A.; Quail, M. A.; Churcher, C.; Barrell, B. G.; Parkhill, J.; Cole, S. T., *Proc. Natl. Acad. Sci. USA* **2007**, *104*, 5596-601.
12. Stinear, T. P.; Seemann, T.; Harrison, P. F.; Jenkin, G. A.; Davies, J. K.; Johnson, P. D.; Abdellah, Z.; Arrowsmith, C.; Chillingworth, T.; Churcher, C.; Clarke, K.; Cronin, A.; Davis, P.; Goodhead, I.; Holroyd, N.; Jagels, K.; Lord, A.; Moule, S.; Mungall, K.; Norbertczak, H.; Quail, M. A.; Rabbinowitsch, E.; Walker, D.; White, B.; Whitehead, S.; Small, P. L.; Brosch, R.; Ramakrishnan, L.; Fischbach, M. A.; Parkhill, J.; Cole, S. T., *Genome Res.* **2008**, *18*, 729-41.
13. Seki, M.; Honda, I.; Fujita, I.; Yano, I.; Yamamoto, S.; Koyama, A., *Vaccine* **2009**, *27*, 1710-6.
14. Mohan, A.; Padiadpu, J.; Baloni, P.; Chandra, N., *Genome Announc.* **2015**, *3*, e01520-14.
15. Kalinowski, J.; Bathe, B.; Bartels, D.; Bischoff, N.; Bott, M.; Burkovski, A.; Dusch, N.; Eggeling, L.; Eikmanns, B. J.; Gaigalat, L.; Goesmann, A.; Hartmann, M.; Huthmacher, K.; Kramer, R.; Linke, B.; McHardy, A. C.; Meyer, F.; Mockel, B.; Pfefferle, W.; Puhler, A.; Rey, D. A.; Ruckert, C.; Rupp, O.; Sahm, H.; Wendisch, V. F.; Wiegrabe, I.; Tauch, A., *J. Biotechnol.* **2003**, *104*, 5-25.
16. Ilisz, I.; Berkecz, R.; Peter, A., *J. Pharm. Biomed. Anal.* **2008**, *47*, 1-15.
17. Brennan, P. J., *Tuberculosis* **2003**, *83*, 91-97.
18. Hett, E. C.; Rubin, E. J., *Microbiol. Mol. Biol. Rev.* **2008**, *72*, 126-56.
19. Okazaki, Y.; Otsuki, H.; Narisawa, T.; Kobayashi, M.; Sawai, S.; Kamide, Y.; Kusano, M.; Aoki, T.; Hirai, M. Y.; Saito, K., *Nat. Commun.* **2013**, *4*, 1510.
20. Cole, S. T.; Brosch, R.; Parkhill, J.; Garnier, T.; Churcher, C.; Harris, D.; Gordon, S. V.; Eglmeier, K.; Gas, S.; Barry Iii, C. E.; Tekaiia, F.; Badcock, K.; Basham, D.; Brown, D.; Chillingworth, T.; Connor, R.; Davies, R.; Devlin, K.; Feltwell, T.; Gentles, S.; Hamlin, N.; Holroyd, S.; Hornsby, T.; Jagels, K.; Krogh, A.; McLean, J.; Moule, S.; Murphy, L.; Oliver, K.; Osborne, J.; Quail, M. A.; Rajandream, M. A.; Rogers, J.; Rutter, S.; Seeger, K.; Skelton, J.; Squares, R.; Squares, S.; Sulston, J. E.; Taylor, K.; Whitehead, S.; Barrell, B. G., *Nature* **1998**, *393*, 537.
21. Sartain, M. J.; Dick, D. L.; Rithner, C. D.; Crick, D. C.; Belisle, J. T., *J. Lipid Res.* **2011**, *52*, 861-72.
22. Layre, E.; Sweet, L.; Hong, S.; Madigan, C. A.; Desjardins, D.; Young, D. C.; Cheng, T. Y.; Annand, J. W.; Kim, K.; Shamputa, I. C.; McConnell, M. J.; Debono, C. A.; Behar, S. M.; Minnaard, A. J.; Murray, M.; Barry, C. E., 3rd; Matsunaga, I.; Moody, D. B., *Chem. Biol.* **2011**, *18*, 1537-49.
23. Richardson, M. B.; Williams, S. J., *Front. Immunol.* **2014**, *5*, 288.
24. Smith, D. G.; Williams, S. J., *Carbohydr. Res.* **2016**, *420*, 32-45.

25. Calabi, F.; Milstein, C., *Semin. Immunol.* **2000**, *12*, 503-9.
26. Cala-De Paepe, D.; Layre, E.; Giacometti, G.; Garcia-Alles, L. F.; Mori, L.; Hanau, D.; de Libero, G.; de la Salle, H.; Puzo, G.; Gilleron, M., *J. Biol. Chem.* **2012**, *287*, 31494-502.
27. Shah, S.; Nagata, M.; Yamasaki, S.; Williams, S. J., *Chem. Commun.* **2016**, *52*, 10902-5.
28. Borg, N. A.; Wun, K. S.; Kjer-Nielsen, L.; Wilce, M. C.; Pellicci, D. G.; Koh, R.; Besra, G. S.; Bharadwaj, M.; Godfrey, D. I.; McCluskey, J.; Rossjohn, J., *Nature* **2007**, *448*, 44-9.
29. Rossjohn, J.; Gras, S.; Miles, J. J.; Turner, S. J.; Godfrey, D. I.; McCluskey, J., *Annu. Rev. Immunol.* **2015**, *33*, 169-200.
30. Gra, O. A.; Sidorova, J. V.; Nikitin, E. A.; Turygin, A. Y.; Surzhikov, S. A.; Melikyan, A. L.; Sudarikov, A. B.; Zasedatelev, A. S.; Nasedkina, T. V., *J. Mol. Diagn.* **2007**, *9*, 249-257.
31. Van Rhijn, I.; Kasmar, A.; de Jong, A.; Gras, S.; Bhati, M.; Doorenspleet, M. E.; de Vries, N.; Godfrey, D. I.; Altman, J. D.; de Jager, W.; Rossjohn, J.; Moody, D. B., *Nat. Immunol.* **2013**, *14*, 706-13.
32. Fodran, P.; Minnaard, A. J., *Org. Biomol. Chem.* **2013**, *11*, 6919-28.
33. Cohen, N. R.; Garg, S.; Brenner, M. B., **2009**, *102*, 1-94.
34. Suhr, R.; Scheel, O.; Thiem, J., *J. Carbohydr. Chem.* **2006**, *17*, 937-968.
35. Cao, B.; Williams, S. J., *Nat. Prod. Rep.* **2010**, *27*, 919-47.
36. Mishra, A. K.; Krumbach, K.; Rittmann, D.; Appelmelk, B.; Pathak, V.; Pathak, A. K.; Nigou, J.; Geurtsen, J.; Eggeling, L.; Besra, G. S., *Mol. Microbiol.* **2011**, *80*, 1241-59.
37. Morita, M.; Motoki, K.; Akimoto, K.; Natori, T.; Sakai, T.; Sawa, E.; Yamaji, K.; Kozuka, Y.; Kobayashi, E.; Fukushima, H., *J. Med. Chem.* **1995**, *38*, 2176-2187.
38. Koch, M.; Stronge, V. S.; Shepherd, D.; Gadola, S. D.; Mathew, B.; Ritter, G.; Fersht, A. R.; Besra, G. S.; Schmidt, R. R.; Jones, E. Y.; Cerundolo, V., *Nat. Immunol.* **2005**, *6*, 819-26.
39. Mastronicolis, S. K.; Arvanitis, N.; Karaliota, A.; Magiatis, P.; Heropoulos, G.; Litos, C.; Moustaka, H.; Tsakirakis, A.; Paramera, E.; Papastavrou, P., *Appl. Environ. Microbiol.* **2008**, *74*, 4543-9.
40. Sedwick, C., *PLoS Biol.* **2008**, *6*, e181.
41. Kinjo, Y.; Tupin, E.; Wu, D.; Fujio, M.; Garcia-Navarro, R.; Benhnia, M. R.; Zajonc, D. M.; Ben-Menachem, G.; Ainge, G. D.; Painter, G. F.; Khurana, A.; Hoebe, K.; Behar, S. M.; Beutler, B.; Wilson, I. A.; Tsuji, M.; Sellati, T. J.; Wong, C. H.; Kronenberg, M., *Nat. Immunol.* **2006**, *7*, 978-86.
42. Ben-Menachem, G.; Kubler-Kielb, J.; Coxon, B.; Yergey, A.; Schneerson, R., *Proc. Natl. Acad. Sci. USA* **2003**, *100*, 7913-8.
43. Kinjo, Y.; Illarionov, P.; Vela, J. L.; Pei, B.; Girardi, E.; Li, X.; Li, Y.; Imamura, M.; Kaneko, Y.; Okawara, A.; Miyazaki, Y.; Gómez-Velasco, A.; Rogers, P.; Dahesh, S.; Uchiyama, S.; Khurana, A.; Kawahara, K.; Yesilkaya, H.; Andrew, P. W.; Wong, C.-H.; Kawakami, K.; Nizet, V.; Besra, G. S.; Tsuji, M.; Zajonc, D. M.; Kronenberg, M., *Nat. Immunol.* **2011**, *12*, 966-974.
44. Mattner, J.; DeBord, K. L.; Ismail, N.; Goff, R. D.; Cantu Iii, C.; Zhou, D.; Saint-Mezard, P.; Wang, V.; Gao, Y.; Yin, N.; Hoebe, K.; Schneewind, O.; Walker, D.; Beutler, B.; Teyton, L.; Savage, P. B.; Bendelac, A., *Nature* **2005**, *434*, 525.
45. Long, X.; Deng, S.; Mattner, J.; Zang, Z.; Zhou, D.; McNary, N.; Goff, R. D.; Teyton, L.; Bendelac, A.; Savage, P. B., *Nat. Chem. Biol.* **2007**, *3*, 559-64.
46. Chaudhary, V.; Albacker, L. A.; Deng, S.; Chuang, Y.-T.; Li, Y.; Umetsu, D. T.; Savage, P. B., *Org. Lett.* **2013**, *15*, 5242-5245.
47. Hirai, Y.; Haque, M.; Yoshida, T.; Yokota, K.; Yasuda, T.; Oguma, K., *J. Bacteriol.* **1995**, *177*, 5327-5333.
48. Lotter, H.; Gonzalez-Roldan, N.; Lindner, B.; Winau, F.; Isibasi, A.; Moreno-Lafont, M.; Ulmer, A. J.; Holst, O.; Tannich, E.; Jacobs, T., *PLoS Pathog.* **2009**, *5*, e1000434.
49. Exley, M. A.; Tahir, S. M.; Cheng, O.; Shaulov, A.; Joyce, R.; Avigan, D.; Sackstein, R.; Balk, S. P., *J. Immunol.* **2001**, *167*, 5531-4.

50. Kohnen, G.; Tosoni, M.; Tussetschläger, S.; Baro, A.; Laschat, S., *Eur. J. Org. Chem.* **2009**, 5601-5609.
51. Jahng, A.; Maricic, I.; Aguilera, C.; Cardell, S.; Halder, R. C.; Kumar, V., *J. Exp. Med.* **2004**, *199*, 947-57.
52. Fuss, I. J.; Joshi, B.; Yang, Z.; Degheidy, H.; Fichtner-Feigl, S.; de Souza, H.; Rieder, F.; Scaldaferrri, F.; Schirbel, A.; Scarpa, M.; West, G.; Yi, C.; Xu, L.; Leland, P.; Yao, M.; Mannon, P.; Puri, R. K.; Fiocchi, C.; Strober, W., *Gut* **2014**, *63*, 1728-36.
53. Yang, S. H.; Lee, J. P.; Jang, H. R.; Cha, R. H.; Han, S. S.; Jeon, U. S.; Kim, D. K.; Song, J.; Lee, D. S.; Kim, Y. S., *J. Am. Soc. Nephrol.* **2011**, *22*, 1305-14.
54. Rhost, S.; Lofbom, L.; Rynmark, B. M.; Pei, B.; Mansson, J. E.; Teneberg, S.; Blomqvist, M.; Cardell, S. L., *Eur. J. Immunol.* **2012**, *42*, 2851-60.
55. Nair, S.; Boddupalli, C. S.; Verma, R.; Liu, J.; Yang, R.; Pastores, G. M.; Mistry, P. K.; Dhodapkar, M. V., *Blood* **2015**, *125*, 1256-71.
56. Dasgupta, S.; Kumar, V., *Immunogenetics* **2016**, *68*, 665-76.
57. Chang, D. H.; Deng, H.; Matthews, P.; Krasovskiy, J.; Ragupathi, G.; Spisek, R.; Mazumder, A.; Vesole, D. H.; Jagannath, S.; Dhodapkar, M. V., *Blood* **2008**, *112*, 1308-16.
58. Tatituri, R. V.; Watts, G. F.; Bhowruth, V.; Barton, N.; Rothchild, A.; Hsu, F. F.; Almeida, C. F.; Cox, L. R.; Eggeling, L.; Cardell, S.; Rossjohn, J.; Godfrey, D. I.; Behar, S. M.; Besra, G. S.; Brenner, M. B.; Brigl, M., *Proc. Natl. Acad. Sci. USA* **2013**, *110*, 1827-32.
59. Wolf, B. J.; Tatituri, R. V.; Almeida, C. F.; Le Nours, J.; Bhowruth, V.; Johnson, D.; Uldrich, A. P.; Hsu, F. F.; Brigl, M.; Besra, G. S.; Rossjohn, J.; Godfrey, D. I.; Brenner, M. B., *J. Immunol.* **2015**, *195*, 2540-51.
60. Zeissig, S.; Murata, K.; Sweet, L.; Publicover, J.; Hu, Z.; Kaser, A.; Bosse, E.; Iqbal, J.; Hussain, M. M.; Balschun, K.; Rocken, C.; Arlt, A.; Gunther, R.; Hampe, J.; Schreiber, S.; Baron, J. L.; Moody, D. B.; Liang, T. J.; Blumberg, R. S., *Nat. Med.* **2012**, *18*, 1060-8.
61. Van Rhijn, I.; Young, D. C.; Im, J. S.; Levery, S. B.; Illarionov, P. A.; Besra, G. S.; Porcelli, S. A.; Gumperz, J.; Cheng, T. Y.; Moody, D. B., *Proc. Natl. Acad. Sci. USA* **2004**, *101*, 13578-83.
62. Le Nours, J.; Praveena, T.; Pellicci, D. G.; Gherardin, N. A.; Ross, F. J.; Lim, R. T.; Besra, G. S.; Keshipeddy, S.; Richardson, S. K.; Howell, A. R.; Gras, S.; Godfrey, D. I.; Rossjohn, J.; Uldrich, A. P., *Nat. Commun.* **2016**, *7*, 10570.
63. Uldrich, A. P.; Patel, O.; Cameron, G.; Pellicci, D. G.; Day, E. B.; Sullivan, L. C.; Kyparissoudis, K.; Kjer-Nielsen, L.; Vivian, J. P.; Cao, B.; Brooks, A. G.; Williams, S. J.; Illarionov, P.; Besra, G. S.; Turner, S. J.; Porcelli, S. A.; McCluskey, J.; Smyth, M. J.; Rossjohn, J.; Godfrey, D. I., *Nat. Immunol.* **2011**, *12*, 616-23.
64. Fischer, K.; Scotet, E.; Niemeyer, M.; Koebernick, H.; Zerrahn, J.; Maillet, S.; Hurwitz, R.; Kursar, M.; Bonneville, M.; Kaufmann, S. H.; Schaible, U. E., *Proc. Natl. Acad. Sci. USA* **2004**, *101*, 10685-90.
65. Karakousis, P. C.; Bishai, W. R.; Dorman, S. E., *Cell. Microbiol.* **2004**, *6*, 105-116.
66. Sturgill-Koszycki, S.; Schlesinger, P. H.; Chakraborty, P.; Haddix, P. L.; Collins, H. L.; Fok, A. K.; Allen, R. D.; Gluck, S. L.; Heuser, J.; Russell, D. G., *Science* **1994**, *263*, 678-81.
67. Van Rhijn, I.; Moody, D. B., *Immunol. Rev.* **2015**, *264*, 138-53.
68. Moody, D. B.; Guy, M. R.; Grant, E.; Cheng, T.-Y.; Brenner, M. B.; Besra, G. S.; Porcelli, S. A., *J. Exp. Med.* **2000**, *192*, 965.
69. Layre, E.; Collmann, A.; Bastian, M.; Mariotti, S.; Czaplicki, J.; Prandi, J.; Mori, L.; Stenger, S.; De Libero, G.; Puzo, G.; Gilleron, M., *Chem. Biol.* **2009**, *16*, 82-92.
70. Sieling, P. A.; Chatterjee, D.; Porcelli, S. A.; Prigozy, T. I.; Mazzaccaro, R. J.; Soriano, T.; Bloom, B. R.; Brenner, M. B.; Kronenberg, M.; Brennan, P. J.; et, a., *Science* **1995**, *269*, 227.
71. Ernst, W. A.; Maher, J.; Cho, S.; Niazi, K. R.; Chatterjee, D.; Moody, D. B.; Besra, G. S.; Watanabe, Y.; Jensen, P. E.; Porcelli, S. A.; Kronenberg, M.; Modlin, R. L., *Immunity* **1998**, *8*, 331-340.

72. de la Salle, H.; Mariotti, S.; Angenieux, C.; Gilleron, M.; Garcia-Alles, L.-F.; Malm, D.; Berg, T.; Paoletti, S.; Maître, B.; Mourey, L.; Salamero, J.; Cazenave, J. P.; Hanau, D.; Mori, L.; Puzo, G.; De Libero, G., *Science* **2005**, *310*, 1321.
73. Gilleron, M.; Stenger, S.; Mazorra, Z.; Wittke, F.; Mariotti, S.; Bohmer, G.; Prandi, J.; Mori, L.; Puzo, G.; De Libero, G., *J. Exp. Med.* **2004**, *199*, 649-59.
74. Goren, M. B., *Am. Rev. Respir. Dis.* **1982**, *125*, 50-69.
75. Guiard, J.; Collmann, A.; Gilleron, M.; Mori, L.; De Libero, G.; Prandi, J.; Puzo, G., *Angew. Chem. Int. Ed.* **2008**, *47*, 9734-8.
76. Van Rhijn, I.; van Berlo, T.; Hilmenyuk, T.; Cheng, T.-Y.; Wolf, B. J.; Tatituri, R. V. V.; Uldrich, A. P.; Napolitani, G.; Cerundolo, V.; Altman, J. D.; Willemsen, P.; Huang, S.; Rossjohn, J.; Besra, G. S.; Brenner, M. B.; Godfrey, D. I.; Moody, D. B., *Proc. Natl. Acad. Sci. USA* **2016**, *113*, 380-385.
77. Jackson, M.; Stadthagen, G.; Gicquel, B., *Tuberculosis* **2007**, *87*, 78-86.
78. Anderson, R. J., *J. Biol. Chem.* **1929**, *83*, 505-522.
79. Spielman, M. A., *J. Biol. Chem.* **1934**, *106*, 87-96.
80. Ryhage, R.; Stenhagen, E., *J. Lipid Res.* **1960**, *1*, 361-90.
81. Prout, F. S.; Cason, J.; Ingersoll, A. W., *J. Am. Chem. Soc.* **1948**, *70*, 298-305.
82. Bijvoet, J. M.; Peerdeman, A. F.; van Bommel, A. J., *Nature* **1951**, *168*, 271.
83. Sonnet, P. E.; Carney, R. L.; Henrick, C., *J. Chem. Ecol.* **1985**, *11*, 1371-1387.
84. Acharya, P. V. N.; Goldman, D. S., *J. Bacteriol.* **1970**, *102*, 733-739.
85. Wolucka, B. A.; McNeil, M. R.; Kalbe, L.; Cocito, C.; Brennan, P. J., *Biochim. Biophys. Acta.* **1993**, *1170*, 131-136.
86. Cao, B.; Chen, X.; Yamaryo-Botte, Y.; Richardson, M. B.; Martin, K. L.; Khairallah, G. N.; Rupasinghe, T. W.; O'Flaherty, R. M.; O'Hair, R. A.; Ralton, J. E.; Crellin, P. K.; Coppel, R. L.; McConville, M. J.; Williams, S. J., *J. Org. Chem.* **2013**, *78*, 2175-90.
87. Goletti, D.; Petruccioli, E.; Joosten, S. A.; Ottenhoff, T. H. M., *Infect Dis Rep.* **2016**, *8*, 6568.
88. Ter Horst, B.; Seshadri, C.; Sweet, L.; Young, D. C.; Feringa, B. L.; Moody, D. B.; Minnaard, A. J., *J. Lipid Res.* **2010**, *51*, 1017-22.
89. Maloney, E.; Lun, S.; Stankowska, D.; Guo, H.; Rajagoapalan, M.; Bishai, W. R.; Madiraju, M. V., *Front Microbiol.* **2011**, *2*, 19.
90. Maloney, E.; Stankowska, D.; Zhang, J.; Fol, M.; Cheng, Q. J.; Lun, S.; Bishai, W. R.; Rajagopalan, M.; Chatterjee, D.; Madiraju, M. V., *PLoS Pathog.* **2009**, *5*, e1000534.
91. Lerouge, P.; Lebas, M. H.; Agapakis-Causse, C.; Prome, J. C., *Chem. Phys. Lipids.* **1988**, *49*, 161-6.
92. Laneelle, M. A.; Prome, D.; Laneelle, G.; Prome, J. C., *J. Gen. Microbiol.* **1990**, *136*, 773-8.
93. Tschumi, A.; Nai, C.; Auchli, Y.; Hunziker, P.; Gehrig, P.; Keller, P.; Grau, T.; Sander, P., *J. Biol. Chem.* **2009**, *284*, 27146-56.
94. Lennarz, W. J.; Scheuerbrandt, G.; Bloch, K.; With a note by, R. R., *J. Biol. Chem.* **1962**, *237*, 664-671.
95. Jaureguiberry, G.; Lenfant, M.; Toubiana, R.; Azerad, R.; Lederer, E., *Chem. Commun.* **1966**, 855-857.
96. Yang, W.; Dostal, L.; Rosazza, J. P., *Appl. Environ. Microbiol.* **1993**, *59*, 281-4.
97. el-Sharkawy, S. H.; Yang, W.; Dostal, L.; Rosazza, J. P., *Appl. Environ. Microbiol.* **1992**, *58*, 2116-2122.
98. Mekala, S.; Hahn, R. C., *J. Org. Chem.* **2015**, *80*, 1610-7.
99. Patil, P. S.; Cheng, T. J.; Zulueta, M. M.; Yang, S. T.; Lico, L. S.; Hung, S. C., *Nat. Commun.* **2015**, *6*, 7239.
100. Roberts, I. O.; Baird, M. S., *Chem. Phys. Lipids* **2006**, *142*, 111-7.

101. Rankin, G. M.; Compton, B. J.; Johnston, K. A.; Hayman, C. M.; Painter, G. F.; Larsen, D. S., *J. Org. Chem.* **2012**, *77*, 6743-59.
102. Liu, X.; Stocker, B. L.; Seeberger, P. H., *J. Am. Chem. Soc.* **2006**, *128*, 3638-3648.
103. Chauvin, Y., *Angew. Chem. Int. Ed.* **2006**, *45*, 3740-3747.
104. Chatterjee, A. K.; Choi, T.-L.; Sanders, D. P.; Grubbs, R. H., *J. Am. Chem. Soc.* **2003**, *125*, 11360-11370.
105. Miao, X.; Fischmeister, C.; Bruneau, C.; Dixneuf, P. H., *ChemSusChem*. **2009**, *2*, 542-545.
106. Louie, J.; Bielawski, C. W.; Grubbs, R. H., *J. Am. Chem. Soc.* **2001**, *123*, 11312-11313.
107. Inokuma, Y.; Yoshioka, S.; Ariyoshi, J.; Arai, T.; Hitora, Y.; Takada, K.; Matsunaga, S.; Rissanen, K.; Fujita, M., *Nature* **2013**, *495*, 461-6.
108. Seco, J. M.; Quinoa, E.; Riguera, R., *Chem. Rev.* **2012**, *112*, 4603-41.
109. Hoye, T. R.; Jeffrey, C. S.; Shao, F., *Nat. Protoc.* **2007**, *2*, 2451-8.
110. Dale, J. A.; Dull, D. L.; Mosher, H. S., *J. Org. Chem.* **1969**, *34*, 2543-2549.
111. Wenzel, T. J.; Wilcox, J. D., *Chirality* **2003**, *15*, 256-270.
112. Yasaka, Y.; Matsumoto, T.; Tanaka, M., *Anal. Sci.* **1995**, *11*, 295-297.
113. Akasaka, K.; Ohru, H., *Biosci. Biotechnol. Biochem.* **1999**, *63*, 1209-1215.
114. Cochrane, S. A.; Lohans, C. T.; van Belkum, M. J.; Bels, M. A.; Vederas, J. C., *Org. Biomol. Chem.* **2015**, *13*, 6073-81.
115. Still, W. C.; Kahn, M.; Mitra, A., *J. Org. Chem.* **1978**, *43*, 2923-2925.
116. Pangborn, A. B.; Giardello, M. A.; Grubbs, R. H.; Rosen, R. K.; Timmers, F. J., *Organometallics* **1996**, *15*, 1518-1520.
117. Roberts, I. O.; Baird, M. S., *Chem. Phys. Lipids* **2006**, *142*, 111-117.
118. Furse, S., *J. Chem. Biol.* **2017**, *10*, 1-9.
119. Boudiere, L.; Michaud, M.; Petroustos, D.; Rebeille, F.; Falconet, D.; Bastien, O.; Roy, S.; Finazzi, G.; Rolland, N.; Jouhet, J.; Block, M. A.; Marechal, E., *Biochim. Biophys. Acta* **2014**, *1837*, 470-80.
120. Benson, A. A.; Maruo, B., *Biochim. Biophys. Acta.* **1958**, *27*, 189-195.
121. Benson, A. A.; Maruo, B., *Biochim. Biophys. Acta.* **1989**, *1000*, 447-458.
122. Frentzen, M., *Curr. Opin. Plant Biol.* **2004**, *7*, 270-6.
123. Ikawa, M., *Bacteriol. Rev.* **1967**, *31*, 54-64.
124. Horvath, S. E.; Daum, G., *Prog. Lipid. Res.* **2013**, *52*, 590-614.
125. Kiyasu, J. Y.; Pieringer, R. A.; Paulus, H.; Kennedy, E. P., *J. Biol. Chem.* **1963**, *238*, 2293-2298.
126. Schlame, M., *J. Lipid Res.* **2008**, *49*, 1607-20.
127. Smith, P. B. W.; Snyder, A. P.; Harden, C. S., *Anal. Chem.* **1995**, *67*, 1824-1830.
128. Hsu, F. F.; Turk, J.; Williams, T. D.; Welti, R., *J. Am. Soc. Mass. Spectrom.* **2007**, *18*, 783-90.
129. Hsu, F., *J. Am. Soc. Mass Spectrom.* **2003**.
130. Tatituri, R. V. V.; Wolf, B. J.; Brenner, M. B.; Turk, J.; Hsu, F.-F., *Anal. Bioanal. Chem.* **2015**, *407*, 2519-2528.
131. Sowden, J. C.; Fischer, H. O. L., *J. Am. Chem. Soc.* **1941**, *63*, 3244-3248.
132. Burgos, C. E.; Ayer, D. E.; Johnson, R. A., *J. Org. Chem.* **1987**, *52*, 4973-4977.
133. Ali, S.; Bittman, R., *J. Org. Chem.* **1988**, *53*, 5547-5549.
134. Stamatov, S. D.; Kullberg, M.; Stawinski, J., *Tetrahedron Lett.* **2005**, *46*, 6855-6859.
135. Lok, C. M., *Chem. Phys. Lipids* **1978**, *22*, 323-337.
136. Martinez, L. E.; Leighton, J. L.; Carsten, D. H.; Jacobsen, E. N., *J. Am. Chem. Soc.* **1995**, *117*, 5897-5898.
137. Hansen, K. B.; Leighton, J. L.; Jacobsen, E. N., *J. Am. Chem. Soc.* **1996**, *118*, 10924-10925.
138. Sutter, M.; Silva, E. D.; Duguet, N.; Raoul, Y.; Méta, E.; Lemaire, M., *Chem. Rev.* **2015**, *115*, 8609-8651.

139. Nielsen, L. P. C.; Stevenson, C. P.; Blackmond, D. G.; Jacobsen, E. N., *J. Am. Chem. Soc.* **2004**, *126*, 1360-1362.
140. Jacobsen, E. N.; Kakiuchi, F.; Konsler, R. G.; Larrow, J. F.; Tokunaga, M., *Tetrahedron Lett.* **1997**, *38*, 773-776.
141. Baer, E.; Buchnea, D., *J. Biol. Chem.* **1958**, *232*, 895-901.
142. D'Arrigo, P.; de Ferra, L.; Pedrocchi-Fantoni, G.; Scarcelli, D.; Servi, S.; Strini, A., *J. Chem. Soc., Perkin Trans. 1* **1996**, 2657-2660.
143. D'Arrigo, P.; Servi, S., *Molecules* **2010**, *15*.
144. Baer, E.; Fischer, H. O. L., *J. Biol. Chem.* **1939**, *128*, 491-500.
145. Baer, E.; Fischer, H. O. L., *J. Biol. Chem.* **1939**, *128*, 475-489.
146. Baer, E.; Fischer, H. O. L., *J. Biol. Chem.* **1939**, *128*, 463-473.
147. Fischer, E., *Ber. Dtsch. Chem. Ges.* **1920**, *53*, 1621-1633.
148. Dreef, C. E.; Elie, C. J. J.; Hoogerhout, P.; van der Marel, G. A.; van Boom, J. H., *Tetrahedron Lett.* **1988**, *29*, 6513-6515.
149. van Boeckel, C. A. A.; Visser, G. M.; van Boom, J. H., *Tetrahedron* **1985**, *41*, 4557-4565.
150. Caruthers, M. H.; Barone, A. D.; Beaucage, S. L.; Dodds, D. R.; Fisher, E. F.; McBride, L. J.; Matteucci, M.; Stabinsky, Z.; Tang, J. Y., *Methods Enzymol.* **1987**, *154*, 287-313.
151. Sparling, M. L.; Zidovetzki, R.; Muller, L.; Chan, S. I., *Anal. Biochem.* **1989**, *178*, 67-76.
152. Chen, N.; Xie, J., *J. Org. Chem.* **2014**, *79*, 10716-21.
153. Front, S.; Court, N.; Bourigault, M.-L.; Rose, S.; Ryffel, B.; Erard, F.; Quesniaux, V. F. J.; Martin, O. R., *ChemMedChem* **2011**, *6*, 2081-2093.
154. Rankin, G. M.; Compton, B. J.; Johnston, K. A.; Hayman, C. M.; Painter, G. F.; Larsen, D. S., *J. Org. Chem.* **2012**, *77*, 6743-6759.
155. Benson, A. A., *Annu. Rev. Plant Physiol.* **1964**, *15*, 1-16.
156. Shaw, N., *Bacteriol. Rev.* **1970**, *34*, 365-377.
157. Wilkinson, S. G., *Biochim. Biophys. Acta, Lipids Lipid Metab.* **1969**, *187*, 492-500.
158. Hunter, S. W.; McNeil, M. R.; Brennan, P. J., *J. Bacteriol.* **1986**, *168*, 917-922.
159. Schultz, J. C.; Elbein, A. D., *J. Bacteriol.* **1974**, *117*, 107-115.
160. Mahajan, S.; Dkhar, H. K.; Chandra, V.; Dave, S.; Nanduri, R.; Janmeja, A. K.; Agrewala, J. N.; Gupta, P., *J. Immunol.* **2012**, *188*, 5593-603.
161. Richardson, M. B.; Torigoe, S.; Yamasaki, S.; Williams, S. J., *Chem. Commun.* **2015**, *51*, 15027-30.
162. Tatituri, R. V.; Illarionov, P. A.; Dover, L. G.; Nigou, J.; Gilleron, M.; Hitchen, P.; Krumbach, K.; Morris, H. R.; Spencer, N.; Dell, A.; Eggeling, L.; Besra, G. S., *J. Biol. Chem.* **2007**, *282*, 4561-72.
163. Takahashi, M.; Ono, Y., Pulse-Chase Analysis of Protein Kinase C. In *Protein Kinase C Protocols*, Newton, A. C., Ed. Humana Press: Totowa, NJ, 2003; pp 163-170.
164. Mishra, A. K.; Klein, C.; Gurcha, S. S.; Alderwick, L. J.; Babu, P.; Hitchen, P. G.; Morris, H. R.; Dell, A.; Besra, G. S.; Eggeling, L., *Antonie Van Leeuwenhoek.* **2008**, *94*, 277-87.
165. Girardi, E.; Zajonc, D. M., *Immunol Rev.* **2012**, *250*, 167-79.
166. Murr, B. L.; Conkling, J. A., *J. Am. Chem. Soc.* **1970**, *92*, 3462-3464.
167. Hanashima, S.; Mizushina, Y.; Yamazaki, T.; Ohta, K.; Takahashi, S.; Sahara, H.; Sakaguchi, K.; Sugawara, F., *Bioorgan. Med. Chem.* **2001**, *9*, 367-376.
168. Peci, L. M.; Stick, R. V.; Tilbrook, D. M. G.; Winslade, M. L., *Aust. J. Chem.* **1998**, *50*, 1105-1108.
169. Moitessier, N.; Chrétien, F.; Chapleur, Y., *Tetrahedron: Asymmetry* **1997**, *8*, 2889-2892.
170. Suhr, R.; Scheel, O.; Thiem, J., *J. Carbohydr. Chem.* **1998**, *17*, 937-968.
171. Dawe, R. D.; Molinski, T. F.; Turner, J. V., *Tetrahedron Lett.* **1984**, *25*, 2061-2064.
172. Kruizinga, W. H.; Strijtveen, B.; Kellogg, R. M., *J. Org. Chem.* **1981**, *46*, 4321-4323.
173. Stamatov, S. D.; Stawinski, J., *Org. Biomol. Chem.* **2010**, *8*, 463-77.
174. Lok, C. M.; Mank, A. P. J.; Ward, J. P., *Chem. Phys. Lipids* **1985**, *36*, 329-334.

175. Hanamoto, T.; Sugimoto, Y.; Yokoyama, Y.; Inanaga, J., *J. Org. Chem.* **1996**, *61*, 4491-4492.
176. Rosseto, R.; Bibak, N.; DeOcampo, R.; Shah, T.; Gabrielian, A.; Hajdu, J., *J. Org. Chem.* **2007**, *72*, 1691-1698.
177. Epp, J. B.; Widlanski, T. S., *J. Org. Chem.* **1999**, *64*, 293-295.
178. Nooy, A. E. J. d.; Besemer, A. C.; Bekkum, H. v., *Synthesis* **1996**, *1996*, 1153-1176.
179. Milkereit, G.; Morr, M.; Thiem, J.; Vill, V., *Chem. Phys. Lipids* **2004**, *127*, 47-63.
180. Tian, G.-Z.; Wang, X.-L.; Hu, J.; Wang, X.-B.; Guo, X.-Q.; Yin, J., *Chin. Chem. Lett.* **2015**, *26*, 922-930.
181. Vetro, M.; Costa, B.; Donvito, G.; Arrighetti, N.; Cipolla, L.; Perego, P.; Compostella, F.; Ronchetti, F.; Colombo, D., *Org. Biomol. Chem* **2015**, *13*, 1091-9.
182. Zhdankin, V. V., Hypervalent Iodine Reagents in Organic Synthesis. In *Hypervalent Iodine Chemistry*, John Wiley & Sons Ltd: 2013; pp 145-336.
183. Thomas, E. J., Philip J. Kocienski, Georg Thieme Stuttgart, *Protecting groups. Philip J. Kocienski. Georg Thieme, Stuttgart, 2000 xv + 260 pages. 99 DM (corrected edition). ISBN 3-13-137002-5 (Stuttgart); 0-86577-993-7 (New York)*. John Wiley & Sons, Ltd.: 2001; Vol. 15, p 725-725.
184. Avery, M. A., *J. Med. Chem.* **1999**, *42*, 5285-5285.
185. Guo, J.; Ye, X.-S., *Molecules* **2010**, *15*, 7235-65.
186. Mootoo, D. R.; Konradsson, P.; Udodong, U.; Fraser-Reid, B., *J. Am. Chem. Soc.* **1988**, *110*, 5583-5584.
187. Cicero, D.; Varela, O.; De Lederkremer, R. M., *Tetrahedron* **1990**, *46*, 1131-1144.
188. Kondo, Y.; Miyahara, K.; Kashimura, N., *Can. J. Chem.* **1973**, *51*, 3272-3276.
189. David, S.; Hanessian, S., *Tetrahedron* **1985**, *41*, 643-663.
190. Wilkinson, B. L., *Aust. J. Chem.* **2013**, *66*, 910.
191. Holý, A.; Souček, M., *Tetrahedron Lett.* **1971**, *12*, 185-188.
192. Pautard, A. M.; Evans, S. A., *J. Org. Chem.* **1988**, *53*, 2300-2303.
193. Stawinski, J.; Hozumi, T.; Narang, S. A., *J. Chem. Soc. Chem. Commun.* **1976**, 243-244.
194. Ishikawa, N.; Shin-ya, S., *Chemistry Lett.* **1976**, *5*, 673-676.
195. Brown, L.; Koreeda, M., *J. Org. Chem.* **1984**, *49*, 3875-3880.
196. Kim, S.; Chang, H.; Kim, W. J., *J. Org. Chem.* **1985**, *50*, 1751-1752.
197. Konig, W.; Geiger, R., *Chem Ber.* **1970**, *103*, 788-98.
198. Sheikh, M. C.; Takagi, S.; Yoshimura, T.; Morita, H., *Tetrahedron* **2010**, *66*, 7272-7278.
199. Matsukawa, Y.; Isobe, M.; Kotsuki, H.; Ichikawa, Y., *J. Org. Chem.* **2005**, *70*, 5339-5341.
200. Hakki, Z.; Cao, B.; Heskes, A. M.; Goodger, J. Q.; Woodrow, I. E.; Williams, S. J., *Carbohydr. Res.* **2010**, *345*, 2079-84.
201. Balalaie, S.; Mahdidoust, M.; Eshaghi-Najafabadi, R., *Chin. J. Chem.* **2008**, *26*, 1141-1144.
202. Wang, Y.; Gao, J.; Gu, G.; Li, G.; Cui, C.; Sun, B.; Lou, H., *ChemBioChem* **2011**, *12*, 2418-2420.
203. Wehrstedt, K. D.; Wandrey, P. A.; Heitkamp, D., *J. Hazard. Mater.* **2005**, *126*, 1-7.
204. El-Faham, A.; Funosas, R. S.; Prohens, R.; Albericio, F., *Chem. Eur. J.* **2009**, *15*, 9404-9416.
205. Itoh, M., *Bull. Chem. Soc. Jpn.* **1973**, *46*, 2219-2221.
206. Twibanire, J.-d. A. K.; Grindley, T. B., *Org. Lett.* **2011**, *13*, 2988-2991.
207. El-Faham, A.; Subirós-Funosas, R.; Albericio, F., *Eur. J. Org. Chem.* **2010**, *2010*, 3641-3649.
208. Jad, Y. E.; Khattab, S. N.; de la Torre, B. G.; Govender, T.; Kruger, H. G.; El-Faham, A.; Albericio, F., *Org. Biomol. Chem.* **2014**, *12*, 8379-85.
209. Jad, Y. E.; Khattab, S. N.; de la Torre, B. G.; Govender, T.; Kruger, H. G.; El-Faham, A.; Albericio, F., *Molecules* **2014**, *19*, 18953-65.
210. Dev, D.; Palakurthy, N. B.; Kumar, N.; Mandal, B., *Tetrahedron Lett.* **2013**, *54*, 4397-4400.

211. Burugupalli, S.; Shah, S.; van der Peet, P. L.; Arora, S.; White, J. M.; Williams, S. J., *Org Biomol Chem* **2016**, *14*, 97-104.
212. Hansch, C.; Leo, A.; Taft, R. W., *Chem. Rev.* **1991**, *91*, 165-195.
213. Jungmann, O.; Pfliederer, W., *Nucleosides, Nucleotides and Nucleic Acids* **2009**, *28*, 550-585.
214. Perrocheau, J.; Carrié, R.; Fleury, J.-P., *Can. J. Chem.* **1994**, *72*, 2458-2467.
215. Duguay, G.; Guémas, J.-P.; Meslin, J.-C.; Pradère, J.-P.; Reliquet, F.; Reliquet, A.; Tea-Gokou, C.; Quiniou, H.; Rabiller, C., *J. Heterocyclic Chem.* **1980**, *17*, 767-770.
216. Kalabin, G. A.; Krivdin, L. B.; Shcherbakov, V. V.; Trofimov, B. A., *J. Mol. Struct.* **1986**, *143*, 569-572.
217. Charton, M., Structural Effects on Reactivity and Properties of Oximes and Hydroxamic Acids. In *The Chemistry of Hydroxylamines, Oximes and Hydroxamic Acids*, Rappoport, Z.; Liebman, J. F., Eds. John Wiley & Sons, Ltd: 2008; pp 553-608.
218. Biehler, J.-M.; Fleury, J.-P.; Perchais, J.; Regent, A., *Tetrahedron Lett.* **1968**, *9*, 4227-4230.
219. Sawada, M.; Tsuno, Y.; Yukawa, Y., *Bull. Chem. Soc. Jpn.* **1972**, *45*, 1206-1209.
220. Pelyvás, I. F.; Lindhorst, T. K.; Streicher, H.; Thiem, J., *Synthesis* **1991**, *1991*, 1015-1018.
221. Bell, D. J.; Lorber, J., *J. Chem. Soc.* **1940**, 453-455.
222. Jarrell, H. C.; Szarek, W. A., *Can. J. Chem.* **1978**, *56*, 144-146.
223. Küster, J. M.; Dyong, I., *Liebigs Ann. Chem.* **1975**, *1975*, 2179-2189.
224. Sheldrick, G., *Acta Crystallogr. A* **2008**, *64*, 112-122.
225. Farrugia, L. J., *J. Appl. Cryst.* **1999**, *32*, 837-838.





Minerva Access is the Institutional Repository of The University of Melbourne

**Author/s:**

Burugupalli, Satvika

**Title:**

Synthesis of immunogenic mycobacterial cell wall lipids

**Date:**

2017

**Persistent Link:**

<http://hdl.handle.net/11343/208937>

**File Description:**

Synthesis of immunogenic mycobacterial cell wall lipids

**Terms and Conditions:**

Terms and Conditions: Copyright in works deposited in Minerva Access is retained by the copyright owner. The work may not be altered without permission from the copyright owner. Readers may only download, print and save electronic copies of whole works for their own personal non-commercial use. Any use that exceeds these limits requires permission from the copyright owner. Attribution is essential when quoting or paraphrasing from these works.